EFFECT OF VARYING DEGREES OF WATER SATURATION ON REDOX CONDITIONS IN A YELLOW BROWN APEDAL B SOIL HORIZON

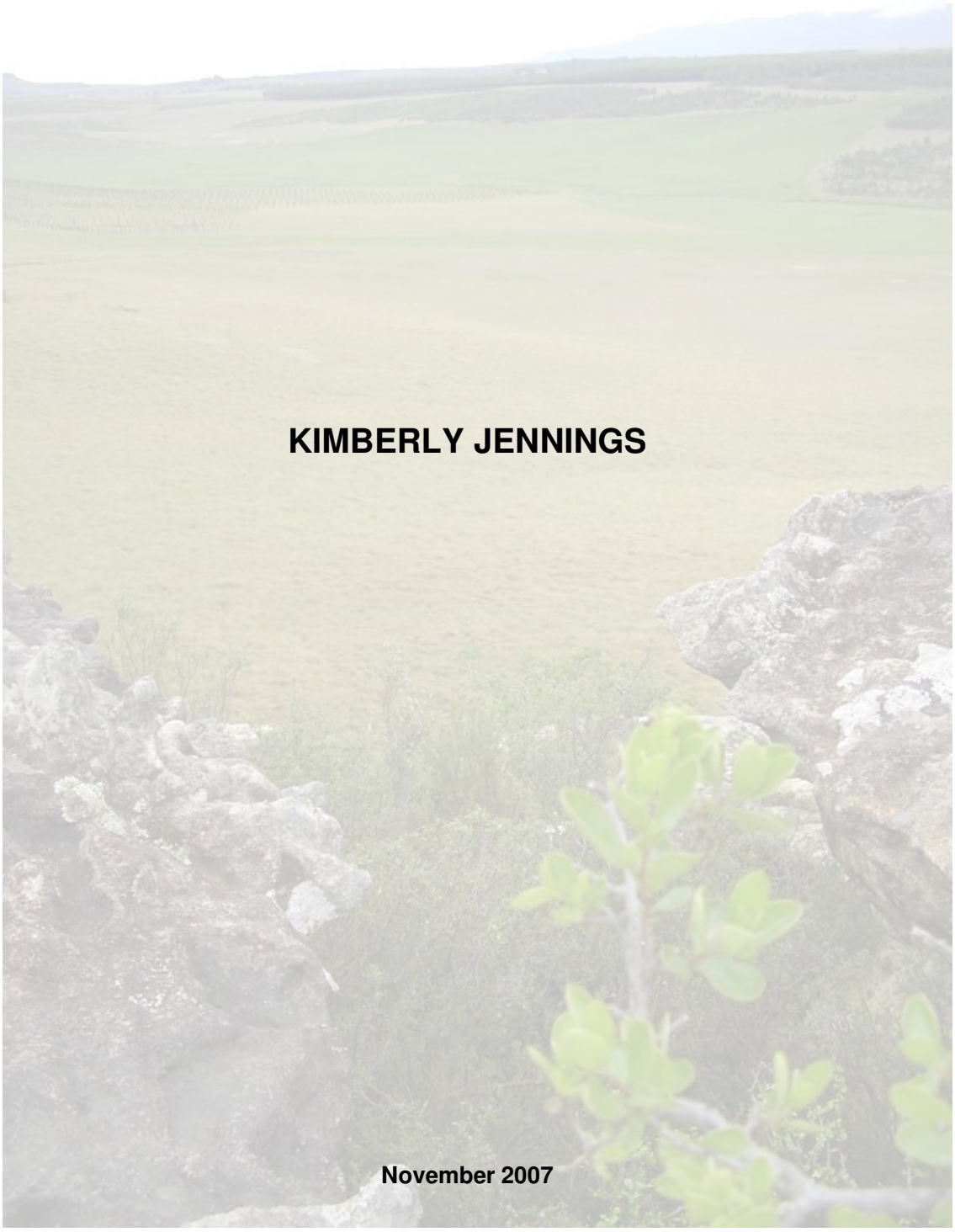

KIMBERLY JENNINGS

November 2007

Effect of varying degrees of water saturation on redox conditions in a yellow brown apedal B soil horizon

By

KIMBERLY JENNINGS

A dissertation submitted in accordance
with the requirements for the
Magister Scientiae degree
in the
Faculty of Natural and Agricultural Sciences
Department of Soil, Crop and Climate Sciences
University of the Free State
Bloemfontein

November 2007

Supervisor: Dr C. W. van Huyssteen

DECLARATION

I hereby declare that this dissertation hereby submitted for the Magister Scientiae degree at the University of the Free State, is my own work and has not been submitted to any other University.

I also agree that the University of the Free State has the sole right to the publication of this dissertation.

Signed: _____ Date: _____

ACKNOWLEDGEMENTS

I acknowledge the following organizations and persons for their endless contribution to this dissertation.

Dr. C. W. van Huyssteen my supervisor for his continuous guidance, support and encouragement during the laboratory phase, data analysis and writing of this dissertation.

Dr. M. Hensley for his advice, guidance and informative conversations. I would have been at a loss without him.

The Department of Soil, Crop and Climate Sciences is acknowledged for providing me with office space, laboratory facilities, and funding.

My sincere gratitude to Mrs. G. C. van Heerden and Mrs. Y. M. Dessels who always assisted me so willingly.

My parents, Greg and Heather and brother, Darren for their guidance and love and for providing me with the opportunity to equip myself for my life ahead.

Sampie for his much needed love and support.

Most importantly, my Lord and Savior, Jesus Christ.

"I can do all things through Christ who strengthens me"
Philippians 4:13

"Soli Deo Gloria"

TABLE OF CONTENTS

LIST OF SYMBOLS AND ABBREVIATIONS

A	Orthic A horizon of the Avalon 2100 used in this study
$AD_{s>0.7}$	Annual duration of water saturation above 70 % of porosity
Av	Avalon soil form (orthic A – yellow-brown apedal B – soft plinthic B)
B1	Yellow brown apedal B1 horizon of the Avalon 2100 used in this study
B2	Yellow brown apedal B2 horizon of the Avalon 2100 used in this study
C	Unspecified material with signs of wetness of the Avalon 2100 used in this study
Cl	Clay
coSa	Coarse sand
DUL	Drained upper limit
Eh	Redox potential
ETo	Reference evaporation determined by the FAO Penman-Monteith equation
fiSa	Fine sand
fiSi	Fine silt
meSa	Medium sand
NWM	Neutron water meter
OM	Organic matter
on	Unspecified material with signs of wetness
ot	Orthic A horizon
pe	Negative common logarithm of the free-electron activity
rH	Negative logarithm of a hypothetical hydrogen pressure (bars)
s	Degree of saturation (volume of water per volume of pores)
S>0.7	Degree of water saturation above 0.7 of porosity
$S_{0.6}$	Degree of saturation at which the pores are saturated to 60 % of porosity
$S_{0.7}$	Degree of saturation at which the pores are saturated to 70 % of porosity
$S_{0.8}$	Degree of saturation at which the pores are saturated to 80 % of porosity
$S_{0.9}$	Degree of saturation at which the pores are saturated to 90 % of porosity
Si	Silt
sp	Soft plinthic B horizon
vfSa	Very fine sand
f	Porosity
θ_v	Volumetric soil water content (mm)

LIST OF FIGURES

LIST OF TABLES

ABSTRACT

Various studies have been conducted into redox potential (Eh), redox indicators and the measured soil water contents in soil (Franzmeier *et al*., 1983; Schwertmann & Fanning, 1976; Veneman *et al*., 1976). Although a measure of success has come from these studies, there are still vast knowledge gaps within this field.

The degree of water saturation where reduction in the soil is initiated cannot be determined from literature, although it was approximated that 70% of water saturation ($S_{0.7}$) was sufficient to initiate reduction (Van Huyssteen *et al*., 2005). This value will vary for different soil temperatures, varying bulk densities as well as soils with different organic matter contents.

This study aimed to determine if it was possible to identify a degree of water saturation at which reduction is initiated for a soil in a closed system. It also aimed to determine the effect of bulk density on reduction. Reduction was defined by a decrease in pe (Eh) of a soil and an increase in the soluble Fe^{2+} concentration. There were three key aims to the study: to establish the relationship between the degree of water saturation (s) and the onset of reduction; to establish the relationship between the degree of water saturation (s) and the duration of reduction and to establish the effect of bulk density on the above-mentioned processes.

A yellow brown apedal B horizon from an Avalon soil form (profile 234) in the Weatherley catchment was used in this study. A soil core experiment was carried out to determine the effect of degree and duration of water saturation on Eh, pH, Fe^{2+}, Mn^{2+}, Ca^{2+}, Mg^{2+}, K^{+}, and Na^{+}. Soil cores were packed to a bulk density of 1.6 Mg m^{-3} and individually saturated to $S_{0.6}$ (60% of the pores saturated with water), $S_{0.7}$ (70% of the pores saturated with water), $S_{0.8}$ (80% of the pores saturated with water), and $S_{0.9}$ (90% of the pores saturated with water). Measurements were done in triplicate. The cores were sealed with a double layer of plastic wrap and stored in a laboratory at 23°C until needed. Analysis started three days after initial water saturation. A set of cores (four degrees of saturation with triplicates of each) was analysed every 3.5 days for the first three months after which a set was analysed once a week for the remaining month of analyses. The experiment was terminated after 121 days.

The same soil and experimental setup was used for the bulk density experiment. The experiment consisted of a set of three cores packed to an initial bulk density of 1.4, 1.6 and 1.8 Mg m^{-3}. The cores were all saturated to $S_{0.8}$, each packed in triplicate. The bulk density experiment was terminated after 23 days.

There was a good correlation between an increase in degree of water saturation and pe (R^2 = 0.95); Mn^{2+} (R^2 = 0.91) and Fe^{2+} (R^2 = 0.92) concentrations. Eh, pH, Fe^{2+}, Mn^{2+}, Ca^{2+}, Mg^{2+}, K^+, and Na^+ were significantly affected by duration of water saturation and all except Ca^{2+} and K^+ significantly affected by degree of water saturation. Fe^{2+} and Mn^{2+} accumulations and depletions (visible segregations or mottles) occurred within 12 months of water saturation in a separate experiment where cores were packed to a bulk density of 1.6 Mg m^{-3} in a core saturated to $S_{0.9}$. It was therefore evident that this soil with 0.22% organic carbon and a bulk density of 1.6 Mg m^{-3} will produce morphological features due to reduction within a year of water saturation at $S_{0.9}$.

An experiment was set up with cores kept at a constant degree of water saturation ($S_{0.8}$) with varying bulk densities, namely 1.4, 1.6 and 1.8 Mg m^{-3}. All the factors measured (Eh, pH, Fe^{2+}, Mn^{2+}, Mg^{2+} and K^+) except Ca^{2+} and Na^+ were significantly affected by a variation in bulk density. In another part of the experiment two different water temperatures were used to saturated the cores, namely 23°C and 30°C respectively. It was determined that the temperature difference of 7°C caused the cores to react significantly different to each other.. The higher water temperature caused the Eh to decrease more rapidly and therefore a higher Fe^{2+} concentration occurred in these cores.

It was concluded that for this soil at 23°C, Fe^{3+} and to a certain extent Mn^{4+} will start to become reduced at a pe of 6 at $S_{0.78}$. These findings show that the first approximation of Van Huyssteen *et al*. (2005) where $S_{0.7}$ was found to be sufficient for reduction is very similar for this soil.

***Keywords**: B horizon, basic cations, bulk density, iron, manganese, redox, degree of water saturation, duration of water saturation*

OPSOMMING

Menigte studies is uitgevoer om die verwantskap tussen grond morfologiese eienskappe, redoks potensiaal (Eh) en die gemete grondwaterinhoud van 'n profiel te bepaal (Franzmeier *et al*., 1983; Schwertmann & Fanning, 1976; Veneman *et al*., 1976). Hierdie studies was suksesvol maar daar is nog steeds groot kennis gapings in hierdie veld.

Literatuur verwys nie na 'n spesifieke graad van waterversading in die grond waar reduksie intree nie, alhoewel na studies deur Van Huyssteen *et al.* (2005) is daar aanbeveel dat $S_{0.7}$ (70% van water versadiging) voldoende sal wees vir die intree van reduksie. Hierdie waarde sal varieer vir verskillende gronde temperature, verskillende brutodigtheide en variërende organiese koolstof inhoude.

Die doel van hierdie studie was om te bepaal of 'n graad van versading bepaal kan word waar reduksie intree vir hierdie grong in 'n geslote systeem. Dit het ook ten doel gehad om die verwantskap tussen brutodigtheid en reduksie te bepaal. Reduksie was aangedui deur 'n daling in Eh en 'n styging in die oplosbare yster (Fe^{2+}) in die grond. Daar was drie doelwitte vir die studie: om die verwantskap tussen die graad van water versading (s) en die intree van reduksie te bepaal; om die verwantskap tussen die graad van water versadiging (s) en die duur van versadiging te bepaal; en om die effek van brutodigtheid op die bogenoemde te bepaal.

'n Geel-bruin apedale B horison van profiel 234 in die Weatherley opvangsgebied is in hierdie studie gebruik. Hierdie studie het gewys dat grondkerne meer suksesvol as kolomeksperimente was om redoks analises te doen. 'n Kernanalise is uitgevoer om die effek van graad en duur van versading op Eh, pH, Fe^{2+}, Mn^{2+}, Ca^{2+}, Mg^{2+}, K^{+} en Na^{+} te bepaal. Die kerne was met 'n dubbele laag plastiek geseël en tot hulle benodig was teen 'n konstante temperatuur van 23°C (met 'n maksimum variasie van 2°C) gestoor. Analise het drie dae na waterversadiging begin. 'n Stel kerne (vier grade van versading, elk in triplikaat) was elke 3.5 dae vir die eerste drie maande geanaliseer en daarna 'n stel een keer per week vir 'n maand. Die eksperiment was na 121 dae gestaak.

Dieselfde grond en eksperimentele uitleg was gebruik vir die brutodigtheid eksperiment. Die eksperiment het bestaan uit 'n stel van drie kerne, wat individueel tot brutodigthede van 1.4,

1.6 en 1.8 Mg m^{-3} gepak is en is in triplikaat uitgevoer. Al die kerne was tot $S_{0.8}$ versadig. Die brutodigtheid eksperiment was na 23 dae gestaak.

Daar was ‘n goeie korrelasie tussen ‘n verhoging in graad van versading en ‘n daling in pe (R^2 = 0.95), Mn^{2+} (R^2 = 0.91) en Fe^{2+} (R^2 = 0.92) konsentrasie. Eh, pH, Fe^{2+}, Mn^{2+}, Ca^{2+}, Mg^{2+}, K^+ en Na^+ was betekenisvol deur duur van versading geaffekteer en almal behalwe Ca^{2+} en K^+ was betekenisvol deur graad van versading geaffekteer. Fe^{2+} and Mn^{2+} akkumulasies en verwydering het binne 12 maande in ‘n kern teen ‘n water versaging van $S_{0.9}$ verskyn. Daar kan dus met sekerheid gesê word dat hierdie grond, met 22% organiese materiaal en ‘n brutodigtheid van 1.6 Mg m^{-3}, morfologiese eienskappe binne ‘n jaar van water versadiging by $S_{0.9}$ sal vorm.

‘n Experiment was opgestel waar al die kerne teen ‘n konstante graad van waterversadiging ($S_{0.8}$) gehou is met ‘n variasie in brutodigtheid, naamlik 1.4, 1.6, 1.8 Mg m^{-3}. In die brutodigtheid eksperiment was all die gemete faktore (Eh, pH, Fe^{2+}, Mn^{2+}, Mg^{2+} en K^+) behalwe Ca^{2+} en Na^+ betekenisvol deur ‘n variasie in brutodigtheid geaffekteer. Dit was verwag dat Eh sal afneem soos wat die brutodigtheid toeneem, maar dit was nie die geval nie. Die laer brutodigtheid (1.4 Mg m^{-3}) het die laagste Eh en die hoogste Fe^{2+} konsentrasie gehad. Daar was vermoed dat ‘n hoër water temperatuur (7°C), wat gebruik was om die kerne te versadig, die onverwagse resultaat veroorsaak het.

Na die afloop van die studie was tot die gevolgtrekking gekom dat in ‘n grond by 23°C, Fe^{3+} en tot ‘n sekere mate Mn^{4+} by ‘n pe van 6 en ‘n waterversadiging van $S_{0.78}$ sal begin reduseer. Die bevindinge is in lyn met die studie van Van Huyssteen *et al*. (2005) waar $S_{0.7}$ voldoende gevind was vir die intree van reduksie.

***Sleutlewoorde**: B horison, basiese katione, brutodigtheid, duur van versadiging, graad van versadiging, mangaan, redox, yster*

CHAPTER 1

INTRODUCTION

This study explores the relationship between duration and degree of water saturation, with varying degrees of bulk density, and the effect of these factors on the reduction of Mn^{4+} and Fe^{3+}. It also explores the impact of these factors on cations in the soil. The project was based upon previous research done by Van Huyssteen *et al.* (2005): "The relationship between soil water regime and soil profile morphology in the Weatherley catchment, an afforestation area in the Eastern Cape". Their report stressed the need for further research into detailed redox studies, with the emphasis on the role of the frequency and duration of water saturation events, and bulk density.

1.1 Problem statement

The proper use and management of soils requires identification of reliable indicators of permanently wet or fluctuating water saturation, i.e. the soil's water regime (Jacobs *et al*., 2002). Redox status is an important indicator of the water regime in a soil. It can allude to the degree as well as the duration of water saturation in a soil horizon. Therefore the study of redox is vital in soil science (Vepraskas, 2001).

Oxidation and reduction reactions contribute to soil formation through the breakdown of clays and the reducing effect on iron oxides and other cations. The redox potential (Eh) which is a recording of voltage over time (Fiedler *et al.,* 2007), can be used to determine the tendency of a soil to reduce or oxidize certain elements (Fiedler & Sommer, 2004). The voltage results from an exchange of electrons between a redox couple during the process of reduction and oxidation. Therefore the electrons found in a soil solution at a given point in time give a good indication of the redox status of the soil (Fiedler *et al.,* 2007).

The Eh of a soil can be used to estimate the nutrient availability and mobility of heavy metals for agricultural and environmental management purposes (Phillips & Greenway, 1998). It can aid in combating pollution of water supplies and wetlands with toxic metals as well as understanding and combating the production of toxic atmospheric pollutants (Paul & Clark, 2001). A better understanding of pedogenetic processes and phenomena such as colour changes, concretions and mottles can also be achieved (Fiedler *et al.,* 2002).

The oxidation and reduction of iron oxides is initiated by a high degree of soil water saturation. This is due to the lack of sufficient oxygen diffusion through the soil, leading to anaerobic soil conditions. Molecular O_2 is the preferred electron acceptor for soil microbes. Once all the O_2 has been depleted microbes will use the next best electron acceptor which will yield the most energy. After O_2, microbes reduce NO_3^-, Mn^{4+}, Fe^{3+}, SO_4^{2-} and finally CO_2 in that order (Fiedler *et al.,* 2007).

While Fe^{2+} and Mn^{2+} are good indicators of the redox status of a soil, cations have also been known to react in relation to the redox status. Published information on soil nutrients other than Fe^{2+} and Mn^{2+}, such as soluble and exchangeable cations is scarce (Phillips & Greenway, 1998). Increases in Ca^{2+}, Mg^{2+}, K^+ and Na^+ have been attributed to increased solubility of organic carbon and from increased competition of the CEC sites due to elevated Fe^{2+} and Mn^{2+} concentrations (Larson *et al*., 1991; Wolt, 1994; Phillips & Greenway, 1998).

Soil properties that are associated with the profile's water regime are for example low base status, accumulation or removal of colloidal matter (iron oxides, silicate clay and organic matter) which can lead to dystrophic, bleached, luvic as well as mottled horizons. Redox reactions are the main force driving the removal and accumulation of iron oxides (Vepraskas, 2001). One can therefore conclude that there is a close relationship between the water regime of a soil profile and its morphology (Brinkman, 1977; Evans & Franzmeier, 1986).

The degree of water saturation (s) measures the fraction of pores filled with water. It is calculated by dividing the volumetric water content with the soil pore volume (Hillel, 1980). In a saturated profile, all the pores are theoretically filled with water and s = 1.00 or 100%, although due to hysteresis, 100% saturation will never or seldom be reached under field conditions. As the soil becomes less saturated the s value will decrease. There is, however, a level of water saturation at which a sufficient fraction of soil pores are filled with water to inhibit normal oxidative respiration, causing the onset of reduction. This level is probably related to the ratio of micropore to macropore porosity, because it is the macropores (> 0.06 mm in diameter) that are responsible for aeration in the soil. If the soil pore volume diminishes (increased bulk density), the volume of water a soil can hold will also diminish. A compact soil will therefore hold less water to obtain the same degree of water saturation than a soil with a lower density. This can possibly affect the degree of water saturation at which reduction will set in.

According to this hypothesis, bulk density will have a significant effect on the oxidation status at different s values. If there is no limitation to drainage, these pores drain within 48 hours after wetting, therefore, the fewer the macropores, the greater the possibility that anaerobic conditions will occur (Van Huyssteen, 2004). This will only be the case if there is no impervious layer below the macropores to prevent drainage. If there is an impervious layer, water will not be able to leach from the horizon and saturated conditions will prevail. Van Huyssteen *et al*. (2005) postulated that reduction can set in at a 70 % degree of water saturation. This limit was chosen because 100 % water saturation is seldom reached (Hillel, 1980) and because it was thought that at this degree of water saturation all micro pores will be saturated with water, creating the possibility for reduction to set in. Van Huyssteen *et al*. (2005) further postulated that this limit would be specific for a specific soil and proposed further studies in this regard.

The purpose of this study was to determine at what degree of water saturation reduction is initiated in this particular soil in a closed system and if bulk density has a significant influence on the dynamics of this process.

CHAPTER 2

LITERATURE REVIEW

2.1 Introduction

Soil, described as, “the unconsolidated mineral fraction on the surface of the earth, which has been subjected to and shows the effects of environmental factors such as water”, designates a close relationship between the soil water regime, and soil profile morphology (Soil Science Society of America, 1997). The soil water regime controls the soil forming processes resulting in soil properties (Soil Survey Staff, 1999).

Numerous soil properties are associated with the soil water regime, for example base status, distribution of colloidal matter (iron oxides, silicate clay and organic matter), colour, mottles, clay mineralogy, clay content and presence of calcium carbonate ($CaCO_3$) (Buol *et al*., 1989; Tarekegne, 2001; Fiedler *et al.,* 2002). These serve as diagnostic criteria in most soil classification systems, e.g. the USDA (United States Department of Agriculture) soil classification system (Soil Survey Staff, 1999), FAO’s classification system which is known as the WRB (World Reference Base) system (FAO, 1998) and the South African Taxonomic system for soil classification (Soil Classification Working Group, 1991). These soil properties are the result of soil forming processes such as hydrolysis, hydration, eluviation, leaching, ferrolysis and shrink swell properties (Brinkman, 1970; Buol *et al.,* 1989; Le Roux *et al*., 2005).

Three major soil water regimes can be identified; a saturated regime, a regime of leaching and a regime of no leaching (Soil Survey Staff, 1999). Saturated, in which the profile is saturated with water for most of the year; leaching, in which water drains freely and a class of no leaching, where water is withdrawn by evaportanspiration leaving precipitates behind. Soil Classification - A Taxonomic System for South Africa (Soil Classification Working Group, 1991) refers to soil water regimes in the definition of three diagnostic horizons namely the E, G and soft plinthic B horizon. The E horizon is formed as a result of water leaching laterally out of the profile. Eluviation results in “marked *in situ* net removal of colloidal matter (iron oxides, silicate clay and organic matter) as evidenced by a comparison of its properties with those of overlying and underlying horizons" (Soil Classification Working Group, 1991). The G horizon, however, is saturated for long periods and “has not undergone marked net removal of colloidal matter (silicate clay and organic matter) on the

contrary, accumulation of colloidal matter has usually taken place". The soft plinthic B horizon has undergone localization and accumulation of iron (Fe) and manganese (Mn) oxides under conditions of a fluctuating water table (Soil Classification Working Group, 1991). Other horizons such as red and yellow apedal B horizons are well drained horizons where water does not stagnate to allow for the formation of redoximorphic features. Wetter soil water regimes can result in the formation of specific redoximorphic features. Microbes deplete the available oxygen (O_2) and in order to survive, use other elements as terminal electron acceptors, e.g. NO_3^-, Mn^{4+} and Fe^{3+}. When Mn^{4+} and Fe^{3+} are reduced they become soluble, for example Fe^{3+} which is insoluble is reduced to soluble Fe^{2+}. These elements will become insoluble again once the environment becomes oxidative (Vepraskas, 2001).

Redoximorphic features occur as redox concentrations and depletions (Vepraskas, 2001). Redox depletions are zones of low chroma colours (lower than the surrounding matrix) where either or both Fe and Mn oxides as well as clay have been removed through reduction. Redox accumulations are areas with high chroma colours, mottles, and Fe^{3+} and Mn^{4+} concretions. The latter features occur due to the oxidation of reduced (soluble) Fe^{2+} and Mn^{2+} (Soil Survey Staff, 1999).

Many factors aid in reduction as well as maintaining reducing conditions. Firstly the O_2 content within the soil has to be low enough to inhibit aerobic respiration. In this regard the duration and frequency of water saturation plays an important role. After anaerobic conditions have been established, an iron oxide reducing microbial colony has to be present, as well as enough organic matter for the microbes to oxidise as an energy source (Simonson & Boersma, 1972).

Reduction will only take place if the water saturation event is present for an adequate amount of time, thereby initiating anaerobic respiration. The relationship between the duration and frequency of saturation events will determine what morphological features occur within the soil. Short durations of water saturation will not produce as prominent or as many mottles as would longer durations of water saturation (Crown & Hoffman, 1970). Therefore the size and abundance of Fe^{3+} and Mn^{4+} mottles will increase from a well-drained to a poorly drained soil (Simonson & Boersma, 1972). Permanent water saturation with no dry period in-between saturation events will produce a reduced grey matrix with very little to no soil mottling (Vepraskas, 2001).

Soil Fe^{2+} content, temperature and time also play an important role in reduction through their influence on soil microbes. Soil bulk density influences reduction through the pore size distribution and amount of pores available for respiration. A decrease in pores leads to a decrease in O_2 content, thereby increasing the propensity for a soil to reduce once saturated (Herbauts *et al*., 1996; Casey & Ewel, 1998; Czyz, 2004).

It is possible to determine the redox state of the soil by determining the reduced elements present in the soil solution or by leaching them from a soil sample. A more direct method is to measure the redox potential (Eh) of the soil and thereby one can speculate which elements will be in solution, as each element has its unique redox potential at which it will reduce and become soluble (Vepraskas, 2001).

When the major redox sensitive components (O_2, NH_4^+, HS^-, Mn^{4+}, Fe^{3+}), and some trace elements in soil undergo microbial redox transformations they behave very differently with regard to reactivity, mobility and toxicity depending on their redox state (Sigg, 2000). Fe^{3+} reduction in soil is an important indicator of the aeration status of a soil and it can aid in determining trace element mobility under reducing conditions. It is therefore of interest to predict the behavior of those elements on the basis of the redox conditions in a soil system (Sigg, 2000).

Since Fe^{3+} oxides are prevalent in aerated environments, reduction of Fe^{3+} results in a pronounced change in the chemical and physical properties of soil (Ponnamperuma, 1972). Once the Fe^{3+} is reduced to soluble Fe^{2+}, it can either be removed from the soil profile, leaving a grey soil matrix, or it can re-precipitated. Once the soluble Fe^{2+} reaches an oxidative soil environment it oxidises and precipitates as a mottle. Soil mottle colours vary depending on the element reduced. These soil morphological features are of importance when it comes to understanding the water regime of a soil profile. They are the primary indicator of the profile's water regime and can be used to deduce information about the soil profile before any chemical or physical soil analyses are done (Vepraskas, 2001).

2.2 Oxidation and reduction

The term "redox" is derived from the processes of reduction and oxidation. Reduction is the reception and oxidation the donation of an electron. Therefore during redox, electrons are transferred among atoms (Vepraskas & Faulkner, 2001). A complete redox reaction consists of an oxidation as well as a reduction reaction, called half-reactions (Glinski &

Stepniewski, 1985). During oxidation the environment becomes deficient in electrons and during reduction, electron rich (Dowdy & Stelly, 1981).

An important example of oxidation and reduction reactions in soil is when Fe^{3+} is reduced to Fe^{2+}:

$$Fe(OH)_3 + e^- + 3H^+ \rightarrow Fe^{2+} + 3H_2O \quad (2.1)$$

Solid minerals can dissolve and dissolved ions can become volatile when changes in the valence of such atoms occur, as the phase in which the atom occurs in the soil changes (Vepraskas & Faulkner, 2001).

Aerobic respiration can be described through oxidation of carbohydrate glucose to CO_2, as shown in the following reaction (Vepraskas & Faulkner, 2001):

$$C_6H_{12}O_6 + 6O_2 \rightarrow 6CO_2 + 6H_2O \quad (2.2)$$

The half reactions for the equation are:

$$C_6H_{12}O_6 + 6H_2O \rightarrow 6CO_2 + 24e^- + 24H^+ (\text{Oxidation}) \quad (2.3)$$

and

$$6O_6 + 24e^- + 24H^+ \rightarrow 12H_2O (\text{Reduction}) \quad (2.4)$$

The simultaneous processes of oxidation and reduction are more easily understood when the oxidation and reduction half reactions are considered separately. This is appropriate in soil science as each reaction affects the soil differently (Vepraskas & Faulkner, 2001), as discussed in section 2.9

2.3 Thermodynamic principles of redox potential

The driving force of any chemical reaction is a tendency to decrease free energy of the system until, at equilibrium, the sum of the free energies of the products is equal to that of the remaining substrates, as what happens in redox reactions (Glinski & Stepniewski, 1985). Redox reactions can be expressed thermodynamically using the redox potential (Eh). Eh is

a voltage that can be measured and used to predict the types of reduced species that would be expected in the soil solution.

The theory behind the Eh can be explained by considering the following general reducing equation (Vepraskas & Faulkner, 2001):

$$\text{Oxidized molecule} + mH^+ + ne^- \leftrightarrow \text{reduced molecule} \quad (2.5)$$

where:

m = number of moles of protons

n = number of moles of electrons

This reaction can be expressed quantitatively by calculating the Gibbs free energy (ΔG) for the reaction:

$$\Delta G = \Delta G^\circ + RT \ln \frac{(Red)}{(Ox)(H+)^m} \quad (2.6)$$

where:

ΔG° = standard free energy change

R = gas constant

T = absolute temperature

Red and Ox = activities of reduced and oxidised species

This equation can be transformed into a more applicable format by converting the Gibbs free energy into a unit of voltage using the relationship ΔG = -nEF which is then known as the Nernst equation:

$$Eh = E_o + \frac{RT}{nF} \ln \frac{(Ox)}{(Red)} + \frac{m}{n} \frac{RT}{F} \ln(H^+) \quad (2.7)$$

or

$$Eh = E_o + \frac{2.303\,RT}{nF} \log \frac{(Ox)}{(Red)} - \frac{m}{n} \frac{2.303\,RT}{F} pH \quad (2.8)$$

Where:

Eh = electrode potential (redox potential)

E° = potential of the half reaction under standard conditions (unit activities of reactions under 1 atmosphere of pressure and a temperature of 298°K)

F = Faraday constant.

The Nernst equation can be further simplified to:

$$Eh(mV) = E^{\circ} - \frac{59}{n}\log\frac{[Red]}{[Ox]} - \frac{59m}{n}pH \qquad (2.9)$$

The Nernst equation shows that the reduction of an element will create a specific Eh value when at equilibrium. This Eh value will vary according to the pH of the solution or the soil being measured. It will also vary according to the concentration or activity of the oxidised and reduced species in the soil (Vepraskas & Faulkner, 2001).

The theoretical order of reduction requires that the soil's Eh must be in equilibrium and that all redox half reactions adjust to it. The Eh of the soil must remain stable across the horizon for a certain time period and all electron acceptors must react at a similar rate. However, a soil's Eh is never stable for long periods of time if the soil is affected by a fluctuating water table. The Eh will also vary across soils due to the lack of uniformity in the distribution of soil organic matter (Vepraskas & Faulkner, 2001).

The disadvantage of using Eh as an experimental parameter is that for any redox pair the value of Eh depends on the pH. There is an inverse relationship between Eh and pH in the soil. This is due to the fact that H^+ ions are used in the reducing reactions, during the oxidation of organic matter. This causes a decrease in H^+ ion concentration, resulting in an increase in soil pH. Moreover, the effect of pH differs for each reaction (Glinski & Stepniewski, 1985).

Soil acidity is expressed quantitatively by the negative common logarithm of the free-proton activity, the pH value;

$$pH = -\log[H^+] \qquad (2.10)$$

Ponnamperuma (1972) showed that the amount of change in pH due to reduction varies among soils, although it generally causes the soil pH to shift towards seven. Reduction in

acid soils generally increases the pH with the opposite taking place in an alkaline soil. The amount of pH change can be as high as three pH units, following several weeks of water saturation. Changes of less than 2 pH units are more typical. The degree of change depends on the amount of reduction taking place which is in turn determined by the amount of oxidisable organic matter, as well as the amount of reducible electron acceptors. According to Ponnamperuma (1972), pH values remain less than 6.5 in acid soils which contain low amounts of organic matter and reducible Fe oxides or hydroxides (Vepraskas & Faulkner, 2001). Other studies have found that a linear relationship between pH and Eh in soils is questionable (Bohn, 1969; Patrick *et al*., 1996). In prolonged water saturation the pH of soils is governed by the partial pressure of carbon dioxide (Glinski & Stepniewski, 1985).

Due to the fact that Eh is pH dependant, a measure of oxidation intensity comprising of both Eh and pH was developed, rH. It was defined as the negative logarithm of a hypothetical hydrogen pressure (in bars) corresponding to given Eh and pH conditions (Clark, 1923):

$$\mathrm{rH} = \frac{2\mathrm{Eh}}{0.059} \times 2\mathrm{pH} \tag{2.11}$$

It was later realized that in the case where oxidised or reduced forms are basic or acidic, the system does not resemble a simple hydrogen electrode. Therefore respective dissociation constants should be included in the formula (Hesse, 1971). Due to this the rH concept was discarded by its developer (Clark, 1923), although Glinski & Stepniewski (1985) have reported that it is still being misused by some researchers, for example by the IUSS Working Group (2006).

The use of pe in describing the redox state in the soil is a more widely accepted term. Similar to soil pH, soil oxidisability can be expressed by the negative common logarithm of the free-electron activity, the pe value (Ponnamperuma, 1972; Glinski & Stepniewski, 1985; Vepraskas & Faulkner, 2001):

$$\mathrm{pe} = -\log\left[\mathrm{e}^{-}\right] \tag{2.12}$$

If the electrons in Equation 2.13 are treated as normal reactants, the equilibrium constant K can be expressed as follows:

$$\mathrm{K} = \frac{[\mathrm{Red}]}{[\mathrm{Ox}][\mathrm{e}]^{n}[\mathrm{H}^{+}]^{m}} \tag{2.13}$$

The pe value is then:

$$pe = \frac{1}{n}\log K + \frac{1}{n}\log\frac{Ox}{Red} - \frac{m}{n}pH \qquad (2.14)$$

Denoting 1/n log K as pe_o, being the negative logarithm of electron activity when [Ox] = [Red] and pH = 0 gives:

$$pe = pe_o + \frac{1}{n}\log\frac{[Ox]}{[Red]} - \frac{m}{n}pH \qquad (2.15)$$

Comparison of Equations 2.15 and 2.9 shows that:

$$pe = \frac{Eh \cdot F}{2.303\,RT} \qquad (2.16)$$

and

$$pe_o = \frac{E_o \cdot F}{2.303\,RT} \qquad (2.17)$$

Therefore, because the factor 2.303 RT/F is 0.0591 V at 25°C:

$$pe = \frac{Eh(V)}{0.059} \qquad (2.18)$$

or

$$pe = \frac{Eh(mV)}{59} \qquad (2.19)$$

Thus, descriptions of a redox system in terms of redox potential and pe are equivalent to each other (Glinski & Stepniewski, 1985).

Large values of pe favour the existence of electron-poor (oxidised) species just as large values of pH favour the existence of proton-poor species (bases). Similarly small values of pe favour electron-rich or reduced species, just as small values of pH favour proton-rich

species, acids (Glinski & Stepniewski, 1985). Unlike pH, however, pe can take on negative values (Sposito, 1989).

Eh ranges from 800 to -400 mV in soil, the related pe range being from 14 to -7. The upper Eh or pe values correspond to the equilibrium of the soil water with atmospheric O_2, while the lower values correspond to the equilibrium of the soil water with gaseous hydrogen at atmospheric pressure (Glinski & Stepniewski, 1985).

The term (pe + pH) can be used as a convenient single-term expression to define the redox status of aqueous systems (Vepraskas & Faulkner, 2001). The sum of pe + pH can be plotted on one axis of a two-dimensional graph, while the activities of the reduced and oxidised species are plotted on the second axis. This addition can be done with ease due to the fact that the numerical ranges of pe and pH are smaller and each has an approximate weight in the sum (Bohn *et al.,* 1985).

2.4 Redox reactions in soil

Reduction in soil is a microbial process and does not occur when the soil has undergone sterilization. For this discussion, bacteria will be considered the major group of organisms initiating the redox processes in soil (Glinski & Stepniewski, 1985). Oxidation in soil occurs whenever respiring heterotrophic microbes consume organic matter, which is the major source of electrons in soil (Chen *et al.,* 2003). This results in the decomposition of organic matter and the production of CO_2 in aerobic environments and when oxidised the electrons released are used in reducing reactions. When organic matter is not present, or when bacteria are not respiring, redox reactions of the type discussed in this study will not occur in soil. Reduction of O_2 can occur in a saturated soil, but only while O_2 is still dissolved in the soil solution (Vepraskas & Faulkner, 2001).

Soil pores are filled with air, which consists of the same elements as the atmosphere, N_2, O_2, CO_2, as well as trace gases (Richardson *et al.,* 2001). Oxygen is the strongest electron acceptor and therefore yields the most energy from oxidation; therefore microbes prefer to consume O_2 first (Bohn *et al.,* 1985). The proportions of these gases change in response to soil microbe respiration (Richardson *et al.,* 2001).

A high O_2 demand is caused by the presence of readily decomposable organic compounds and by growth conditions that favour microbial activity (Bohn *et al.,* 1985). This does not cause a problem in well aerated soils as the O_2 is replenished by diffusion and the CO_2 is

rapidly expelled. In water saturated soil, O_2 diffusion is not efficient and is therefore insufficient to maintain aerobic respiration (Richardson *et al.,* 2001). This microbial O_2 demand can exhaust the dissolved O_2 in a waterlogged soil within 24 hours (McBride, 1994).

Several conditions must be met for reducing reactions to occur (Vepraskas & Faulkner, 2001). The soil must be saturated with water to a degree that excludes the free movement of air supplying O_2. In the field water saturation (s) is generally limited to less than $S_{0.9}$ (Hillel, 1980). Reducing conditions are anticipated to start at levels of water saturation as low as $S_{0.7}$ (Van Huyssteen *et al.,* 2005). With slow O_2 diffusion, anaerobic respiration occurs and soil microbes will start to utilize other electron acceptors. The theoretical path of electron acceptors reduced after O_2 is: NO_3^-, MnO_2, Fe_2O_3, SO_4^{2-}, and CO_2 (Turner & Patrick, 1968; Ponnamperuma 1972; Vepraskas & Faulkner, 2001). These elements are reduced in order of decreasing redox potential and therefore energy released. The order ensures the most energy possible is released by each reaction. The water should also be stagnant or moving very slowly through the soil profile to prevent an influx of oxygenated water. Oxidisable organic matter must be present to fuel a respiring microbial population (Vepraskas & Faulkner, 2001). Although these are the critical conditions that need to be met, there are many other factors that influence the rate of redox reactions, for example temperature, bulk density and soil Fe content. These factors will be discussed in more detail in the following sections.

Oxidation and reduction are important processes in soil as they influence soil morphology as well as the availability of elements within the soil, such as nitrogen (N), sulphur (S), Mn, Fe and cations (Dowdy & Stelly, 1981). Redox reactions are the main force driving the removal and accumulation of Fe oxides. The redox status of Fe serves as a convenient boundary for separating oxidised from reducing conditions in soils. The activity of Fe^{2+} will increase within the soil solution with a decrease in redox potential (Eh) and pH (Schwertmann, 1985). Under reducing conditions Fe^{2+} and Mn^{2+} can be depleted locally from an individual ped or regionally to the extent that it is depleted from the whole landscape (Figure 2.2). Accumulation occurs where and when oxidizing conditions occur. It is during anaerobic respiration that major chemical processes occur in soils such as denitrification, production of mottled soil colours due to the spatial and temporal variation in redox conditions (Stolt *et al.,* 1998), and production of hydrogen sulphide and methane gases (McBride, 1994; Vepraskas & Faulkner, 2001).

2.5 Redox potential ranges

In a water saturated soil, the movement of O_2 from the atmosphere into the soil stops or slows down dramatically. Bacteria that are still respiring by oxidizing organic compounds can then reduce dissolved O_2 in the water. Once all the dissolved O_2 has been depleted, the redox potential starts to fall and bacteria then start using other electron acceptors to respire. The Eh continues to fall (Figure 2.1) as long as water saturation is maintained and bacteria continue to respire (Vepraskas, 2001)

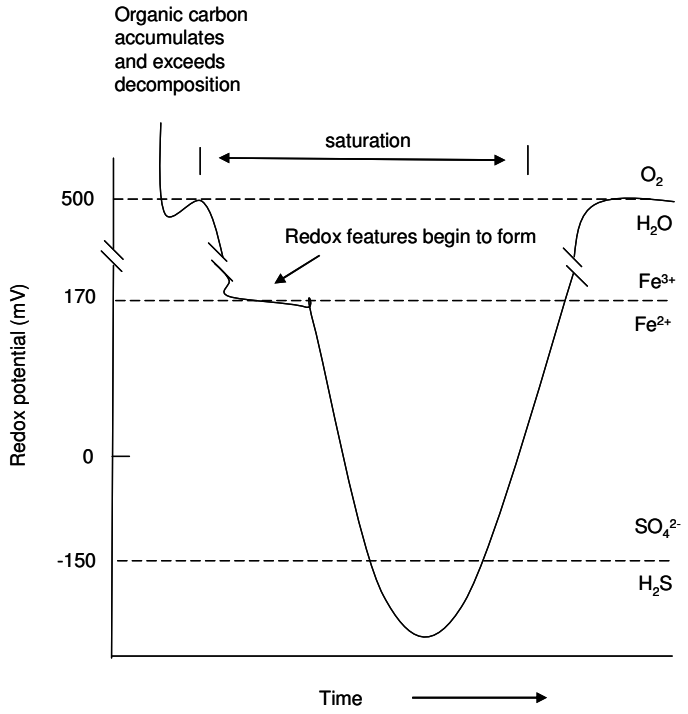

Figure 2.1 Theoretical changes in Eh under saturated conditions (adapted from Vepraskas, 2001).

An air dry soil that is submerged into water can cause the Eh to drop rapidly. Values of 500 mV have been reported to fall to -400 mV within the first day. The rate of decrease and the minimum value of Eh depends on the intensity of reduction being related mainly to temperature, organic matter and the amount of bio-reducible oxidised inorganic compounds which act as electron acceptors (Glinski & Stepniewski, 1985).

Following the Nernst-equation, several empirical ranges of Eh can be derived where different redox systems are active and could support bacterial metabolism (Schüring *et al.,* 2000). Reducing reactions proceed in a theoretical order, from a higher Eh to a lower Eh

(Table 2.1). This order is related to the elements that will release the highest amount of energy when reduced (Bohn *et al.,* 1985).

When the soil is unsaturated and oxidised, the Eh is relatively high (>500 mV at soil pH7). Morphological features related to reduction do not occur at such high Eh values (Vepraskas, 2001). In a water saturated soil, under anaerobic conditions, there is a rapid exhaustion of O_2 and nitrate which leads to biological reduction of Mn oxides. This process depends on soil pH (Lovley, 2001), and the intensity of Mn reduction depends on the organic matter content and temperature. Oxidation and reduction of Mn^{4+} are thermodynamically favored at relatively higher redox potentials than Fe^{3+}, which is the next element to be reduced (Glinski & Stepniewski, 1985).

Table 2.1 Reducing reactions and their accompanying redox potentials in soil (Bohn *et al.,* 1985)

Half reaction	Redox potential measured in soil (mV)
$O_2 + 4\ e^- + 4\ H^+ \rightarrow 2\ H_2O$	600 to 400
$NO_3^- + 2\ e^- + 2\ H^+ \rightarrow NO_2^- + H_2O$	500 to 200
$MnO_2 + 2\ e^- + 4\ H^+ \rightarrow Mn^{2+} + 2\ H_2O$	400 to 200
$FeOOH + e^- + 3\ H^+ \rightarrow Fe^{2+} + 2\ H_2O$	300 to 100
$SO_4^{2-} + 6\ e^- + 9\ H^+ \rightarrow H_2S + 4\ H_2O$	0 to -150
$2\ H^+ + 2\ e^- \rightarrow H_2$	-150 to -220
$2\ CH_2O \rightarrow CO_2 + CH_4$	-150 to -20

When the Eh reaches approximately 170mV (pH 7), the Fe^{3+} will reduce to Fe^{2+} and become soluble in the soil solution (Bohn *et al*., 1985; Lovley, 2001). The soluble Fe^{2+} may diffuse through the soil and when it reaches oxidised conditions it will re-oxidize. It may also move with the soil water and be taken out of the horizon. In most cases, as long as the Eh stays below 170 mV, the Fe^{2+} will remain reduced. The leaching of Fe^{2+} from a soil horizon leads to greyer soil colours. The grey colour occurs because Fe^{2+} is colourless and the colour of the soil is determined by the colour of the sand, silt, and clay particles (Bohn *et al*., 1985).

McDaniel and Buol (1991) were able to demonstrate a spatial relationship between Mn^{2+} and Fe^{2+} precipitation in horizontal sand columns in response to increased redox potential. Fe^{2+} precipitated at low redox potentials while most Mn^{2+} did not precipitate until leaching the more oxidised portions of the columns. In well-drained soil profiles, secondary Mn^{4+} is

found deeper than Fe^{3+} because Mn^{2+} remains in a reduced, soluble form longer than Fe^{2+}, with increasing redox potential. Reduced Mn^{2+} is therefore typically re-oxidised in subsoil where higher pe and pH conditions prevail (Bartlett, 1986).

Once all the Fe^{3+} has been reduced, the Eh will continue to decrease. When the Eh reaches values below -150mV, SO_4^{2-} anions may be reduced to H_2S gas. This usually requires a relatively long period of water saturation and anaerobic respiration. The H_2S gas is produced only while the Eh is below -150mV (Vepraskas, 2001).

2.6 Spatial and temporal variability of reduced soils

Physical properties of a soil greatly affect microbial respiration. This limits the O_2 diffusion to the bulk of the soil. Therefore soil structure as well as water regime aid in the varying heterogeneity of soils. As a result of this heterogeneity, anaerobic microsites with an oxidative soil matrix occur. Therefore redox conditions in soils vary widely over short distances (Glinski & Stepniewski, 1985).

Redox conditions in saturated and flooded soils are more homogenous than in drier soils (Bohn *et al.,* 1985). Soils which crack due to the action of growing plant roots are likely to be more affected by heterogeneity than apedal soils with weaker structure. The O_2 supply may be adequate for aerobic plant and microbial activity along the walls of large pores or peds while the bulk of the soil may be O_2 deficient. This process leads to a soil with reduced inner peds exhibiting grey colours, and oxidised ped surfaces of the same colour as the original oxidised soil matrix. In an opposite scenario, water enters via macropores or cracks and saturates the outer edges of the ped. The Fe^{2+} on the ped surface will reduce and either move into the ped or will move out of the horizon. This will cause a depletion of Fe oxides on the ped surface (Figure 2.2; Figure 2.3), i.e., a grey colour, while the ped core will stay the same colour as the original oxidised soil matrix (Vepraskas & Faulkner, 2001).

Redox potential measurements made at a single point in the soil may change over the course of a year by 1000 mV or more. This occurs especially in soils that are periodically saturated or flooded where reducing conditions prevail. Less variation is anticipated in permanently saturated soils as well as dry soils that are never saturated for periods long enough to initiate reduction. The variation in redox potential across a saturated soil horizon, can be over 600 mV during the first few days of measuring. Within two months of water saturation the range in redox potentials can still vary by approximately 100 mV even though the mean potential can be near 0 mV, as reported by Vepraskas and Faulkner, (2001). This

variability is caused by the oxidation of organic matter and the corresponding reducing reactions occurring in microsites, hotspots or micro-habitats. These microsites are areas of soil that surround organic matter and therefore have a higher population of respiring bacteria (Parkin, 1987; Crozier *et al.,* 1995; Vepraskas & Faulkner, 2001).

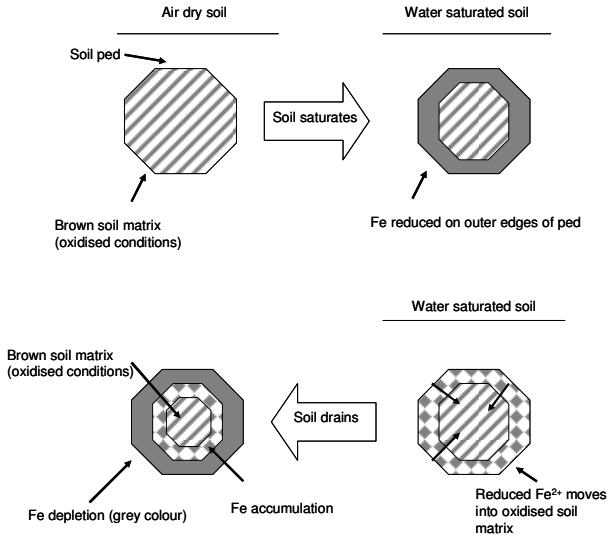

Figure 2.2 Fe^{2+} depletions on the outer edges of a ped under saturated conditions (adapted from Vepraskas, 2001).

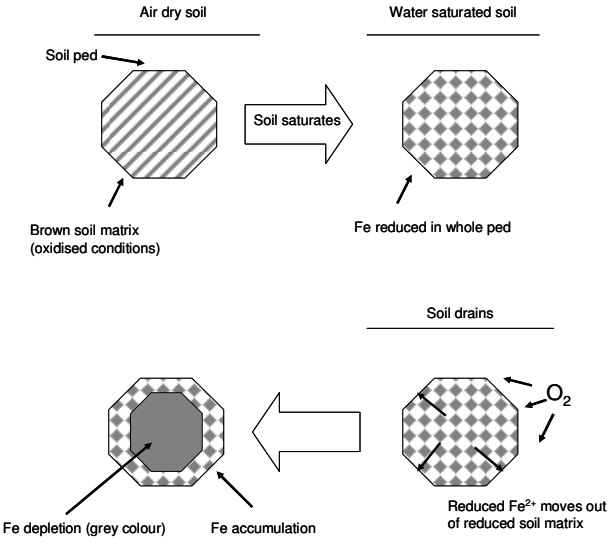

Figure 2.3 Fe^{2+} depletions in the center of a ped under saturated conditions (adapted from Vepraskas, 2001).

Once anaerobic conditions have been reached, the ranges in Eh are wider due to the effect of microsites, but over time the range in Eh narrows as the dissolved O_2 in the soil solution is depleted and a greater soil volume becomes reduced (Vepraskas & Faulkner, 2001). Eh may fluctuate between 0 to 800 mV within horizontal distances of 10 mm. Due to temperature and pH dependent error the deviation can be from around 100 mV up to 300 mV between sampling points at the same depth (McKeague, 1965). Measurements at the same depth are therefore unsuitable to obtain a meaningful mean value. However, they are suitable to reflect the specific ranges of Eh values within a horizon. Eh measurements must be considered as local measurements, only representative for the surrounding soil matrix at a scale approximately of 1 mm^3 (Fiedler & Sommer, 2000).

Vepraskas & Faulkner (2001) suggest that at least five redox potential measurements need to be taken at each depth to account for the variability expected in the redox potentials. The most effective way to overcome the problem of spatial heterogeneity of a soil is therefore through replication of measurements.

2.7 Measuring reduction in soils

Measuring reduction in soils can be done by chemical analyses, dyes and redox potential measurements. These measurements can be done in a soil solution or by measuring the soil directly. The type of redox measurement used will depend on the accuracy needed for the measurement as well as where the measurement will take place, i.e. in the field or in the laboratory (Vepraskas & Faulkner, 2001).

2.7.1 Chemical analyses

There are a variety of methods that can be used to extract oxidised Fe^{3+} from the soil. Dithionite-citrate-bicarbonate (CBD) extracts all secondary Fe^{3+} oxides that are not part of the clay lattice. Acid ammonium oxalate extracts the poorly crystalline and organic complexed Fe oxides, while pyrophosphate extracts organic complexed Fe oxides (Mehra & Jackson, 1960; McKeadue *et al.,* 1971). Just as it is possible to measure the concentration of oxidised Fe^{3+} species in solution, it is possible to measure the concentrations of reduced species in a solution (Schwertmann, 1985; FAO, 1998).

Atomic absorption spectroscopy can be used to determine the soluble Fe^{2+} concentration in a soil solution. Once Fe^{2+} is detected in solution one can only predict that the soil is anaerobic and be sure that denitrification of NO_3^- and reduction of Mn already occurred. A disadvantage of this procedure is micro site reduction, which can occur when a small part of

the soil is more reduced than the surrounding soil matrix due to the occurrence of localized organic matter particles (Vepraskas & Faulkner, 2001). A higher Fe^{2+} concentration can therefore be found less than 10 mm away from a patch of soil with a low to non existent amount of Fe^{2+} (Jahn *et al*., 2003; Fiedler *et al.,* 2007). To overcome this a representative soil sample must be taken. It is important to remember that one can also only predict that the soil was anaerobic if Fe^{2+} was found in the soil solution, therefore Fe^{2+} concentration on its own is not sufficient when studying reduction (Vepraskas, 2001).

2.7.2 Dyes

The use of soil dyes is a practical way to determine if reduction in soil has taken place up to that point. Dyes are used that react with reduced forms of key elements and can be measured against colour cards. The most widely used dyes, both of which detect soluble Fe^{2+} when sprayed onto a soil sample are ά, ά - dipyridyl (Childs, 1981; Soil Survey Staff, 1999) and 1, 10-phenanthroline (Richardson & Hole, 1979).

The disadvantage of dyes is that if there is no reaction, all one can assume is that there is no Fe^{2+} present in the soil. Therefore one does not know if the soluble Fe^{2+} has already been washed out of the horizon and it does therefore not give a definite answer to whether the soil is anaerobic or not (Vepraskas & Faulkner, 2001).

2.7.3 Redox potential measurements

Using redox potential (Eh), one can predict the types of reduced species that could be expected in the soil solution (Sigg, 2000). The Eh measurements are evaluated along with soil pH data and can then be interpreted in the form of an Eh/pH phase diagram (Vepraskas & Faulkner, 2001).

Electron transfers between solution and an inert electrode result in an electrode potential difference, which is measurable as a voltage. Any electron conducting material can be used as an electron selective electrode. The electrode should equilibrate with the electric potential of the sample, but it should not change itself, it should not react with parts of the solution nor should it have any catalytic effect on the equilibrium in the solution. Nobel metals are the most widely used, as these metals are only inert when their standard potential is more than 100 mV higher than the redox potential of the sample. Platinum is preferred to gold for measuring redox potential (Galster, 2000). A reference electrode is used in conjunction with a Pt electrode to create a standard set of conditions (Galster, 2000; Vepraskas & Faulkner, 2001). In dilute solutions, measurements with Ag/AgCl reference

electrodes and a 1 mol ℓ^{-1} potassium chloride electrolyte have proved to be successful (Galster, 2000). Calomel electrodes can also be used in conjunction with a Pt electrode (Mansfeld, 2003)

Reduced soils transfer electrons to the Pt electrode, while oxidised soils tend to take electrons from the electrode. The potential or voltage developed between the soil solution and the reference electrode is measured with a volt meter, designed to detect small voltages. Voltages developed in soil range from approximately +1 to -1 V, and are usually expressed in mV (Vepraskas & Faulkner, 2001).

A solution can be extracted from the soil and the Eh can be measured immediately or a modified electrode can be inserted into the soil with a reference electrode and the Eh of the soil can thus be measured directly. Pt electrodes can be left in the soil for long periods, up to 5 years having been recorded (Austin & Huddleston, 1999; Reuter & Bell, 2001). Leaving a Pt electrode in the soil for long periods can cause problems in the measured redox potential, however, two main problems usually arise, contamination, where the surface of the Pt gets coated with substances that affect the measured potential, and the second is electrode breakdown, where the casing is damaged or resin leakage takes place (Mansfeldt, 2003).

For direct measurements of redox potential a hole must first be driven into the soil to a depth 10 - 20 mm less than the desired measurement depth. Before any measurements are taken, contamination and precipitation on the surface of electrodes must be removed, which will aid in an accelerated response time. Without exception, the Pt-oxides that form on the surface of the electrode must be removed. Hydrochloric acid is an appropriate cleaning agent (Jahn *et al*., 2003). It is necessary to clean the Pt-surface extensively from all oxides prior to each measurement. It is safest to abrade and polish the electrode mechanically. A fine polish is better, as a rough open surface would intensify the catalytic activity (Galster, 2000). Sandpaper can be used for this purpose (Jahn *et al*., 2003). A pretreatment of chinhydrone in a buffer solution with pH = 4.01 is also useful (Galster, 2000). Once the Pt surface is cleaned it should then be pushed 10 mm deeper than the prepared hole. A measurement can be taken after at least 30 minutes against a reference electrode (Jahn *et al*., 2003). Due to the fact that Eh in soil is such a variable parameter, duplicate, but preferably triple measurements must be taken (Patrick *et al*., 1996)

2.8 Factors affecting redox reactions

Exclusion of O_2 occurring under saturated conditions is probably the major factor that determines when reduction can occur in the soil, whereas the presence of oxidisable organic matter is likely the most important factor determining whether or not reduction occurs in a saturated soil (Vepraskas & Faulkner, 2001). Apart from the exclusion of O_2 and the presence of oxidisable organic matter there are also other factors that influence redox reactions and the activity of soil microbes. The effect of soil aeration and organic matter content on redox as well as other factors will be discussed below.

2.8.1 Soil oxygenation

Aeration is of extreme importance. It influences soil physical quality, soil fertility, soil microbial populations and ultimately determines which fauna and flora can survive within it (Czyz, 2004). Gas exchange within the soil takes place mainly through diffusion. This is an important mechanism for supplying O_2 to plant roots as the rate of influx of O_2 is more important that the O_2 content within the soil (Glinski & Stepniewski, 1985).

An ideal soil consists of 50% solids, 25% water and 25% air. Soil air fills that part of the soil pore volume that is not occupied by water. The basic composition of soil air is nitrogen (78%), O_2 (21%), carbon dioxide (0.36%) and vaporized water, of which the percentage will depend on the temperature of the soil, normally close to 100%. Water vapor causes the dilution of the other gaseous components of atmospheric air. These components are unevenly distributed between the liquid and gas phases of the soil. In certain cases, when soil oxygenation is insufficient, other gasses, such as CH_4, H_2S, N_2O, C_2H_4, and H_2 occur in the soil. These gasses are an important indicator of the aeration status of the soil despite their presence in low concentrations (Glinski & Stepniewski, 1985).

The air content within soil (E_g) is often referred to as the air-filled porosity of the soil and is therefore equal to the difference between the total porosity of the soil (f) and its current volumetric water content (θ_v) (Glinski & Stepniewski, 1985):

$$E_g = f - \theta_v \tag{2.20}$$

The total porosity (f) is calculated as:

$$f = 1 - \frac{\rho_b}{\rho_s} \tag{2.21}$$

Where: ρ_b = bulk density (Mg m^{-3})

ρ_s = particle density (Mg m^{-3})

Volumetric water content (θ_v) can be calculated as:

$$\theta_v = \theta_w \times \rho_b \quad (2.22)$$

Where: θ_w = gravimetric water content (water content by weight)

ρ_b = bulk density (Mg m^{-3})

The basic physical parameter determining the air content is the soils air filled porosity, which is decisive for the rate of gas exchange. A decrease in air filled porosity leads to a decrease in the soil O_2 concentration. This occurs due to the decrease in space for O_2 storage and O_2 diffusion. At a certain critical value of air filled porosity, O_2 concentration drops to zero, due to the lack of O_2 diffusing in from the surface. This critical value of the air-filled porosity varies in different soils (Glinski & Stepniewski, 1985).

Soil O_2 is contained primarily in the gaseous phase of the soil and usually decreases with depth. In poorly drained soils the O_2 concentration may even fall to zero. Maximum concentrations of carbon dioxide in the soil air occur during periods of increased degree of water saturation and soil temperature. Carbon dioxide content in the soil air is affected by the inverse of the factors that affect the O_2 content (Glinski & Stepniewski, 1985).

The exchange of gasses, particularly O_2 and carbon dioxide between the soil and the atmosphere takes place under the influence of pressure gradients (mass flow) and concentration gradients (diffusion flow). Both kinds of flow may take place in the soil pores and also in the tissue of plants. The relative contribution of the two fundamental mechanisms of gas exchange, mass and diffusion flow, may vary within broad limits due to the fact that soil structure and degree of water saturation greatly affect the soil air concentration (Glinski & Stepniewski, 1985).

Diffusion flow through a concentration gradient in soil takes place through water films as well as through air-filled pores. For both these pathways, the diffusion process can be described by Ficks law (Hillel, 1998)

$$J_g = -D\, dc / dz \qquad (2.23)$$

where

J_g = diffusive flux of gas

D = diffusion coefficient

c = mass of diffusion substance per volume

z = distance

dc / dz = concentration gradient

If partial pressure (ρ) is used instead of the concentration of the diffusing components;

$$J_g = -(D/\beta)(dp/dz) \qquad (2.24)$$

Where:

β = ratio of the partial pressure to concentration

D = diffusion coefficient

The gaseous diffusivity coefficient (D) in bulk air varies with the molecular weight of the diffusing gas. It also depends on the temperature and pressure of the gaseous medium within which diffusion takes place. In porous bodies, the diffusion constant generally depends on the fractional volume of the continuous gas phase, that is, on the pore volume available for diffusion. Since the mean free path of the diffusing molecules is generally much smaller than the width of the pores, gaseous diffusivity is little affected by the shape of the solid surfaces or by the distribution of pore sizes, although it is affected by pore tortuosity. In this respect, gaseous diffusivity differs fundamentally from the transmission coefficients for mass flow such as conductivity, permeability, and hydraulic diffusivity (Hillel, 1998).

Considering the diffusive path in the air phase of the soil, the diffusion coefficient in soil (D_s) must be smaller than that in bulk air (D_o), because of the limited fraction of the total volume occupied by continuous air-filled pores, and also because of the tortuous nature of these pores. Therefore we can expect (D_s) to be some function of the air-filled porosity (f_a) (Hillel, 1998).

As a soil's degree of water saturation drops, there is a threshold value where discontinuity occurs within the soil pores and the O_2 content drops. The value for this threshold will differ

for different soils and it will even differ for the same soil at different levels of compaction. With a high degree of compaction, there will be less pores especially macropores. Hence discontinuity will occur at a lower degree of water saturation in low bulk density soils. Application of manure, green fertilizers and slurry can also decrease the soil O_2 concentration. Increasing O_2 concentration can take place by loosening the soil (Glinski & Stepniewski, 1985), which will create a higher porosity and a higher probability for contiguous air filled pores.

Soil air, particularly O_2 as its most important component, significantly affects biological and chemical transformations that occur in soil. Under anaerobic conditions, changes in the microbial population are induced which bring about changes in the respiration in the soil, its enzyme activity, and redox potential. O_2 deficiency in soil leads to a variation in soil reaction and chemical transformations of many soil components, organic and inorganic, leading to characteristic morphological features in the soil profile (Glinski & Stepniewski, 1985). These changes are discussed in section 2.9.

2.8.2 Microorganisms

Soil respiratory activity is a result of the activity of the microbial population in the soil, it depends largely on the composition, size, and metabolic activity of the population. The microbe activity is in turn influenced by factors such as O_2 availability, organic matter availability and decomposability and mineral nutrients. Parameters such as temperature, carbon dioxide content, soil bulk density, pH, the presence of heavy metals or pesticides as well as soil water content play a large role (Glinski & Stepniewski, 1985).

Microbes are divided into three groups with respect to their water requirements; hygrophiles, mesophiles, and xerophiles (Table 2.2).

Table 2.2 Soil water requirements for 3 groups of microbes (Glinski & Stepniewski, 1985)

Group	Disappearance of activity (kPa)	Microorganism (group/*spp*)
Hygrophiles	7 000	Majority bacteria, yeasts, certain fungi
Mesophiles	7 000 – 30 000	Majority fungi, certain bacteria
Zerophiles	30 000 – 48 000	*Phycomycetes*

A reduction in the respiration rate at low water contents is caused by a low availability of soil water, i.e., a low degree of water saturation. Therefore the relationship between soil microbial activity and soil water content is curvilinear. Soil respiration comes to a standstill at a soil water potential above 10 000 kPa, after the permanent wilting point for plants has been reached. In the range of high water contents, a decrease in the observed respiration rate is caused by limitation of O_2 accessibility in the soil due to water filled pores. There is thus an indirect effect of water on soil microbes due to the physical blocking of O_2 transport in soil (Glinski & Stepniewski, 1985).

The soil contains many different varieties of microorganisms, of which each have their own function (Lovley, 2001). Microbes are divided into three groups according to their O_2 needs: aerobic, which need O_2, facultative anaerobic which can use both O_2 and other elements as terminal electron acceptors and obligate anaerobic which can only use elements other than O_2 as an electron acceptor. Only a few of these microbes have the ability to reduce Fe^{3+} oxides. These Fe reducing bacteria need to be present in active colonies for Fe^{3+} reduction to take place (Glinski & Stepniewski, 1985). Anaerobic conditions in the soil force microbes to use other elements as electron acceptors. Through this process, insoluble Fe^{3+}, which is the most common form of Fe in the soil, is reduced to soluble Fe^{2+} (Lovley, 2001)

One of the most striking characteristics of the Fe reducing bacteria is their ability to utilize a large range of alternative terminal electron acceptors. This aspect, coupled with the environmental abundance of Fe^{3+}, accounts for the bacteria's widespread distribution. Fe reducing bacteria have been found in almost every place on earth (Lovley, 2001). Freshwater, saline and aquifer sediments harbor Fe reducing bacteria. Examples of Fe reducing bacteria are *Geobacter spp* and *Shewanella spp.* which are found in saline environments. Strains of *Shewanella spp.* have been detected in a wide range of habitats, including oil field fluids, fresh and estuarine sediments, deep sea sediments, as well as in Antarctic sea ice. Other strains of Fe reducing bacteria such as *G. sulferrducens* and *Feovibrio ferrireducens* have been found in hydrocarbon contaminated environments (Paul & Clark, 2001)

Thiobacillus ferrooxidans, *Leptospirillum ferrooxidans*, *Sulfolobus spp.*, *Acidianus spp.*, and *Gallionella spp* are all Fe-oxidizing bacterium species (Paul & Clark, 2001). The enzymatic oxidation of Fe^{2+} takes place as follows:

$$2Fe^{2+} + 2H^{+} + \tfrac{1}{2}\, O_2 \rightarrow 2Fe^{3+} + H_2O \qquad (2.25)$$

Organic matter promotes anaerobic respiration due to the increased biological O_2 demand during the breakdown of organic matter. Laboratory studies, using the bacterial strain *S. putrefaciens* were done to determine the effect of organic matter fractions on the microbial reduction of Fe^{3+}. The reduction of Fe^{3+} was greatly enhanced, although the reaction rate appeared to vary significantly depending on different organic matter fractions (Chen *et al.,* 2003). In Schwertmann (1991) it was noted that in experiments done with *Clostridium butyricum* and *Bacillus plymyxa*, ferrihydrite was more readily reduced than goethite and hematite. Microbes therefore greatly enhance the reduction of Fe^{3+}, for all organic matter fractions compared with abiotic reactions (Chen *et al.,* 2003).

2.8.3 Soil organic matter

Soil organic matter (SOM) refers to the sum total of all organic carbon containing substances in soil compounds with varying molecular sizes and structural functional properties (Table 2.3) (Schulten, 1993). The content of organic matter varies widely from less than 1% in sandy soils up to almost 100% in peat soils (Glinski & Stepniewski, 1985).

Table 2.3 Different components of soil organic matter (Glinski & Stepniewski, 1985)

Component	Dry weight (%)
Cellulose	15-20
Hemicelluloses	10-30
Lignin	5-30
Simple saccharides, amino acids, alphatic acids	5-30

Anaerobic microbes can reduce organic matter as an electron acceptor and then donate electrons to reduce Fe^{3+} containing minerals to soluble Fe^{2+}. Iron-reducing microbes such as *G. metallireducens*, *S. putrefaciens*, and a variety of fermenting bacteria have been shown to use humic substances as terminal electron acceptors (Chen *et al.,* 2003).

A study done by Dobos *et al.* (1990), determined that the addition of organic matter to soil columns caused mottles to occur within 35 weeks. Organic matter contents of 3.2 g kg^{-1} up to 15.4 g kg^{-1} (15%) were used, with the latter creating the highest mottle contrast, although the treatment with 3.2 g kg^{-1} (0.3%) organic carbon did cause mottle formation. The quality of organic matter content also plays a major role in mottle formation. The quality of soil organic matter quality is determined by the nonstructural carbohydrate content, a higher nonstructural carbohydrate content leading to a higher organic matter quality. A treatment

that lasted for 7 weeks had a higher mottle Munsell hue with a higher quality organic matter content than a treatment that lasted 21 weeks with a lower quality organic matter content. The matrix Munsell hue of a soil is less affected by organic carbon quality. Typically, each increment of added organic carbon produces a response in the matrix hues and percentage of occurrence (Dobos *et al.,* 1990).

2.8.4 Duration, frequency and total duration of water saturation

The degree of water saturation (s) is indicative of the volume of water in a soil relative to its total pore volume. It ranges from zero in a dry soil to one, when all the soil pores are filled with water. Complete water saturation is seldom reached under normal field conditions because some air is almost always trapped by the water (Hillel, 1980). The degree of water saturation is calculated as:

$$s = \frac{V_w}{V_f} \tag{2.26}$$

Where: s = degree of water saturation (as a fraction)
V_w = water content (mm^3)
Vf = total pore volume (mm^3)

In a soil with a small pore volume, a smaller about of water will be needed to saturate the soil than a soil with a larger pore volume.

Van Huyssteen *et al.* (2005) approximated that the critical saturation parameter of $S_{0.7}$ would be sufficient for reduction in a soil . This fraction was chosen as a first approximation, based on the following observations. Experience has shown that the drained upper limit (DUL) of a soil is generally around $S_{0.6}$ (M. Hensley, personal communication[1]). Since it is reasonable to expect that significant reduction will only occur above DUL, the critical value should be above $S_{0.6}$. Secondly, a study of the degree of water saturation versus time graphs in Van Huyssteen *et al.* (2005) provided the following evidence that $S_{0.7}$ is a reasonable first approximation: (a) in horizons that are known to drain rapidly, the degree of water saturation only exceeded $S_{0.7}$ for very short times and normally occurred during periods of heavy rainfall; (b) the inflection point in the “water loss” curves in rapidly drying horizons was

[1] Dr. M. Hensley. 2006. Department of Soil Science, Faculty of Natural and Agricultural Science, University of the Free State, Bloemfontein, South Africa.

always well below $S_{0.7}$ indicating that DUL is < 0.7 of porosity; (c) in horizons that were known to be very wet, e.g. G horizons, the degree of water saturation exceeds $S_{0.7}$ for long periods. Therefore soils in the Weatherley catchment at water contents below $S_{0.7}$ should probably not show signs of reduction and soils which are at water contents above $S_{0.7}$ for long enough periods should reduce if there is sufficient organic matter, Fe and soil temperatures are above 5°C.

Cycles of wetting and drying have a pronounced effect on soil. The respiration rate of an air-dry soil immediately after its re-wetting is relatively high. The respiration rate then decreases, stabilizing after several days, sometimes only after several weeks. Re-wetting an air-dry soil goes hand in hand with an increase in the number of soil microbes due to the increased decomposability of organic matter after prolonged drying caused by chemical processes such as decarboxylation or oxidation. Repeated cycles of wetting and drying, as well as aerobic and anaerobic cycles, increase respiration which implies an increased rate of organic matter depletion compared to conditions with constant water contents (Glinski & Stepniewski, 1985). These varying cycles of aerobic and anaerobic conditions lead to Fe and other minerals being oxidised and reduced resulting in soil mottling (Vepraskas & Faulkner, 2001).

Pioneering work was done by Crown and Hoffman (1970) to determine whether or not specific kinds of mottles could be recognized, defined and related to the depth of the water table. The depth of the water table was measured over a four month period. Trends could be noted toward more diffuse boundaries and increases in mottle size and abundance with increased duration of water saturation in soil horizons. Horizontal banding of mottles occurred in two soils in which there had been the highest frequency of water table fluctuation. The accumulation of Fe^{3+} in horizontal bands may have resulted partially from textural differences in the stratified soil material. However, this banding of mottles was not observed in the other two horizons where there was no continued fluctuation in depth to water table, even though all soils had developed in stratified materials. Therefore, the banded mottles appeared to be a function of fluctuating water table. Vertical streaking of mottles occurred in the first horizon, which also was situated on the highest spot in the landscape, in which the water table fluctuated only once during the measuring period. Vertically streaked mottles were not observed in any of the other three horizons. Mottles in horizons almost permanently saturated were large, nebulous (vague) features while those in horizons rarely saturated during the measuring period were generally smaller and had more distinct boundaries with the matrix. Hseu and Chen (1996) found that grey matrix colours, indicating reduced Fe, generally occurred when the soil was saturated for 50% or more of

the year, but there were soils with some grey colours that were saturated for less than 50% of the year.

Vepraskas and Faulkner (2001) measured the redox potential of three different soils in three locations in the landscape. The soils consisted of one wetland soil, and two non-wetland soils - one on a transition zone and one on an upland zone. The soils all had a pH of 5. The wetter the soil the higher the redox potential among the three landscape positions. The upland soil never became saturated during the study period, and it was clear that its redox potential remained high and fairly constant. The transitional soil was saturated for short periods, but the redox potential never fell to a point where Fe reduction would have been expected. On the other hand the wetland soil was saturated for an extended period, and Fe reducing conditions occurred for approximately 150 days.

The term “saturation” was not specified in Hseu and Chen (1996) and Vepraskas and Faulkner (2001) and therefore the degree of water saturation of the respective soils could not be determined.

It can be concluded that fluctuations in the water table, e.g., cycles of wetting and drying cause a greater amount of mottles and higher matrix colour hues than a soil that never saturates or a soil with a permanent water table.

2.8.5 Soil iron content

Fe is found in most igneous rocks and is a component of several minerals, for example hornblende, olivine and biotite (Fitzpatrick, 1980). Fe is released from these minerals through protolysis or oxidation. The most common Fe oxide minerals in soils and sediments are hematite, goethite, ferrihydrite, and lepidocrocite. The most stable and recurrent of these tend to be goethite and hematite (Schwertmann, 1971). The forms of oxidised Fe and Mn in soil also dictate the rate and extent of Fe and Mn reduction. Most oxidised Fe and Mn in soils exist as insoluble oxides that vary in physical and chemical composition. The concentration of Fe oxides in various soils ranges between <0.1 and >50% (Schwertmann, 1991).

The Fe released from the weathering of igneous rocks has a strong tendency to hydrolyse where the soil pH is in excess of 3 to form hematite (Fe_2O_3) which produces a red colour or goethite (FeOOH) which produces a yellowish brown colour (Table 2.4). Below a pH of 3, Fe is normally present in the reduced form (Schwertmann, 1985).

Table 2.4 General characteristics of iron oxide minerals (Schwertmann, 1985)

Mineral	Hematite	Goethite	Lepidocrocite	Ferrihydrite	Magnetite
Composition	Fe_2O_3	FeOOH	FeOOH	$5\ Fe_2O_3 \cdot 9H_2O$	Fe_3O_4
Density (kg m^{-3})	5 260	4 260	4 090	3 960	5 180
Colour	bright red	yellowish-brown	orange	redder than goethite	black
Munsell value	5R – 2.5YR	7.5YR – 2.5Y	5YR – 7.5YR	5YR – 7.5YR	
Size (nm)	10 to 20	50 to 100		3 to 7	
Surface area (X 10^3 m^2 kg^{-1})	50 to 120	60 to 200		200 to 500	

The Fe content in most soils exceeds that of nitrate or manganese. Therefore, the presence of reducible Fe^{3+} induces a buffering capacity which protects soil against a rapid decrease in Eh and resultant mobilization of toxic ions (Glinski *et al.,* 1996). Highly crystalline forms of oxidised Fe are less susceptible to Fe reduction, while soluble chelated Fe oxides are readily reduced. The reductive portion of the Fe biogeochemical cycle in non-phototropic environments is driven by the direct enzymatic reduction of Fe^{3+} oxides to Fe^{2+} by Fe reducing bacteria, or directly via the redox cycling of humic acids (Zachara *et al*., 2000).

Most of the reducible Fe in soils consists of poorly crystalline Fe^{3+} oxides. Ferrihydrite is the most predominant form of reduced Fe and can be dissolved and reprecipitated within a few days (Schwertmann, 1985). It has been shown that Al substitution in the structures of both goethite and hematite can significantly lessen their propensity for being reduced and solubilized. Goethite can accommodate greater amounts of Al than hematite and therefore goethite would be less susceptible to reduction than hematite (Rabenhorst & Parikh, 2000; Schwertmann, 1991). Fe oxides have an extremely low solubility therefore it can be assumed that in the common pH range of well aerated soils, the activity of soluble Fe would be extremely low and would not be sufficient to meet the Fe requirements for plants (Schwertmann, 1991; Lovley, 2001). Reduction of Fe is therefore important to aid in the plant uptake (Schwertmann, 1991).

2.8.6 Temperature

Like any other organism, soil microbes function at optimal temperatures (Vepraskas, 2001). Changes in temperature can induce changes in microbial activity, thereby causing a change in Eh. The Nernst equation also shows that temperature influences the reaction equilibrium (see section 2.3).

Under normal conditions, soil comprises many varieties of microbes, and their respiratory activity takes place as a function of temperature. Microbes in general, including those in the soil, are divided into three groups according to their temperature requirements (Table 2.5).

Table 2.5 Three groups of microbes and their optimal temperatures in which they function (Glinski & Stepniewski, 1985)

Group	Optimum temperature (℃)
Cryophiles	<20
Mesophiles	20-40
Thermophiles	>40

In soils, a respiratory maximum usually occurs within the temperature range of around 40 to 70℃. It is generally believed that soil temperatures must be above approximately 5℃. At temperatures below 5℃ microbial respiration will be too slow to deplete the soil water of O_2 (Vepraskas, 2001). A soil may therefore not show any signs of reduction if the temperature is to low to allow the soil microbes to function optimally. In a study done by Dobos *et al.* (1990), temperature effects on mottle chromas were seen mainly between 5 and 15℃. Optimal microbial Fe reduction occurred at temperatures near 30 to 35℃ at a pH of 7.

Respiratory maximums are not usually reached under normal soil temperatures. O_2 uptake and carbon dioxide production therefore increases with an increase in soil temperature. This phenomenon can be adequately explained by two different equations which are applied for chemical reactions, namely the Van't Hoff or Arrhenius equations (Glinski & Stepniewski, 1985).

Thus respiration rate q:

$$\ln q = c + T\frac{\ln Q_{10}}{10} \qquad (2.27)$$

Where:

q = respiration rate at temperature (T)

c = constant

Q_{10} = the Q_{10} temperature coefficient (showing by how many times the respiration intensity increases when the temperature increases by 10℃).

Van't Hoffs law is based upon the assumption that a temperature increase of 10°K enhances the reaction rate of redox reaction by a of factor 2 to 3. For chemical processes Q_{10} = 2 to 3 and for physical processes it ranges between of 1.2 to 1.3. The Q_{10} value for soils is of little value because even for the same soil it is not constant and decreases with temperature (Glinski & Stepniewski, 1985). A second, more precise description of the dependence of chemical reaction rate upon temperature is the equation of Arrhenius:

$$\ln k = \frac{-E}{RT} + a \qquad (2.28)$$

Where:

k = reaction rate constant
E = activation energy of the reaction
R = universal gas constant
T = absolute temperature
a = constant

For respiration activities q_1 and q_2 at temperatures T_1 and T_2:

$$\ln \frac{q_2}{q_1} = \frac{E}{R} \frac{(T_1 - T_2)}{T_1 T_2} \qquad (2.29)$$

According to this model, the actual respiration rate should be a linear function of the reciprocal of T. The equation also implies a decrease in Q_{10} with temperature. T_2-T_1 = 10°C, the higher the absolute temperature, the higher T_1T_2, and the lower q_2q_1 would be (Glinski & Stepniewski, 1985).

Neither of the above models are always satisfactory for describing the influence of temperature on soil respiratory activity because of the impact of some other environmental factors such as soil water, microbial composition, the kind of organic matter and its degree of decomposition, as well as the time factor (Glinski & Stepniewski, 1985).

2.8.7 Time

For a soil to become reduced it must comply with the factors needed for reduction, and these factors have to be present for a certain amount of time. The O_2 demand of soils can exhaust the dissolved O_2 in a waterlogged soil within 24 hours (McBride, 1994).

Vepraskas (2001) reported that soluble Fe^{2+} was detected in solution after only one day of ponding in field plots in which fresh organic matter was added. The Fe in solution reached its peak after approximately 4 to 5 days following the initial ponding. It was reported by Ponnamperuma (1972) that soils high in organic matter reached a peak Fe^{2+} content within one to three weeks after ponding. There is also a lag between the onset of water saturation and the onset of Fe^{3+} reduction which can be correlated to the soil temperature as well as the organic matter content. The reason for this being that these two factors directly influence microbial activity. Fe oxidation on the other hand can occur very rapidly. It has been noted in laboratory experiments that approximately 78% of the Fe^{2+} was oxidised to Fe^{3+} after 8 hours at 20°C (Vepraskas, 2001).

2.8.8 Bulk density

Soil physical parameters indirectly influence soil organism respiratory activity, through their influence on the transport of O_2 and carbon dioxide. A sharp drop in Eh is observed at a certain critical air-filled porosity value, where the soil pores become discontinuous. At low air filled porosities (< 0.2 m^3m^{-3}) a decrease in soil respiratory activity occurs. This is caused by unsatisfactory O_2 distribution (Glinski & Stepniewski, 1985).

Bulk density influences soil respiration by changing its air-filled porosity (Glinski & Stepniewski, 1985). Increased bulk density leads to a reduction in pore space and a change in aeration and water balance. Soil bulk density can be used as a useful indicator of the extent to which a soil has become compacted. The extent of soil compaction largely depends on texture and structure. A serious consequence of soil compaction is that it reduces space for adequate air and water storage as well as movement (Foth, 1978).

Czyz (2004) showed that traffic over a land caused the bulk density to increase, especially in the topsoil (Table 2.6). Increased compaction reduced the aeration of the soil as measured by a decrease in Eh. A decrease in Eh was noted after only one pass of a wheel over the test area (Table 2.7). The same was found to happen in another experiment where the harvesting of trees growing in swamp areas resulted in soil compaction. The compaction led to a decreased hydraulic conductivity and Eh (Aust & Lea, 1992).

Table 2.6 Increase in bulk density through wheel traffic (Czyz, 2004)

Soil	Depth (cm)	Bulk Density (Mg m^{-3})		
		Natural State	One wheel pass	Four wheel passes
A	2-7	1.54	1.58	1.64
	17-22	1.51	1.56	1.60
	32-37	1.54	1.59	1.63
	47-52	1.52	1.54	1.59
B	2-7	1.45	1.60	1.65
	17-22	1.59	1.62	1.67
	32-37	1.75	1.74	1.76
	47-52	1.72	1.72	1.73
C	2-7	1.51	1.63	1.71
	17-22	1.58	1.63	1.65
	32-37	1.75	1.67	1.67
	47-52	1.71	1.70	1.70
D	2-7	1.54	1.66	1.71
	17-22	1.66	1.67	1.74
	32-37	1.77	1.80	1.80
	47-52	1.79	1.79	1.79

Table 2.7 Eh (mV) values as affected by tractor wheel passes (Czyz, 2004)

Soil	Depth (cm)	Redox Potential (mV)		
		Original State	One Wheel Pass	Four Wheel passes
A	0-10	371.6	341.9	282.1
	10-20	369.3	339.8	288.1
B	0-10	380.4	350.0	277.5
	10-20	358.0	329.4	276.3
C	0-10	382.8	329.2	306.3
	10-20	374.4	329.5	303.0
D	0-10	385.8	358.8	310.6
	10-20	361.0	335.7	310.2

In Table 2.7, soil A has a higher organic matter content than soil D, and could be one of the reasons for the lower Eh values in soil A. More carbon is available for the microbes to feed on, even though soil D had a higher bulk density. Soil A, with a loam texture, has a higher clay content than soil D which has a sandy texture, soil B and C are sandy loam soils (Czyz, 2004).

Casey and Ewel (1998) characterized the natural variation in soil Eh to identify important factors that affect Eh and to assess the short and long-term impact of harvesting trees in a swamp area (Figure 2.4).

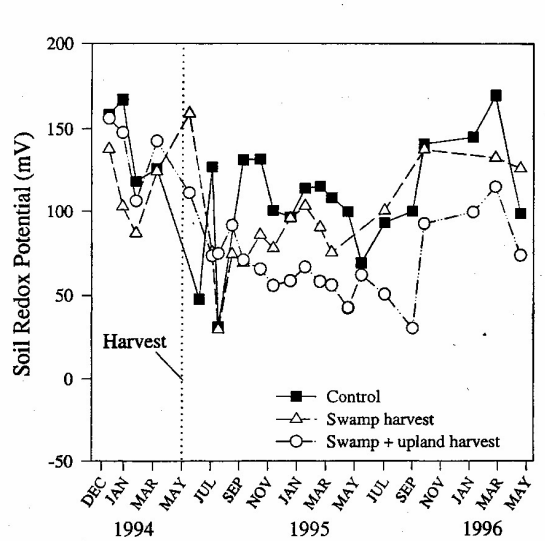

Figure 2.4 Natural variation in monthly mean soil redox potential over a period of three years (Casey & Ewel, 1998).

A control swamp was allocated where no trees were harvested. Two test blocks were allocated, one where all the trees were removed, excluding the upland swamp (swamp harvest treatment), and block two where all the trees were removed from both the swamps and the uplands (swamp and upland harvest). Prior to harvesting, there was no significant difference in surface area or Eh of the swamps. Two years after harvesting, Eh was significantly lower in areas where harvesting took place than in the control area (Figure 2.4). It was unfortunate that the article did not note what the bulk densities before and after the experiment were, though it can be assumed that the harvested areas had a lower bulk density due to compaction through harvesting vehicles as reported by Czyz (2004).

It can be concluded that the decrease in redox potential can be as a result of temporary water logging due to the reduction in macropores through soil compaction (Herbauts *et al.,* 1996; Czyz, 2004).

2.9 Changes in soil morphology due to redox reactions

The most noticeable feature of a soil profile is its colour. Soil colour can be affected through many different factors, including parent material, organic matter content as well as redox reactions within the soil. The specific soil colour observed is determined by the colour of the

various components, particularly the colour of the silicate mineral grains and the quantity and nature of the various natural pigments which may occur and coat the mineral grains (Dobos *et al*, 1990).

Two of the most common pigments are organic matter and Fe oxides. Organic matter is the pigment most active in topsoil horizons. This pigment becomes limited and less noticeable in the subsoil horizons (Vepraskas, 2001).

Saturation and reduction lead to the dissolution, mobilization, and precipitation of Fe and Mn compounds. The resultant soil colour patterns and mineral forms will reflect the long term average soil water status (FAO, 2006). Thus, soil colour features have been routinely used to infer seasonal patterns of soil water saturation and biochemical reduction (Soil Survey Staff, 1975; FAO, 1998). Using soil colour and morphological feature to predict the soil water regime is not always as easy in all soils. It has been reported by Mokma and Sprecher (1994) soil colour was not a good indicator of duration of water saturation in spodsols as the colour differences tended to be related to differences in eluviation and illuviations rather than saturation. Soil mottles can also be indications of relict water regimes and the water regime of the profile can therefore be misinterpreted.

Morphological features of seasonally reduced soils include unique colour patterns, the smell of rotten eggs (sulphur) and colour changes that occur on exposure to air. A predetermined abundance or soil depth of a certain feature is not a defining factor in the determination of soil morphological features. The principal reducing reactions that form the morphological features of reduction involve four elements: O, Mn, Fe, and S, which are used as electron acceptors in bacterial respiration. The reactions for Mn and Fe are reversible and produce different features as the reactions proceed in either direction (Vepraskas, 2001).

Coatings of Fe oxides have a more prominent effect on soil colour (Table 2.8). Mn oxides can also be strong soil pigments, causing the soil to become dark brown or black. Hematite (Fe_2O_3) produces a red colour in the soil matrix and is indicative of an oxidative environment. Goethite (FeOOH) gives the soil a yellow colour and is indicative of a less well drained soil (Table 2.8). In more extreme cases, the Fe oxides are not only depleted from small zones, but may be largely removed from the soil, leading to what is called a depleted or gleyed matrix (Rabenhorst & Parikh, 2000).

Table 2.8 Reducing reactions related to saturated soils (McBride, 1994; Vepraskas, 2001)

Reducing Reaction	Eh (pH 7) mV	Morphological Feature Formed	
		Group Name	Example
$O_2 + 4e^- + 4H^+ \rightarrow 2H_2O$	600	Organic C-based features	Dark to black soil horizons
$MnO_2 + 2e^- + 4H^+ \leftrightarrow Mn^{2+} + 2H_2O$	300	Mn-based features	Black and grey mottles
$2FeOOH + 4e^- + 4H^+ \leftrightarrow 2Fe^{2+} + 4H_2O$	100	Fe-based features	Fe masses and Fe depletions, red, yellow and gray mottles
$SO_4^{2-} + 8e^- + 10H^+ \rightarrow H_2S + 4H_2O$	-200	S-based features	Odor of rotten eggs

Studies on how much time is necessary for the formation of soil morphological features to occur within soil are limited (Stolt *et al.*, 1998). Vepraskas and Bouma (1976) saturated cores with water treated with dextrose to increase the microbial activity. Accumulation and depletion of Fe and Mn were observed within 150 days of water saturation. Redoximorphic features related to fluxes in Fe and Mn concentrations were observed within the interior and exterior of peds buried for two years in a wetland. The most prominent features were Fe masses on ped exteriors, and Fe pore linings and Fe depletions within the interior (Stolt *et al.,*1998).

Mottle values show no obvious trend with an increase in organic carbon content or temperature. Typically, the yellow component of the soil matrix colour Munsell hue increases in area as temperature increases. Matrix colour hues tend to be influenced by increased time (Dobos *et al.,* 1990).

Table 2.9 Reductimorphic colour pattern and occurrence of Fe compounds (FAO, 2006)

Colour	Munsell colour	Formula	Mineral
Green/blue, after oxidation red	5-GY-5-B2-3/1-3	Fe_2/Fe_3	Fe-mix compounds
White, after oxidation brown	N7-8 → 10 YR4/5	Fe_2CO_3	Siderite
White, after oxidation blue	N7-8 → 5-B	$Fe23(PO_4)2 \bullet 8\ H_2O$	Vivanite
Bluishblack (H_2S- smell)	5-10-B1-2/1-3	FeS, FeS_2 (or Fe_3S_4)	Fe sulphides
White, after oxidation white	N8 → N8	--	Complete loss of Fe compounds

In cases where saturated soils do not display signs of reduction (Daniels *et al.,* 1973; Cuoto *et al.,* 1985; Vepraskas & Faulkner, 2001), oxygenated soil water usually prevents the development of redoximorphic features. This water can be provided in the form of flowing water either in the form of ground water (interflow) or flood water. The flowing water carries O_2 through the soil making the O_2 difficult to deplete. Another factor can be that such soils simply lack the oxidisable organic matter needed to supply the electrons used in reduction (Vepraskas & Faulkner, 2001). If enough organic matter and a stagnant water source is present the of lack morphological features can be attributed to the fixation of Fe to organic matter. The Fe will be unavailable to precipitate and therefore the redoximorphic features will not reflect the water regime of the soil (Ticehurst, *et al*., 2007).

2.10 Effect of redox reactions on basic cations

All natural elements on the periodic table have a certain charge. An element with a positive charge is referred to as a cation. In soil, basic cations are calcium (Ca^{2+}), magnesium (Mg^{2+}), potassium (K^{+}) and sodium (Na^{+}) and the acidic cations are, hydrogen (H^{+}) and aluminum (Al^{3+}). The amount of these positively charged cations a soil can hold is determined by the cation exchange capacity (CEC). The CEC is expressed in $cmol_c\ kg^{-1}$. The larger this number, the more cations the soil can hold.

Cations are attracted to negatively charged clay colloids. Different rates and orders of adsorbtion exist among cations, since the adsorbtion reaction depends on the surface potential, valence, and hydrodynamic radius. When monovalent and divalent ions are present in a soil solution, adsorbtion is usually shifted in favour of the divalent ions.

Specific adsorbtion of cations is affected by the hydrodynamic radii. Ions with smaller hydrated radii usually have preference when adsorbed by the clay complex (Tan, 1993). A decreasing order of preference for adsorbtion of monovalent cations by clays has been reported by Gast (1977):

$Cs^{+} > Rb^{+} > K^{+} > Na^{+}$

Such a series of ions, listed in decreasing order of preferential adsorbtion is called a *lyotropic series.* The lyotropic series for divalent cations (Taylor & Ashcroft, 1972) is:

$Th^{2+} > La^{2+} > Ba^{2+} > Sr^{2+} > Ca^{2+} > Mg^{2+}$

The lyotropic series may differ in different clay types (Tan, 1993).

Ca^{2+} and Mg^{2+} are present in most soils and are components of several primary and secondary minerals in the soil. These are essentially insoluble for agricultural considerations, although they are also present in a soluble form, as a cation, Ca^{2+} and Mg^{2+} which are adsorbed to the soil colloidal complex. The availability of calcium and magnesium in the soil is related to the soil CEC. They are in competition with each other as well as in competition with other major cations such as sodium (Na^{+}), potassium (K^{+}) and iron (Fe^{2+}), for uptake by the crop and adsorbtion on the soil colloidal complex. High levels of soil Na^{+} displace Ca^{2+} and lead to Ca^{2+} leaching. This results in poor soil structure (Havlin *et al*., 1999*)*.

Potassium (K^{+}) does not form a structural part of any plant component or compound, although it is required for various metabolic activities and physiological functions. It plays a role in sugar and carbohydrate production, transport, and storage. Soil K content varies widely. Very little of this K is available to plants, as much of the unavailable K is a structural part of various soil minerals. Plant-available soil K is in the ionic form K^{+}. K^{+} in soil is affected by soil pH. If the soil pH decreases (increasing soil acidity) the availability of K often decreases. Cold, compaction and soils with a low degree of water saturation often reduced the availability of K^{+} in soil for plant use (Havlin *et al*., 1999*)*.

In the past, considerable attention has been given to the behaviour of N, P and organic matter under reducing and oxidizing conditions (Moore *et al*., 1992; Patrick & Jugsujinda, 1992; Chen *et al*., 2003). Published information on other soil nutrients such as soluble and exchangeable cations and anions and the cation exchange capacity is scarce. It has been noted that in calcareous soils the Ca, Mg, K, Mn and Fe concentrations increase with increased water saturation of a soil (Larson *et al*., 1991). There have been reports that an increase in solubility of these cations is due to dissolved organic carbon (Wolt, 1994). Increases in concentration can also be attributed to the increased competition between the cations for the negatively charged sites due to the increased levels Fe^{2+} and Mn^{2+} under reducing conditions (Phillips & Greenway, 1998).

Phillips and Greenway (1998) studied the effects of waterlogging and drying on the cation composition of the soil phase. They reported that waterlogging caused a decline in Eh, a rise in pH and an increase in soluble Ca, Mg, K, Na, Mn and Fe. The changes were more evident in the soils containing higher levels of organic carbon, thereby more intense reducing conditions. The increased concentrations of soluble Ca, Mg, K and Na can be

attributed to either a loss of exchange/adsorbtion sites due to the solubilization of organic carbon and hydrous oxides of Fe and Mn, or the displacement from the CEC sites due to increased concentrations of soluble Fe and Mn. Waterlogging and subsequent drying did not significantly affect the concentration of the exchangeable Ca, Mg, K, and Na (Phillips & Greenway, 1998)

It can therefore be concluded that Ca^{2+} and Mg^{2+} should react similarly and K^{+} and Na^{+} will react similarly due to these cations having the same valence as well as similar hydrated radii. The soluble Ca^{2+}, Mg^{2+}, K^{+} Na^{+} concentrations in soil should increase under saturated conditions in conjunction with an increase in the Mn^{2+} and Fe^{2+} concentration. This is due to the solubilisation of organic carbon and hydrous oxides of Fe and Mn, or their displacement from the CEC sites due to increased concentrations of soluble Fe^{2+} and Mn^{2+}.

2.11 Hydropedology

The U.S.A. National Research Council (NRC) has identified integrated studies of the earth's critical zone as a compelling research area for the 21st century (NRC, 2001). The NRC (2001) defined this zone to include the land surface and its canopy of vegetation, rivers, lakes and shallow seas and then extend through the root zone, deep vadose zone, and ground water zone. The term "critical zone" was coined through the life-sustaining interaction between the solid earth and its fluids. Soil and water are two critical components of this zone and the soil-water interaction is the key interface between the biotic and abiotic (Lin *et al*., 2005).

A common term used to describe the status of the soil water is the soil water regime. There have been conflicting ideas on the definition for soil water regime, one being a qualitative term referring to the state and availability of soil water (Van der Watt & Van Rooyen, 1995) and the other referring to the degree of wetness of the soil (Van Huyssteen *et al*., 2005). Another term used, is soil hydrology, which can be defined as the physical interpretation of phenomena which govern hydrological events related to soil or the uppermost mantle of the earth's crust (Kutilek & Nielsen, 1994).

In earlier years it was thought that soil hydrology and hydropedology were the same concept (Schoeneberger & Wysocki, 2005), although this thought pattern was soon shrugged off by the new age of hydropedologists. The new interdisciplinary subject "hydropedology" is developing owing to the necessity to sustain optimal environments within the earths critical zone. Therefore the need for a more integrated approach for studying landscape-soil-water

interactions across spatial and temporal scales. Hydropedology provides this bridge. It combines the disciplines of pedology, including soil macro- and micromorphology and vadose zone hydrology together with other disciplines dealing with land, air and water interfaces as well as data translations from soil survey databases into soil hydraulic properties (Lin *et al*., 2005; Kutilek & Nielsen, 2007). Hydropedology aids in shifting the science of geology-orientated pedology towards a more hydrology-orientated pedology which reflects the crucial role that water plays in many environmental, ecological, geological, agricultural and natural resource issues (Lin *et al*., 2005). Through this bridging, a unique situation arises in which hydropedology aids in integrating the soil and water sciences.

Lin *et al*. (2005) summarized the fundamental scientific issues of hydropedology in four interrelated areas:

(a) Soil structure and layering as indicators or determinants of flow and transport characteristics in soils. In the context of hydropedology the term "soil structure" is used to encompass both pedality and pore space, because soil structure refers to a specific soil horizon, soil layering is thus treated separately to reflect the overall organization of the profile (Lin *et al*., 2005);

(b) Soil morphology used as signatures of soil hydrology. Soil morphology reflects both profile and landscape hydrology by integrating soil changes over time. The soil's morphology is also the testimony of the long-term persistent flow and transport process of water, resulting in visible pedological features (Lin *et al*., 2005) such as oximorphic and redoximorphic features, as well as the accumulation or lack of clay in a horizon. Wetlands and hydric soils have been of growing public interest in recent years. Several authors (Hseu & Chen, 1996; Vepraskas & Sprecher, 1997; Rabenhorst & Lindbo, 1998; Vepraskas, 2001) have underlined the importance of using soil morphology in interpreting soil hydrology (Lin *et al*., 2005). Soil hydrology is the factor that drives the development of hydromorphic features, water saturation, and reduction in wet soils (Mausbach & Richardson, 1994);

(c) Water movement over the landscape in relation to soil cover. Conceptual models of water movement over the landscape, overland flow, are key aspects of contaminant transport, watershed management, wetland delineation, and terrestrial ecosystem functions. Hydropedological studies in various major land resource areas could provide insights regarding water movement over a range of landscapes of various scales as it is important to understand where, when and how water moves through

the landscape. It is also of further interest to understand how this water moves through different size landscapes and how water flow impacts soil processes and subsequently soil spatial and temporal patterns (Lin *et al*., 2005);

(d) Hydrology as a factor of soil formation and a driving force of the dynamic soil system. The fluvial system can be seen as the life blood of the landscape. It is of critical importance to soil morphology, genesis, classification, and mapping. All of the five natural soil forming factors, climate, vegetation, time, topography, and parent material affect and are affected by hydrology (Lin *et al*., 2005).

Understanding the redox behaviour of elements within a soil profile will aid in interpreting soil profile hydrology. Interactions between the solid earth and its fluids control almost every life-sustaining activity. Due to this, hydropedology holds significant potential to enhance our understanding of the earth's critical zone and to improve the modeling of flow and transport phenomena occurring in the earth's surface and subsurface environments (Lin *et al*., 2005).

2.12 Summary

Oxidation and reduction (redox) processes play an important role in the soil through the process of soil formation. The reduction of Fe within the soil through water saturation leads to the Fe becoming soluble. Moving water carries the soluble Fe through the profile until it reaches oxidised conditions which renders the Fe insoluble after which it precipitates. This precipitated Fe as well as other oxides form soil morphological features, such as soil mottles. Very little literature is available on how long it takes for these mottles to form.

Several factors influence the redox process by either retarding or intensifying it. In the presence of factors such as a high soil O_2 content, a lack of organic matter, low soil Fe and water contents and a low bulk density, reduction will not take place. Whereas if there is a lack of O_2, with sufficient organic matter and Fe, the soil will have a higher propensity to reduce. Due to the fact that redox processes are sensitive to these factors a lack in any one of them can retard reduction. Therefore it is important to understand the dynamics of the soil redox system so that it becomes easier to interpret redox features in relation to these influential factors.

Redox processes in soil from an integral part of soils and a better understanding on the subject can lead to a better understanding of a broad spectrum of fields within soil science. Hydropedology and wetland delineation are two new examples. Understanding of redox

processes in soils can aid in better understanding of the hydrology of the profile and thereby lead to more accurate hydrological interpretations.

The effect of organic matter as well as temperature on redox processes have been widely documented. On the other hand, literature on soil degree of water saturation, time and bulk density and their effect on redox is scarce. A better understanding of the influence of the latter factors on redox can aid one in relating these properties to the water regime of a soil profile.

CHAPTER 3

HYPOTHESIS AND AIMS

3.1 Hypothesis

For any given soil material with a particular combination of those factors affecting redox potential (e.g. organic matter, iron oxides, micro-organism population, temperature) and a particular physical structure and porosity, a critical degree of water saturation can be identified at which detectable reduction of Fe will commence.

3.2 Aims

There were three key aims to the study of a selected soil horizon from the Weatherley catchment:

a) To establish the relationship between the degree of water saturation (s) and the onset of reduction.

b) To establish the relationship between the degree of water saturation (s) and the duration of reduction.

c) To establish the effect of bulk density on the above-mentioned processes.

3.3 Experimental approach

To address the first and second aim, a detailed soil core study was done. Soil cores using the same soil and bulk density were saturated to four different degrees of water saturation ($S_{0.6, 0.7, 0.8, 0.9}$). The experiment was terminated after 121 days. Redox was measured *in situ* every 3.5 days for the first three months after which weekly measurements were made for a further one month. The onset of reduction was taken to be a measured pe value of 6 corresponding to an increase in detectable soluble Fe. To address the third aim, a second experiment was set up with three bulk densities and a constant degree of water saturation ($S_{0.8}$). Redox was measured *in situ* every 3.5 days and the experiment was terminated after 23 days of water saturation.

CHAPTER 4

GEOGRAPHY OF THE STUDY SITE

4.1 Introduction

This chapter describes profile 234, a 1.6 m deep, sandy loam Avalon 2100 (Appendix A, Figure A1), situated in the Weatherley catchment, Eastern Cape Province. This soil can also be classified as a Ferric-Hyperdistric Cambisol FAO (1998) or an Aquic Ustipsamments (Soil Survey Staff, 1999).

4.2 Site description

The Weatherley catchment is situated on the footslopes of the Drakensberg mountain range in the north-eastern part of the Eastern Cape Province. The catchment totals 160 ha and occupies a large part of the farm Weatherley (Figure 4.1). The geographical coordinates for the catchment are 31° 06' South and 28° 20' East with a mean elevation of 1 300 m above sea level.

Elliot sandstone covers the upper part of the eastern and southern slopes of the catchment. Two prominent dolerite dykes occur within the catchment. A prominent sandstone shelf of the Molteno formation is found at 1 320 m above sea level with sandstone and mudstone of this formation below this level. Sandstone and mudstone of the Elliot formation overlie the Molteno shelf (Esprey, 1997).

The catchment receives moderately high summer rainfall, with a mean annual rainfall of 1 064 mm (calculated from 9 years data) (BEEH, 2003) (Figure 4.2). The summers are hot, with mean maximum temperatures of 25°C and mean winter minimum temperatures of 4°C (Table 4.1). Profile 234 is situated in an upper midslope position, with a western aspect and slope of 11%. The profile has Elliot sandstone as parent material (Figure 4.3). The soils in the catchment display a large spatial variation. Primarily deep freely drained soils occur on the southern and western slopes (apedal and neocutanic B horizons) with a mixture of soils located immediately below the Molteno shelf and on the south-eastern end of the catchment. Soils range from very wet in the marsh areas to dry in the uplands where the Hutton and Oakleaf soil forms occur. The soils in the catchment are acidic with a low cation exchange capacity due to the high rainfall and siliceous lithology (Van Huyssteen *et al.,* 2005).

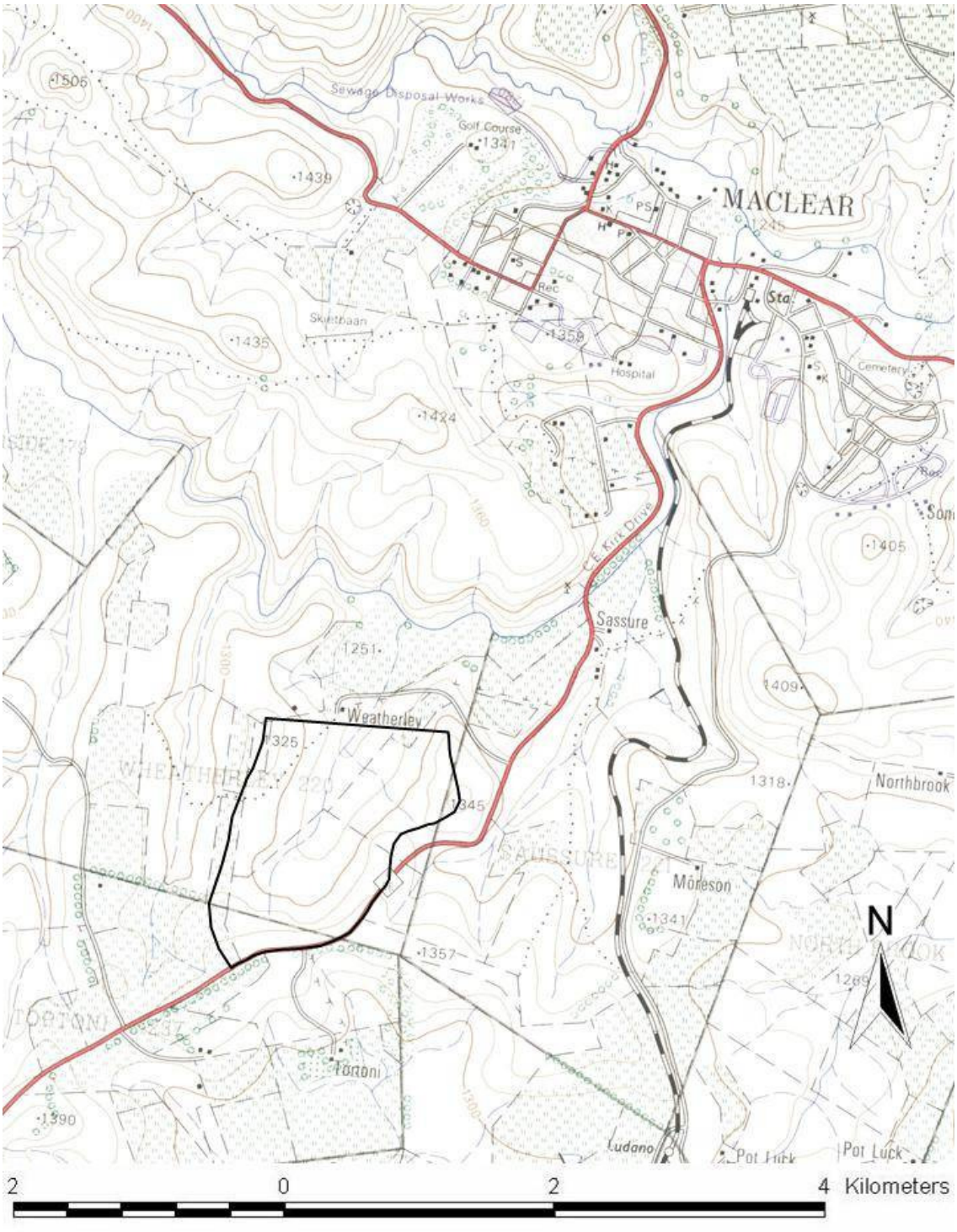

Figure 4.1 Location of the Weatherley catchment, 4 km south of the town Maclear (Chief Director of Surveys and Mapping, 1993).

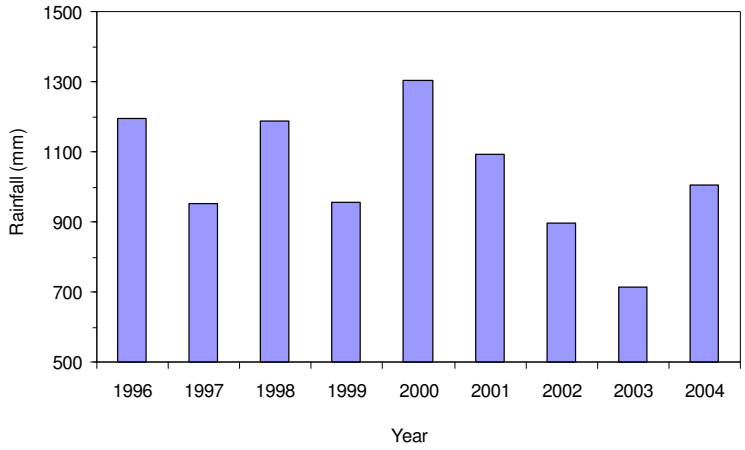

Figure 4.2 Yearly rainfall, measured at Weatherley (BEEH, 2003).

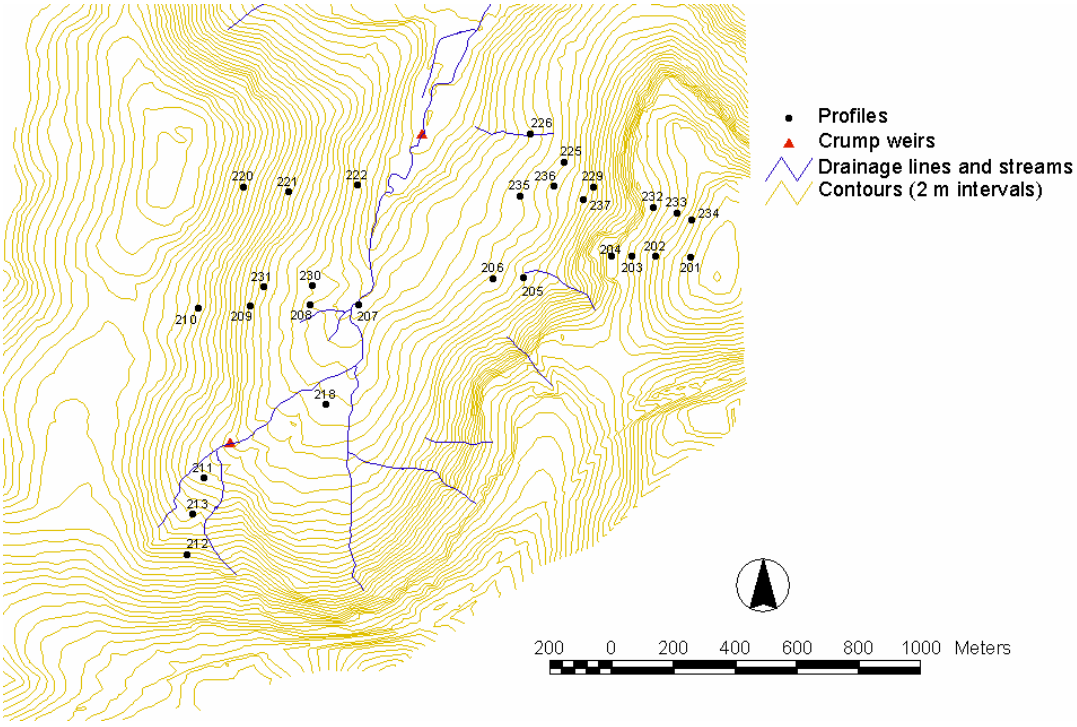

Figure 4.3 Location of profile 234 within the Weatherley catchment, Eastern Cape (Van Huyssteen *et al.,* 2005).

Table 4.1 Monthly mean rainfall for Weatherley (seven-year means, from 1996 to 2002) (BEEH, 2003), and temperature from a weather station 4 km from the study area (Roberts *et al.,* 1996)

Month	Rainfall (mm)	Temperature (°C)		
		Maximum	Minimum	Mean
January	195.3	25	14	20
February	154.3	25	14	20
March	140.4	24	12	18
April	61.6	24	11	18
May	30.3	21	7	14
June	24.9	18	4	11
July	15.2	19	4	11
August	28.8	19	6	11
September	36.6	21	8	14
October	65.2	21	10	15
November	131.3	24	12	18
December	180.5	24	13	19
Total	1064.3			

4.3 Profile description

Profile 234, an Avalon 2100 (Appendix A, Figure A1), consists of a very dark greyish brown (10YR3/2) orthic A horizon (0 – 500 mm), overlying a dark yellowish brown (10YR4/4) yellow-brown apedal B1 (500 – 880 mm), on a yellowish brown (10YR5/4) yellow-brown apedal B2 (880 – 1 070 mm) on an yellowish brown (10YR5/6) soft plinthic B3 (1 070–1 300 mm) on light yellowish grey (10YR6/2) unspecified material with signs of wetness (1 300–1 500 mm) on yellowish brown (10YR5/4) unspecified material with signs of wetness (1 500–1 600 mm). Soil colour was read in the moist state using a soil Munsell colour chart (Munsell Color Company, 1980). A detailed profile description is given in Table 4.2 and in Appendix A, Table A1.

The profile description in Appendix A, Table A1 and Table 4.2 are representative of the diagnostic horizon although soil samples for chemical and physical analysis were taken at 100 mm intervals in Table A2, hence the discrepancy in horizon depths.

Table 4.2 Description of profile 234, an Avalon 2100 (Van Huyssteen *et al.,* 2005)

Horizon	Depth (mm)	Description	Diagnostic horizons / material
A	0 - 500	Water status: moist; dry colour: 10YR4/2 (95%), 10YR4/3 (5%); moist colour: 10YR3/2 (95%), 10YR4/3 (5%); 9.8% clay; coarse sandy loam; no 10YR4/3 dry, 10YR3/2 moist, humus mottles; apedal massive; hard, friable, non-sticky, non-plastic; few normal fine and very fine pores; few normal medium and coarse pores; no slickensides; no cracks; no cutans; no coarse fragments; water absorption 1 second(s); many normal roots; gradual smooth transition;	orthic A horizon
B1	500 - 880	Water status: moist; dry colour: 10YR5/4 (90%), 10YR4/2 (10%); moist colour: 10YR4/4 (90%), 10YR3/2 (10%); 14.3% clay; coarse sandy loam; common medium distinct 10YR4/2 dry, 10YR3/2 moist, humus mottles; apedal massive; hard, friable, non-sticky, non-plastic; few normal fine and very fine pores; few normal medium and coarse pores; no slickensides; no cracks; no cutans; no coarse fragments; water absorption 1 second(s); many normal roots; gradual smooth transition;	yellow-brown apedal B horizon
B2	880 - 1070	Water status: moist; dry colour: 10YR6/4 (85%), 10YR6/6 (10%), 10YR5/2 (5%); moist colour: 10YR5/4 (85%), 10YR4/6 (10%), 10YR3/2 (5%); 17.1 % clay; sandy loam; common medium distinct 10YR6/6 dry, 10YR4/6 moist, humus mottles; apedal massive; hard, friable, non-sticky, non-plastic; many normal fine and very fine pores; few normal medium and coarse pores; no slickensides; no cracks; no cutans; no coarse fragments; water absorption 1 second(s); common normal roots; gradual smooth transition;	yellow-brown apedal B horizon
B3	1070 - 1300	Water status: moist; dry colour: 10YR7/3 (90%), 10YR8/1 (10%); moist colour: 10YR5/6 (90%), 10YR5/6 (10%); 18.7% clay; loam; common fine distinct 10YR8/1 dry, 10YR5/6 moist, iron oxide mottles; common fine distinct 10YR8/1 dry, 10YR5/6 moist, iron oxide mottles; apedal massive; very hard, friable, very sticky, plastic; many normal fine and very fine pores; few normal medium and coarse pores; no slickensides; no cracks; no cutans; no coarse fragments; water absorption 1 second(s); few bleached roots; clear smooth transition;	soft plinthic B horizon
C1	1300 - 1500	Water status: moist; dry colour: 10YR8/1 (70%), 2.5YR4/8 (30%); moist colour: 10YR6/2 (70%), 10YR4/8 (30%); 15.1% clay; loam; common fine distinct 2.5YR4/8 dry, 10YR4/8 moist, iron oxide mottles; many fine prominent 2.5YR4/8 dry, 10YR4/8 moist, iron oxide mottles; moderate coarse prismatic; very hard, very firm, very sticky, very plastic; few bleached fine and very fine pores; few bleached medium and coarse pores; many slickensides; no cracks; common clay & cutans; very few 2-6 mm round Fe & Mn concretions; water absorption 4 second(s); very few bleached roots; abrupt smooth transition;	unspecified material with signs of wetness
C2	1500 - 1600	Water status: moist; dry colour: 10YR7/1 (60%), 10YR5/8 (40%); moist colour: 10YR5/4 (60%), 10YR4/6 (40%); 15.1% clay; loam; many coarse distinct 10YR5/8 dry, 10YR4/6 moist, iron oxide mottles; moderate coarse prismatic; very hard, very firm, very sticky, very plastic; few bleached fine and very fine pores; few bleached medium and coarse pores; many slickensides; no cracks; common clay & cutans; no coarse fragments; water absorption 1 second(s); no roots; transition not reached;	unspecified material with signs of wetness

4.4 Soil analyses

4.4.1 Chemical analyses

Chemical analyses were done for all the horizons, although it was decided to only use a mixed soil sample from the B1 (500 - 880 mm) and B2 horizon (880 - 1 100 mm) in the experiments. The two horizons were mixed in a 2:1 ratio before analyses were done. The mixing took place in a 2:1 ratio as the B1 horizon was 380 mm and the B2 horizon 200 mm. Mixing of the B1 and B2 horizon took place by spreading the air dry soil on a 10 X 10 m plastic sheet. The sheet was then repeatedly pulled at 120° angles, after which the soil was sieved through a 2 mm sieve (M. Hensley, personal communication[2]). The end product was a homogenously mixed 2:1 ratio between the B1 and B2 horizon.

All chemical analyses were done according to standard methods (The Non-Affiliated Soil Analysis Work Committee, 1990). Soil samples were analysed for particle size distribution (7 fractions), pH (H_2O), exchangeable cations, cation exchange capacity (CEC), organic carbon, nitrogen, as well as dithionite-citrate-bicarbonate (Mehra & Jackson, 1960) extractable Fe and Mn.

The exchangeable cations for all the horizons, including a mixed sample of the B1 + B2 horizon were determined with ammonium acetate (NH_4OAc) extraction (Table 4.3). Detailed results of chemical analyses for profile 234 is given in Appendix A, Figure A2.

The soluble Fe concentration was high in the A horizon (13.5 mg kg^{-1}) and then decreased dramatically in the B2 (0.4 mg kg^{-1}) and stayed low right through to the C horizon. The CBD extractable Fe concentration decreased from the A horizon to the B2 horizon after which it increased through to the C horizon.

The organic carbon content was highest in the A horizon and then decreased through to the C horizon. The average organic carbon content of the profile was relatively low with averages below 1 %.

[2] Dr. M. Hensley. 2006. Department of Soil Science, Faculty of Natural and Agricultural Science, University of the Free State, Bloemfontein, South Africa.

Table 4.3 Chemical analyses for profile 234 as well as for combined B1 and B2 horizon

Horizon	Soluble cations			CEC soil	Exchangeable cations					
	Ca	Mg	Na		Ca	K	Mg	Na	Fe	Mn
	$cmol_c\ kg^{-1}$				$mg\ kg^{-1}$					
A	0.55	0.52	0.15	7.3	1.60	0.16	0.78	0.05	13.5	20.8
B1	0.38	0.49	0.18	7.1	0.46	0.09	0.49	0.06	0.4	1.0
B2	0.92	0.50	0.17	4.2	0.49	0.07	0.58	0.05	0.2	1.4
B3	0.88	1.03	0.18	10.6	2.11	0.27	2.46	0.11	0.5	1.2
C	0.81	0.89	0.70	14.5	2.85	0.35	2.70	0.13	0.4	1.4
B1+B2	0.61	0.47	0.16	5.4	0.47	0.07	0.52	0.05	0.4	1.1

Horizon	pH H_2O	Org C	Fe	Mn
			CBD	
	%		$mg\ kg^{-1}$	
A	5.14	1.10	6253	6.5
B1	5.33	0.25	5412	13.5
B2	5.55	0.15	4487	6.0
B3	5.81	0.29	5219	6.5
C	5.69	0.26	6318	7.0
B1+B2	5.47	0.22	4856	8.8

The pH (water) increased from 5.14 in the A horizon to 5.81 in the B3 horizon after which it decreased to 5.69 in the C horizon (Figure 4.4).

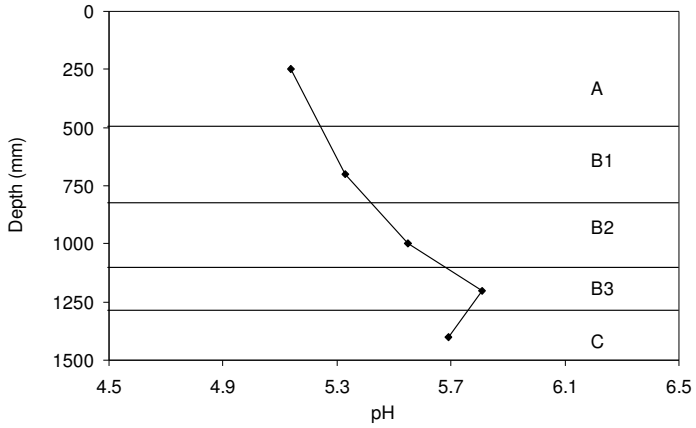

Figure 4.4 pH (H_2O) taken in the middle of each horizon for profile 234 (Avalon 2100).

4.4.2 Particle size analyses

Particle size analyses were done using the pipette method (Handbook of standard soil testing methods for advisory purposes, 1990).

Sand sizes were determined by dry sieving and fractionation of the coarse, medium, fine, and very fine sand. Silt and clay fractions were determined by the modified pipette method using calgon as the dispersing agent. All texture analyses were done in triplicate.

For the coarse segments a set consisting of five sieves, with a receiving pan was used. The five sieve openings consisted of 2.0; 0.5; 0.25; 0.106 and 0.053 mm. The soil was first sieved through a 2 mm aperture sieve after which 10 cm^3 calgon dispersion agent was added to 50 g of the pretreated oven dry soil. The solution was then mixed in an electric mixer for 5 minutes. The solution was washed on a 0.053 mm sieve, passing the silt and clay through the sieve via a funnel into a 1 000 cm^3 cylinder. Once the percolate was clear, the sand left in the sieve was transferred to an evaporating dish and dried at 105°C until a constant mass was reached. It was then transferred to the set of sieves arranged in decreasing order. The sieves were shaken on a sieve shaker for approximately 10 minutes. The mass of each sand fraction was determined by weighing the content of each sieve as well as the residual silt plus clay that passed through the 0.053 mm sieve into the receiving pan.

To determine the silt and clay fraction with the pipette the 1 000 cm^3 cylinder into which the percolate was washed, was filled to the 1 dm^3 mark. A temperature measurement was taken before the solution was stirred with a hand stirrer for 30 seconds to ensure all the clay was in suspension. Pipette extractions were then done according to the temperature of the solution. The pipette extraction was transferred into an evaporating container and placed in an oven and dried at 105°C until all the water had evaporated. The silt, fine silt and clay were then determined by weighing the containers. The first pipette measurement contained all the fractions of silt, fine silt and clay. By the time the second measurement was taken, the silt had settled at the bottom of the cylinder and only the fine silt and clay were in suspension. The last pipette measurement contained only the clay fraction. The percentage of each fraction in the soil sample was then calculated.

The coarse sand fraction was the highest in the A horizon with 32.7% whereafter it decreased to a mere 2.13% in the C horizon, while the clay content increased from 19% in the A horizon to 54% in the C horizon (Table 4.4). The A, B1 and B2 horizons had a sandy loam texture, while the B3, C1 and C2 horizons had a loam texture. The clay content was

stable in the first three horizons after which it increased considerably in the B3 and C horizon (Figure 4.5).

Table 4.4 Texture analyses for all horizons including B1 + B2 mixed sample

Horizon	Texture Analysis						
	coSa	meSa	fiSa	vfSa	Si	fiSi	Cl
	%						
A	32.7	22.9	9.5	5.5	3.4	6.3	19.1
B1	33.4	21.0	10.7	5.8	6.0	3.7	20.3
B2	19.5	19.6	15.7	9.8	6.9	7.0	22.3
B3	7.5	8.0	16.0	12.6	5.2	6.7	45.3
C	2.1	5.7	18.1	11.9	3.2	5.0	54.0
B1 + B2	25.3	19.3	14.2	6.8	7.4	5.7	21.5

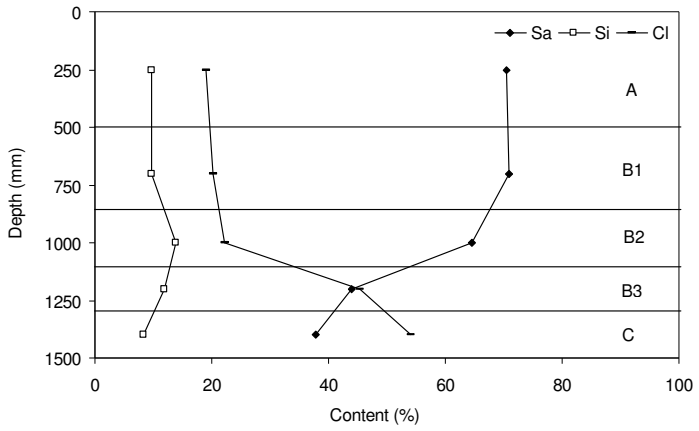

Figure 4.5 Sand, silt and clay percentages for profile 234 (Avalon 2100).

4.4.3 Bulk density

Bulk density is a measure of the weight of the soil per unit volume. Variation in bulk density is attributable to the relative proportion and density of the solid organic and inorganic particles and to the porosity of the soil.

Two main methods of determining bulk density are the clod method and the core method. The core method was used for the determination of the bulk density of profile 234 (Blake & Hartge, 1986).

A core sample was taken by inserting a cylinder of a known volume, 0.00085 m^3 into the core sampler. The surface of the soil area to be sampled was scraped clean and level. The core sampler was placed over the area and hit firmly but gently into the soil. Once the sampler was deep enough it was removed carefully without damaging the soil structure. The surface was leveled on both sides and the roots were removed with a pair of scissor. Once the exposed surfaces of the core were cleaned perfectly, the contents were put into a bag of known weight and dried for 24 hours at 105°C. The contents were then weighed and the bulk density and porosity was calculated. The particle density of quartz (2.65 Mg m^{-3}) was used in calculating the porosity.

The bulk density increased from an average of around 1.6 Mg m^{-3} in the A horizon to 1.7 Mg m^{-3} in the C horizon.

Table 4.5 Field measured bulk density

			Bulk density			
Horizon	Depth	Diagnostic	Replication			Average
		horizon	1	2	2	
	(mm)		(Mg m^{-3})			
A	0 – 500	ot	1.55	1.61	1.56	1.57
B1	500 – 880	ye	1.66	1.58	1.61	1.62
B2	880 – 1070	ye	1.68	1.66	1.59	1.64
B3	1300 – 1500	sp	1.69	1.75	1.74	1.73
C	1500 – 1600	on	1.70	1.71	1.73	1.71

4.5 Summary

A soil profile in the Weatherley catchment was selected due to the considerable amount of data available on the area. It was also aimed at adding valuable data to the already large database of the soils in the catchment.

The profile chosen for the study was an Avalon 2100. It consisted of an orthic A, on a yellow brown B1 and B2 horizon, with a soft plinthic B, on an unspecified horizon with signs of wetness. The yellow brown B1 and B2 horizon was used for all further analyses. The profile has Elliot sandstone as parent material.

The profile has a bulk density ranging from an average of 1.6 Mg m^{-3} in the A horizon to 1.7 Mg m^{-3} in the C horizon. The Fe and Mn concentrations in the profile is fairly low, with the most Fe and Mn occurring in the A horizon. The clay content increased from the A through to the C horizon, at the expense of the sand fraction.

CHAPTER 5

EXTRACTION OF WATER FROM A SOIL COLUMN

5.1 Introduction

The ratio between water and air within the soil porous media determines the availability of O_2. A decrease in soil air constrains the O_2 availability and may lead to anaerobic conditions. Reduction is then initiated leading to a decrease in Eh (Vepraskas, 2001).

A wide range of information can be derived from soil Eh. It is therefore an important soil parameter. Eh can be used to determine the tendency of a soil to reduce or oxidize certain elements (Fiedler & Sommer, 2004). It can used to estimate the nutrient availability and mobility of heavy metals for agricultural and environmental management purposes, such as the protection of wetlands (Phillips & Greenway, 1998). Eh can also aid in understanding pedogenetic processes and phenomena such as colour changes, concretions and mottles formation (Fiedler *et al.,* 2002).

Insoluble Mn^{4+} and Fe^{3+} are rendered soluble (Mn^{2+} and Fe^{2+}) through reduction and can therefore be used together with Eh as a good indication of the redox status of soil (Vepraskas & Faulkner, 2001). Cation concentrations can also be used as indicators of the reduction. Increases in Ca^{2+}, Mg^{2+}, K^{+} and Na^{+} can be correlated with the increased competition for the CEC sites due to elevated Mn^{2+} and Fe^{2+} concentrations in the soil solution (Phillips & Greenway, 1998). Increases in Ca^{2+}, Mg^{2+}, K^{+} and Na^{+} can therefore be related to reduced of Mn^{2+} and Fe^{2+}.

It is not always possible to determine the Mn^{2+} and Fe^{2+} concentrations in the field, therefore it is important to be able to determine the Eh of the soil efficiently and correctly.

Eh is measured with a platinum (Pt) electrode, either directly in the soil or from extracted soil solution. Each method poses its own problems. Direct measurements are subject to the influence of microsites. Microsites are areas where an increase or decrease in microbial consumption of organic matter causes a local change in Eh (Vepraskas & Faulkner, 2001). By extracting the soil solution, one can run the risk of the solution oxidizing during the extraction process and therefore giving an incorrect measurement. It will also be more desirable to extract the soil solution from the soil core or column when doing laboratory

studies. Furthermore many measurements can be taken from a core or column without the soil being disturbed.

The aim of this chapter was to determine if water could be extracted efficiently through suction applied to tensiometer cups installed in a soil column. The column was wetted through capillary rise.

It was hypothesised that in a column wetted through capillary rise, the wetness of the column would vary from wettest at the bottom (saturated) and driest at the top of the column. The extracted soil water could then be used to investigate the redox status of the soil at different degrees of water saturation.

5.2 Material & methods

5.2.1 Soil

The soil used in this experiment was from the combined B1 and B2 horizons (500 – 1 070 mm) of the profile 234 discussed in Chapter 4, section 4.4.

5.2.2 Soil column

An artificial soil column was constructed by packing the soil in a PVC pipe, 1 m high, and 0.104 m in inner diameter. The method used in constructing the column was based on the method used by Vepraskas and Bouma (1976). The complete column consisted of ten 0.1 m sections sealed with silicon sealant and held together with duct tape (Figure 5.2). The column was packed to a bulk density of 1.6 Mg m^{-3} using the method proposed by Klute (1986). The bottom of the column was sealed with a PVC base and silicon sealant.

The volume of the column was calculated from the equation:

$$V = \pi r^2 h \qquad (5.1)$$

Where:

V = volume (m^3)
r = radius (m)
h = height (m)
π = pi

The total volume of the 1 m column was therefore 0.0085 m^3.

The mass of the dry soil (M) needed to fill the column to the specified bulk density could be calculated from the volume of the column, (V_s = 0.0085 m^3) and the desired bulk density, (D_b = 1.6 Mg m^{-3}):

$$M = D_b \times V_s \qquad (5.2)$$
$$= 13.59 \text{ kg}$$

Micro tensiometer cups, 6 mm in diameter, were inserted through holes drilled in the side of the column. The cups were inserted into the centre of each segment at 0.1 m intervals. The holes through which the tensiometer cup and its tubing were inserted were sealed with silicon sealant to prevent air leaking in and soil water leaking out. Once packed, the top of the column was left uncovered to allow for evaporation and hence water movement through the column.

A layer of glass beads was placed in the bottom 0 - 50 mm of segment 1. A piece of cheese cloth was placed over the beads to prevent the mixing thereof with soil. The beads allowed for even distribution of the water. The base of the column was connected via plastic tubing to a 5 ℓ glass bottle. The pre-determined water level was then established by filling the reservoir bottle to the desired depth. The water table in the soil column was maintained at a height of 0.3 m from the base of the soil column by means of a Marriot bottle connected to the surface of the reservoir water by a glass tube. A lowering of the water table level, as water evaporated through the soil column resulted in the siphoning of water from the Marriot bottle to re-establish the correct water level in the reservoir bottle (Figure 5.1). Room temperature (23℃) distilled water was used throughout the experiment.

Water was allowed to move into the column through capillary rise. The column was left for two days to equilibrate after which the first extraction took place. An attempt was made to extract water samples from all 10 segments of the column. The intention was to extract soil water daily for the first three days and then roughly every third day. The extraction was done under suction from a vacuum pump (-85 kPa). A minimum of 15 cm^3 of soil solution was needed to determine the Eh, pH and soluble cations.

Extraction took place by inserting two needles into a test tube stopper (Figure 5.3). One needle was connected to a manifold which was connected to the suction pump. The second needle was connected to the tube which was connected to the tensiometer cup in the soil

column. Soil water could then be extracted from the soil column and would be sucked directly into the test tube. This limited the exposure of the sample to air and therefore the risk of subsequent oxidation.

Immediately after extraction, a redox electrode was inserted into the test tube to determine the Eh of the extracted soil solution. A platinum (Pt) electrode with a combined Ag/AgCl reference electrode used was. The electrode was connected to a millivolt meter.

The pH was read in the same solution. The sample was transferred to a storage container and 3 cm^3 HCl was added to prevent Fe^{2+} and Mn^{2+} oxidation (Weaver, 1992; Franson *et al*., 1995). Atomic absorption spectrometry (AAS) was used to determine Fe^{2+}, Mn^{2+}, Ca^{2+}, Mg^{2+}, K^+ and Na^+ concentrations in the extracted soil solution.

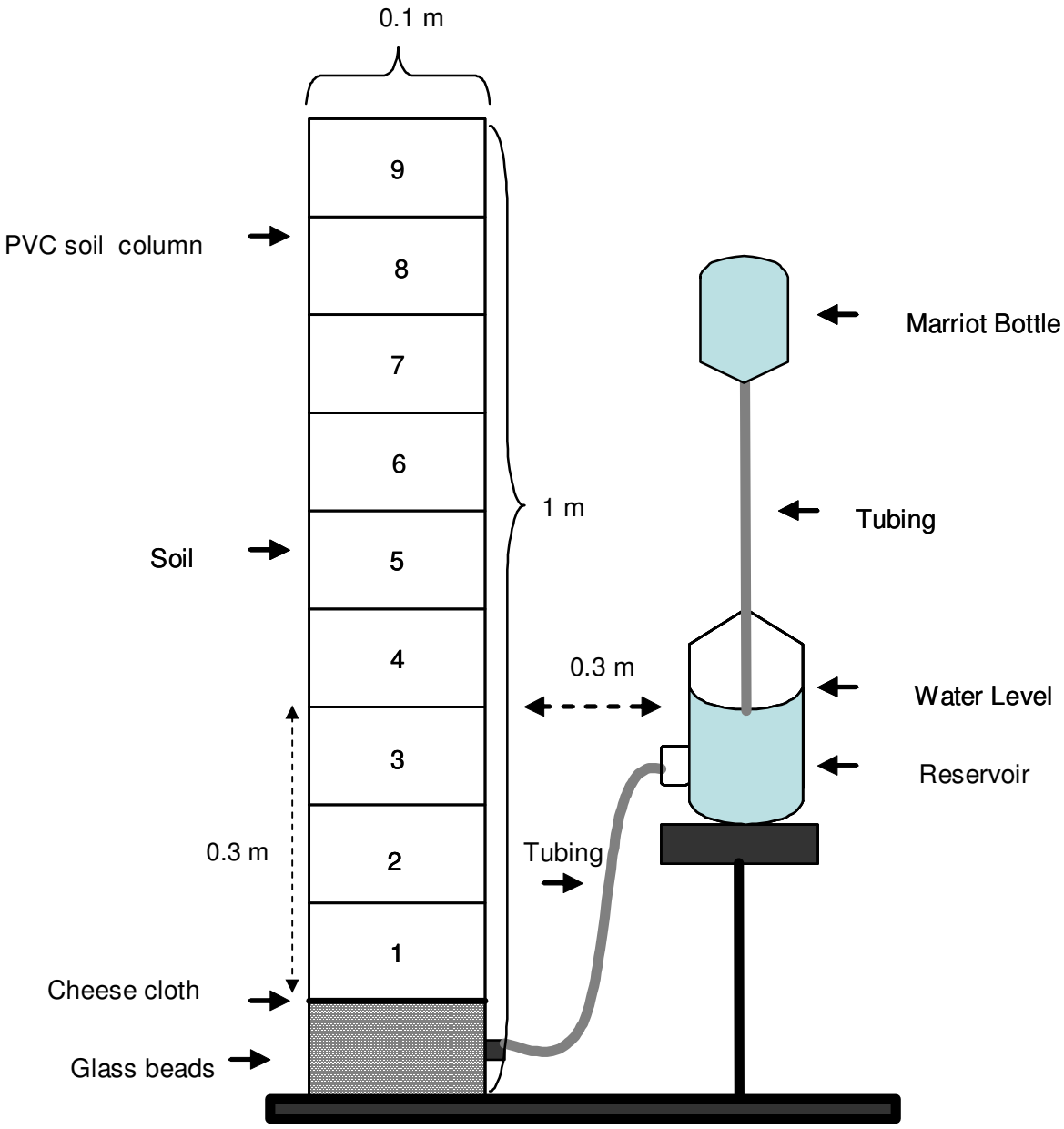

Figure 5.1 Graphic representation of the soil column constructed from ten 0.1 m segments with an established water table at 0.3 m above the cheese cloth, using a Marriot bottle (adapted from Ashworth & Shaw, 2004).

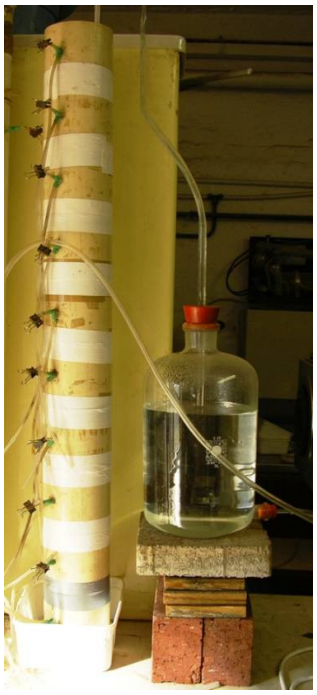

Figure 5.2 Soil column constructed from ten 0.1 m segments with a permanent water table at 0.3 m from the base of the column using a Marriot bottle (Marriot bottle not visible in picture).

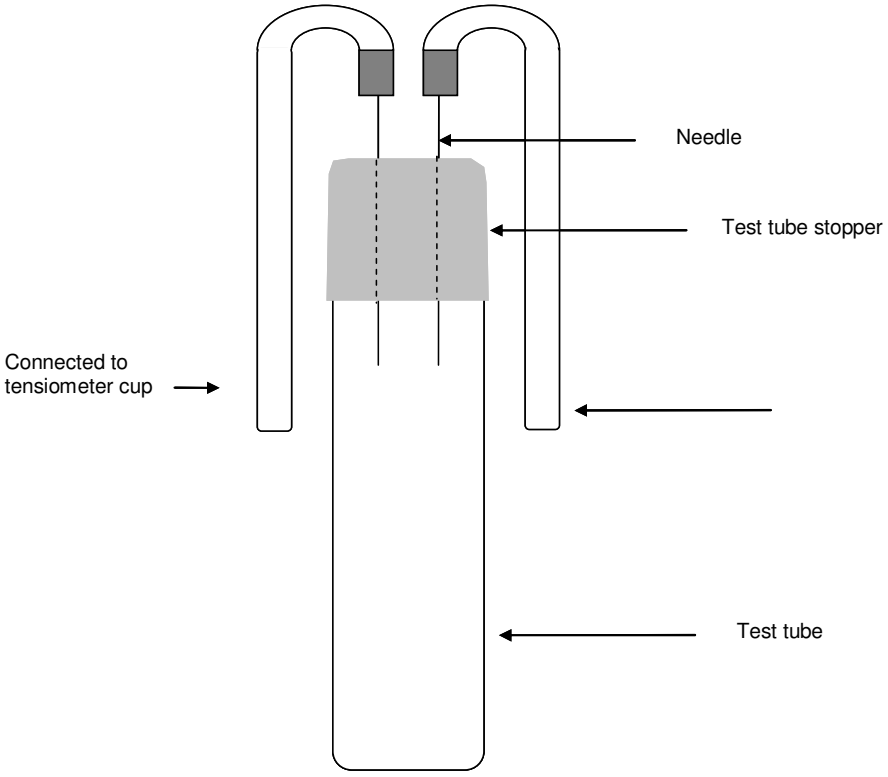

Figure 5.3 Test tube setup for sampling of extracted soil water.

5.3 Results & discussion

5.3.1 Column wetted by capillary rise

It was found that water could be extracted from below the water table, but above it, even from segment 4, proved difficult. It took approximately 4 hours to extract 1 cm^3 of soil solution from segment 4 which was 0.1 m above the water table. The water saturation was assumed to be at 90% of porosity in segment 4. It was virtually impossible to extract enough solution to be analysed from segment 5. Data collection was terminated after 42 days due to the difficulty experienced in extracting soil solution. The column was then left intact for 7 months. The full data set for segment 1 (Table B1), Segment 2 (Table B2) and Segment 3 (Table B3) is given in Appendix B.

The Eh data was analysed using the pe of each segment. The calculation and reason for the use of pe is given in section 2.3. It was observed that a decrease in pe lead to an increase in pH (Figure 5.4) and *vice versa*. In general, reduction caused the soil pH to shift toward seven. This was due to the loss of H^+ ions during reducing reactions. As the pe decreased in segment 1 to 3, the pH increased toward 7. The pH reached 7 in some instances, but never exceeded it (Figure 5.4). This is supported in Fiedler & Sommer (2004), who reported that the pH increases under reducing conditions in low pH soils.

3

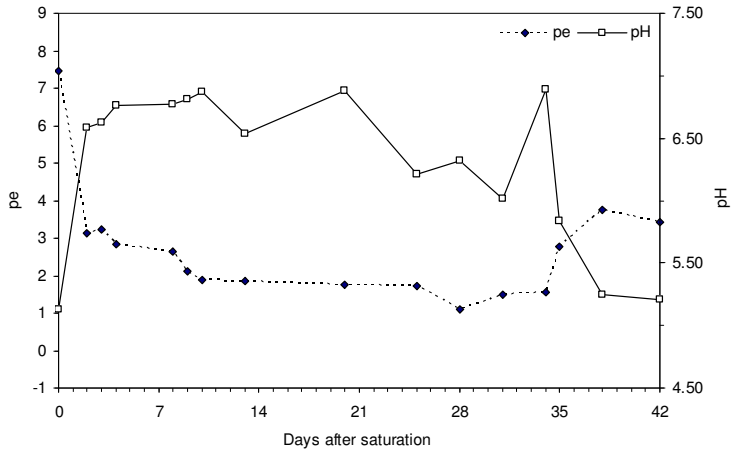

2

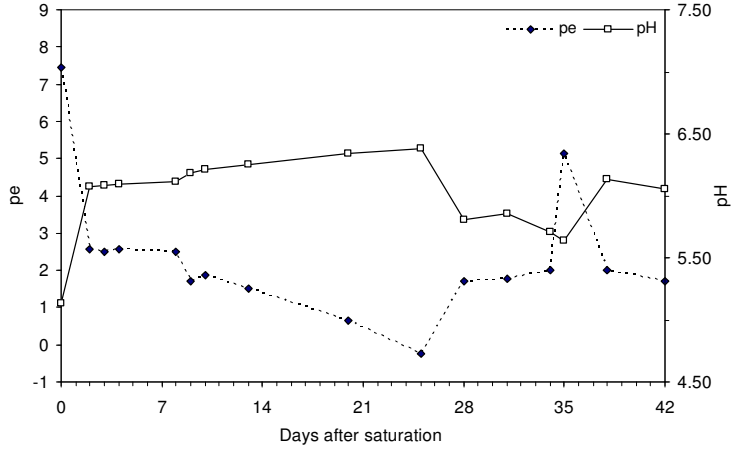

1

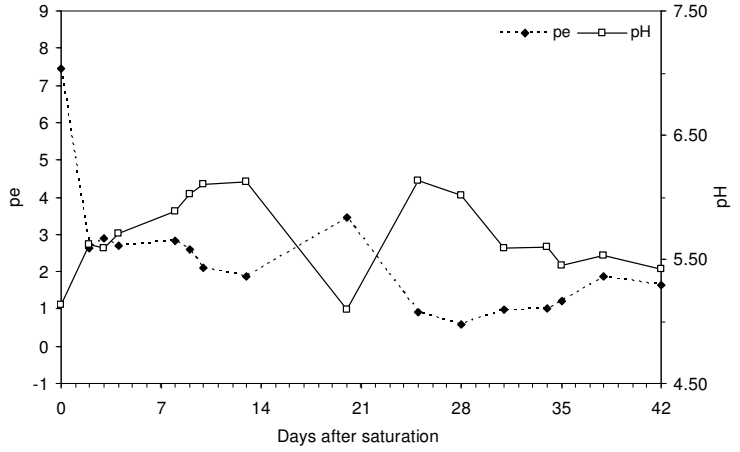

Figure 5.4 pe and pH values over a 42 day period for segment 1 (0.0 - 0.1 m), segment 2 (0.1 - 0.2 m) and segment 3 (0.2 - 0.3 m), with segment 1 being at the bottom of the column.

Soluble Mn^{2+} was detected in all three segments after the first reading which was 3 days after water saturation. This was anticipated, as Mn becomes soluble at a pe of below 7.6

units (Fiedler & Sommer, 2004). In all the segments where water was extracted the pe was constantly below 7.6 units. In segment 1, the Mn^{2+} concentration decreased steadily over 31 days. It reached its lowest point after 31 days after which it increased to a maximum concentration over the next 4 days and then again decreased. In segment 2, the Mn^{2+} concentration decreased for 13 days after which the concentration stabilized over the next 14 days. An overall decrease in Mn^{2+} concentration took place in all three segments. The reason for the Mn^{2+} being in solution in all the segments from the first measurement could also be as a result of the low pH and therefore it lead to a higher solubility of Mn^{2+} (Figure 5.6).

In segment 1, soluble Fe^{2+} was not evident in the soil solution for the first four days, after which it steadily increased over a period of 28 days (Figure 5.6). The Fe^{2+} concentration increased in conjunction with a decrease in pe + pH, it increased to a maximum of 11.84 mg kg^{-1} after 35 days of saturation. The sudden increase in Fe^{2+} could not be related to the pe + pH, which remained low. The pe + pH decreased sharply after the first measurement and then continued to decrease at a slower rate. The sudden fall in pe + pH did not cause the Fe to reduce immediately, as Fe^{2+} was not evident in the solution for the next 8 days, although the overall decrease in pe + pH lead to an increase in Fe^{2+} concentration. In segment 2 the Fe^{2+} concentration was very sensitive to decreases in pe + pH. As the pe + pH decreased, a simultaneous increase in Fe^{2+} concentration took place. In segment 3, which was the last segment from which adequate soil water could be extracted, the pe + pH decreased after the first measurement for 31 days after which it increased. The soluble Fe^{2+} concentration in segment 3 remained present in very low concentrations throughout the 42 day period. The pe + pH levels did not fall as low in segment 3 as in the other two segments. This could be as a result of segment 3 having a slightly lower degree of water saturation due to insufficient capillary rise of water. The lower pe + pH levels therefore did not lead to Fe^{2+} reduction in this segment.

When the pe was analysed separately, the pe of all 3 segments are very similar (Figure 5.5). Therefore one can conclude that the pe did not have such a big influence on the reduction of Fe^{2+}. After 10 days Fe^{2+} was only detected in solution in segment 1 and 2, even though the pe of all three segments was similar. When the pe + pH data for all the segments are compared, the pe + pH for segment 1 and 2 are very similar, and the pe + pH in segment 3 is higher. It might therefore be that the higher pH in segment 3 could have prevented Fe reduction.

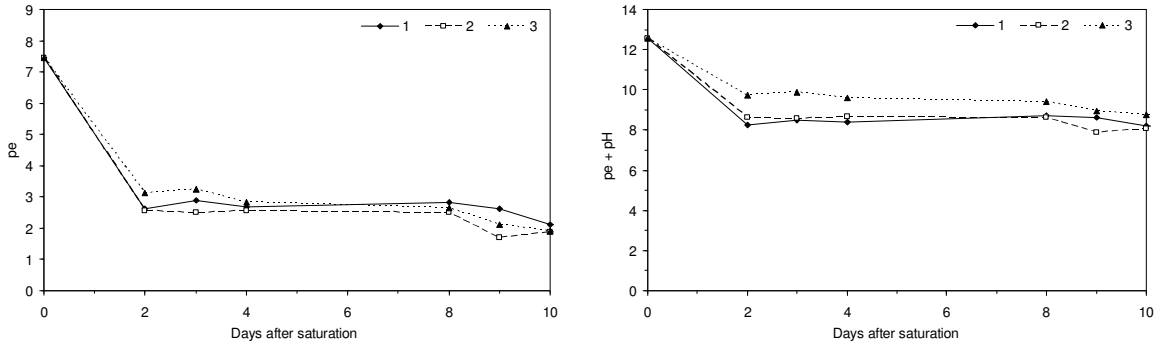

Figure 5.5 pe and pe + pH values for the first 10 day period for segment 1 (0.0 - 0.1 m), segment 2 (0.1 - 0.2 m) and segment 3 (0.2 - 0.3 m), with segment 1 being at the bottom of the column.

It was assumed that the degree of water saturation in segments 1 to 4 was between $S_{1.0}$ and $S_{0.9}$ due to the presence of the water table. An increase in Fe^{2+} concentration in segment 1 took place 8 days after initial water saturation. The Fe^{2+} content increased from 0.01 to 1.58 mg kg^{-1}. Therefore reduction in segment 1 took place within 8 days. The Fe^{2+} concentration reached a maximum of 12.00 mg kg^{-1} after 35 days of saturation. An increase in Fe^{2+} was detected 9 days after water saturation in segment 2, from a minimum of 0.01 to a maximum of 3.59 mg kg^{-1}. The Fe^{2+} concentration reached a maximum of 13.00 mg kg^{-1} after 28 days of saturation. There was very little Fe^{2+} present in the soil solution in segment 3, except for a slight increase to 1.94 mg kg^{-1} after 28 days of water saturation. This showed that segment 3 might not have been at the same degree of water saturation as segment 1 and 2, or that segment 3 might have had an air leak through the tensiometer coupling, allowing oxidation to take place. Reduction diminished after approximately 42 and 35 days in segments 1 and 2 respectively.

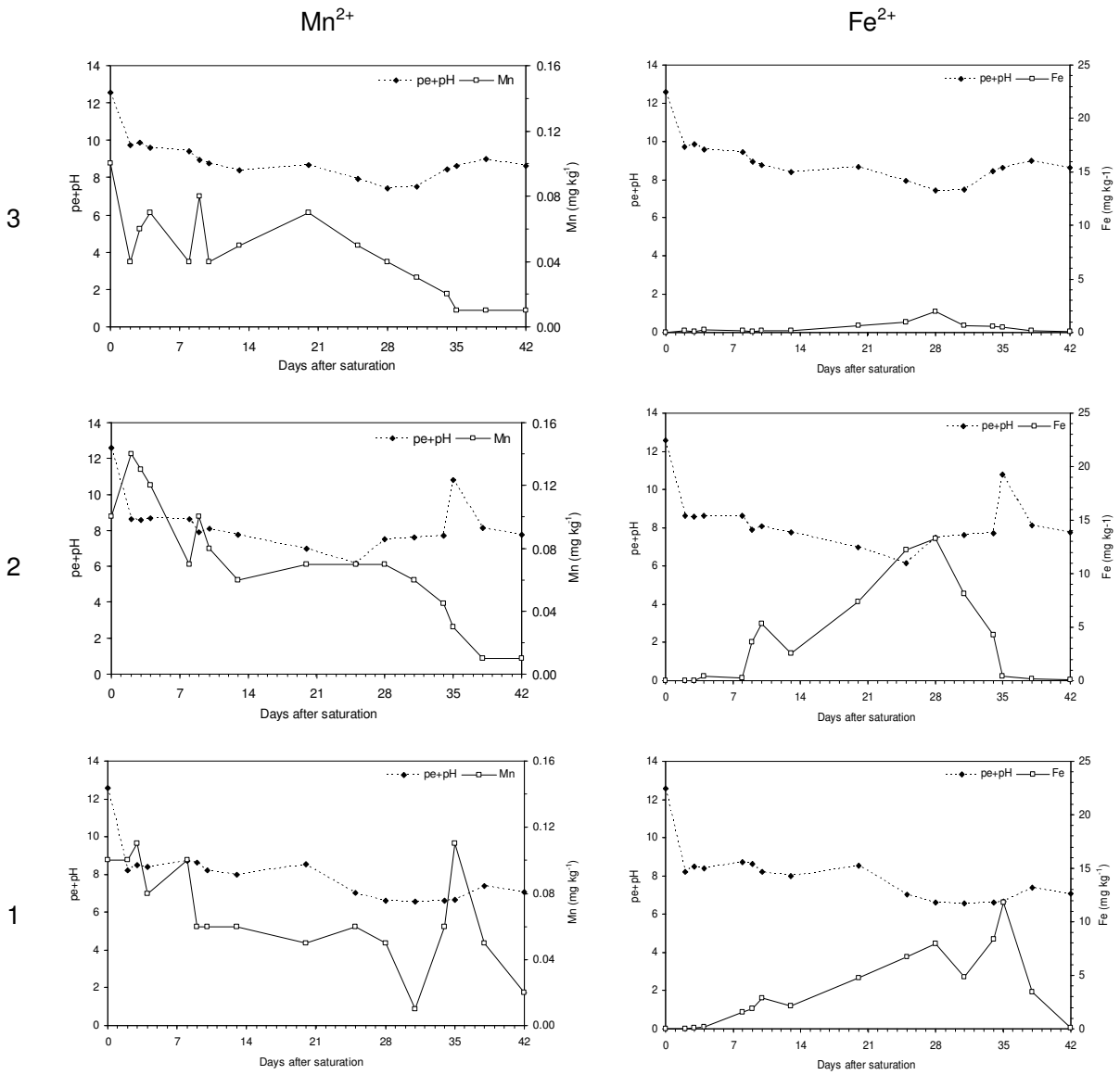

Figure 5.6 Mn^{2+} and Fe^{2+} concentration and pe + pH values for segment 1 (0.0 - 0.1 m), segment 2 (0.1 - 0.2 m) and segment 3 (0.2 - 0.3 m) over a 42 day period, with segment 1 being the bottom of the column.

By the fourth measurement in segment 1 and 2 the Ca^{2+} and Mg^{2+} concentrations reached their maximum concentrations for the 42 day saturation period after which a constant decrease took place (Figure 5.7). In almost all the segments the Ca^{2+} and Mg^{2+} concentrations were lower at the end of the 42 day water saturation period than after the first measurement.

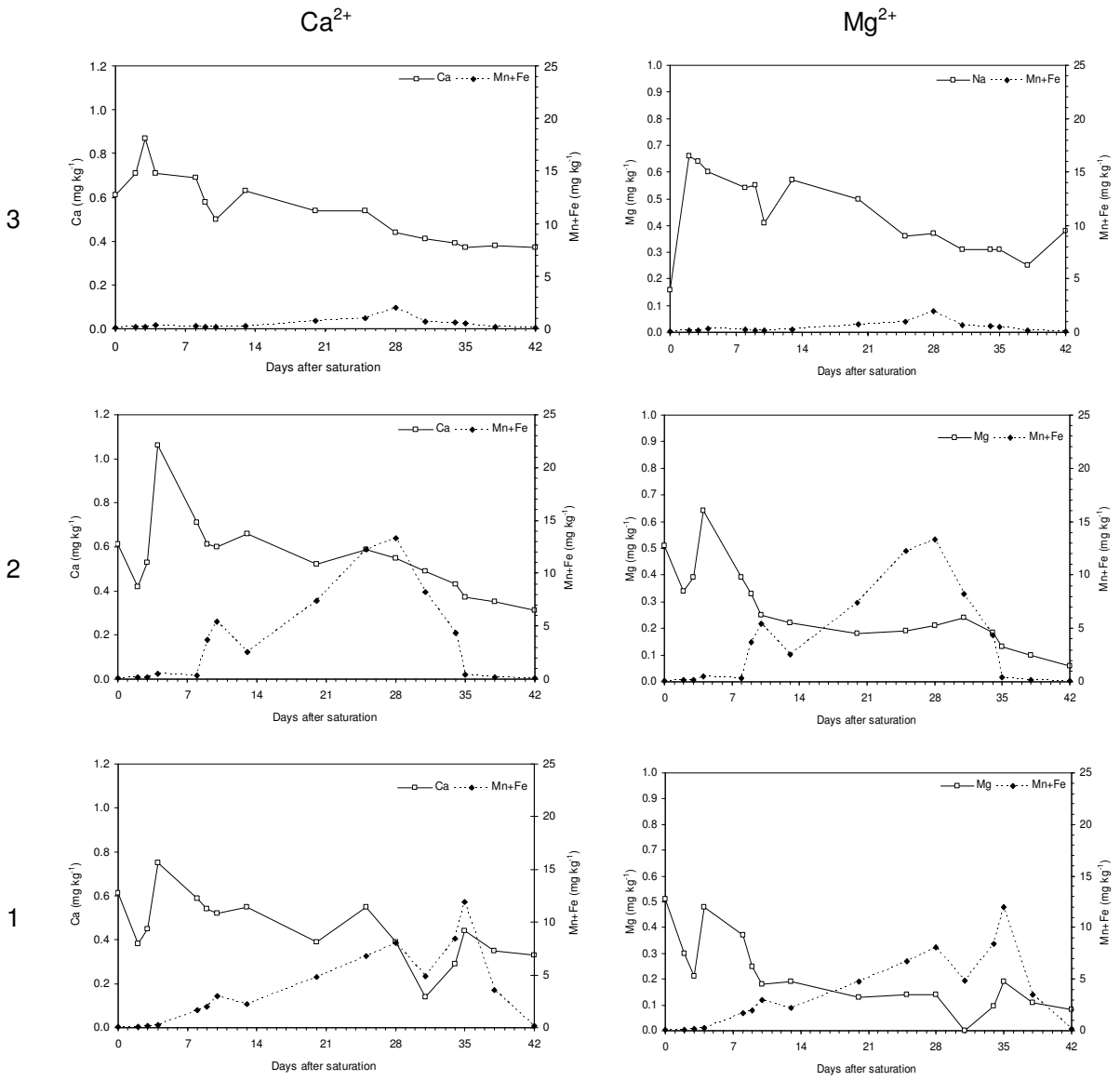

Figure 5.7 Ca^{2+} and Mg^{2+} concentration and pe + pH values for segment 1 (0.0 - 0.1 m), segment 2 (0.1 - 0.2 m) and segment 3 (0.2 - 0.3 m) over a 42 day period, with segment 1 being the bottom of the column.

No relationship could be found between the concentrations of Ca^{2+} and Mg^{2+} and the pe + pH in any segment. The Ca^{2+} and Mg^{2+} concentrations were then compared to the combined Mn^{2+} + Fe^{2+} concentration in the cores. In segment 3 the Ca^{2+} and Mg^{2+} concentrations increased to a maximum within the first three days after which they steadily decreased. The average Ca^{2+} and Mg^{2+} concentrations were the lowest in segment 1, this segment being the most reduced. The average Ca^{2+} and Mg^{2+} concentrations of segment 2 and 3 were very similar. In segment 1 the Ca^{2+} and Mg^{2+} concentrations reacted in unison with the Mn^{2+} + Fe^{2+} concentration, although this relationship could not be found in segments

2 and 3. The reason for this could be the higher pe in segment 2 and 3. Ca^{2+} and Mg^{2+} reacted very similar, with simultaneous increases and decreases taking place. The reason for the similarity between the Ca^{2+} and Mg^{2+} concentrations in the soil was probably because these two cations have the same valence and hydrated radii and therefore behave similarly within the soil.

There seemed to be a similarity between an increase in K^+ and an increase in Na^+ for all 3 segments (Figure 5.8). The similarity between the K^+ and Na^+ concentrations could be attributed to the fact that these cations have the same valence. In segment 1 there was a relationship between an increase in the Mn^{2+} + Fe^{2+} concentration and an increase in the K^+ and Na^+ concentrations. This could not be found in segment 2 or 3.

An increase in soluble Fe^{2+} and Mn^{2+} concentrations could be attributed to reduction. The increase in Ca^{2+}, Mg^{2+}, K^+ and Na^+ was attributed to increased competition between cations for the negatively charged sites on the clay complex due to increased concentrations of Mn^{2+} and Fe^{2+} in the soil solution under reducing conditions. Therefore an increase in the Mn^{2+} and Fe^{2+} concentration lead to an increase in the concentrations of Ca^{2+}, Mg^{2+}, K^+ and Na^+ in the soil solution, through displacement from the solid phase.

After 7 months (252 days) the soil column was separated into 0.1 m sections. All the segments were moist except the top segment. No colour change was observed in the moist or dry state. The lack of change in colour could be as a result of insufficient water saturation or the lack of fluctuating water saturation. The degree of water saturation was however sufficient to cause reduction and an increase in Fe^{2+} extracted from the soil solution.

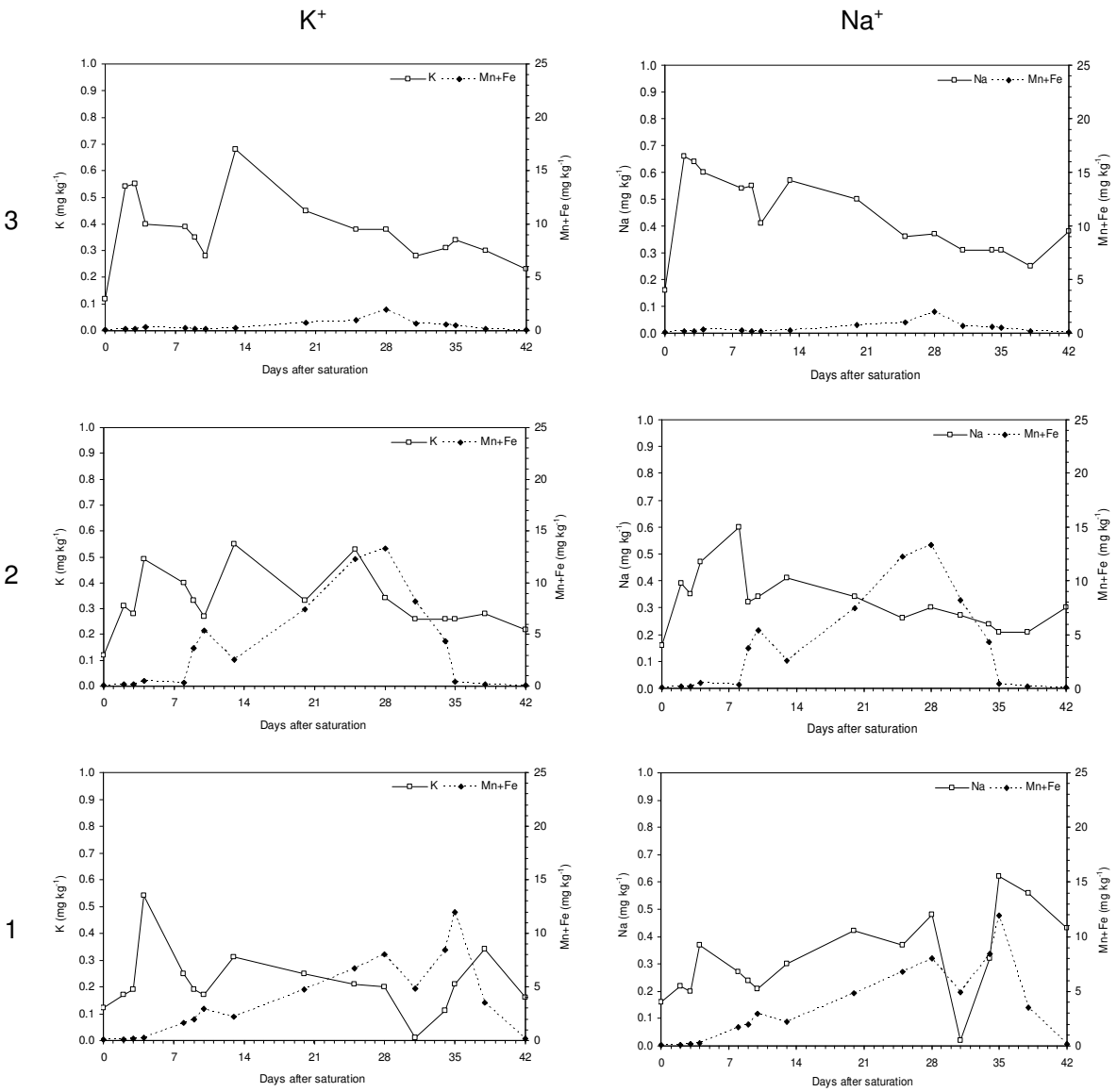

Figure 5.8 K^+ and Na^+ concentration and pe + pH values for segment 1 (0.0 - 0.1 m), segment 2 (0.1 - 0.2 m) and segment 3 (0.2 - 0.3 m) over a 42 day period, with segment 1 being the bottom of the column.

5.3.2 Column wetted by suction

The extraction of water from a soil column wetted by capillary rise proved to be unsatisfactory in relation to the data required to fulfill the aims of this study. The extraction process was too slow and an insufficient sample volume was retrieved for segments with S<0.9 for routine determination. It was thought that the tensiometer cups were not making sufficient contact with the soil thereby making it difficult to extract the water. After one month there were no signs of wetness at the top of the column indicating limited movement of water into the column by capillary rise. This inhibited soil water extraction by the tensiometer cups.

A second column was built in an attempt to accelerate the wetting process by creating a vacuum at the top of the column. Fine silica powder was placed around each tensiometer cup, when inserted into the column. The purpose of the silica powder was to promote good contact between the soil and the ceramic of the tensiometer cup and therefore a greater water flux into the ceramic cup. The column was set up in the exact manner as the previous column. The column was first wetted through capillary rise. A total of 4 ℓ of water was needed to saturate the whole column, and after 6 days only 177 cm^3 water entered the column through capillary rise. Suction was then applied to the top of the column.

A sealed lid was placed at the top of the column and a suction of -85 kPa was then applied. The suction proved to be too strong and soil was sucked into the system. After the first suction attempt, 1 925 cm^3 water was sucked into the column. Another attempt was made to increase the amount of water in the column by lowering the suction to -50 kPa and then finally to -10 kPa. This was abandoned due to more soil entering into the system at both suctions. Due to the fact that the top segment was wet it was assumed that the rest of the column had been wetted.

Soil water was extracted in the same manner as in the first column. The extraction was done under suction through a vacuum (-85 kPa) with a direct couple from the tensiometers in the soil column, not using a manifold as in the previous column. Soil water could be extracted at 70 $cm^3\ h^{-1}$ below the water table. It seemed that the silica flour packed around each tensiometer cup had promoted contact between the soil and the ceramic. The volume of soil water extracted above the water table was, however, still insufficient for analyses. The permanent nature of the column set up made it difficult to determine at which degree of saturation each segment was during the extraction process. Continual feeding of the

column with distilled water was inadequate for studying redox due to the continual introduction of O_2 through the applied water, therefore this method needed reviewing.

The full data set for the column wet through suction is given in Appendix C, Table C1.

5.4 Summary

The aim of this experiment was to determine the extent to which water could be extracted from all segments in a soil column wetted through capillary rise. It was thought that the degree of water saturation would decrease from the bottom of the column upwards. Once the water was extracted it could be analysed to determine if and when reduction took place through the measurement of Eh, pH, Mn^{2+}, Fe^{2+}, Ca^{2+}, Mg^{2+}, K^{+} and Na^{+}.

An artificial soil column was constructed by packing the soil in a PVC pipe, 1 m high, and 0.104 m in inner diameter. The complete column consisted of ten 0.1 m sections sealed with silicon sealant and held together with duct tape. The column was packed to a bulk density of 1.6 Mg m^{-3}. The bottom of the column was sealed with a PVC base and silicon sealant. A water table was established at 0.3 m and kept constant by means of a Marriott bottle.

Capillary rise was very slow through the column. The first extraction took place 3 days after water saturation. Water could only be sufficiently extracted from the first three segments and from the fourth one with difficulty, even though the fourth segment was below the water table. Thirty nine days after wetting of the column started, extraction rates through the ceramic tensiometers cups were approximately 1 cm^3 h^{-1} from 0.1 m below the water table. This was too slow for routine analyses. After 42 days there were no signs of wetness at the top of the column, and the experiment was terminated. The column was left intact for 7 months, after which there was still no sign of wetness at the top of segment 10. This slow water movement contributed to the difficulty in soil water extraction.

There was a good relationship between a decrease in pe and an increase in pH in all three segments analysed. The Mn^{2+} and Fe^{2+} concentrations were also well correlated with pe. A decrease in pe + pH lead to an increase in the Mn^{2+} and Fe^{2+} concentration in all the segments. An increase in Ca^{2+}, Mg^{2+}, K^{+} and Na^{+} was correlated with an increase in Fe^{2+} and Mn^{2+} concentration. The increase was attributed to increased competition between cations for the negatively charged sites on the clay complex due to increased levels of Mn^{2+} and Fe^{2+} in the soil solution under reducing conditions.

After 7 months the column was cut into 0.1 m sections. All the segments were moist except the top segment. No colour or morphological feature changes had occurred in the soil. The lack of development of morphological features could be due to the low degree of water saturation or the lack of a fluctuating degree of water saturation which would lead to alternating oxidation and reduction cycles.

A second soil column was built in an attempt to accelerate the wetting process by creating a vacuum at the top of the column. It was thought that the tensiometer cups had not made sufficient contact with the soil to ensure a sufficient flow of soil water from the soil matrix into the tensiometer cups. Silica flour, which has a very fine texture, was thought to enhance the movement of water from the soil matrix into the tensiometer cup. The suction was applied to the top segment through a -85 kPa suction pump. This proved too strong and was lowered in phases to around -10 kPa, which still proved to be too strong as it sucked muddy water into the pump system. After the suction was applied, the top of the column was sufficiently wetted and extraction of soil water through tensiometer cups commenced.

Extraction of soil water still proved to be too difficult. The extraction process through tensiometer cups was too slow even though the silica flour around the tensiometer cups aided slightly. It was also thought that a continual feeding of distilled water into the column, as water was extracted, would tend to neutralize any tendency to reduce due to the continual introduction of oxygenated water.

The saturation of a soil column through capillary rise was deemed unpractical for the analyses of redox conditions at different degrees of water saturation, because very little soil solution could be extracted below the water table and no water could be extracted above it. Another problem with this column method was that there was no way to determine what the exact degree of water saturation of the segments was during the extraction process.

It was decided to change the experimental setup to single cores, each with its unique degree of water saturation. *In situ* Eh measurements would be done. pH would be measured by making a soil solution and the soluble cations leached from a representative soil sample of each core. It was also determined that creating a decreasing degree of wetness in a column needed more research as it had been unsuccessful on two occasions. The methodology for the single core method is discussed in the next chapter.

CHAPTER 6

EFFECT OF DURATION AND DEGREE OF WATER SATURATION ON IRON, MANGANESE AND SELECTED BASIC CATIONS

6.1 Introduction

In natural soils, redox potential (Eh) varies widely over time, thus continuous *in situ* measurements are preferable to trace Eh. Continuous Eh measurements are of great importance as Eh is an important parameter used to study transformation and translocation processes of redox sensitive elements (Fiedler *et al.,* 2007).

It was determined by two separate experiments that column analyses of redox was inadequate to meet the aims set out in the study. It was thought that the validity of investigations into soil redox using Eh data acquired solely in soil suspensions was limited due to the artificial conditions established once the soil solution was extracted. The soil solution was subjected to atmospheric O_2 during extraction therefore creating a greater margin of error.

It was decided to change the experimental set up to single cores, each with their own degree of water saturation. Soil cores were packed to a bulk density of 1.6 Mg m^{-3} and saturated to four different degrees of water saturation, namely $S_{0.6}$ (60% of pores saturated with water), $S_{0.7}$ (70% of pores saturated with water), $S_{0.8}$ (80% of pores saturated with water), and $S_{0.9}$ (90% of pores saturated with water). Eh was measured *in situ* and pH (H_2O) was measured from a representative soil sample taken from the core. A separate soil sample was leached with ammonium acetate (NH_4OAc) and analysed using atomic absorption spectroscopy to determine the Mn^{2+}, Fe^{2+}, Ca^{2+}, Mg^{2+}, K^+ and Na^+ concentrations.

6.2 Material & methods

6.2.1 Single core

Soil from the combined yellow brown apedal B1 and B2 horizon described in Chapter 4 was used in the core analyses. A core was constructed by packing the soil in a PVC pipe, 0.1 m high and 0.104 m in diameter. Extreme caution was taken not to create layers of varying bulk densities during the packing process. A thin metal rod was used to break up layers

while packing and the core was constantly turned over in order to prevent the particle sizes from separating.

The volume of a core was derived from the equation:

$$V_s = \pi r^2 h \quad (6.1)$$

Where:

V_s = volume (m^3)

r = radius (m)

π = pi

h = height (m)

The volume of the core was therefore 0.00085 m^3.

From the volume of the core (V_s) and the desired bulk density (ρ_b), the mass of the dry soil (M) needed for each core sample was calculated:

$$M = \rho_b \times V_s \quad (6.2)$$

= 1.36 kg per segment

The correct amount of distilled water needed to bring each individual core to the desired degree of water saturation (Table 6.1) was obtained by equation 5.3:

$$\text{Water Volume} = \text{fraction} \times (1 - (p_b \div p_s)) \quad (6.3)$$

Where:

Fraction = $S_{0.6}, S_{0.7}, S_{0.8}, S_{0.9}$

p_b = Bulk density (1.6 Mg kg^{-1})

p_s = Particle density (2.65 Mg kg^{-1})

The water used to saturate the cores was distilled freshly and stored at room temperature (23℃). The storage container prevented any air from diffusing into the water. This method was used to ensure that the O_2 content of the water added to the cores was constant and kept minimal.

Table 6.1 Volume of water needed to bring cores to correct degree of water saturation when packed to a bulk density of 1.6 Mg m^{-3}

Degree of saturation	Fraction of water per core	Water volume added per core (cm^3)
$S_{0.9}$	0.36	306
$S_{0.8}$	0.31	263
$S_{0.7}$	0.28	238
$S_{0.6}$	0.24	204

The cores were brought to these specific degrees of water saturation through capillary rise. A piece of damp cheesecloth was attached to the bottom of the core and the core was put in a dry container. The correct amount of distilled water was then added to the container and was allowed to seep into the core. It was determined that the water redistributed to the middle of the column within 5 minutes. Once all the water had been absorbed, the top and bottom of the core was covered with a double layer of plastic wrap, and sealed tightly with elastic bands. It was determined by a trial experiment that no significant evaporation took place through the plastic wrap.

To determine if the proposed methodology used in the core method would allow for sufficient reduction, two core samples were prepared as described above. One core was saturated to $S_{0.9}$ with distilled water while the other was left air-dry. The saturated core was covered with plastic wrap and sealed with elastic bands to prevent air moving into the core. After 10 days, soil was excavated from the two cores and divided into two batches. One batch was leached with alcohol and one with distilled water, to determine which would produce the best results. Extractions were done in triplicate. The results are presented in Table 6.2.

The results for the H_2O extraction indicated that there was a definite increase in Fe^{2+} concentration from the air-dry soil to the saturated soil. The average Fe^{2+} concentration observed in the H_2O extraction after saturation was 0.70 mg kg^{-1} whereas the air dry soil only yielded an average Fe^{2+} concentration of 0.15 mg kg^{-1}. The alcohol extraction did not deliver results for Fe^{2+} and therefore the results were not interpreted. The soluble Fe^{2+} leached with H_2O could only have been released through reduction. It was therefore concluded that single core analyses were suitable to study redox processes in a disturbed soil.

Table 6.2 Soluble cation extractions using alcohol and distilled water, from an air-dry and saturated core

		Replication	Mn	Fe	Ca	K	Mg	Na
			(mg kg^{-1})					
H_2O extraction	Air-dry	1	0.32	0.17	52.10	24.60	46.50	16.50
		2	0.85	0.14	59.32	34.50	45.25	15.25
		3	0.25	0.15	45.50	35.65	42.58	15.25
		Average	0.47	0.15	52.31	31.58	44.78	15.67
	Saturated	1	0.00	0.57	62.58	33.54	44.89	16.25
		2	0.00	0.93	61.25	34.69	43.54	17.25
		3	0.00	0.59	55.58	33.38	45.58	16.24
		Average	0.00	0.70	59.80	33.87	44.67	16.58
Alcohol extraction	Air-dry	1	0.00	0.00	91.25	20.15	38.58	16.25
		2	0.00	0.00	81.32	15.82	39.50	18.25
		3	0.00	0.00	78.58	19.58	42.58	15.58
		Average	0.00	0.00	83.72	18.52	40.22	16.69
	Saturated	1	0.00	0.00	92.35	22.25	38.58	14.25
		2	0.00	0.00	85.21	26.35	39.58	13.25
		3	0.00	0.00	81.36	25.25	42.25	14.55
		Average	0.00	0.00	86.31	24.62	40.14	14.02

A test experiment was set up to determine what leachate would produce the best results when leaching the soil sample. Soil from the mixed B1 + B2 soil horizon was used. A dry sample as well as a sample that had been saturated for 30 days was used. Three different extractant methods were used to test for Mn^{2+}, Fe^{2+} and basic cations. The extraction methods tested were distilled H_2O, ammonium acetate (NH_4OAc) and diethylenetriaminepentaacetate (DTPA).

The water extraction yielded Fe^{2+} in the air-dry as well as the saturated soil (Table 6.3); this is also confirmed in Table 6.2. The DTPA method yielded the highest amount of Fe^{2+} in the saturated soil as well as in the air-dry soil. It was decided that leaching for the duration of the experiment would be done with NH_4OAc as it extracted only the reduced Fe^{2+} and yielded no Fe in the air-dry soil.

Table 6.3 Three methods used to extract soluble Mn^{2+}, Fe^{2+} and cations

		Replication	Mn	Fe	Ca	K	Mg	Na
			(mg kg^{-1})					
H_2O extraction	Air-dry	1	1.25	0.58	48.75	28.80	45.31	15.74
		2	0.25	0.15	61.50	35.50	43.51	17.54
		3	0.25	0.25	55.80	33.30	41.50	14.65
		Average	0.58	0.32	55.35	32.53	43.44	15.98
	Saturated	1	0.00	5.25	66.30	34.80	44.32	15.55
		2	0.00	7.00	59.10	33.72	42.82	17.35
		3	0.00	6.75	58.81	37.80	44.33	16.35
		Average	0.00	6.33	61.40	35.44	43.82	16.42
Ammonium Acetate	Air-dry	1	0.50	0.00	89.90	39.52	51.32	15.52
		2	0.50	0.00	78.90	44.80	51.95	17.38
		3	0.25	0.00	85.80	38.53	53.33	21.28
		Average	0.42	0.00	84.87	40.95	52.20	18.06
	Saturated	1	1.51	25.50	91.80	42.85	53.30	22.56
		2	1.48	17.75	88.58	41.50	54.14	18.53
		3	1.50	19.25	89.82	38.20	52.87	21.89
		Average	1.50	20.83	90.07	40.85	53.44	20.99
DTPA	Air-dry	1	0.48	6.48	738.00	4.40	48.00	24.00
		2	0.44	6.40	754.00	4.46	50.00	24.20
		3	0.46	6.46	726.00	4.54	44.00	23.80
		Average	0.46	6.45	739.33	4.47	47.33	24.00
	Saturated	1	1.42	26.12	700.00	5.60	50.00	22.20
		2	1.64	27.26	716.00	5.96	50.00	22.20
		3	1.52	29.46	704.00	5.90	48.00	22.80
		Average	1.53	27.61	706.67	5.82	49.33	22.40

Once the trial experiment was conducted and it was ensured that the experiment would be successful, the main experiment was set up. The experiment consisted of a set of 4 cores packed to an initial bulk density of 1.6 Mg m^{-3} with three replications. Each core was subjected to a different degree of water saturation, i.e., $S_{0.6,}$ $S_{0.7,}$ $S_{0.8}$ and $S_{0.9}$. A laboratory temperature of 23°C and a core temperature of 22°C was maintained with a fluctuation of not more than 2°C. The experiment was terminated after 121 days.

Analysis of the cores started 3.5 days after initial water saturation. Eh was measured directly in the soil core. The plastic wrap was kept on the core throughout the measurements to minimize O_2 diffusion.

The redox electrode used to measure the Eh was a platinum (Pt) electrode with a separate Ag/AgCl reference electrode with an electrolyte solution of 3.5 M KCl (Figure 6.1). The Pt electrode was built by Prof. H. P. Blume at the University of Kiel (Jahn *et al*., 2003). A Pt wire was welded on a copper (Cu) wire which was connected to a Cu lead. A PVC casing was placed around the copper lead and allowed a 2 mm Pt tip to protrude from the casing.

The Pt was the only metal that had contact with the solution in which the electrode was placed. The casing was then sealed and filled with a waterproof resin to prevent the copper wire from moving around in the casing. The copper wire was then fitted with a male connector that could fit on to a millivolt meter. This electrode design similar to electrodes used in Muellar *et al*. (1985) and Faulkner *et al*. (1989).

The Eh measurements took place by driving a hole through the plastic wrap into the soil using a glass rod 2 mm greater than the redox electrode to a depth of 40 mm, about 10 mm less than the desired measuring depth. The redox electrode was then inserted through this hole and the Pt tip was then pushed about 10 mm deeper into the soil to ensure a good soil/Pt contact.

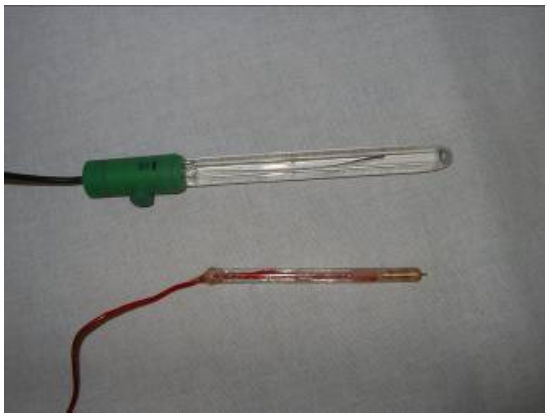

Figure 6.1 Glass Ag/AgCl reference electrode with accompanying Pt redox electrode.

The calibration of the Pt electrode used in this experiment was performed by using Hanna instruments HI7020 redox solution (Potassium Hydrogen Phthalate (877-24-7); Quinhydrone (106-34-3)) having a redox potential of between 200 - 270 mV at 25℃ (Patrick *et al*., 1996). No drifting of the Pt electrode occurred through the 121 days.

The Pt surface of the redox electrode was cleaned with sandpaper immediately before inserting it into the soil. The reference electrode was inserted in the middle of the core and kept in place while the Pt electrode was moved around for 3 replicate measurements (Figure 6.2).

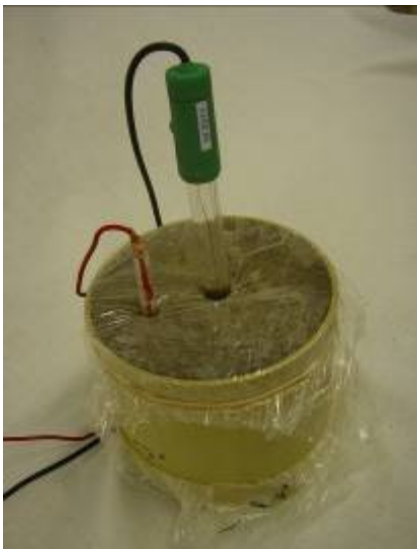

Figure 6.2 Glass Ag/AgCl reference electrode is placed in the middle of the core with the accompanying Pt redox electrode moved around to the desired area in the core.

The electrode was allowed to stabilize before a measurement was taken, this usually took between 10 to 30 minutes per replication. The more reduced the soil, the longer the electrode took to stabilize. Hanna instruments pH 221 microprocessor pH meter was used to measure the Eh against the reference electrode.

The results were interpreted by calculating pe values (Equation 5.4):

$$pe = \frac{Eh(mV)}{59} \tag{6.4}$$

The pH was determined by making a soil solution of 20 g soil to 50 cm^3 distilled water (1:2.5 soil:water ratio). The volume of water in each sample was taken into account (Table 6.4) and the weight of the soil was corrected accordingly. Once the soil was added to the distilled water it was stirred and allowed to stand for 30 minutes.

Table 6.4 Amount of water needed to correct water volume for pH determination to ensure a 1:2.5 soil water ratio

Degree of saturation	Fraction of water	Mass of water (g)	Mass of soil + water (g)
$S_{0.9}$	0.36	7.1	27.1
$S_{0.8}$	0.31	6.2	26.2
$S_{0.7}$	0.28	5.6	25.6
$S_{0.6}$	0.24	4.8	24.8

Extraction of Mn^{2+}, Fe^{2+}, Ca^{2+}, Mg^{2+}, K^{+} and Na^{+} was done using 12.5 g of soil (The non-affiliated soil analysis work committee, 1990). The weight of soil was corrected to compensate for the soil's degree of water saturation. A representative soil sample from each core was leached with 250 ml NH_4OAc. The sample was taken by excavating four samples from a depth of approximately 50 mm. To prevent the Fe^{2+} from oxidizing, 5 cm^3 HCl was added to the leached soil solution (Weaver, 1992; Franson *et al.*, 1995). . The Mn^{2+} and Fe^{2+} concentration, as well as the soluble cation concentrations (Ca^{2+}, Mg^{2+}, K^{+} and Na^{+}) were determined by atomic absorption spectrometry (AAS).

For the first three months a set of cores (four degrees of saturation with three replications each) were analysed every 3.5 days, thereafter analyses were done once per week (every 7 days) for a month. The experiment was done in triplicate, giving 336 cores for the duration of the experiment. Once all data was collected from the individual cores, the cores were discarded and a new set of cores was used for the next day's measurements. A total of 408 cores were packed, enough for the experiment to last 6 months (Figure 6.3).

Temperature corrections were not considered necessary as the laboratory temperature was constant at 23 ℃ ±2 degrees over the 121 days of analyses. An adjustment to pH 7 was also not carried out. Data was statistically analysed and the analysis of variance was computed at a 95 % confidence level using the NCSS software package of Hintze (1997). Significant differences between averages were determined using the analysis of variance (ANOVA) procedure.



Figure 6.3 The 408 soil cores stored at a constant temperature (23°C).

6.2.2 Column wet by suction

After 330 days, the column described in Chapter 5 was cut up into 100 mm sections. The sections were immediately covered with a double layer of plastic wrap to prevent any changes in redox state. The separate cores were analysed for soil degree of water saturation, Eh, pH, Mn^{2+}, Fe^{2+}, Ca^{2+}, Mg^{2+}, K^{+} and Na^{+}. Eh was determined *in situ*, pH, Mn^{2+}, Fe^{2+}, Ca^{2+}, Mg^{2+}, K^{+} and Na^{+} concentrations were determined following the same procedure as for the single core method. Soil colour was read using a Munsell colour chart in the dry and wet state. Results are discussed in section 6.3.2.

6.3 Results & discussion

6.3.1 Single core

The analyses of variance was computed at a 95 % confidence level using the NCSS software package of Hintze (1997). The significant effects of degree of water saturation and duration of water saturation are represented in Table 6.5.

Table 6.5 Summary of the analyses of variance indicating the significant effects on pH, Eh, Mn^{2+}, Fe^{2+}, Ca^{2+}, Mg^{2+}, K^{+} and Na^{+} at a 95% confidence level

Treatments[a]	pH	Eh	Mn^{2+}	Fe^{2+}	Cations			
					Ca^{2+}	Mg^{2+}	K^{+}	Na^{+}
A	*	*	*	*	*	*	*	*
B		*	*	*		*		*
AB	*	*	*	*	*	*	*	*

[a] A: Duration of saturation, B: Degree of saturation, AB: Duration of saturation and degree of water saturation

The full data set for $S_{0.6}$ (Table D1), $S_{0.7}$ (Table D2), $S_{0.8}$ (Table D3) and $S_{0.9}$ (Table D4) is given in Appendix D. These as well as the ANOVA results are discussed separately in the following sections.

6.3.1.1 pH

The pH data represented in Figure 6.4 is the average of each set of replications for the duration of water saturation. Each data point was calculated from 30 measurements over a period of 121 days. Each data point per replication was taken at the same degree of water saturation, although they were horizontally slightly spread out to aid in a better understanding of the graph. The data represented in Figure 6.5 is an average of three daily replications.

The soil's average pH before water saturation was 5.1. At the end of 121 days of water saturation at $S_{0.6}$ the average pH was 4.86, $S_{0.7}$ had an average of 4.84, $S_{0.8}$ an average of 4.81 and $S_{0.9}$ had an average pH of 4.85. The average pH decreased in all the cores once the cores were saturated. The standard deviation increased with an increase in degree of water saturation although the pH between the treatments did not differ significantly (Table 6.5). Therefore degree of water saturation did not play a role in the pH of the soil, although the treatments differed significantly over the duration of saturation (Table 6.5). In Figure 6.5 the pH increased and decreased over time. The standard deviation's between the $S_{0.6}$ and $S_{0.7}$ treatments were very similar, whereas the standard deviation increased in the cores saturated to $S_{0.8}$ and $S_{0.9}$. The greater standard deviation was due to the increased redox activity in the higher water saturations, and thereby the possibility for increased occurrence of microsites. The pH of a soil tends towards 7 when reduction takes place as H^+ ions are used in reducing reactions (Glinski & Stepniewski, 1985).

One can therefore conclude that for this soil, at a bulk density of 1.6 Mg m^{-3}, pH was not affected by the degree of water saturation, although it did change significantly over time in all the treatments. Even though the pH was not affected by degree of water saturation, the standard deviation increased with an increase in water saturation. This was due to the fact that H^+ ions were used in reducing reactions, thereby increasing the pH, and causing a greater standard deviation in the$S_{0.9}$ treatment than in the $S_{0.6}$ treatment, were no reduction took place.

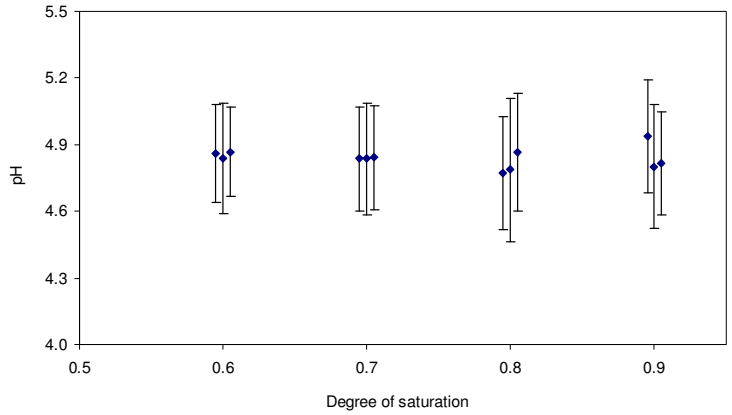

Figure 6.4 Average pH and standard deviation of three sets of replications consisting of 30 measurements over a period of 121 days.

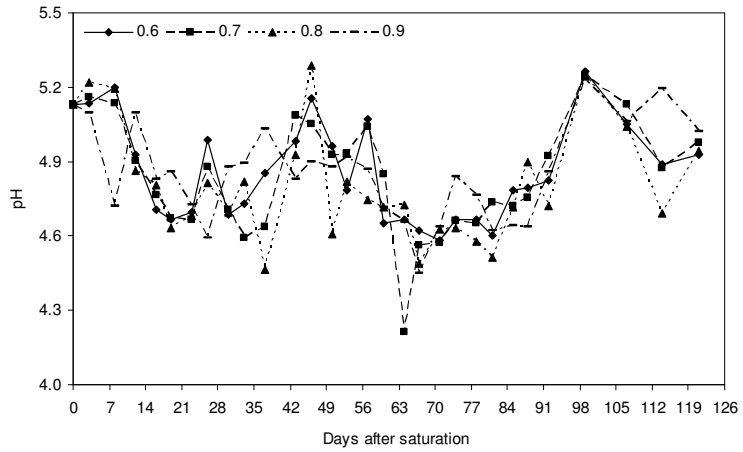

Figure 6.5 pH for all degrees of water saturation over a period of 121 days.

6.3.1.2 pe

The redox potential (Eh) varied markedly during the study (Table 6.6). The average and minimum Eh values decreased as the degree of water saturation decreased. The maximum values of all the treatments were very similar. This was anticipated as the soil did not reduce immediately after water saturation. The range and standard deviation of pe in the cores increased with an increase in degree of water saturation. This was due to the increased redox potential in the higher water saturations. An increased redox potential increased the instances of microsites, which in turn increased the standard deviation. The redox status of a soil is divided into four groups by Mansfeldt (2003). According to Mansfeldt's (2003) groups, the $S_{0.6}$ and $S_{0.7}$ cores were oxidised and the $S_{0.8}$ and $S_{0.9}$ cores were only weakly reduced. This could have been as a result of the low organic matter

content (0.22%) of the cores which prevented the cores from reducing more. The minimum pe of $S_{0.9}$, which was 2.10 units, was only moderately reduced.

It must be kept in mind that the effect of water saturation on Eh is indirect. Once O_2 diffusion is impaired through a high degree of water saturation, and then depleted by microbes, alternate electron acceptors are used. It is the reduction of these alternate electron acceptors that is accompanied with a decrease in Eh (Mansfeldt, 2003)

Table 6.6 Eh statistics for the degree of saturation experiment over a 121 day period

Degree of saturation	Average[a]	Minimum	Maximum	Range	std dev	Redox status[b]
	(----------mV----------)					
$S_{0.6}$	449	398	463	65	17	I
$S_{0.7}$	421	354	455	101	28	I
$S_{0.8}$	326	216	464	248	59	II
$S_{0.9}$	247	124	439	315	72	II

[a] Data calculated from 90 measurements over a period of 121 days; [b] I; oxidizing (>400 mV); II, weakly reducing (400 to 200 mV); III, moderately reducing (200 to -100 mV); IV, strongly reducing (<-100 mV) from Mansfeldt (2003)

To aid in better interpretation and correlation the Eh was interpreted through pe, when compared to Fe^{2+}, Mn^{2+}, Ca^{2+}, Mg^{2+}, K^+ and Na^+. The average pe for a degree of water saturation was calculated from 90 measurements over a period of 121 days (Figure 6.6).

The pe remained stable in the $S_{0.6}$ treatment throughout the saturation period (Figure 6.7). As the degree of water saturation increased, the pe decreased and the standard deviation increased (Figure 6.6). An increase in the fluctuations in pe and therefore the standard deviation can be related to an increase in redox activity, and an increase in the occurrence of microsites.

Callebaut *et al*. (1982), found that Eh correlated with O_2 at low O_2 concentrations (6 to 15%) but not at higher O_2 concentrations (>15%) and stated that Eh measurements did not reflect the soil aeration status in oxygenated environments. Mansfeldt (2003) also found that Eh fluctuations in oxidizing conditions were limited, and stated that performing long-term measurements of soil Eh in an oxidizing environment is not meaningful. The reason for this is that in an O_2 dominated environment, the Pt surface absorbs O_2 thus creating a PtO surface. The Pt surface acts as an oxide electrode that has the function of the hydrogen electrode. Thus, the electrode responds to pH rather than to O_2 at partial pressure

(Whitfield, 1969). Therefore the lack of an Eh reading in the $S_{0.6}$ and $S_{0.7}$ treatments could be due to the Pt electrode not functioning optimally in an oxiginated environment.

There was a good linear relationship (R^2 = 0.95) between pe and the degree of water saturation. Pe decreased on a linear scale with every increase in degree of water saturation (Figure 6.6). A polynomial trend line produced a better fit with R^2 = 1.00, but it was decided to use the linear trend line to facilitate interpretation.

According to the summary of the analysis of variance in Table 6.5, the Eh was significantly affected by degree of water saturation as well as time. In the $S_{0.8}$ and $S_{0.9}$ treatment the pe decreased with duration of water saturation after which it increased. This was in agreement with Mansfeldt (2003) who found that Eh decreased over time. The increase in pe after 90 days was probably due to depletion of the available organic carbon substrate for microbes. The pe remained stable over time in the $S_{0.6}$ and $S_{0.7}$ values.

It can therefore be concluded that this soil with a bulk density of 1.6 Mg m^{-3} will not reduce significantly at a water saturation of $S_{0.7}$ or lower. Significant reduction started at a point between $S_{0.7}$ and $S_{0.8}$.

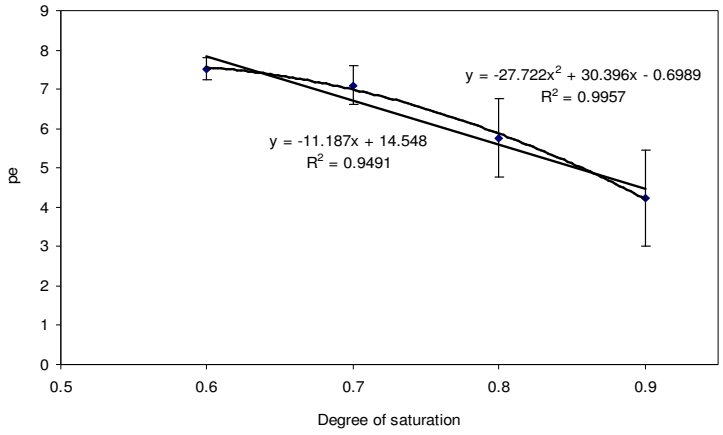

Figure 6.6 Average pe and standard deviation for 90 measurements over a period of 121 days showing a polynomial (R^2 = 1.00) as well as a linear (R^2 = 0.95) trend line.

$S_{0.6}$

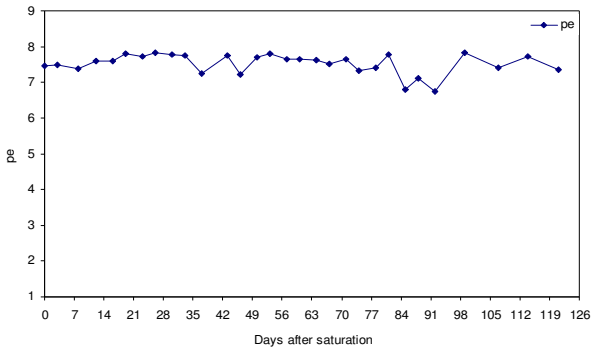

$S_{0.7}$

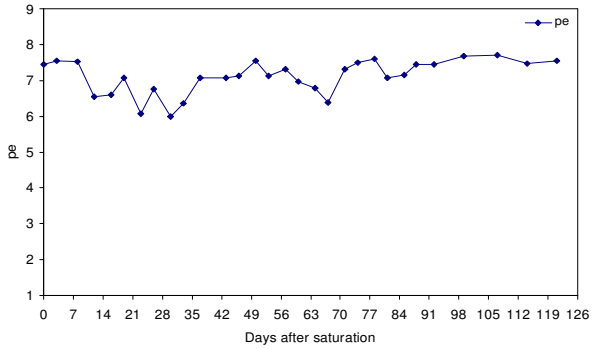

$S_{0.8}$

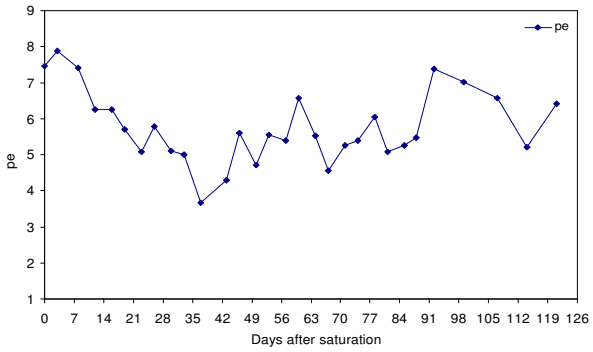

$S_{0.9}$

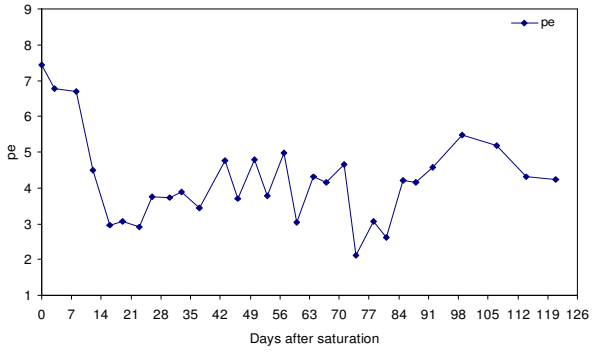

Figure 6.7 pe values for the $S_{0.6,\ 0.7,\ 0.8,\ 0.9}$ during the 121 day period.

6.3.1.3 Manganese

The Mn^{2+} data represented in Figure 6.8 is the average of each set of replications for the duration of water saturation. Each data point was calculated from 30 measurements over a period of 121 days. Each data point per replication was taken at the same degree of water saturation, although they were horizontally slightly spread out to aid in a better understanding of the graph. The data represented in Figure 6.9 is an average of three daily replications and Figure 6.10 represents the Mn^{2+} concentration in each degree of saturation over 121 days showing the relationship with pe+pH and pH.

The Mn^{2+} concentration was significantly influenced by degree of water saturation (Table 6.5). There was a good relationship ($R^2 = 0.91$) between an increase in Mn^{2+} concentration and an increase in the degree of water saturation (Figure 6.8). The soil's average NH_4OAc extractable Mn^{2+} concentration before as well as after 121 days of water saturation was 0.7 mg kg^{-1}. The soil's Mn^{2+} concentration therefore did not change over time. The core saturated to $S_{0.7}$ had an average of 0.8 mg kg^{-1}; $S_{0.8}$ an average of 0.9 mg kg^{-1} and $S_{0.9}$ had an average Mn^{2+} concentration of 1 mg kg^{-1}. The highest Mn^{2+} fluctuations were recorded in the core saturated to $S_{0.9}$ (Figure 6.10). A poor relationship was found between Mn^{2+} concentration and the pe as well as the combined pe + pH values for all the treatments although the relationship improved in the $S_{0.8}$ and $S_{0.9}$ cores. A better relationship was found to exist between the Mn^{2+} concentration and pH in all the treatments (Figure 6.10). Mn^{2+} concentration is very sensitive to pH and becomes more soluble as the pH decreases. The average pH over the duration of the experiment was 4.84 units, which is a low pH for a soil. This is also the reason why the Mn^{2+} was in solution for the duration of the experiment.

The lack of a relationship between fluctuations of Mn^{2+} concentration and pe in the lower degrees of water saturation could be due to the inadequate performance of the Pt electrode in an oxygenated environment. The Pt electrode was therefore not sensitive enough to pick up fluctuations in Eh that could have been related to increases or decreases in the Mn^{2+} concentration. This lead to the inability to relate pe to Mn^{2+} concentration in the $S_{0.6}$ and $S_{0.7}$ cores.

The behavioral pattern of Mn in the soil for the $S_{0.6}$, $S_{0.7}$ and $S_{0.8}$ was very similar (Figure 6.9), and had a similar standard deviation (Figure 6.8). It was only the $S_{0.9}$ that differed from all the rest according to the Tukey-Kramer Multiple-Comparison Test (Hintze, 1997). In the $S_{0.9}$ core, the maximum levels of Mn^{2+} increased significantly (Table 6.5) over time. The

average standard deviation between the $S_{0.6}$, $S_{0.7}$, and $S_{0.8}$ remained an average of 0.2 where in $S_{0.9}$ the average standard deviation increased to 0.3 (Figure 6.8).

The duration of water saturation had a significant influence on the Mn^{2+} concentration (Table 6.5). The maximum levels of fluctuation increased with increased degree as well as duration of water saturation (Figure 6.11). In the $S_{0.6}$, $S_{0.7}$, and $S_{0.9}$ treatments the Mn^{2+} concentration was not affected as much by duration of water saturation as the $S_{0.9}$ treatment. The Mn^{2+} concentration did not stabilize in any of the treatments as fluctuations were continually occurring.

It could therefore be concluded that for this soil, packed to a bulk density of 1.6 Mg m^{-3}, Mn^{2+} is active in all the water saturation treatments. The Mn^{2+} concentration increased with an increase in degree of water saturation and time. The Mn^{2+} was in solution for the duration of the experiment in all water saturation treatments and therefore no point where reduction ceased or slowed down can be coupled to Mn^{2+}. The Mn^{2+} concentration reacted inversely to the pH of the soil. Mn^{2+} becomes more soluble at lower pH values. A decrease in pH caused an increase in Mn^{2+} concentration. This relationship between pH and Mn^{2+} concentration was more apparent as the degree of water saturation increased.

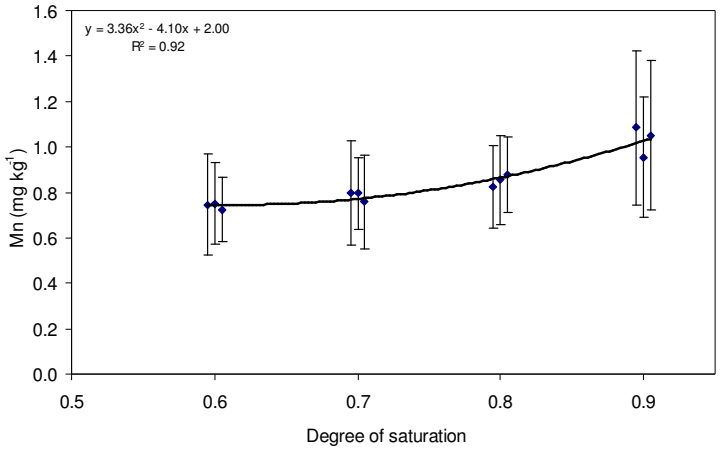

Figure 6.8 Average Mn^{2+} concentration and standard deviation of three sets of replications consisting of 30 measurements each over a period of 121 days.

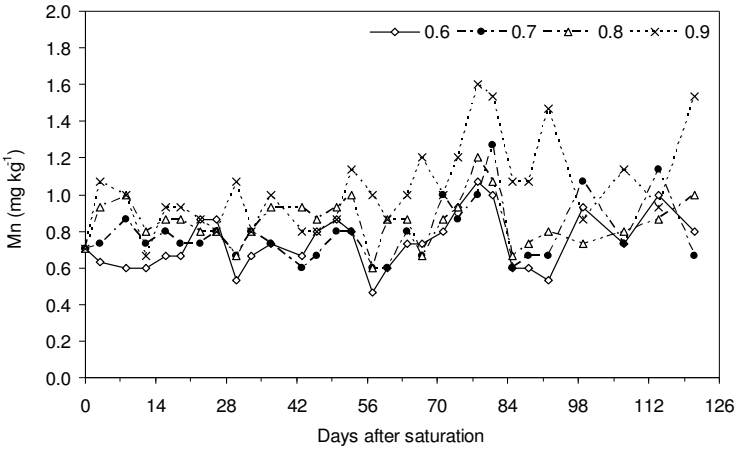

Figure 6.9 Mn^{2+} for all degrees of water saturation over a period of 121 days.

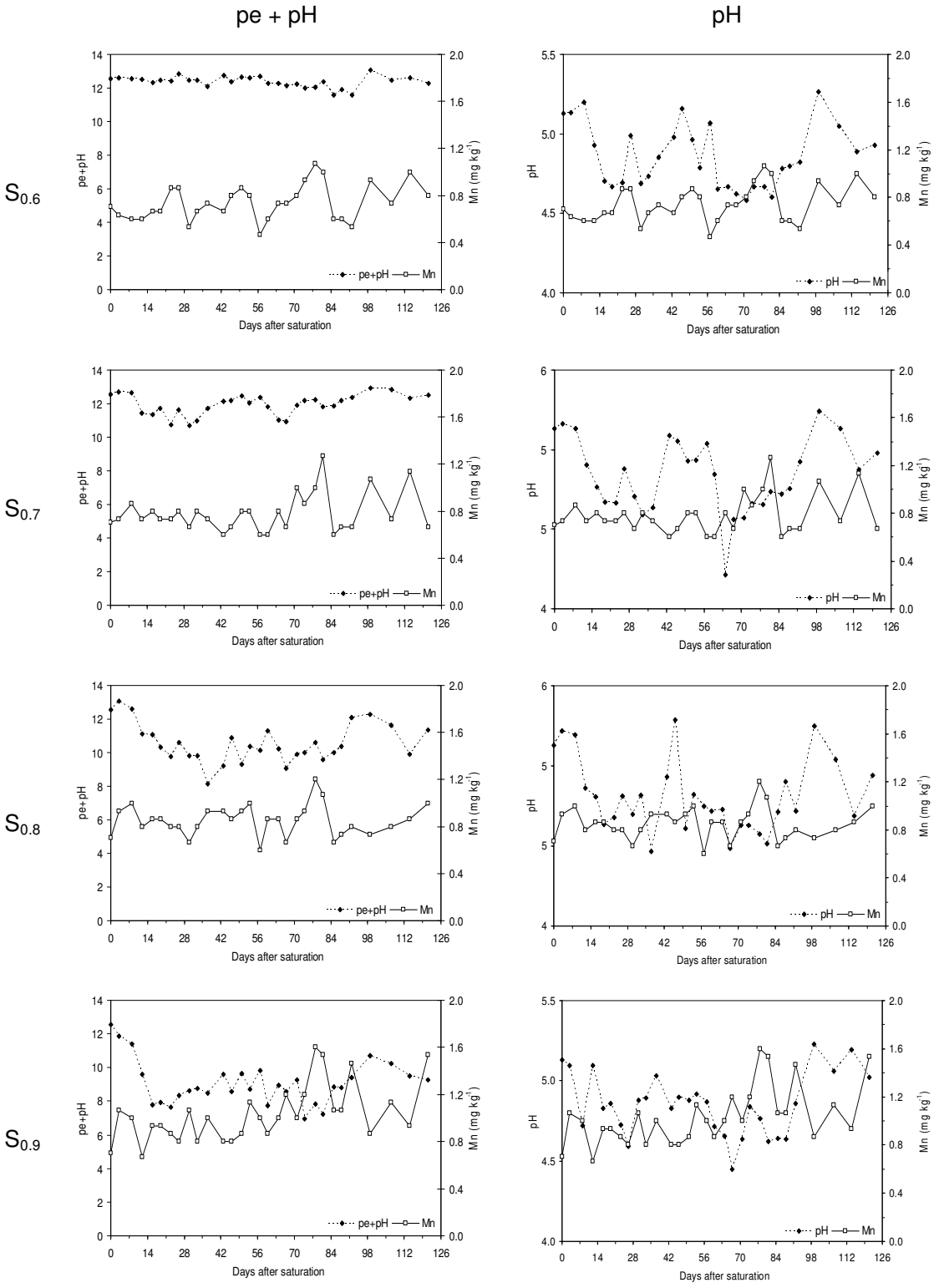

Figure 6.10 Mn^{2+} concentration and pe + pH as well as the pH values for $S_{0.6,\ 0.7,\ 0.8,\ 0.9}$ during the 121 day period.

6.3.1.4 Iron

The Fe^{2+} data represented in Figure 6.11 is the average of each set of daily replications for the duration of water saturation. Each data point was calculated from 30 measurements over a period of 121 days. Each data point per replication was taken at the same degree of water saturation, although they were horizontally slightly spread out to aid in a better understanding of the graph. The data represented in Figure 6.12 is an average of three daily replications.

The Fe^{2+} concentration was significantly influenced by degree of water saturation (Table 6.5), and increased exponentially ($R^2 = 0.92$) with an increase in degree of water saturation (Figure 6.12). The average Fe^{2+} concentration before water saturation was 0.9 mg kg^{-1}. At the end of 121 days of water saturation at $S_{0.6}$ the average Fe^{2+} concentration was 2.36 mg kg^{-1}, $S_{0.7}$ had an average of 4.64 mg kg^{-1}, $S_{0.8}$ an average of 9.33 mg kg^{-1} and $S_{0.9}$ had an average Fe^{2+} concentration of 25.73 mg kg^{-1}. The Fe^{2+} concentration doubled with each increase in degree of water saturation from $S_{0.6}$ to $S_{0.8}$, although the average almost tripled in the $S_{0.9}$. The highest Fe^{2+} fluctuations were recorded in $S_{0.8}$ and $S_{0.9}$. The higher Fe^{2+} fluctuations in the $S_{0.8}$ and $S_{0.9}$ treatments could be attributed to the lower redox potentials in these cores.

The standard deviation in the Fe^{2+} concentration within the cores increased with an increase in water saturation (Figure 6.12). The average Fe^{2+} concentration in the core saturated to $S_{0.6}$ remained stable throughout the water saturation period, and therefore had a very small standard deviation (Figure 6.12). There were fluctuations in the Fe^{2+} concentration in the $S_{0.7}$ and upwards (Figure 6.13), although the greatest fluctuations occurred in the $S_{0.8}$ and $S_{0.9}$ treatments. The relationship between a greater standard deviation and an increase in water saturation can be attributed to the lower redox potentials as the degree of water saturation increases. The more the core reduces over time, the greater the occurrence of microsites. An increase in microsites leads to a greater standard deviation, as the microsites are more reduced or oxidised than the soil matrix.

The duration of water saturation had a significant influence on the Fe^{2+} concentration (Table 6.5). The maximum levels of fluctuation increased with increased degree as well as duration of water saturation (Figure 6.11). In the $S_{0.6}$ and $S_{0.7}$ treatments the Fe^{2+} concentration was not affected as much by duration of water saturation as in the $S_{0.8}$ and $S_{0.9}$ treatments. The slight fluctuations in Fe^{2+} concentration in the two lower water saturations stabilized after 84 days, whereas the Fe^{2+} concentration in the two higher water

saturations never stabilized. This was due to the lower redox potentials in the $S_{0.8}$ and $S_{0.9}$ treatments.

The Fe^{2+} concentration correlated well with the combined pe+pH (Figure 6.13). An increase in pe+pH lead to a decrease in Fe^{2+} concentration and *vice versa*. The lower Fe^{2+} concentrations at higher pe values was as a result of the decreased reduction potential and therefore less Fe^{3+} was reduced. The reason for the good relationship between pH and Fe^{2+} concentration is because as the pH decreases, a shift occurs in the ferric/ferrous couple as the reduction potential increases. At a pH of 2 and 3, the standard reduction potential for Fe^{3+} is ±770 mV, as the pH increases the reduction potential lowers to values close to ± 200 mV (Lovley, 2001).

In $S_{0.9}$ most of the Fe present in the soil for the duration of the experiment was in the form of Fe^{2+} (Figure 6.14). This indicates that the Fe in the $S_{0.9}$ core was reduced and did not precipitate as $Fe(OH)_3$ after reduction. Most of the Fe present in the core saturated to $S_{0.8}$ was Fe^{2+} although a few sampling points did fall into the iron hydroxide ($Fe(OH)_3$) range. In the $S_{0.6}$ and $S_{0.7}$ treatments, half of the measurements fell into the Fe^{2+} and the other half fell into the $Fe(OH)_3$ range (Figure 6.14). $Fe(OH)_3$ is oxidised Fe and it usually occurs under wetter soil conditions, though not anaerobic.

One could therefore conclude that for this soil, at a bulk density of 1.6 Mg m^{-3}, there was an exponential increase in the Fe^{2+} concentration with every increase in the degree of water saturation. Duration of water saturation will only lead to an increased Fe^{2+} concentration where the pe values are low enough to cause reduction. If the pe remains stable over time, the Fe^{2+} concentration will not be affected by increased time. Fe^{2+} was in solution for the duration of the experiment in the $S_{0.8}$ the $S_{0.9}$ saturation treatments. It seemed that in the $S_{0.8}$ core reduction had ceased between the period of 98 and 112 days after initial saturation, although the Fe^{2+} concentration increased again after 112 days. Therefore no point could be identified where reduction ceased.

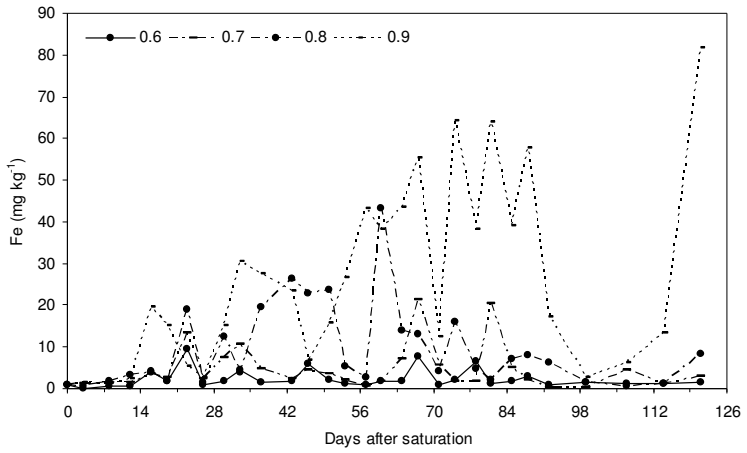

Figure 6.11 Fe^{2+} for all degrees of water saturation over a period of 121 days.

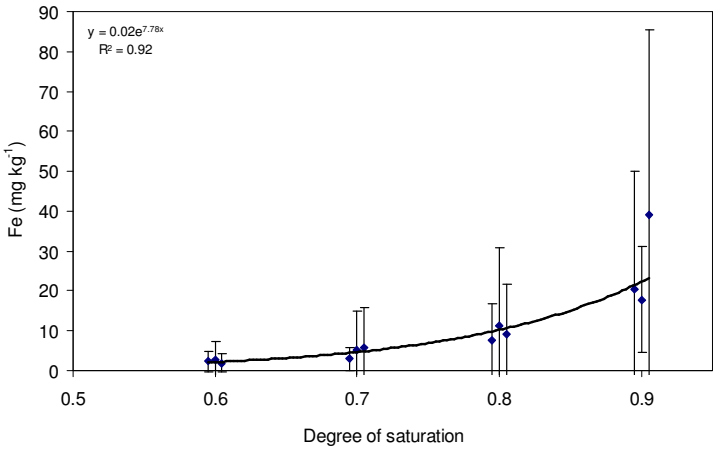

Figure 6.12 Average Fe^{2+} concentration and standard deviation of three sets of replications consisting of 30 measurements each over a period of 121 days.

$S_{0.6}$

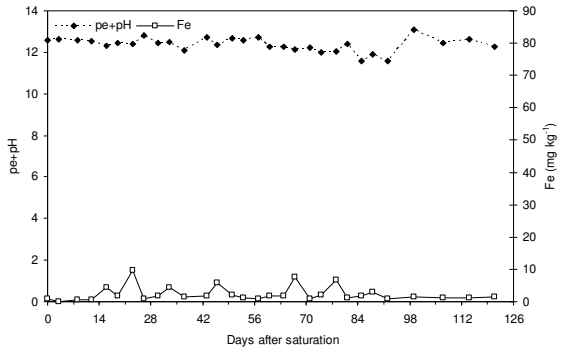

$S_{0.7}$

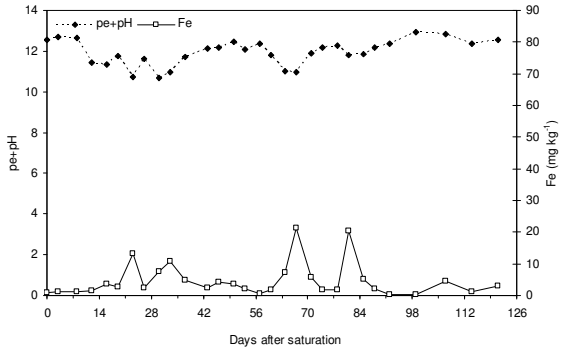

$S_{0.8}$

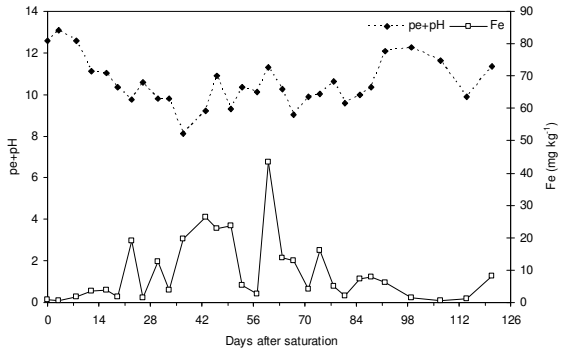

$S_{0.9}$

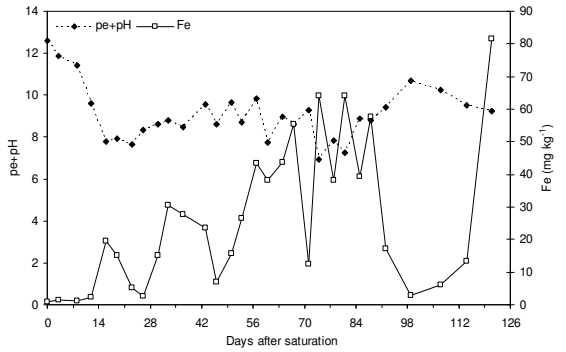

Figure 6.13 Fe^{2+} concentration and pe + pH values for $S_{0.6,\ 0.7,\ 0.8\ 0.9}$ during the 121 day period.

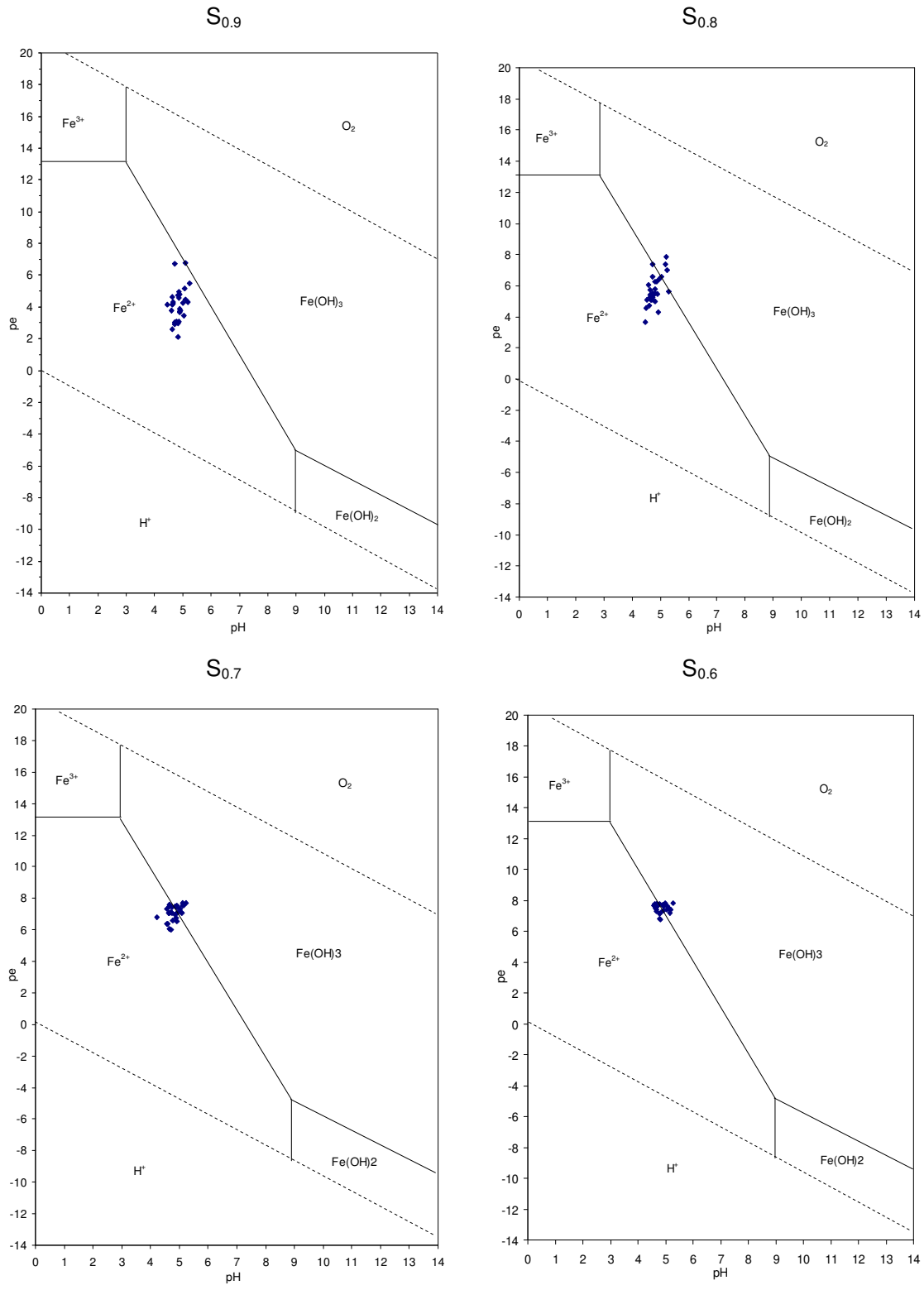

Figure 6.14 Fe^{2+} concentration for 30 measurements over a 121 day period plotted on a pe/pH graph, showing the different parameters of iron (Buol *et al.*, 1989).

6.3.1.5 Calcium

The Ca^{2+} data represented in Figure 6.15 is the average of each set of replications for the duration of water saturation. Each data point was calculated from 30 measurements over a period of 121 days. Each data point per replication was taken at the same degree of water saturation, although they were horizontally slightly spread out to aid in a better understanding of the graph. The data represented in Figure 6.16 is an average of three daily replications.

The soil's average Ca^{2+} concentration before water saturation was 81.0 mg kg^{-1}, whilst at the end of 121 days $S_{0.6}$ had an average Ca^{2+} concentration of 86.1 mg kg^{-1}, $S_{0.7}$ had an average of 85.6 mg kg^{-1}, $S_{0.8}$ an average of 86.5 mg kg^{-1} and $S_{0.9}$ had an average Ca^{2+} concentration of 86.2 mg kg^{-1}. The average concentration over all the s values was very similar and they all increased by around 4.0 to 5.0 mg kg^{-1} over the 121 day period. The highest and lowest Ca^{2+} concentration fluctuations were recorded in the core saturated to $S_{0.9}$. The standard deviation between the cores was very similar except for a higher standard deviation in the $S_{0.9}$ treatment. This was due to an extraneous value at 19 days after water saturation.

Duration of water saturation influenced the Ca^{2+} concentration significantly (Table 6.5). The behavior of the Ca^{2+} concentration of all the treatments was very similar throughout the 121 days of water saturation (Figure 6.16). The Ca^{2+} concentration was stable in all the s values with only slight fluctuations over time. After 88 days of water saturation, the Ca^{2+} concentration of all the cores increased. The increase seemed to correlate with a decrease in the $Mn^{2+} + Fe^{2+}$ of all the treatments except the $S_{0.6}$ treatment where the $Mn^{2+} + Fe^{2+}$ remained stable throughout the testing period.

According to Phillips and Greenway (1998), an increase in Ca^{2+} concentration should be correlated with an increase in the combined $Mn^{2+} + Fe^{2+}$ concentration. The Ca^{2+} is displaced from the CEC sites due to increased concentrations of soluble Fe^{2+} and Mn^{2+}. In Figure 5.7 and Figure 5.8 in Chapter 5, Ca^{2+}, Mg^{2+}, K^{+} and Na^{+} reacted in unison with the $Mn^{2+} + Fe^{2+}$ concentration, although the opposite took place in the core method. This was due to the NH_4OAc used to leach Ca^{2+}, Mg^{2+}, K^{+} and Na^{+} in the core method. In the column experiment the Ca^{2+}, Mg^{2+}, K^{+} and Na^{+} concentrations were determined from the soil solution. The NH_4OAc removes a higher concentration of Ca^{2+}, Mg^{2+}, K^{+} and Na^{+} from the soil, and therefore not only the water soluble Ca^{2+}, Mg^{2+}, K^{+} and Na^{+} as in the column experiment.

A better result in the core method was obtained when the Ca^{2+} concentration was correlated with the pH. An increase in pH lead to an increase in the Ca^{2+} concentration and *vice versa*. This relationship was not found for pe + pH and Ca^{2+} concentration (Figure 6.17).

The Ca^{2+} concentration in the cores did not differ significantly in relation to the degree of water saturation (Table 6.5). In Figure 6.16 it can be seen that the Ca concentration in all four s values followed the same pattern over the period of 121 days. In Figure 6.15 the average of 30 measurements over the period of 121 days for all four s values were very similar. This could be further verified when the groups were compared using the Tukey-Kramer Multiple-Comparison Test (Hintze, 1997) where it was found that none of the groups differed from one another.

It could therefore be concluded that the degree of water saturation did not affect the Ca^{2+} concentration in the soil. Other factors such as Fe^{2+} and Mn^{2+} concentration, pe and to a large extent pH played a role in the solubility of Ca^{2+} in the soil.

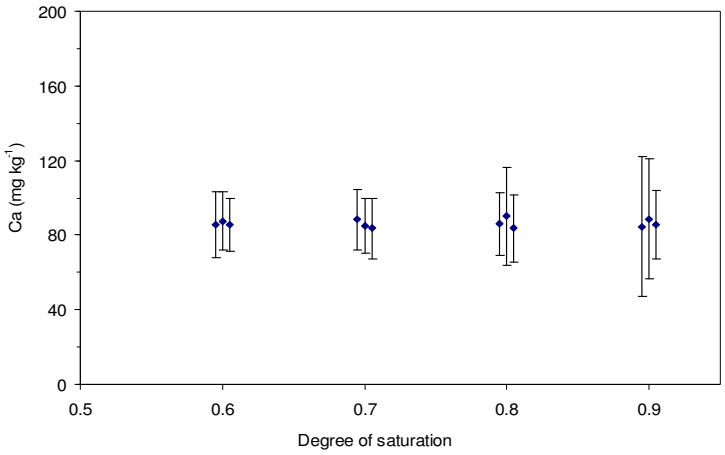

Figure 6.15 Average Ca^{2+} concentration and standard deviation of three sets of replications consisting of 30 measurements each over a period of 121 days.

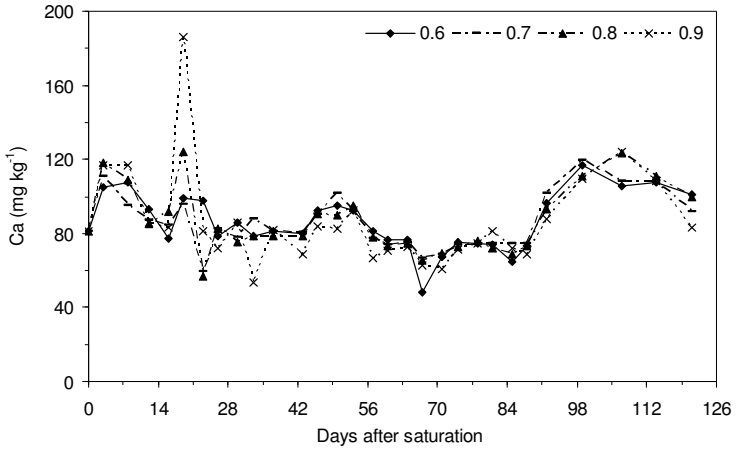

Figure 6.16 Ca^{2+} for all degrees of water saturation over a period of 121 days.

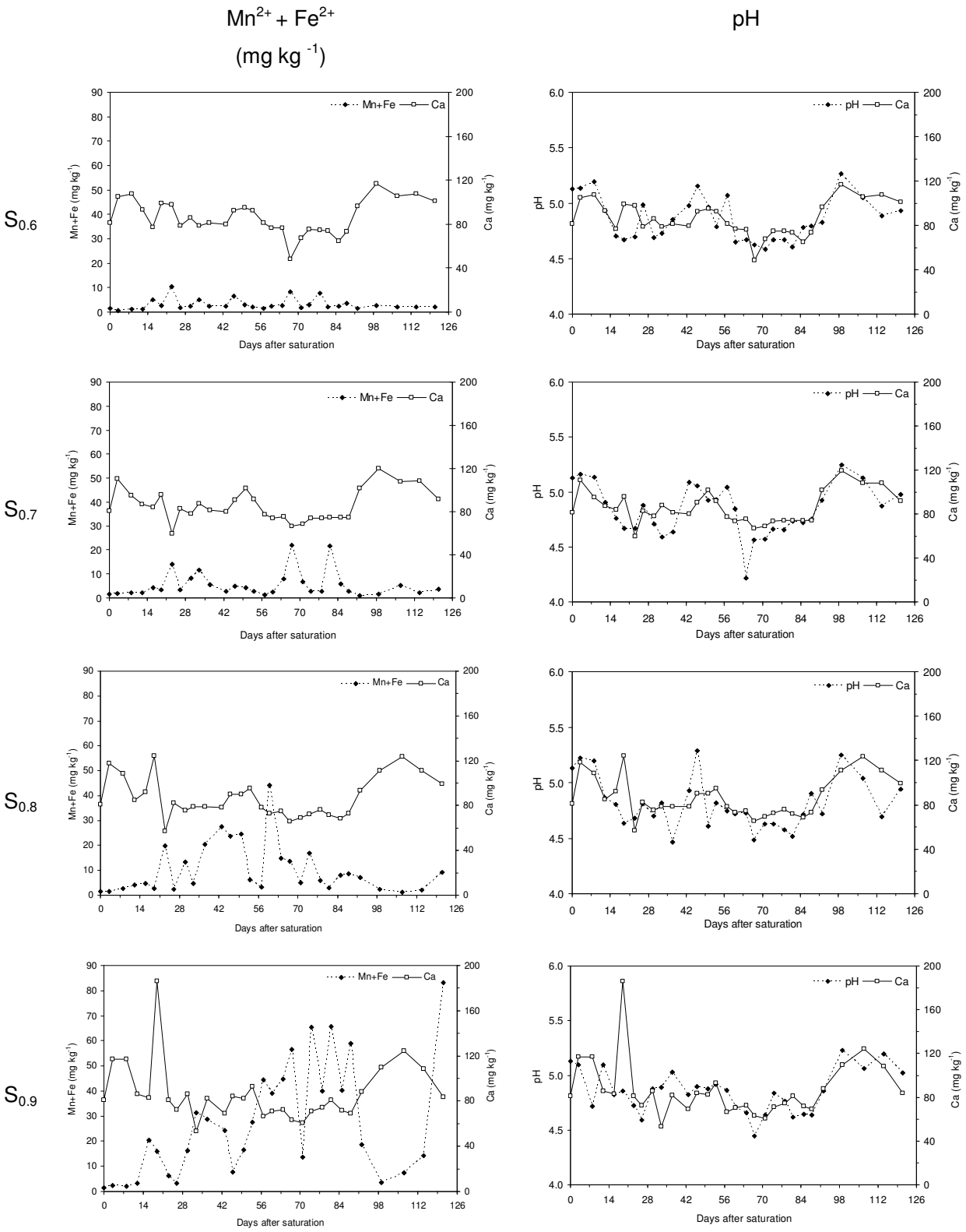

Figure 6.17 Ca^{2+} concentration, $Mn^{2+} + Fe^{2+}$ and pH values for the $S_{0.6, 0.7, 0.8, 0.9}$ during the 121 day period.

6.3.1.6 Magnesium

The Mg^{2+} data represented in Figure 6.18 is the average of each set of replications for the duration of water saturation. Each data point was calculated from 30 measurements over a period of 121 days. Each data point per replication was taken at the same degree of water saturation, although they were horizontally slightly spread out to aid in a better understanding of the graph. The data represented in Figure 6.19 is an average of three daily replications.

There was a good correlation ($R^2 = 0.93$) between the average Mg^{2+} concentration and the degree of water saturation, and the Mg^{2+} concentration was significantly affected by degree of water saturation (Table 6.5). The soils average Mg^{2+} concentration before water saturation was 51.7 mg kg^{-1}. The highest fluctuations in Mg^{2+} concentration were recorded in the core saturated to $S_{0.6}$ although it had the lowest average Mg^{2+} concentration. At the end of 121 days $S_{0.6}$ had an average Mg^{2+} concentration of 54.3 mg kg^{-1}, $S_{0.7}$ had an average of 63.8 mg kg^{-1}, $S_{0.8}$ an average of 62.7 mg kg^{-1} and $S_{0.9}$ had an average Mg^{2+} concentration of 58.0 mg kg^{-1}

The standard deviation in the cores saturated to $S_{0.6}$, $S_{0.7}$ and $S_{0.8}$ was the greatest, after which the standard deviation decreased in the core saturated to $S_{0.9}$ (Figure 6.18). When the treatments were compared using the Tukey-Kramer Multiple-Comparison Test (Hintze, 1997), the $S_{0.6}$ and $S_{0.9}$ cores differed from all the others, and the $S_{0.7}$ and $S_{0.8}$ core were similar to each other. This can be seen when the average Mg^{2+} concentrations between the s values are compared with one another. The $S_{0.6}$ and $S_{0.9}$ values had a similar average and the $S_{0.7}$ and $S_{0.8}$ values had a similar average (Figure 6.18).

There was no apparent correlation between $Mn^{2+} + Fe^{2+}$ and the Mg^{2+} concentration (Figure 6.20), although there was an inverse relationship when pe was plotted against Mg^{2+} for all the s values except $S_{0.6}$. A good correlation was found when Mg^{2+} was plotted against pH. As the pH decreased (became more acidic) the Mg^{2+} concentration would increase and *vice versa* (Figure 6.20).

The Mg^{2+} concentration was influenced more by the lower degree of water saturations $S_{0.6}$, $S_{0.7}$ and $S_{0.8}$ whereas the $S_{0.9}$ had very little effect on the Mg^{2+} concentration (Figure 6.20). This is also depicted in the standard deviation (Figure 6.18). The Mg^{2+} concentration was significantly affected by duration of water saturation (Table 6.5). The Mg^{2+} concentration increased to a maximum of over 80 mg kg^{-1} within the first month of saturation in all the cores except $S_{0.9}$ (Figure 6.20). It then stayed in solution for around 7 days after which it

sank to levels as low as or lower than the Mg^{2+} levels detected in the dry sample. The Mg^{2+} concentration remained at low concentrations of around 53 mg kg^{-1} in all the water saturations, after which it showed another increase in $S_{0.7}$ and $S_{0.8}$ to levels of 80 mg kg^{-1}. This increase did not occur in the $S_{0.6}$ or $S_{0.9}$ treatments (Figure 6.19).

It was therefore concluded that Mg^{2+} was significantly influenced by degree as well as duration of water saturation. The $S_{0.7}$ and $S_{0.8}$ treatments had a higher average Mn^{2+} concentration than the $S_{0.6}$ and $S_{0.9}$ treatments. The $Mn^{2+} + Fe^{2+}$ concentration does not affect the Mg^{2+} concentration to a large extent, although it was found that the Mg^{2+} concentration reacted inversely to the pH of the soil.

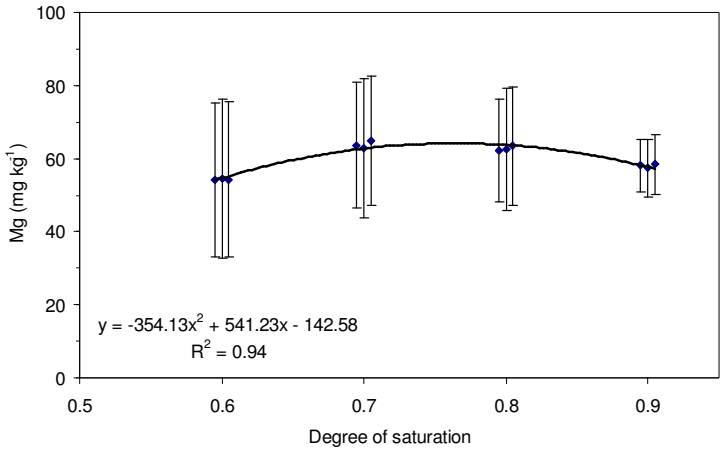

Figure 6.18 Average Mg^{2+} concentration and standard deviation of three sets of replications consisting of 30 measurements each over a period of 121 days.

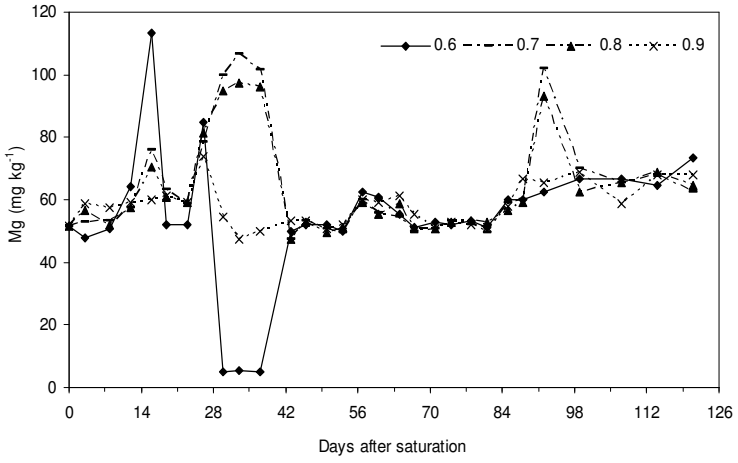

Figure 6.19 Mg^{2+} for all degrees of water saturation over a period of 121 days.

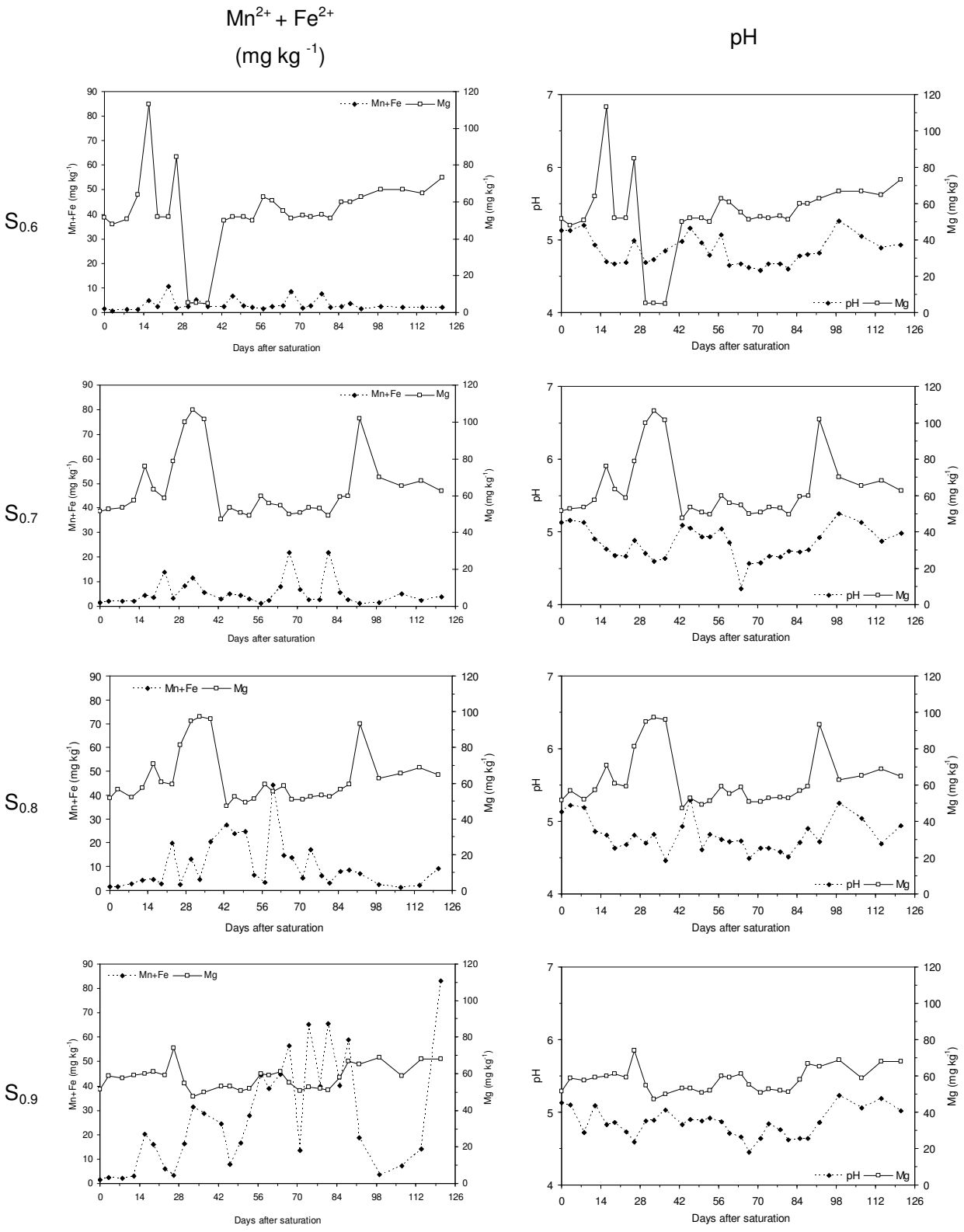

Figure 6.20 Mg^{2+} concentration and Mn^{2+} + Fe^{2+} and pH values for $S_{0.6, 0.7, 0.8, 0.9}$ during the 121 day period.

6.3.1.7 Potassium

The K^+ data represented in Figure 6.21 is the average of each set of replications for the duration of water saturation. Each data point was calculated from 30 measurements over a period of 121 days. Each data point per replication was taken at the same degree of water saturation, although they were horizontally slightly spread out to aid in a better understanding of the graph. The data represented in Figure 6.22 is an average of three daily replications.

The soil's average K^+ concentration before saturation was 25.0 mg kg^{-1}, at the end of 121 days $S_{0.6}$ had an average K^+ concentration of 38.5 mg kg^{-1}, $S_{0.7}$ had an average of 38.4 mg kg^{-1}, $S_{0.8}$ an average of 37.4 mg kg^{-1} and $S_{0.9}$ had an average K^+ concentration of 39.1 mg kg^{-1}. The highest K^+ fluctuations were recorded in the core saturated to $S_{0.9}$. There was no significant difference for between the K^+ concentration and the degree of water saturation (Table 6.5). This can be seen in Figure 6.21 where the average K^+ over a period of 121 days showed almost no difference between the different treatments. This was confirmed when the treatments were compared using the Tukey-Kramer Multiple-Comparison Test (Hintze, 1997) where it was shown that none of the groups differed from one another.

There was no significant difference between the K^+ concentration and the duration of water saturation (Table 6.5). From Figure 6.22 and Figure 6.23 it could be seen that pattern's of K^+ solubility over time for all the degrees of water saturation were almost identical except for the last 20 days of saturation. The K^+ concentration was very stable over a 70 day period after which the K^+ concentration increased in all the water saturations. The increase in the K^+ concentration in $S_{0.9}$, and, to a certain extent in $S_{0.8}$, could be correlated to a decrease in the $Mn^{2+} + Fe^{2+}$ concentration. This link could not be made in the $S_{0.6}$ and $S_{0.7}$ treatments. No trend was found to exist between the K^+ concentration and the pe + pH values or the pH values.

The K^+ concentration was significantly affected by duration of water saturation and not by degree of water saturation. The K^+ concentration behaved very similarly in all the degree of saturation treatments. The K^+ concentration decreased over the first 28 days of saturation after which the concentration stabilised over the next 70 days and then increased.

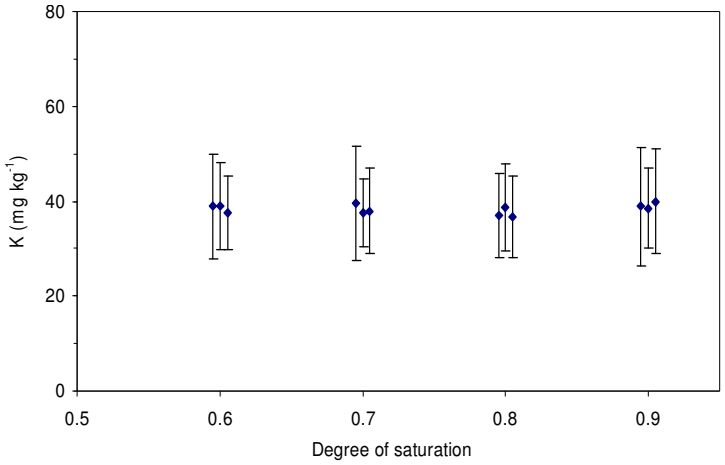

Figure 6.21 Average K^+ concentration and standard deviation of three sets of replications consisting of 30 measurements each over a period of 121 days.

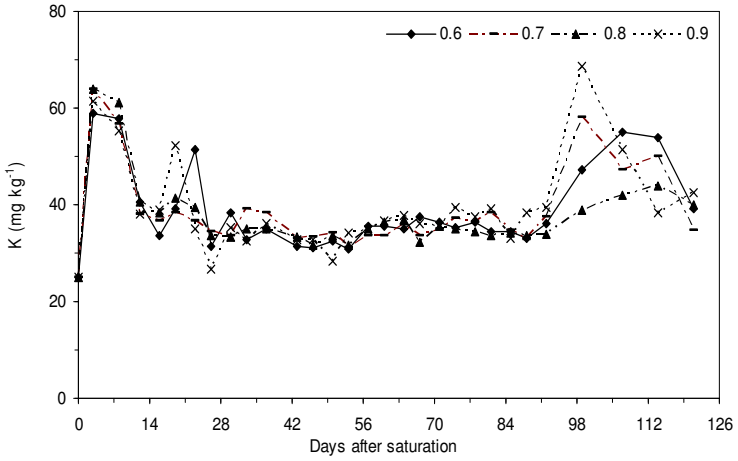

Figure 6.22 K^+ for all degrees of water saturation over a period of 121 days.

$S_{0.6}$

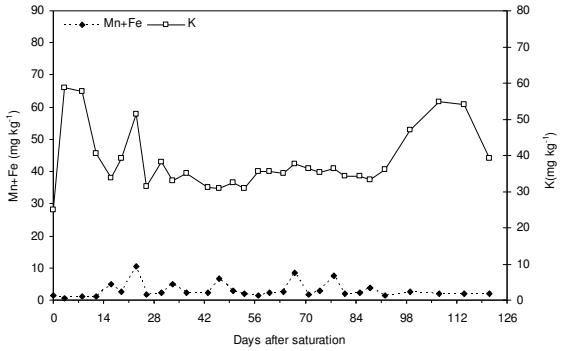

$S_{0.7}$

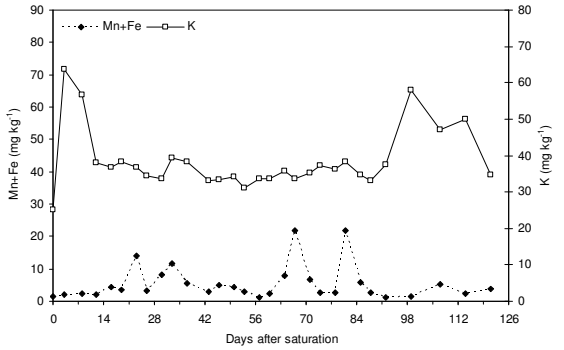

$S_{0.8}$

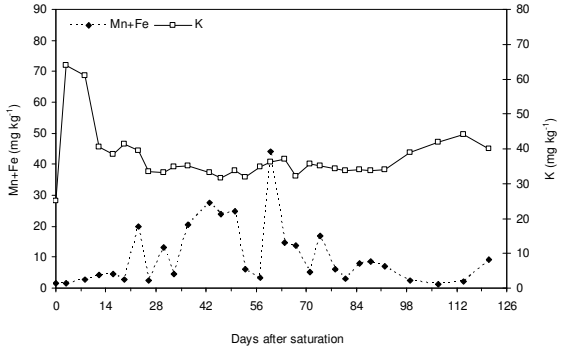

$S_{0.9}$

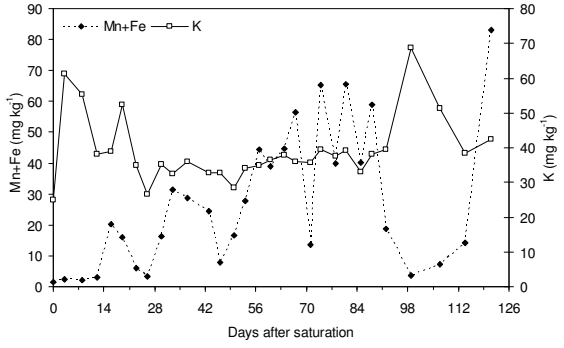

Figure 6.23 K^+ concentration and Mn^{2+} + Fe^{2+} values for the $S_{0.6,\ 0.7,\ 0.8,\ 0.9}$ during the 121 day period.

6.3.1.8 Sodium

The Na^+ data represented in Figure 6.24 is the average of each set of replications for the duration of water saturation. Each data point was calculated from 30 measurements over a period of 121 days. Each data point per replication was taken at the same degree of water saturation, although they were horizontally slightly spread out to aid in a better understanding of the graph. The data represented in Figure 6.25 is an average of three daily replications.

The soil's average Na^+ concentration before saturation was 15.7 mg kg^{-1}, at the end of 121 days $S_{0.6}$ had an average Na^+ concentration of 21.1 mg kg^{-1}, $S_{0.7}$ had an average of 20.3 mg kg^{-1}, $S_{0.8}$ an average of 20.6 mg kg^{-1} and $S_{0.9}$ had an average Na^+ concentration of 21.0 mg kg^{-1}. The highest Na^+ fluctuations were recorded in the core saturated to $S_{0.6}$.

There was a significant difference between degree of water saturation and the Na^+ concentration of the cores. The Na^+ concentration followed the same pattern for all four s values as can be seen in Figure 6.25, except for two extraneous values for $S_{0.6}$. When the treatments were compared using the Tukey-Kramer Multiple-Comparison Test (Hintze, 1997) it showed that $S_{0.6}$ differed from $S_{0.7}$ and $S_{0.8}$ and that $S_{0.9}$ did not differ from any of the other treatments. When the two extraneous values were removed from the $S_{0.6}$ data set, their would be no significant difference between the treatments.

The average Na^+ concentration between all the s values remained very similar as well as did their standard deviations. The $S_{0.6}$ treatment had a slightly higher standard deviation than the remaining treatments. The higher standard deviation in the $S_{0.6}$ treatment can be related to the two extraneous values at day 14 and 98 of saturation.

According to the ANOVA there was a significant difference between duration of water saturation and the Na^+ concentration. A decrease in the sodium concentration took place over the 121 days of saturation for all the treatments.

It was therefore concluded that for this soil at a bulk density of 1.6 Mg m^{-3} the Na^+ concentration did not differ between the water saturations. The Na^+ concentration decreased with time, irrespective of the water saturation. This could be as a result of the Na^+ being adsorbed to the clay complex as the other cations are displaced into the soil solution.

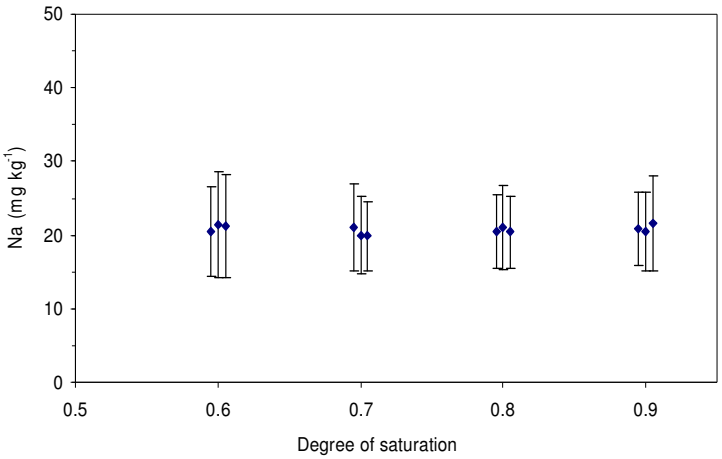

Figure 6.24 Average Na^+ concentration and standard deviation of three sets of replications consisting of 30 measurements each over a period of 121 days.

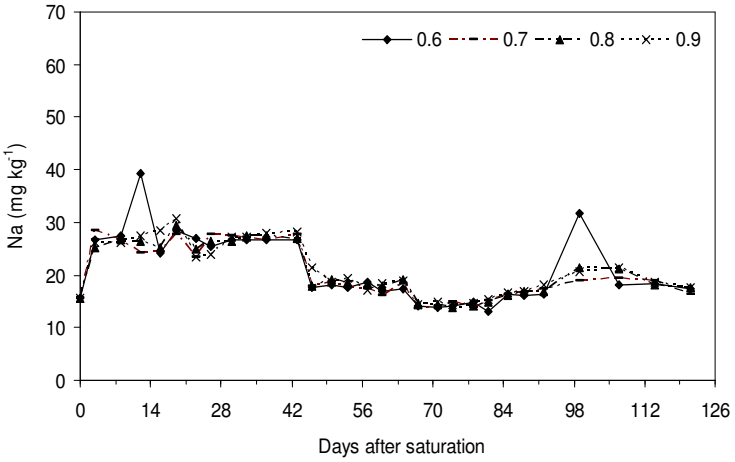

Figure 6.25 Na^+ for all degrees of water saturation over a period of 121 days.

$S_{0.6}$

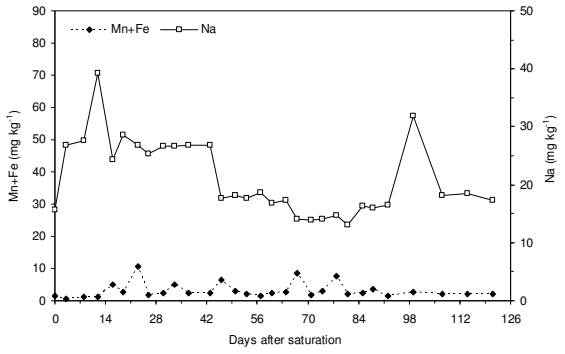

$S_{0.7}$

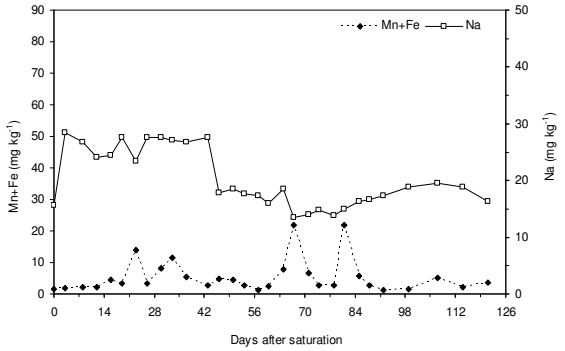

$S_{0.8}$

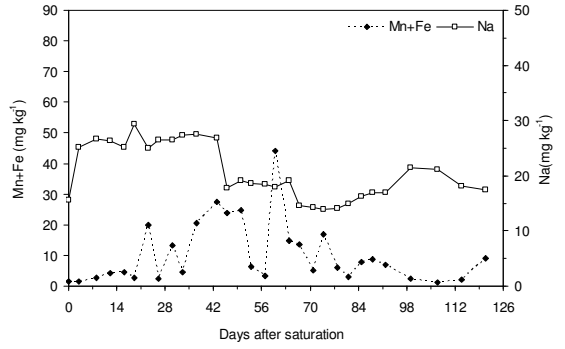

$S_{0.9}$

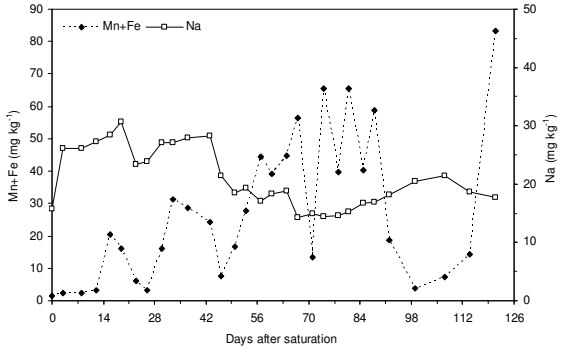

Figure 6.26 Na^+ concentration and $Mn^{2+} + Fe^{2+}$ values for $S_{0.6,\ 0.7,\ 0.8,\ 0.9}$ during the 121 day period.

6.3.2 Column wet by suction

The results presented in this section are from the column packed to a bulk density of 1.6 Mg m^{-3} with soil from the combined B1 + B2 horizon described in Chapter 4. The column was wet by suction as described in chapter 5. After extractions were terminated the column was left in tact for 330 days after which it was cut up into 0.1 m segments and analysed for pH, Eh, Mn^{2+}, Fe^{2+}, Ca^{2+}, Mg^{2+}, K^{+} and Na^{+}. The aim of leaving the column intact over such a long period of time was to determine what would happen to the pH, Eh, Mn^{2+}, Fe^{2+}, Ca^{2+}, Mg^{2+}, K^{+} and Na^{+} over such a long duration of water saturation.

It was found that an irregular wetting pattern was present in the column. This was caused by the suction at the top of the column. It was thought that the column would be uniformly wet due to the suction although this did not prove true (Figure 6.27). The column was the wettest at the base in segment 1 ($S_{0.81}$) and at the top, segment 9 ($S_{0.76}$), with segment 8 being the driest at $S_{0.31}$. The degree of wetness increased uniformly from segment 8 down the column to segment 1. For use as a reference to the core method, only data from segment 1, 2 and 3 could be used as the remaining segment's degree's of water saturation were too low to compare with the degree of water saturations used in the core method. Data from segment 9 could also not be used even though it was at a water saturation of $S_{0.8}$, as it was exposed to O_2. Even though segment 9 was exposed to O_2, it was covered with a lid that prevented any evaporation from the segment, hence the high degree of water saturation.

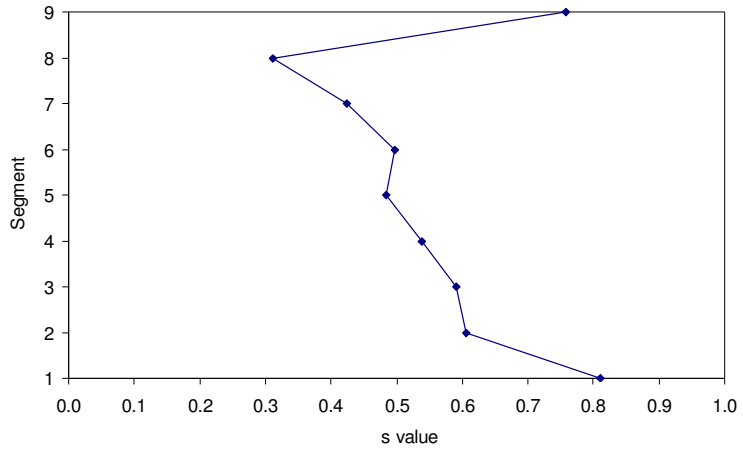

Figure 6.27 Degree of saturation (s) for segment 1 to 9, with segment 9 being the top of the column exposed to O_2.

After 330 days the pe in the column varied from 2.8 in segment 1 to 6.4 in segment 9 (Figure 6.28), and ranged between 7 and 8 in segment 8 to segment 2. Even though the top segment was also saturated to $S_{0.8}$, the pe was not as low as the bottom segment due to the fact that the top segment was not sealed and O_2 prevented the soil from reducing.

The pe data from segment 1, which was at $S_{0.8}$, was compared to the $S_{0.8}$ single core data. The pe in segment 1 was much lower than in the single cores, therefore it could be concluded that with time, the pe in the cores would have decreased to much lower levels as the duration of water saturation continued. The pe in segment 2 and 3 which were both at $S_{0.6}$ were compared to the $S_{0.6}$ single core data. The pe values were very similar, both varied between a pe of 7 and 8. Therefore one can conclude that the pe would not have increased with an increased duration of water saturation in the $S_{0.6}$ single core method.

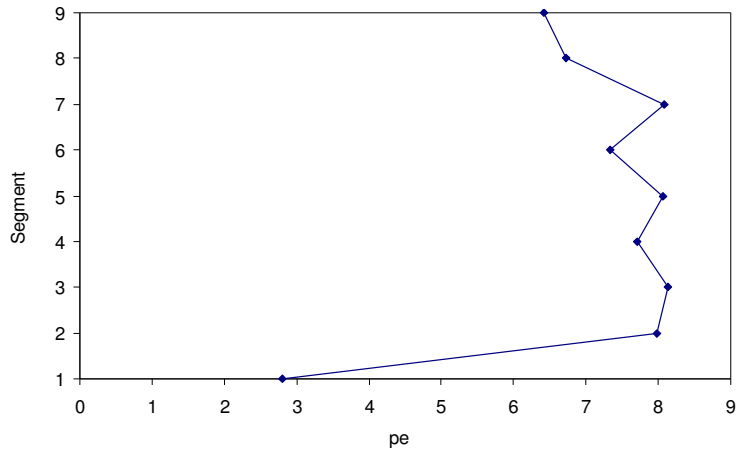

Figure 6.28 The pe after 330 days for segment 1 to 9, with segment 9 being the top of the column exposed to O_2.

The pH differed dramatically over the length of the column, with a variation of 1.5 units from segment 8 to segment 7. When the pH of the $S_{0.6}$ single core data was compared to the pH of segment 2 and 3, the average pH was very similar. It can be stated that with time, the pH at $S_{0.6}$ would not change significantly. The average pH in the $S_{0.8}$ single core data was lower than the pH of segment 1 in the column. Therefore one could conclude that the pH would have increased with time in the $S_{0.8}$ single cores. The pH in the $S_{0.9}$ single core data would also have increased due to the relation between an increase in pH and an increase in water saturation.

The pH in the single core data was significantly influenced (Table 6.5) by duration of water saturation and it therefore concurred with the fact that the pH data in the column varied to such an extent over such a long period of saturation.

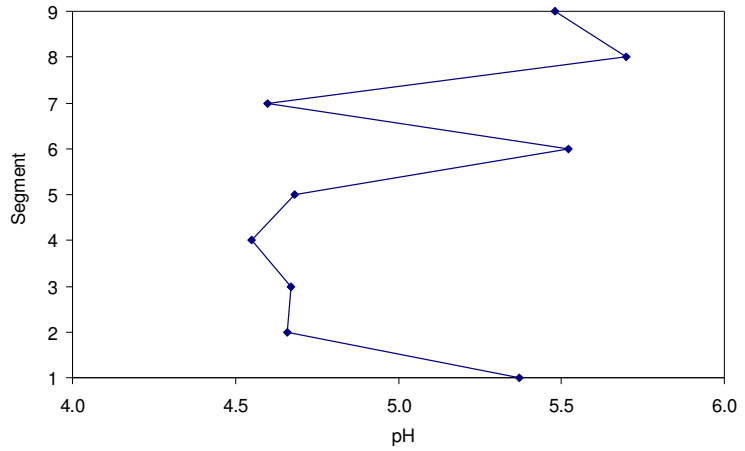

Figure 6.29 The pH after 330 days for segment 1 to 9, with segment 9 being the top of the column exposed to O_2.

The Mn^{2+} concentration in the column followed the same pattern as the degree of water saturation in each segment. The Mn^{2+} concentration was the highest in the first two segments after which it decreased up until segment 8 and then increased in segment 9 (Figure 6.30). The average Mn^{2+} concentration in segment 1 was similar to the average Mn^{2+} concentration in the $S_{0.8}$ single core data. Therefore one can conclude that the Mn^{2+} concentration would not have increased significantly if the single core method was not terminated. The average Mn^{2+} concentration in the $S_{0.6}$ singe core data was also very similar to the Mn^{2+} concentration data in segment 2 and 3.

The Fe^{2+} concentration in segment 9, which was at the top of the column, was 27.3 mg kg^{-1} after which the Fe^{2+} concentration dropped to very low values, increased slightly in segment 5 and then decreased again in segments 3 and 4 (Figure 6.31). The Fe^{2+} concentration increased to 31.0 mg kg^{-1} in segment 2 and the doubled to 66.7 mg kg^{-1} in segment 1 at the base of the column. The pe was also the highest in segment 1. The high pe in segment 2 and 9 indicated non-reducing conditions, although there was a high Fe^{2+} concentration present. Even though the pe had decreased, it must have been lower during the course of the 330 days, causing the Fe to reduce after which the pe increased although the Fe^{2+} still remained soluble. When segment 1 was compared to the $S_{0.8}$ single core treatments, the Fe^{2+} concentrations were very similar. This showed that the Fe^{2+} concentration must have reached its maximum levels in the single core method. In segment 2 the Fe^{2+} concentration

was slightly higher than in the core method. The Fe^{2+} concentration in segment 3 correlated well with the $S_{0.6}$ cores in the singe core method.

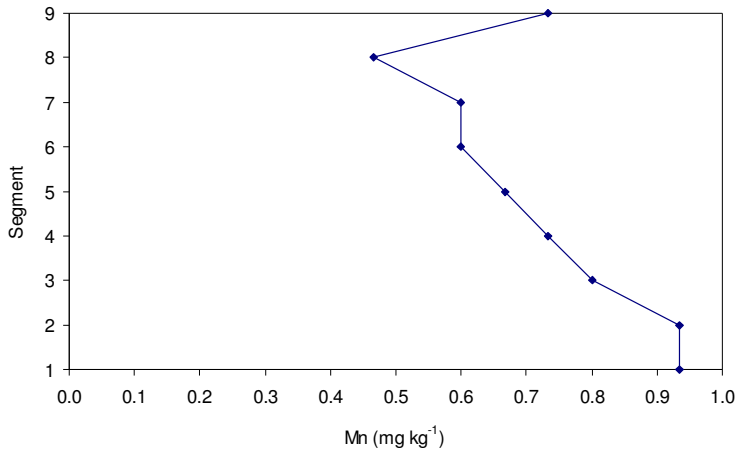

Figure 6.30 Mn^{2+} concentration after 330 days for segment 1 to 9, with 9 being the top of the column.

The Ca^{2+} concentration in segment 2 to 9 was relatively stable, with a dramatic decrease from segment 2 to segment 1 from an average of 85 mg kg^{-1} to 50 mg kg^{-1}. The Ca^{2+} concentration resembles the pe in the column. A lower pe value, being a more reduced soil lead to a lower Ca^{2+} concentration. This was confirmed in section 6.3.1.5, where an increase in Ca^{2+} and a decrease in Mn^{2+} + Fe^{2+} concentration were noted. The average Ca^{2+} concentration in the core analyses for $S_{0.6}$ was similar to the Ca^{2+} concentration for segment 2 and 3 in the column experiment, although the Ca^{2+} concentration was much lower in segment 1 than the $S_{0.8}$ core treatments.

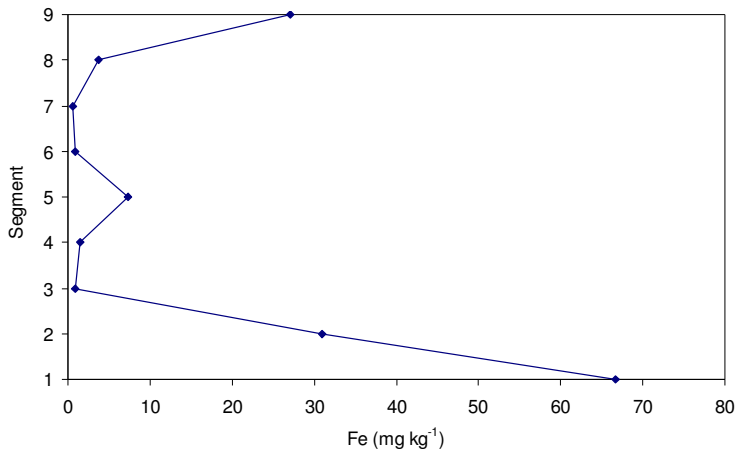

Figure 6.31 Fe^{2+} concentration after 330 days for segment 1 to 9, with 9 being the top of the column.

The Mg^{2+} concentration remained relatively stable throughout the column except for segment 8, where it deviated from its average of 68.0 mg kg^{-1} to a maximum of 90.0 mg kg^{-1}. Segment 8 was also the driest segment ($S_{0.31}$). An inverse correlation was found between Mg^{2+} and pe in the column that was wetted with capillary rise, but this was not the case in this column, although there did appear to be an inverse correlation between degree of water saturation and Mg^{2+} concentration. In the core method the Mg^{2+} concentration correlated well with the pH of the core, although this was not found to be the case in the column experiment.

The K^+ concentration decreased from the top of the column to the base, from an average of 36.8 mg kg^{-1} at the top to an average of 32.2 mg kg^{-1} at the base of the soil column. The K^+ concentration remained stable in segment 9 and 8 after which it decreased dramatically in segment 7 and 6 and then increased again in segment 5; thereafter it decreased steadily to its lowest value in segment 1. When the K^+ concentration in the column was compared to the average K^+ concentration in the single core method the concentration was slightly lower. The K^+ concentration's in segment 8 and 9 were similar to the concentrations found in the single core method, although the remaining segments were lower by about 10.0 to 20.0 mg kg^{-1}.

The Na^+ concentration only varied in a range of between 10.0 mg kg^{-1}. It decreased from the top of the column to the base in the same fashion as the K^+ concentration. Both the K^+ and Na^+ concentrations decreased down the profile as the water saturation increased. Both of them also exhibited an increase in concentration in segment 8, which was the driest

segment of the core. It could therefore be stated that degree of water saturation influenced the displacement of K^+ and Na^+. An increase in water saturation lead to a decrease in concentration of these cations.

An increase in the Ca^{2+}, Mg^{2+}, K^+ and Na^+ is due to the displacement from the CEC sites due to increased concentrations of soluble Fe^{2+} and Mn^{2+} as stated by Phillips and Greenway (1998). All the cations displayed a decrease in concentration from the top of the column (segment 9) to the bottom of the column (segment 1) except for Mg^{2+}. Therefore this statement did not hold true for the core method. This is because these segments were leached with NH_4OA_c and all the cations were leached, not only the soluble cations found in the soil solution as in the first column experiment, where soil solution was extracted from the column.

No colour change occurred in any of the segments over the 330 day saturation period. Soil colour was read using a Munsell colour chart.

Ca^{2+}

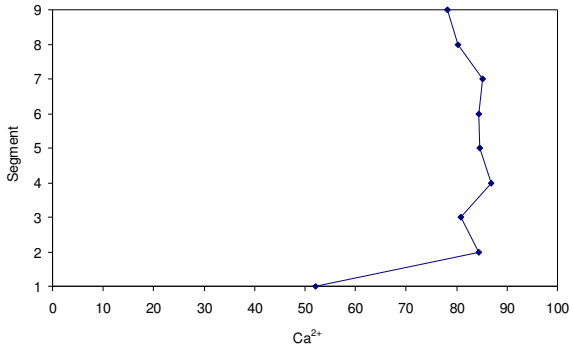

Mg^{2+}

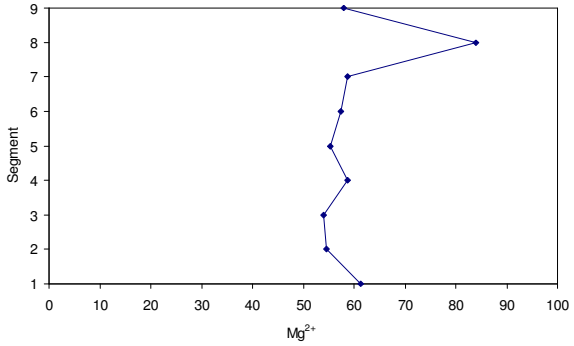

K^{+}

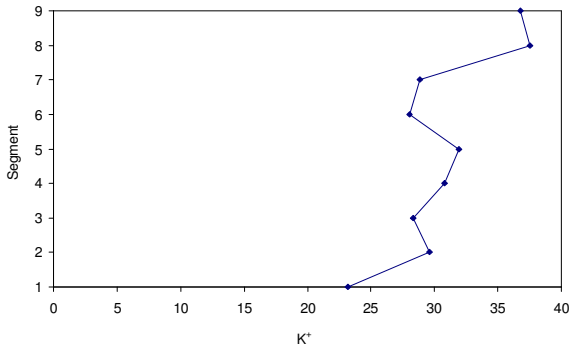

Na^{+}

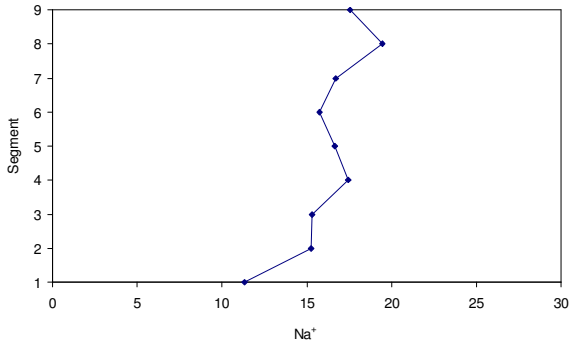

Figure 6.32 Ca^{2+}, Mg^{2+}, K^{+} and Na^{+} concentrations after 330 days for segments 1 to 9.

6.4 Morphological features

Three cores packed to a bulk density of 1.6 Mg m^{-3} and saturated to $S_{0.9}$ in exactly the same manner as described in section 6.2.1 were stored in a laboratory at room temperature (23°C) for twelve months. After twelve months the cores were opened and Mn and Fe accumulations and depletions were found at the interface between the plastic covering and the soil in all three cores (Figure 6.33). Reduced Fe^{2+} must have moved out of the soil to the oxidised outer edges of the core where it precipitated due to the higher O_2 concentration.

Mn concretions were only found in core 1 and core 2 (Figure 6.32). Core 1 only showed Mn accumulations and no Fe accumulations or depletions. The fact that only core 1 contained Mn accumulations could be as a result of the Eh not falling as low as in core 2 and 3, therefore the Fe could not reduce to the extent of the other cores.

Core 2 and 3 contained prominent Fe accumulations and depletions, which were mostly concentrated in the center of the core. The Fe precipitation formed a crust like layer over the surface of the soil and could be lifted up to reveal a depleted grey soil matrix below the accumulations. Lighter and darker Fe accumulations could be seen, with the lighter ones most likely being goethite and the darker ones ferrihydrite.

It could therefore be confirmed that a soil with 0.22% organic carbon will produce morphological features within a year of saturation at $S_{0.9}$.

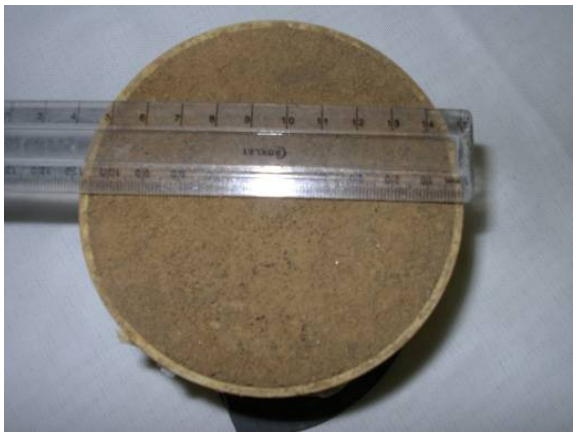

(a)

(b)

(c)

Figure 6.33 Mn^{4+} and Fe^{3+} accumulations and depletions in cores packed to a bulk density of 1.6 Mg m^{-3} and saturated at $S_{0.9}$ for twelve months: (a) Only Mn^{4+} accumulations, (b) Both Mn^{4+} and Fe^{3+} accumulations and depletions, (c) Both Mn^{4+} and Fe^{2+} accumulations and depletions, Fe^{3+} accumulations were found mainly in the centre of the core and the Mn^{4+} accumulations were found mainly at the outer edges.

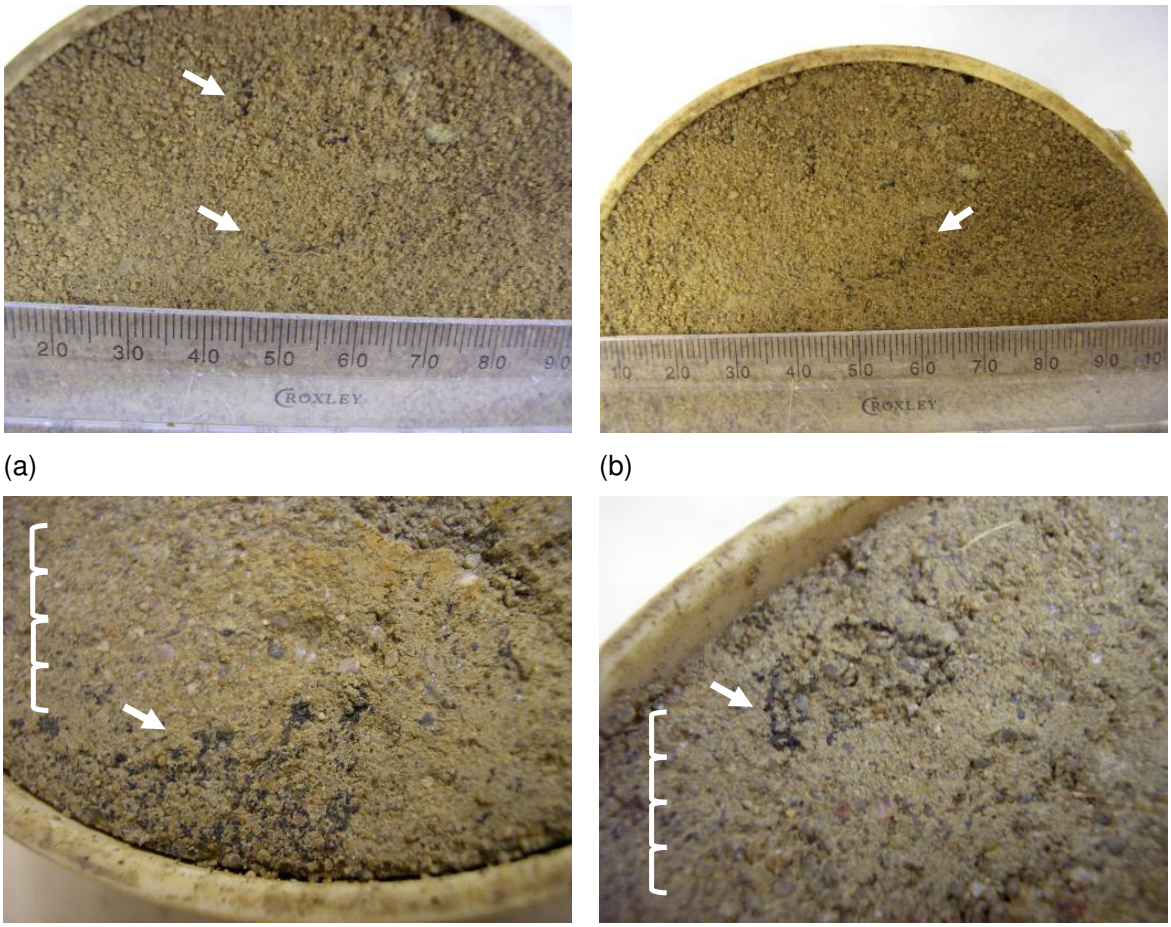

Figure 6.34 Mn^{4+} accumulations in cores packed to a bulk density of 1.6 Mg m^{-3} and saturated at $S_{0.9}$ for twelve months: (a) Mn^{4+} accumulations, (b) Mn^{4+} precipitating in a half moon formation (c) Mn^{4+} accumulations near edge of core (the scale bar is approximately 2 mm scale), (d) Mn^{4+} accumulations in a circular formation near out edge of core (the scale bar is approximately 2 mm scale).

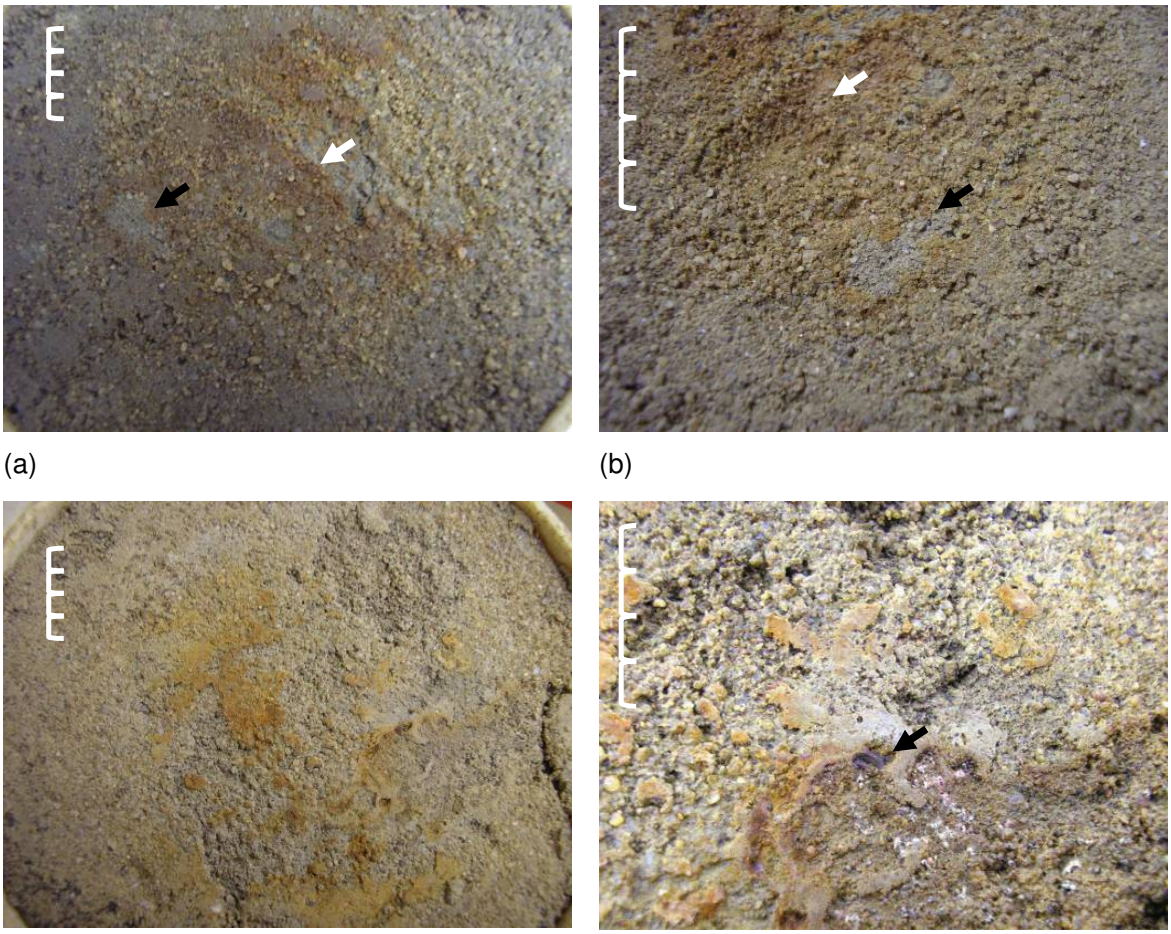

(a) (b)

(c) (d)

Figure 6.35 Fe^{3+} accumulations in cores packed to a bulk density of 1.6 Mg m^{-3} and saturated at $S_{0.9}$ for twelve months: (a) Fe^{3+} accumulations (white arrow) and Fe^{3+} depletions (black arrow) (the scale bar is approximately 2 mm scale), (b) Fe^{3+} accumulations (white arrow) and Fe^{3+} depletions (black arrow) (the scale bar is approximately 2 mm scale), (c) Fe^{3+} accumulations and depletions (the scale bar is approximately 2 mm scale), (d) Fe^{3+} accumulations and depletions with Fe^{3+} concretions (black arrow) (the scale bar is approximately 2 mm scale).

6.5 Proposed degree of water saturation for onset of reduction

One of the aims of this study was to try to determine at which degree of water saturation reduction is most likely to be initiated in this particular soil in a closed (unnatural) system. Van Huyssteen *et al.* (2005) approximated that reduction will set in when the pores are saturated to 70% of porosity, which is $S_{0.7}$. This first approximation was based on experience, and a set of specific conditions, in the absence of scientific research and data in this regard. This obvious lack in scientific knowledge led to the initiation of the current study.

All data represented in this section are averages of each water saturation treatment over a period of 121 days.

Through data analysis in the previous sections of this chapter it was determined that the $S_{0.6}$ and $S_{0.7}$ treatments reacted similarly and were grouped together with a trend line, the same was done for the $S_{0.8}$ and $S_{0.9}$ treatments. The trend lines for Eh were then extrapolated until the trend lines crossed each other, this method was used in an attempt to approximate the degree of saturation required to obtain measurable Fe indicative of reduction.

Using this method, the optimal degree of water saturation where Eh started to decrease significantly was determined to be the point where the lines crossed, which was at $S_{0.72}$ (Figure 6.36).

This point was mathematically determined by solving the two equations given by the trend lines (Equation 6.1):

$$-250x + 594 = -900x + 1060 \quad (6.1)$$

Therefore the x axis will be 0.72

The y axis was then determined by inserting the value found for the x axis into any of the two linear equations provided in the trend line, y = 414.8.

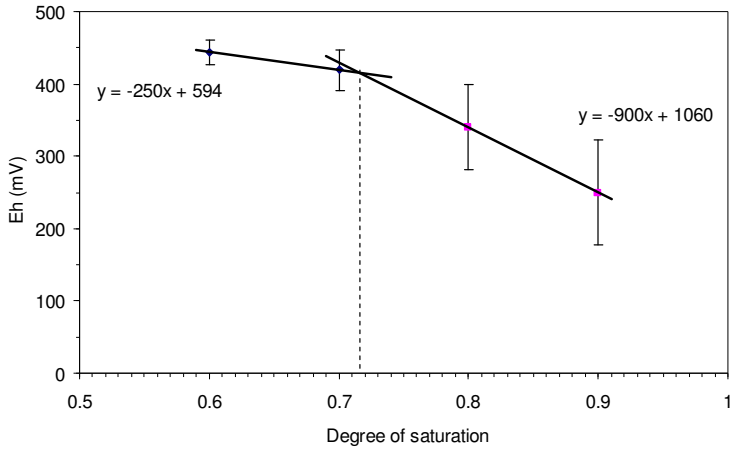

Figure 6.36 Average Eh (mV) and standard deviation for four treatments ($S_{0.6,\ 0.7,\ 0.8,\ 0.9}$) over a period of 121 days, with the linear trend line extrapolated to the point where they crossed; the dotted line indicates degree of water saturation at point of crossing (x = 0.72, y = 414.5).

The optimal degree of water saturation where pe decreased significantly was the same as Eh, calculated at $S_{0.72}$ (Figure 6.37). The y axis gave a pe of 7, therefore an Eh of 414.5 mV. It is well known in literature (Brookins, 1988; Faulkner & Patrick, 1992; Mansfeldt, 2004; Vepraskas, 2001) and through experience in this study that the reduction of Mn^{2+} and Fe^{2+} does not occur at a pe of 7 or an Eh above 400 mV. These values are known to be a sign of oxidizing conditions. Most literature reports Mn^{2+} reduction takes place at values between 300 to 200 mV (Mansfeldt, 2004) and Fe^{2+} reduction takes place at an Eh of between 200 mV (Mansfeldt, 2004) and 170 mV (Brookins, 1988; Faulkner & Patrick, 1992; Vepraskas, 2001). Therefore an Eh at 414.5 mV and $S_{0.72}$ is not a good indication of the optimal point for reduction of Mn^{2+} and Fe^{2+} in this experiment.

The point where the two trend lines crossed for the two groups of treatments were also determined for Mn^{2+} and Fe^{2+} (Figure 6.38 and Figure 6.39). It was found that the optimal water saturation for the reduction of both Mn^{2+} and Fe^{2+} was $S_{0.78}$. This was then plotted against the $S_{0.8}$ trend line (Figure 6.40) for pe. It was found that at a water saturation of $S_{0.78}$ the optimal pe for Mn^{2+} and Fe^{2+} reduction is 6 (Eh = 350 mV).

An optimal pe of 6 for Fe^{2+} reduction was then plotted against the pe and Fe^{2+} concentration graphs (Figure 6.41). It was found that reduction takes place where the pe decreases below 6 units. In Figure 6.41 it could be seen that the pe did not decrease below 6 in treatment $S_{0.6}$ or $S_{0.7}$ during the 121 days of analysis, and the Fe^{2+} concentration did not increase

significantly during this period. In $S_{0.8}$ the Fe^{2+} concentration increased during the periods where the pe was below 6. This was indicated by the period between the dotted lines (Figure 6.41). In $S_{0.9}$ the pe was constantly above 6 and the Fe^{2+} was also constantly in solution. This relationship between an increase in the Fe^{2+} concentration when the pe was below 6 was not found for the Mn^{2+} concentration. The lack of a relationship could be attributed to the fact that Mn^{2+} is more sensitive to pH, and therefore pH also plays a greater role in the reduction of Mn^{2+} (Glinski & Stepniewski, 1985).

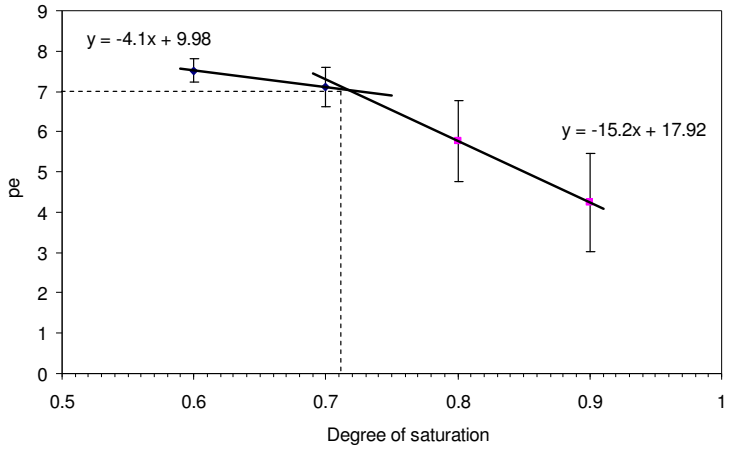

Figure 6.37 Average pe and standard deviation for four treatments ($S_{0.6, 0.7, 0.8, 0.9}$) over a period of 121 days, with the linear trend line extrapolated to the point where they crossed; dotted line indicates degree of water saturation at crossing point (x = 0.72, y = 7).

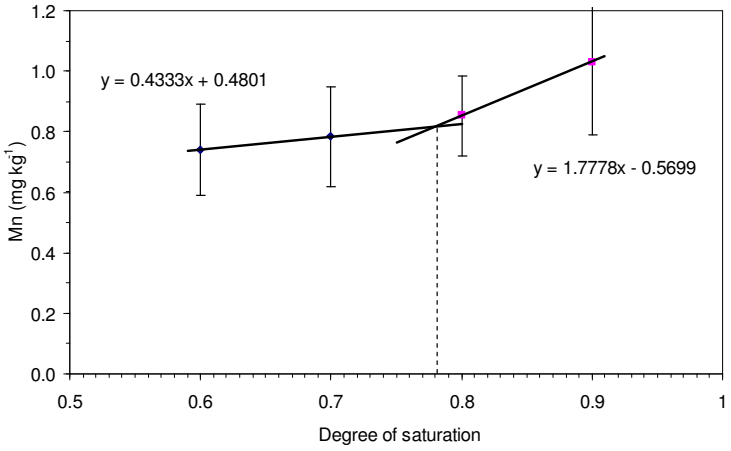

Figure 6.38 Average Mn^{2+} (mg kg^{-1}) concentration and standard deviation for four treatments ($S_{0.6, 0.7, 0.8, 0.9}$) over a period of 121 days, with the linear trend line extrapolated to the point where they crossed; dotted line indicates degree of water saturation at crossing point (x = 0.78, y = 0.82).

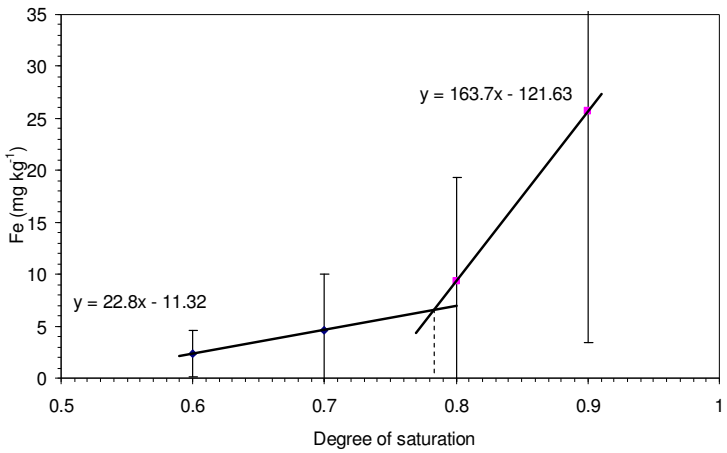

Figure 6.39 Average Fe^{2+} (mg kg^{-1}) concentration and standard deviation for four treatments ($S_{0.6, 0.7, 0.8, 0.9}$) over a period of 121 days, with the linear trend line extrapolated to the point where they crossed; dotted line indicates degree of water saturation at crossing point (x = 0.78, y = 6.46).

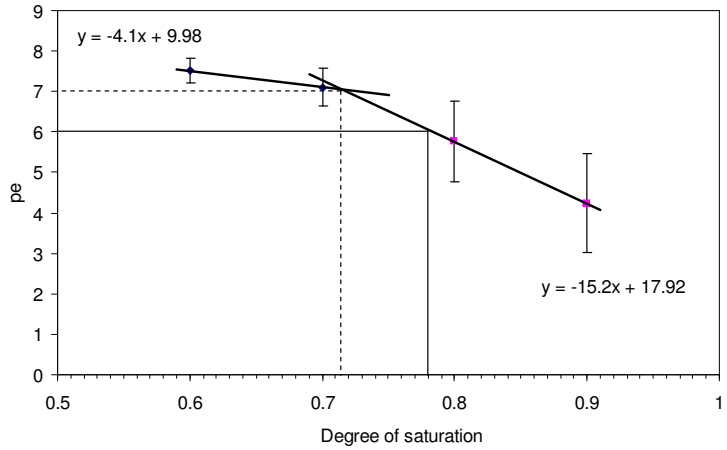

Figure 6.40 Average pe and standard deviation for four treatments ($S_{0.6, 0.7, 0.8, 0.9}$) over a period of 121 days, with the linear trend line extrapolated to the point where they crossed; dotted line indicates degree of water saturation at crossing point (x = 0.72, y = 7.2) and solid line indicates optimal degree of water saturation and pe at which Mn^{2+} and Fe^{2+} will set in (x = 0.78, y = 6).

$S_{0.6}$

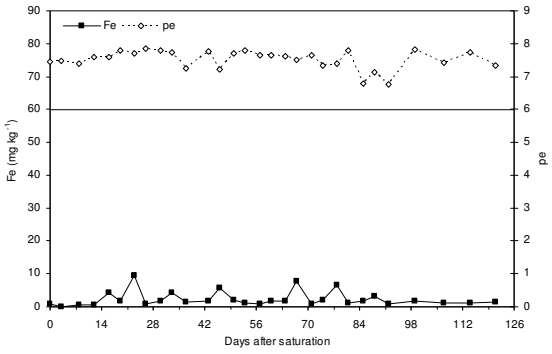

$S_{0.7}$

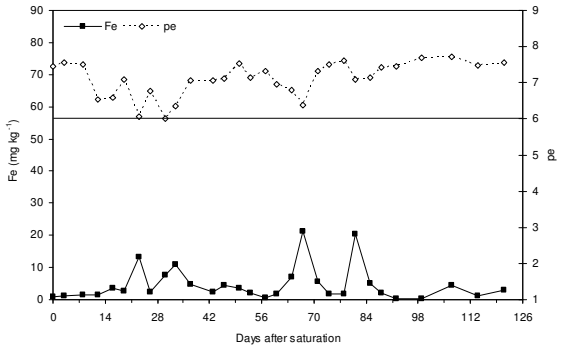

$S_{0.8}$

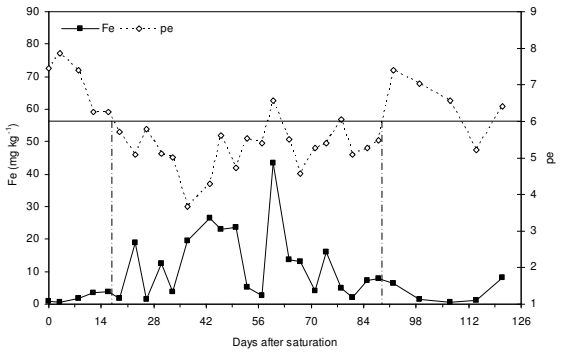

$S_{0.9}$

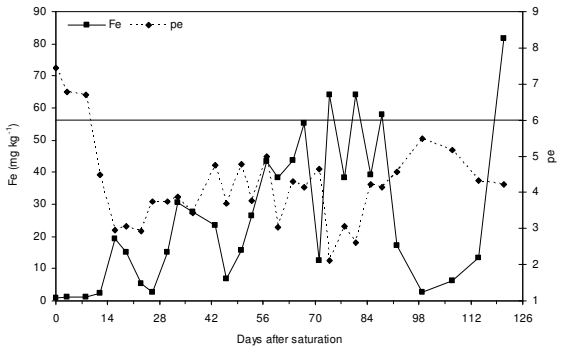

Figure 6.41 Average pe and Fe^{2+} concentration for four treatments ($S_{0.6,\ 0.7,\ 0.8,\ 0.9}$) over a period of 121 days, with the solid line set at a pe of 6. The dotted line in $S_{0.8}$ indicates where the pe decreases below 6.

It was determined that for this soil, Fe^{2+} and to a certain extent Mn^{2+} will start reducing at a pe of 6 and at an optimal degree of water saturation of $S_{0.78}$. This method could not be used for the Eh graph was not used as an indication of Mn^{2+} and Fe^{2+} reduction, as the Eh value was too high. The Eh was indicated at 414.5 mV and according to literature (Brookins, 1988; Faulkner & Patrick, 1992; Mansfeldt, 2003; Vepraskas, 2001) Mn^{2+} and Fe^{2+} do not readily reduce at such high Eh values.

These findings show that the first approximation of Van Huyssteen *et al*. (2005), where it was stated that $S_{0.7}$ was sufficient for reduction was very similar for this soil under these conditions.

6.6 Summary

It was concluded that individual core analysis of redox conditions delivered a better result than column analysis. Individual cores were packed to a bulk density of 1.6 Mg m^{-3}. Four water saturation treatments were used, namely $S_{0.6, 0.7, 0.8, 0.9}$. Triplicates were made of each set. The cores were kept at their respective s values for 121 days after which the experiment was terminated.

The pH showed a significant difference in relation to duration of water saturation, although not in degree of water saturation. Even though there was no significant difference between the different water saturations, the standard deviation between them did vary more with increasing degree of water saturation. This is due to the fact that H^+ ions were used in reducing reactions, thereby increasing the pH.

The Eh varied markedly during the study from a maximum of 463 mV in the $S_{0.6}$ core to a minimum of 124 mV in the $S_{0.9}$ core. The Eh was significantly affected by the duration as well as the degree of water saturation. The Eh was interpreted as pe to aid in better correlation with pH. The pe is directly related to the Eh, therefore it was also significantly affected by these two factors. There was a good correlation ($R^2 = 0.95$) between pe and degree of water saturation, with a decrease in pe from $S_{0.6}$ being 8, through to a pe of 4 in $S_{0.9}$. The standard deviation of Eh also increased as the s value increased from 17 in $S_{0.6}$ to 72 in $S_{0.9}$. This could be as a result of the greater redox activity in the higher water saturations, thereby leading to increased micro site activity.

The Mn^{2+} concentration was significantly affected by degree of water saturation as well as duration of water saturation. There was a good correlation ($R^2 = 0.91$) between the Mn^{2+}

concentration and an increase in degree of water saturation. The standard deviation also increased with an increase in degree of water saturation. This could have been as a result of the increased redox activity as the degree of water saturation increased. It was also found that there was an inverse relationship between Mn^{2+} concentration and pH. Therefore as the pH became more acidic, the Mn^{2+} concentration increased.

The Fe^{2+} concentration was significantly affected by duration of water saturation as well as degree of water saturation. The Fe^{2+} concentration showed a good correlation to pe. The lower the pe in the cores, the higher was the Fe^{2+} concentration in the soil. The average Fe^{2+} concentration increased dramatically from the lower water saturation to the higher degree of water saturation, thereby reinforcing the statement that reduction takes place more intensely the higher the degree of water saturation at a specific bulk density. The maximum Fe^{2+} concentration fluctuations also increased with time. The standard deviation increased with an increase in degree of water saturation. For this soil at a bulk density of 1.6 Mg m^{-3}, all the cation concentrations studied were significantly affected by duration of water saturation, and only Mg^{2+} and Na^{+} were significantly affected by the degree of water saturation.

The Ca^{2+} concentration was significantly affected by duration of saturation although not by degree of saturation. The Ca^{2+} concentration in the soil was affected to a large extent by factors such as $Mn^{2+} + Fe^{2+}$ concentration, pe and pH. There was an inverse relationship between $Mn^{2+} + Fe^{2+}$ concentration and the Ca^{2+} concentration in the soil, and a direct relationship between Ca^{2+} concentration and pH.

The Mg^{2+} concentration was significantly affected by duration of saturation as well as degree of saturation. The $S_{0.7}$ and $S_{0.8}$ treatments had a higher average Mn^{2+} concentration than the $S_{0.6}$ and $S_{0.9}$ treatments. The $Mn^{2+} + Fe^{2+}$ concentration did not affect the Mg^{2+} concentration to a large extent, although it was found that the Mg^{2+} concentration reacted inversely to the pH of the soil.

The K^{+} concentration was significantly affected by duration of water saturation and not by degree of water saturation. The K^{+} concentration behaved very similarly in all the cores and increased with an increase in the duration of water saturation. During the first two weeks of analysis the K^{+} concentration decreased in all the degree of saturation treatments, after which it increased in all the treatments after 98 days of saturation.

The Na^+ concentration did not differ between the different water saturations. The Na^+ concentration decreased with time, irrespective of the water saturation. The decrease in Na^+ concentration was probably as a result of the Na^+ being adsorbed to the clay complex as the other cations were displaced and left the exchange complex.

After 330 days the column packed as described in Chapter 5 was cut up into 0.1 m sections. The individual cores were analysed for pH, Eh, Fe^{2+}, Mn^{2+}, Ca^{2+}, Mg^{2+}, K^+ and Na^+ in exactly the same manner as in Chapter 6. All the cations displayed a decrease in concentration from the top of the column (segment 9) to the bottom of the column (segment 1) except for the Mg^{2+} concentration. Therefore an increase in Mn^{2+} + Fe^{2+} concentration lead to a decrease in Ca^{2+}, K^+ and Na^+ and an increase in Mg^{2+} concentration. No colour change occurred in any of the segments as indicated by a Munsell colour chart.

In another experiment where cores were packed to a bulk density of 1.6 Mg m^{-3} and saturated to $S_{0.9}$ redox accumulations and depletions occurred within 12 months of saturation. It could therefore be confirmed that this soil with 0.22% organic carbon at a bulk density of 1.6 Mg m^{-3} will produce morphological features within a year of saturation at $S_{0.9}$.

Through data analysis over the 121 day period it was determined that the $S_{0.6}$ and $S_{0.7}$ treatments reacted similarly and they were grouped together with a trend line, the same was done for the $S_{0.8}$ and $S_{0.9}$ treatments. The trend lines on the Mn^{2+} and Fe^{2+} graphs were extrapolated until the point was obtained where the trend lines crossed. This point was taken as the optimal degree of water saturation for the reduction of both Mn^{2+} and Fe^{2+} and was found to be $S_{0.78}$. This was very close to the first approximation made by Van Huyssteen *et al*., 2005. This was then plotted against the $S_{0.8}$ trend line for pe. It was found that at a water saturation of $S_{0.78}$ the optimal pe for Mn^{2+} and Fe^{2+} reduction is 6 (Eh = 350 mV). The same was done for the pe graph, although this delivered unsatisfactory results.

An optimal pe of 6 for Fe^{2+} reduction was then plotted against the pe and Fe^{2+} concentration graphs. It was found that the most Fe^{3+} reduction takes place where the pe decreased below 6 units. The pe did not decrease below 6 in treatment $S_{0.6}$ or $S_{0.7}$ during the 121 days of analysis, and the Fe^{2+} concentration did not increase significantly during this period. In $S_{0.8}$ the Fe^{2+} concentration increased during the periods where the pe was below 6. In $S_{0.9}$ the pe was constantly above 6 and the Fe^{2+} was also constantly in solution. This relationship between an increase in the Fe^{2+} concentration when the pe was below 6 was not found for the Mn^{2+} concentration. The lack of relationship could be attributed to the fact

that Mn^{2+} was more sensitive to pH, and therefore pH also played a greater role in the reduction of Mn^{2+}.

In the light of these findings, it was determined that for this soil in a closed system i.e. no lateral feeding by CO_2 rich water, Fe^{2+} and to a certain extent Mn^{2+} will start reducing at an optimal pe of 6 (Eh = 354 mV) and a degree of water saturation of $S_{0.78}$. These findings show that the first approximation of Van Huyssteen *et al.* (2005) where it was stated that $S_{0.7}$ was sufficient for reduction was very accurate.

CHAPTER 7

EFFECT OF BULK DENSITY AND DURATION OF WATER SATURATION ON IRON, MANGANESE AND SELECTED BASIC CATIONS

7.1 Introduction

Soil physical parameters indirectly influence soil respiration through their effect on the transport of O_2 and carbon dioxide. Increased bulk density, of which the extent largely depends on texture and structure, leads to a reduction in pore space and a change in aeration and water balance as well as a change in water movement within the soil. Therefore bulk density influences soil respiration by changing its air-filled porosity (Glinski & Stepniewski, 1985). Soil bulk density can be used as an indicator of the extent to which a soil has become compacted (Foth, 1978). Increased compaction of a soil will reduce soil aeration as measured by a decrease in Eh and hydraulic conductivity (Aust & Lea, 1992; Czyz, 2004).

At low air filled porosities of around < 0.2 m^3m^{-3}, a decrease in soil respiratory activity occurs. A sharp drop in Eh is observed at a certain critical air-filled porosity; at this point the soil pores become discontinuous. This critical value depends largely on soil structure (Glinski & Stepniewski, 1985).

A soil with a lower bulk density, saturated to $S_{0.8}$ will contain more water and air than a soil with a higher bulk density at the same saturation. This concept is represented by Figure 7.1, where the solid, air and water ratio of a soil with a bulk density 1.4, 1.6 and 1.8 Mg m^{-3} was determined.

The air (9%) and water content (38%) would be greatest in a core packed to a bulk density of 1.4 Mg m^{-3}, and would decrease in the 1.6 Mg m^{-3} bulk density to an air content of 8% and a water content of 32%. The air and water contents would be lowest in a core packed to a bulk density of 1.8 Mg m^{-3}, being 6% and 26% respectively. The solid ratio would increase in the opposite direction.

It can therefore be assumed that a soil with a higher bulk density will have a higher propensity to reduce when saturated than a soil with a lower bulk density. This is because there are less macropores in a soil with a higher bulk density and because macropores are responsible for soil aeration (Hillel, 1998). For a given amount of water, a soil with a higher

bulk density will therefore have a higher degree of water saturation than a soil with a lower bulk density.

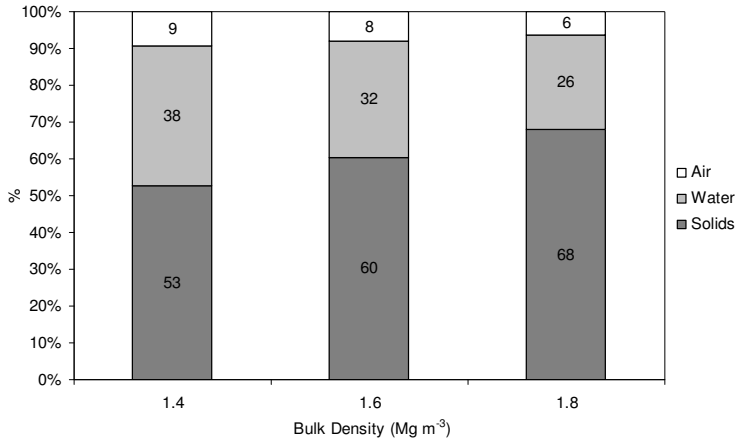

Figure 7.1 Solid, water and air fractions (by volume) for a soil with varying bulk densities at $S_{0.8}$ (80% of porosity).

An experiment was set up to test the hypothesis. The same experimental setup as in Chapter 6 was used, except that the bulk densities varied, while the degree of water saturation remained constant.

7.2 Material and methods

The mixed B1 and B2 horizon of profile 234 described in Chapter 4, was used for this experiment. Cores were constructed by packing the soil in PVC pipes, 0.1 m high, and 0.104 m in diameter. The experiment consisted of a set of 3 cores packed to a initial bulk density of 1.4, 1.6, 1.8 Mg m^{-3}, with three replications. Extreme caution was taken not to create layers of varying bulk densities in the cores. A thin metal rod was used to break up layers while packing and the core was constantly turned over in order to prevent the particle sizes from separating. Cores with a bulk density of 1.6 and 1.8 Mg m^{-3} were first saturated to $S_{0.5}$ to aid in the packing process. It had already been determined in Chapter 6 that reduction did not take place at a water saturation of $S_{0.6}$, therefore $S_{0.5}$ was deemed a safe saturation value to use.

After all the cores were packed, they were saturated to $S_{0.8}$ with distilled water (Table 7.1). The water was used directly from the distiller and was therefore not cooled down to room temperature. Through the use of this method, it was thought to ensure that the water had a very low O_2 content.

Table 7.1 Amount of water needed to bring cores to $S_{0.8}$

Bulk density ($Mg\ m^{-3}$)	Fraction of water	Water volume needed to saturated cores (cm^3)
1.4	0.38	320
1.6	0.32	269
1.8	0.26	218

The cores were saturated as described in section 6.2.1. Once the cores were saturated, they were covered with two layers of plastic wrap and sealed with elastic bands. The cores were then stored at room temperature (± 23℃) until needed.

The first measurement took place three days after saturation. Measurements were then taken every 3 ½ days. Eh, pH, Fe^{2+}, Mn^{2+}, Ca^{2+}, Mg^{2+}, K^+ and Na^+ were all determined by the same method as described in section 6.2.1. The experiment was terminated after 23 days of saturation.

7.3 Results and discussion

In the summary of the analyses of variance (Table 7.2) it can be seen that all the factors showed a significant difference with duration of water saturation except Mg^{2+} and K^+. The Mg^{2+} and K^+ concentrations in the cores remained stable throughout the 23 days. All the factors except Ca^{2+} and Mg^{2+} showed a significant difference with a variation in bulk density.

Table 7.2 Summary of the analyses of variance indicating the significant effects of duration of water saturation and bulk density on pH, Eh, Fe^{2+}, Mn^{2+}, Ca^{2+}, Mg^{2+}, K^+ and Na^+ at a 95% confidence level

Treatments[a]	pH	Eh	Fe^{2+}	Mn^{2+}	Cations			
					Ca^{2+}	Mg^{2+}	K^+	Na^+
A	*	*	*	*	*			*
B	*	*	*	*			*	*
AB					*			

[a] A: Duration of saturation, B: Bulk density, AB: Duration of saturation and Bulk density

The full data set for 1.4 Mg m^{-3} (Table E1), 1.6 Mg m^{-3} (Table E2) and 1.8 Mg m^{-3} (Table E3) is given in Appendix E. These results as well as the ANOVA will be discussed separately in the following sections.

7.3.1 pH

The data represented in Figure 7.2 is an average of three daily replications for 7 days over a period of saturation of 23 days. The data represented in Figure 7.3 is the average of each set of replications for the duration of water saturation and each data point was therefore calculated from 7 measurements over a period of 23 days.

The pH was significantly affected by duration of water saturation as well as a variation in bulk density (Table 7.2). The average pH over the 23 days of saturation was the highest in the 1.4 Mg m^{-3} bulk density core followed by the 1.8 Mg m^{-3} bulk density and lowest in the 1.6 Mg m^{-3} bulk density (Figure 7.2). The pH of all the bulk densities increased after the first measurement after which they all decreased to values lower than the initial pH of the soil. After 8 days of saturation the pH in the 1.4 and 1.8 Mg m^{-3} bulk density cores stabilized with the 1.6 Mg m^{-3} bulk density core initially increasing for 4 measurements and then decreasing.

The standard deviation was the greatest in the 1.6 Mg m^{-3} bulk density cores with the standard deviation being relatively similar in the 1.4 and 1.8 Mg m^{-3} cores.

It was therefore concluded that for this soil saturated to $S_{0.8}$, pH was significantly affected by a change in bulk density as well as duration of water saturation.

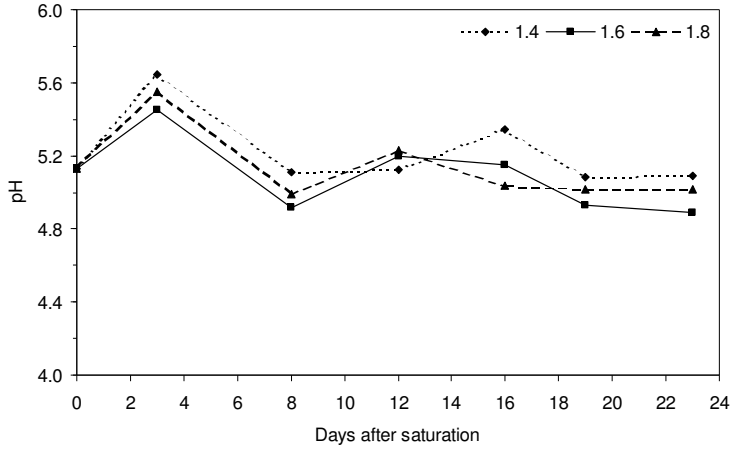

Figure 7.2 pH for all bulk densities over a period of 23 days.

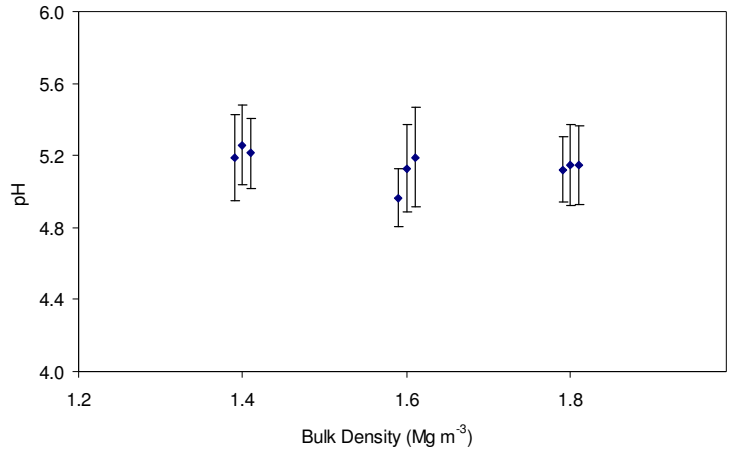

Figure 7.3 Average pH and standard deviation of three sets of replications consisting of 30 measurements each over a period of 23 days.

7.3.2 pe

The Eh was significantly influenced by duration of water saturation and bulk density as indicated through the analysis of variance (Table 7.2). The average and minimum Eh increased with an increase in bulk density. The maximum Eh was the same for all three treatments as the Eh decreased in all the treatments after the first measurement. The range in Eh was much higher in the 1.4 Mg m^{-3} bulk density core and decreased as the bulk density increased. According to Mansfeldt's (2003) reduction status indicators, the 1.4 Mg m^{-3} bulk density core was moderately reducing, the 1.6 Mg m^{-3} bulk density core was weakly reducing and the 1.8 Mg m^{-3} bulk density core was oxidizing (Table 7.3)

Table 7.3 Eh statistics for the bulk density experiment over a 23 day period

Bulk Density (Mg m^{-3})	Average[a]	Minimum	Maximum	Range	std dev	Reduction status[b]
	(----------mV----------)					
1.4	169	-93	439	532	155	III
1.6	388	104	439	335	113	II
1.8	425	321	439	119	52	I

[a] Data calculated from 21 measurements over a period of 23 days; [b] I; oxidizing (>400 mV); II, weakly reducing (400 to 200 mV); III, moderately reducing (200 to -100 mV); IV, strongly reducing (<-100 mV) (Mansfeldt, 2003)

To aid in better interpretation, the Eh was interpreted by using pe. The pe was used when compared with Fe^{2+}, Mn^{2+}, Ca^{2+}, Mg^{2+}, K^{+} and Na^{+}. The average pe calculated from seven sampling days over a 23 day period was much lower in the core packed to a bulk density of

1.4 Mg m^{-3} than in the 1.6 and 1.8 Mg m^{-3} bulk density cores. There was an excellent correlation (R^2 = 0.90) between an increase in pe and an increase in the bulk density. The pe increased on a linear scale with every unit increase in bulk density, from an average pe of 2.9 in the 1.4 Mg m^{-3} bulk density core to an average pe of 6.5 and 7.2 in the1.6 and 1.8 Mg m^{-3} bulk density cores respectivly. A perfect fit on a polynomial trend line exists for pe, although it was rather chosen to represent pe on a linear scale to ease interpretation. The standard deviation was the highest in the 1.4 Mg m^{-3} bulk density core after which it decreased in the 1.6 Mg m^{-3} and was the lowest in the 1.8 Mg m^{-3} bulk density core (Figure 7.5).

Reduction had already taken place within the first three days after saturation. Soil in the core packed to a bulk density of 1.4 Mg m^{-3}, reduced to a greater extent than the soil in the core packed to a bulk density of 1.6 and 1.8 Mg m^{-3}. After three days the pe was -1.6, 1.8 and 5.4 in the 1.4, 1.6 and 1.8 Mg m^{-3} bulk density cores respectively (Figure 7.4). Eight days after saturation the pe values in all the cores increased, after which they stabilized.

It was concluded that the bulk density had an effect on the pe. The pe was the lowest in the lower bulk density. This was contrary to what was anticipated to happen, as it was thought that the 1.8 and then the 1.6 Mg m^{-3} cores would reduce first. Possible reasons for this are discussed in section 7.3.9.

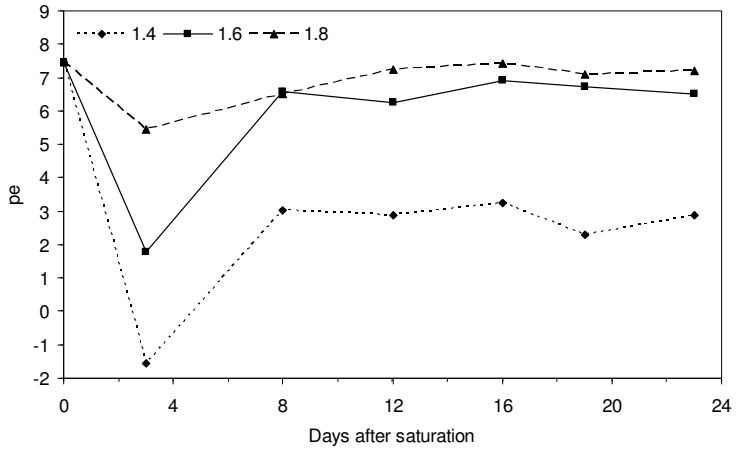

Figure 7.4 pe values for all bulk densities over the duration of the 23 days of saturation.

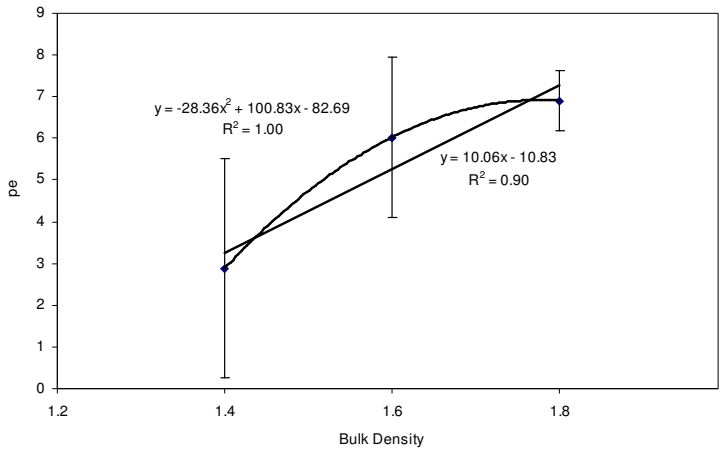

Figure 7.5 Average pe and standard deviation consisting of 7 sampling days over a period of 23 days of saturation.

7.3.3 Manganese

The data represented in Figure 7.6 is an average of three replications for 7 daily measurements over 23 days of saturation. The data represented in Figure 7.7 is the average of each set of replications for the duration of water saturation and each data point was therefore calculated from 7 measurements over a period of 23 days.

The soil's average Mn^{2+} concentration before saturation was 0.7 mg kg^{-1}. At the end of 23 days of saturation at $S_{0.8}$ the average Mn^{2+} concentration in the core packed to a bulk density of 1.4 Mg m^{-3} was 0.9 mg kg^{-1}, the core packed to a bulk density of 1.6 Mg m^{-3} had an average Mn^{2+} concentration of 0.6 mg kg^{-1}, and the core packed to a bulk density of 1.8 Mg m^{-3} an average of 0.7 mg kg^{-1}.

It was shown in the analysis of variance (Table 7.2) that the Mn^{2+} concentration was significantly influenced by duration of water saturation and bulk density. When the groups were compared using the Tukey-Kramer Multiple-Comparison Test (Hintze, 1997) it was found that only the core with a bulk density of 1.4 Mg m^{-3} differed from the rest. This can be seen when the Mn^{2+} concentrations were compared with one another (Figure 7.6), as the 1.4 Mg m^{-3} cores Mn^{2+} concentration was much higher than the other bulk densities. An excellent polynomial correlation (R^2 = 0.91) was found between the Mn^{2+} concentration and the bulk density of the cores (Figure 7.7). A decrease in Mn^{2+} concentration took place from the 1.4 Mg m^{-3} to the 1.6 Mg m^{-3} bulk density core and then a slight increase up to the 1.8 Mg m^{-3} bulk density core. The standard deviation in the 1.4 Mg m^{-3} bulk density core was much greater than in the two higher bulk densities.

It was anticipated that the most reduced core and therefore the highest concentration of Mn^{2+} would occur in the 1.8 Mg m^{-3} bulk density core. This was due to less macropores and therefore less soil aeration. On the contrary, the 1.4 Mg m^{-3} bulk density core had a much higher Mn^{2+} concentration than the 1.6 and 1.8 Mg m^{-3} bulk densities. The 1.4 Mg m^{-3} bulk density core had an average Mn^{2+} concentration of 1.1 mg kg^{-1} at the end of 23 days of water saturation, and the 1.6 and 1.8 Mg m^{-3} bulk density cores had an average Mn^{2+} concentration of 0.7 and 0.9 mg kg^{-1} respectively. The 1.8 Mg m^{-3} bulk density core had the second highest Mn^{2+} concentration and the 1.6 Mg m^{-3} bulk density core had the lowest Mn^{2+} concentration. The Mn^{2+} concentration was not affected by the pe + pH values of the cores, although when compared to the pH on its own, a better correlation was found. This agreed with the results found in Chapter 6.

In the 1.4 Mg m^{-3} bulk density core the Mn^{2+} concentration was directly related to the pH. An increase in pH occurred with an increase in the Mn^{2+} concentration. This correlation could not be made with the two higher bulk densities. This could be because the two higher bulk densities were not as reduced as the 1.4 Mg m^{-3} bulk density cores. In Chapter 6 it was reported that an increase in Mn^{2+} occurred together with a decrease in pH, therefore an inverse relationship existed between the two. As the degree of water saturation increased, this correlation improved. Mn^{2+} concentration is therefore influenced more by the pH at lower pH values than the redox potential of a soil.

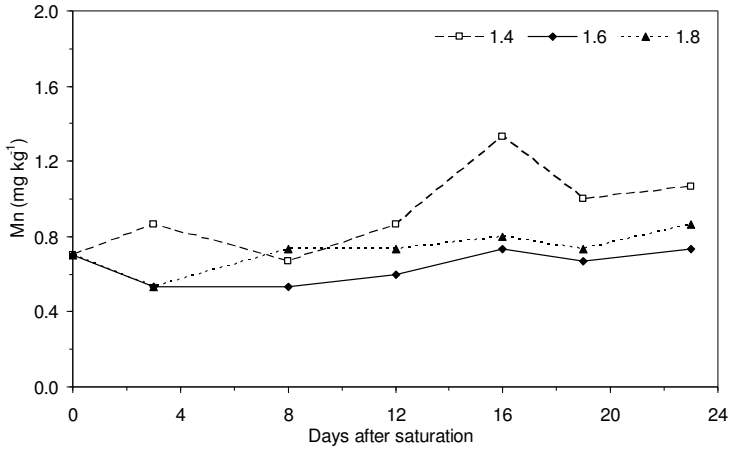

Figure 7.6 Average Mn^{2+} for all bulk densities for the duration of the 23 days of saturation.

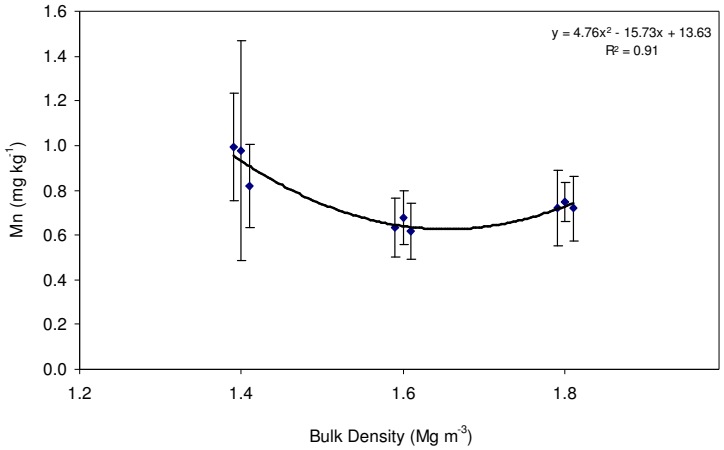

Figure 7.7 Average Mn^{2+} concentration and standard deviation of three sets of replications consisting of 7 measurements each over a period of 23 days.

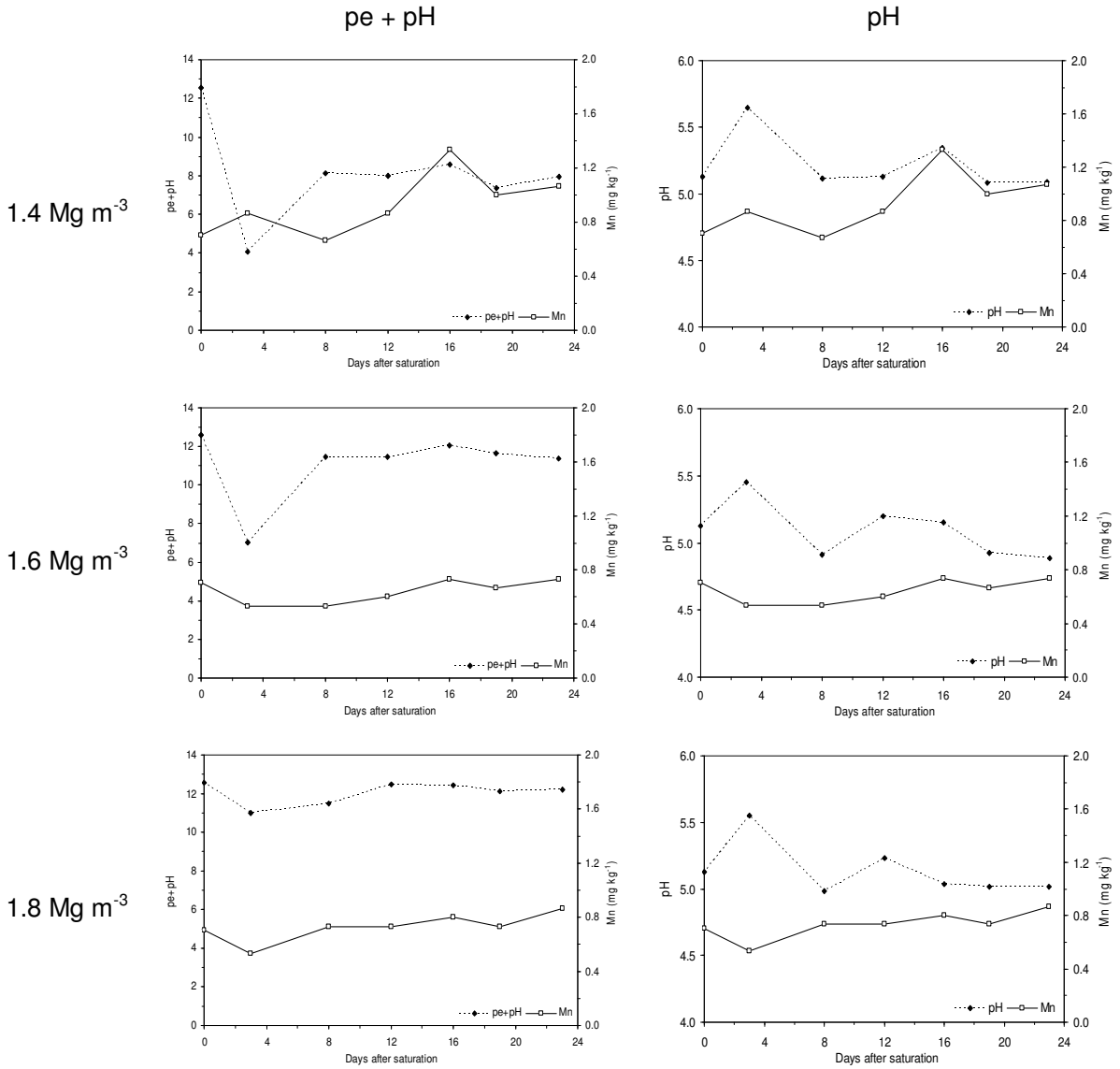

Figure 7.8 Mn^{2+} concentration, pe+pH and pH values for the bulk densities 1.4, 1.6, 1.8 Mg m^{-3}, saturated at $S_{0.8}$.

7.3.4 Iron

The data represented in Figure 7.9 is an average of three daily replications. The data represented in Figure 7.10 is the average of each set of replications over time and each data point was therefore calculated from 7 measurements over a period of 23 days.

The soil's average Fe^{2+} concentration before saturation was 0.9 mg kg^{-1}. At the end of 23 days of saturation at $S_{0.8}$ the average Fe^{2+} concentration in the core packed to a bulk density of 1.4 Mg m^{-3} was 19.3 mg kg^{-1}, the core packed to a bulk density of 1.6 Mg m^{-3} had an average Fe^{2+} concentration of 4.3 mg kg^{-1}, and the core packed to a bulk density of 1.8 Mg m^{-3} an average of 3.6 mg kg^{-1}.

The Fe^{2+} concentration in the 1.4 Mg m^{-3} bulk density increased linearly over time (R^2=0.93). It increased from 0.9 mg kg^{-1} to 18.9 mg kg^{-1} after the first ten days of saturation. Whereas there was only a slight increase in Fe^{2+} in the cores packed to 1.6 and 1.8 Mg m^{-3} bulk densities. The Fe^{2+} content never exceeded 10.0 mg kg^{-1} in these cores (Figure 7.9). It was shown in the analysis of variance (Table 7.2) that the Fe^{2+} concentration was significantly influenced by time and bulk density, although when the groups were compared using the Tukey-Kramer Multiple-Comparison Test (Hintze, 1997) it was found that only the core with a bulk density of 1.4 Mg m^{-3} differed from the rest. This can be seen in Figure 7.9.

No trend was found between Fe^{2+} concentration and bulk density. The standard deviation in the 1.4 Mg m^{-3} was much greater than the two higher bulk densities (Figure 7.11).

It was anticipated that the treatment with the highest concentration of Fe^{2+} should occur in the 1.8 Mg m^{-3} bulk density core. This was due to less macropores and therefore less soil aeration. The contrary happened, with the 1.4 Mg m^{-3} bulk density core reducing to a far greater extent than the 1.6 and 1.8 Mg m^{-3} bulk densities. The 1.8 Mg m^{-3} bulk density core reduced the least of all the cores.

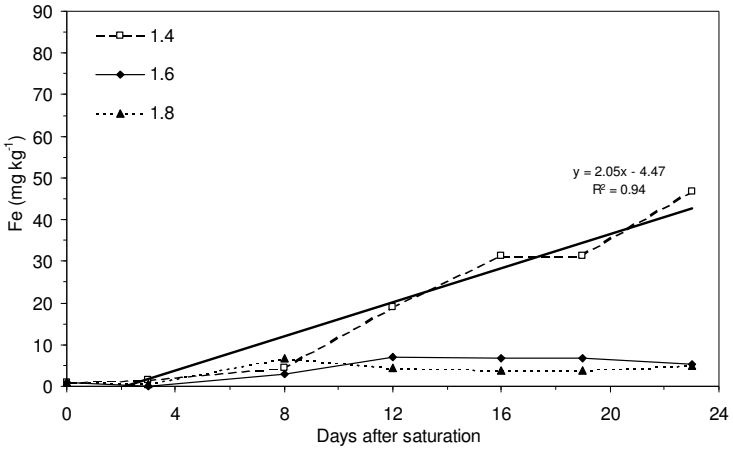

Figure 7.9 Fe^{2+} concentration for all bulk densities over a period of 23 days of saturation.

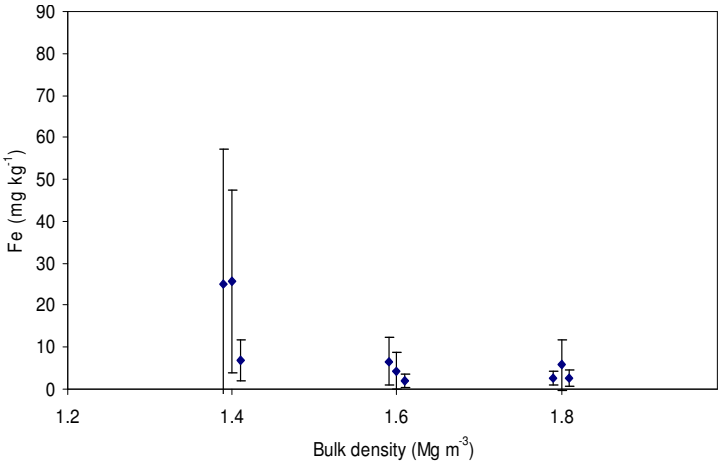

Figure 7.10 Average Fe^{2+} concentration and standard deviation of three sets of replications consisting of 7 measurements each over a period of 23 days.

1.4 Mg m^{-3}

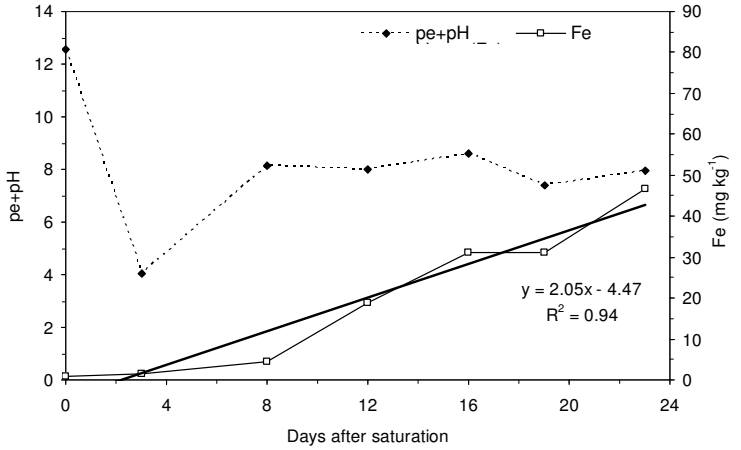

1.6 Mg m^{-3}

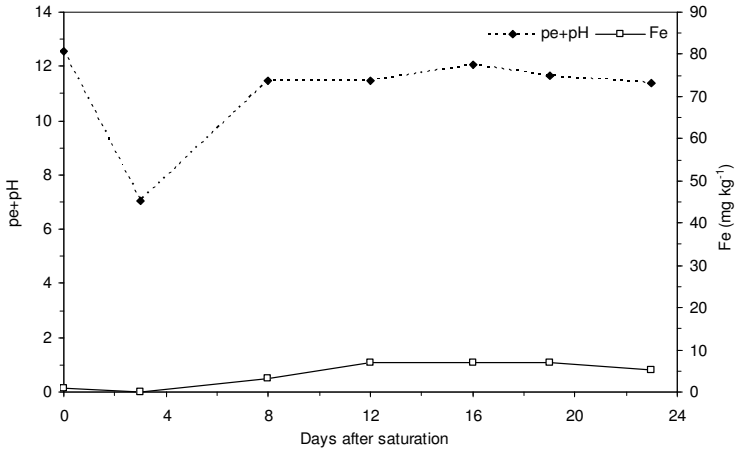

1.8 Mg m^{-3}

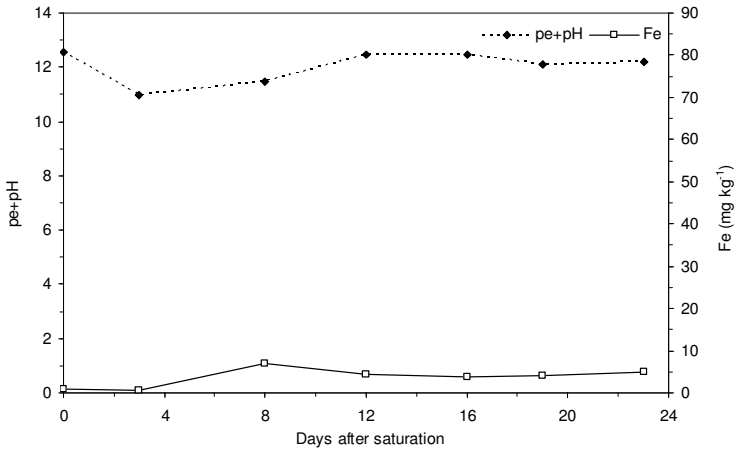

Figure 7.11 Fe^{2+} concentration and pe+pH values for the bulk densities 1.4, 1.6, 1.8 Mg m^{-3}, saturated at $S_{0.8}$.

7.3.5 Calcium

The data represented in Figure 7.12 is the average of each set of replications over time and each data point was calculated from 7 measurements over a period of 23 days. The data represented in Figure 7.13 is an average of three replications per daily measurement for each bulk density.

The soil's average Ca^{2+} concentration before saturation was 81.0 mg kg^{-1}. At the end of 23 days of saturation at $S_{0.8}$ the average Ca^{2+} concentration in the core packed to a bulk density of 1.4 Mg m^{-3} was 77.4 mg kg^{-1}, the core packed to a bulk density of 1.6 Mg m^{-3} had an average Ca^{2+} concentration of 75.4 mg kg^{-1}, and the core packed to a bulk density of 1.8 Mg m^{-3} an average of 78.8 mg kg^{-1}.

No trend was found between Ca^{2+} concentration and bulk density. The standard deviation in the 1.4 Mg m^{-3} was much higher than the 1.6 and 1.8 Mg m^{-3} bulk densities. This could be due to the higher Mn^{2+} + Fe^{2+} concentration in the 1.4 Mg m^{-3} bulk density which lead to an increased Ca^{2+} concentration.

It was shown in the analysis of variance (Table 7.2) that the Ca^{2+} concentration was significantly influenced by duration of water saturation. The Ca^{2+} concentration decreased with duration of water saturation after which it increased on the last day of measurement. The Ca^{2+} concentration was not significantly influenced by bulk density and this was confirmed when the groups were compared using the Tukey-Kramer Multiple-Comparison Test (Hintze, 1997). It was found that none of the cores differed significantly from each other (Figure 7.12).

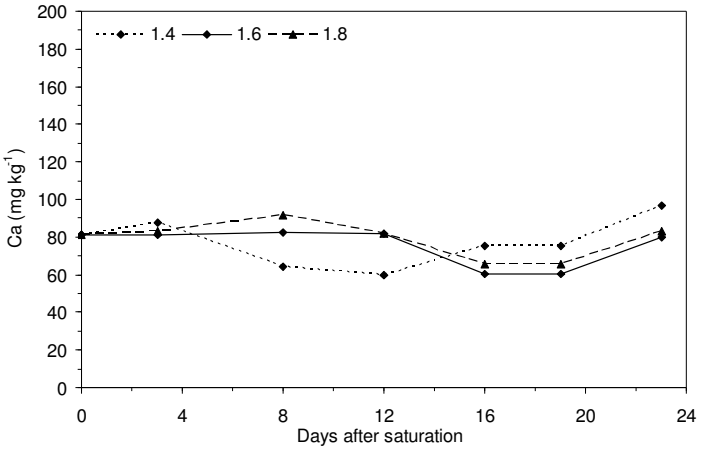

Figure 7.12 Average Ca^{2+} concentration of three sets of replications consisting of 7 measurements each over a period of 23 days.

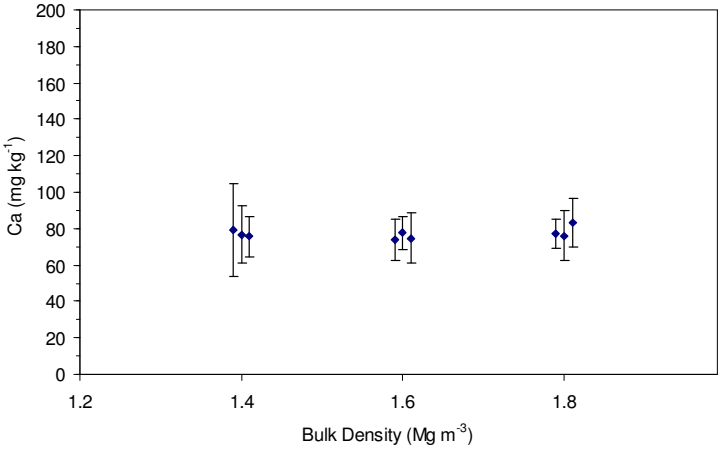

Figure 7.13 Average Ca^{2+} concentration and standard deviation of three sets of replications consisting of 7 measurements each over a period of 23 days.

1.4 Mg m^{-3}

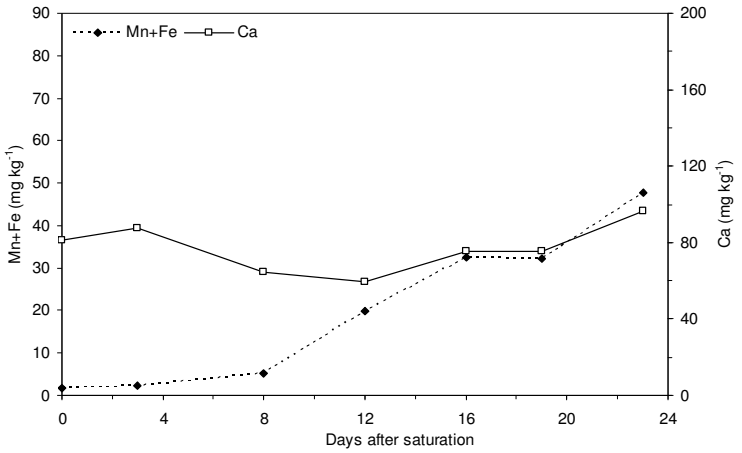

1.6 Mg m^{-3}

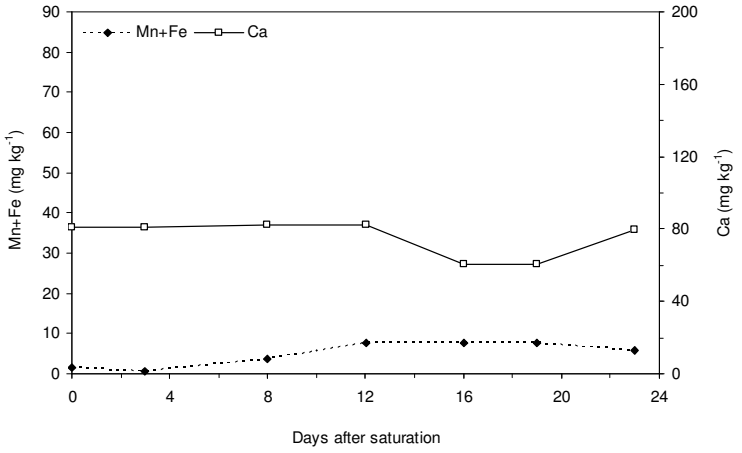

1.8 Mg m^{-3}

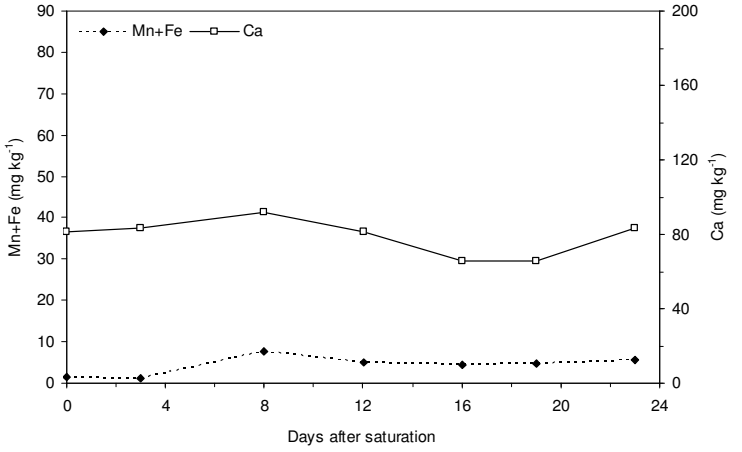

Figure 7.14 Ca^{2+} concentration and Mn+Fe values for the bulk densities 1.4, 1.6, 1.8 Mg m^{-3}, saturated at $S_{0.8}$.

7.3.6 Magnesium

The data represented in Figure 7.15 is the average Mg^{2+} concentration of three daily replications for 7 measurements over a 23 day period. Figure 7.16 is the average of each set of replications over time and each data point was calculated from 7 measurements over a period of 23 days.

The soil's average Mg^{2+} concentration before saturation was 51.7 mg kg^{-1}. At the end of 23 days of saturation at $S_{0.8}$ the average Mg^{2+} concentration in the core packed to a bulk density of 1.4 Mg m^{-3} was 51.5 mg kg^{-1}, the core packed to a bulk density of 1.6 Mg m^{-3} had an average Mg^{2+} concentration of 49.0 mg kg^{-1}, and the core packed to a bulk density of 1.8 Mg m^{-3} an average of 52.2 mg kg^{-1}.

It was shown in the analysis of variance (Table 7.2) that the Mg^{2+} concentration was neither significantly influenced by duration of water saturation nor by bulk density. The Mg^{2+} concentration remained stable during the course of the experiment, and this was confirmed when the groups were compared using the Tukey-Kramer Multiple-Comparison Test (Hintze, 1997). It was found that none of the cores differed from each other. This can also be seen in Figure 7.19 where none of the groups differ from one another. The standard deviation in the 1.4 Mg m^{-3} was greater than the two higher bulk densities (Figure 7.16). The Mn^{2+} + Fe^{2+} concentrations did not affect the Mg^{2+} in any of the bulk densities (Figure 7.17).

It was therefore concluded that the Mg^{2+} concentration was neither influenced by a variation in bulk density nor by a duration of water saturation. In phase 1 of the experiment, where the cores were saturated for 121 days, Mg^{2+} showed a significant difference in relation to duration of water saturation. The duration of water saturation of 23 days could have been too short in this case, to show a significant difference.

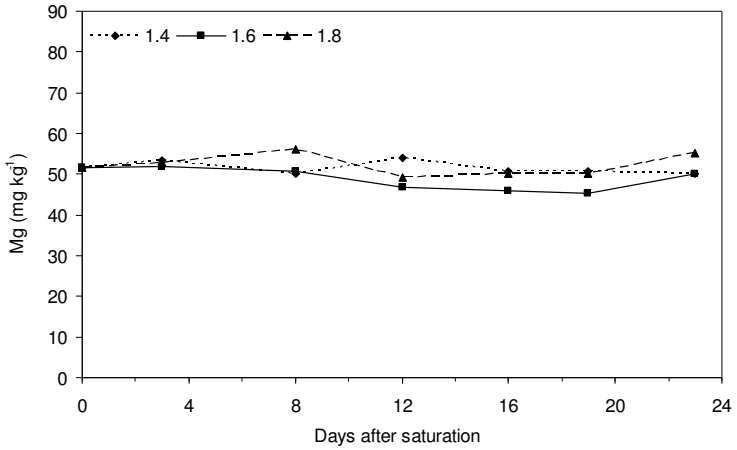

Figure 7.15 The Mg^{2+} concentration for all bulk densities over a period of 23 days.

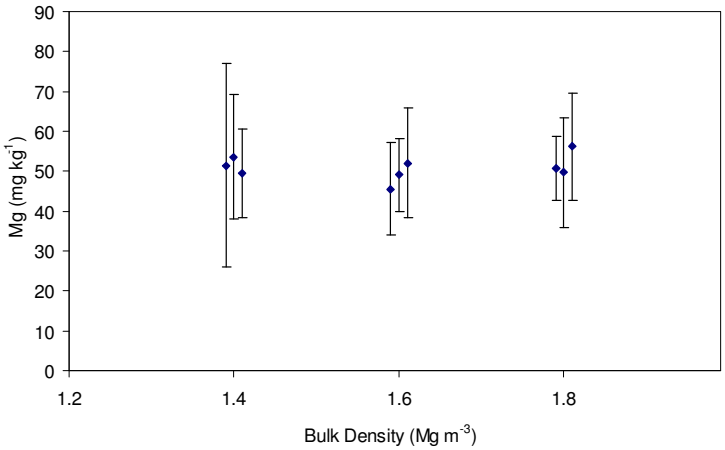

Figure 7.16 Average Mg^{2+} concentration and standard deviation of three sets of replications consisting of 7 measurements each over a period of 23 days.

1.4 Mg m^{-3}

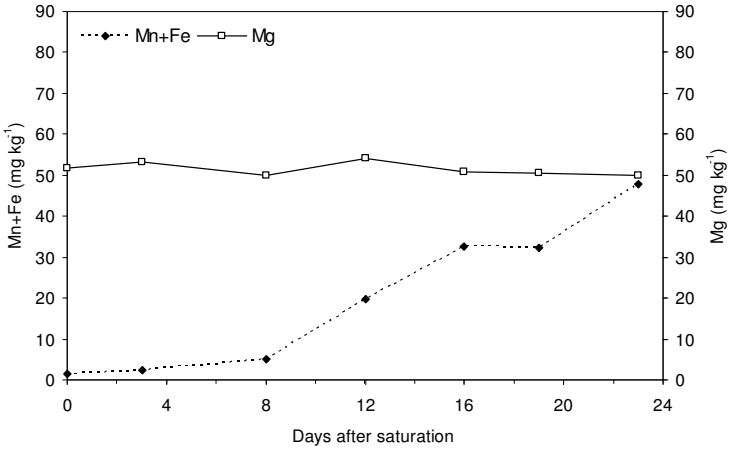

1.6 Mg m^{-3}

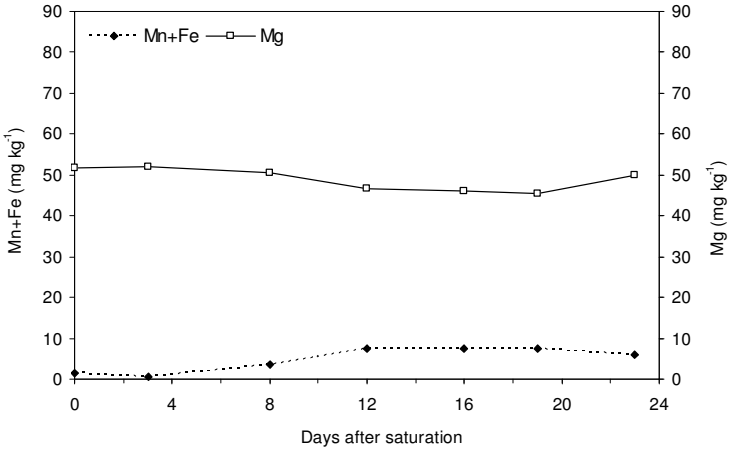

1.8 Mg m^{-3}

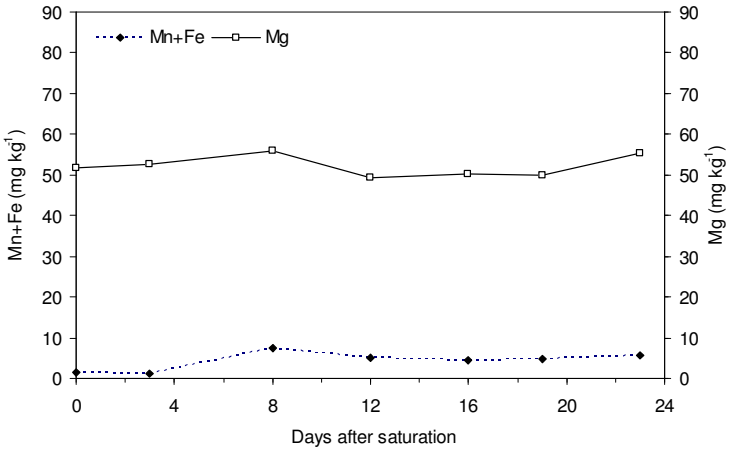

Figure 7.17 Mg^{2+} concentration and Mn+Fe values for the bulk densities 1.4, 1.6, 1.8 Mg m^{-3}, saturated at $S_{0.8}$.

7.3.7 Potassium

The data represented in Figure 7.18 is the average K^+ concentration of three daily replications for 7 measurements over a 23 day period. The data represented in Figure 7.19 is the average K^+ concentration of each set of replications over time and each data point was therefore calculated from 7 measurements over a period of 23 days.

The soil's average K^+ concentration before saturation was 25.0 mg kg^{-1}. At the end of 23 days of saturation at $S_{0.8}$ the average K^+ concentration in the core packed to a bulk density of 1.4 Mg m^{-3} was 36.3 mg kg^{-1}, the core packed to a bulk density of 1.6 Mg m^{-3} had an average K^+ concentration of 32.4 mg kg^{-1}, and the core packed to a bulk density of 1.8 Mg m^{-3} an average of 35.1 mg kg^{-1}.

It was shown in the analysis of variance (Table 7.2) that the K^+ concentration was significantly influenced by a variation in bulk density and not by duration of water saturation. According to the Tukey-Kramer Multiple-Comparison Test (Hintze, 1997), the 1.4 Mg m^{-3} and 1.6 Mg m^{-3} bulk density cores differed from one another, and the 1.8 Mg m^{-3} bulk density core did not differ from either of the two. The standard deviation's between the cores were very similar (Figure 7.24).

It was therefore concluded that the K^+ concentration was influenced by a variation in bulk density and not by duration of water saturation. In phase 1 of the experiment, where the cores were saturated for 121 days, K^+ showed a significant difference in relation to duration of water saturation. The time period of 23 days could have been too short in this case, to show a significant difference.

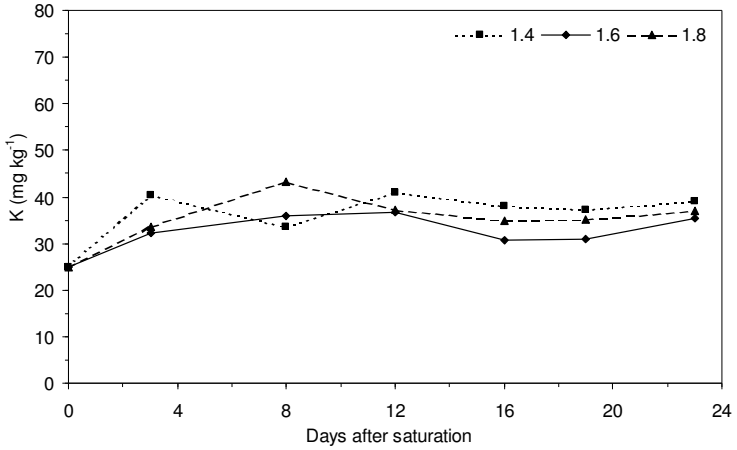

Figure 7.18 The K^+ concentration for all bulk densities over a period of 23 days.

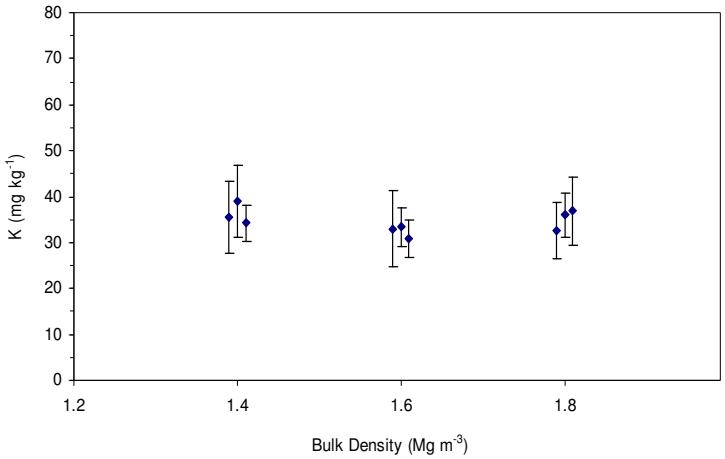

Figure 7.19 Average K^+ concentration and standard deviation of three sets of replications consisting of 7 measurements each over a period of 23 days.

1.4 Mg m^{-3}

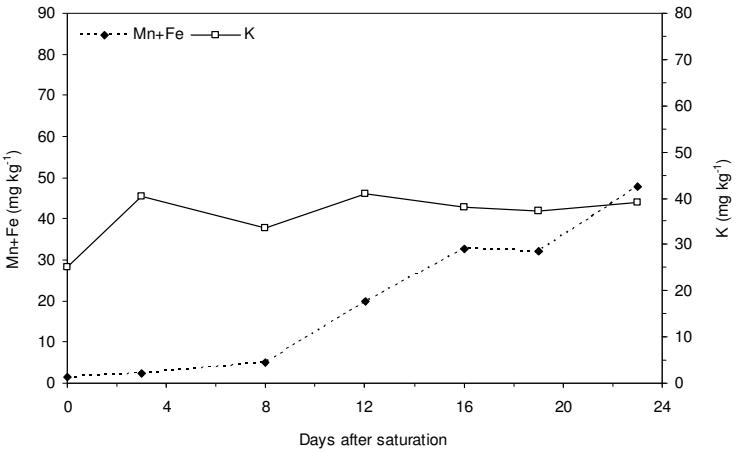

1.6 Mg m^{-3}

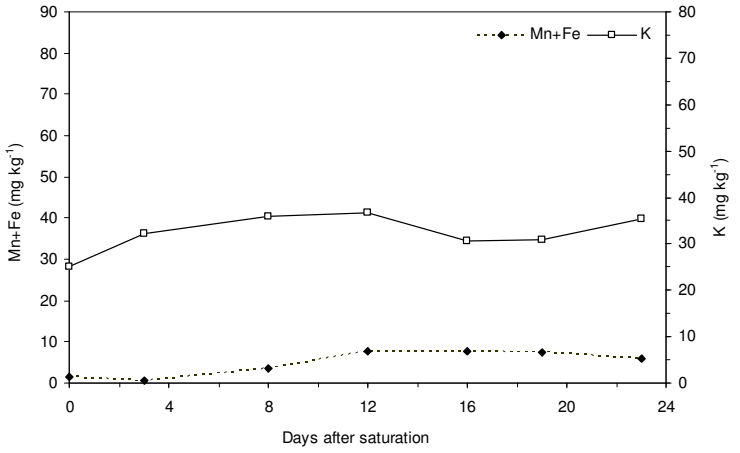

1.8 Mg m^{-3}

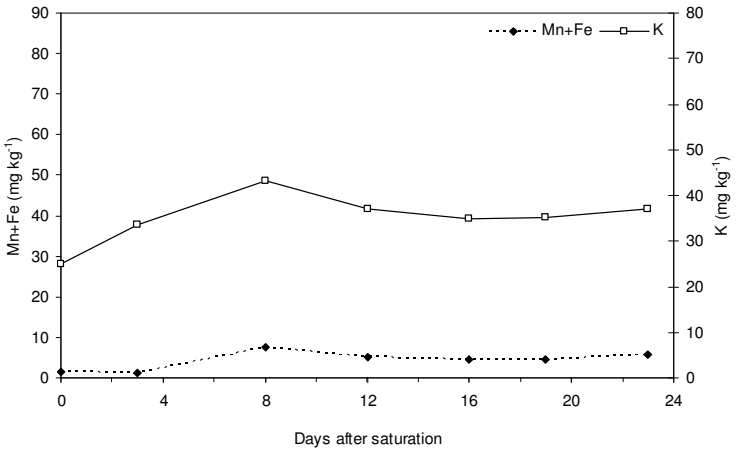

Figure 7.20 K^+ concentration and Mn+Fe values for bulk densities 1.4, 1.6, 1.8 Mg m^{-3}, saturated at $S_{0.8}$.

7.3.8 Sodium

The data represented in Figure 7.21 is the average Na^+ concentration of three daily replications for 7 measurements over a 23 day period. The data represented in Figure 7.22 is the average Na^+ concentration of each set of replications over time and each data point was therefore calculated from 7 measurements over a period of 23 days.

The soil's average Na^+ concentration before saturation was 15.7 mg kg^{-1}. At the end of 23 days of saturation at $S_{0.8}$ the average Na^+ concentration in the core packed to a bulk density of 1.4 Mg m^{-3} was 17.1 mg kg^{-1}, the core packed to a bulk density of 1.6 Mg m^{-3} had an average Na^+ concentration of 16.0 mg kg^{-1}, and the core packed to a bulk density of 1.8 Mg m^{-3} an average of 15.4 mg kg^{-1}.

It was shown in the analysis of variance (Table 7.2) that the Na^+ concentration was significantly influenced by a variation in bulk density as well as the duration of water saturation. No trend was found between Na^+ concentration and bulk density or duration of water saturation. The standard deviation between the cores was very similar. When the Na^+ concentration's between bulk densities were compared using the Tukey-Kramer Multiple-Comparison Test (Hintze, 1997), it was found that the 1.4 Mg m^{-3} bulk density core differed from the 1.8 Mg m^{-3} bulk density core and the 1.6 Mg m^{-3} bulk density core did not differ from either group.

It was therefore concluded that the Na^+ concentration was influenced by a variation in bulk density as well as duration of water saturation. The1.4 Mg m^{-3} bulk density had the highest average Na^+ concentration with an average of 17.1 mg kg^{-1} after 23 days and the1.8 Mg m^{-3} bulk density had the lowest average Na^+ concentration with an average of 15.4 mg kg^{-1} after 23 days. After the first reading until the last measurement the Na^+ concentration decreased in all the bulk densities by an overall average of 5.0 mg kg^{-1}.

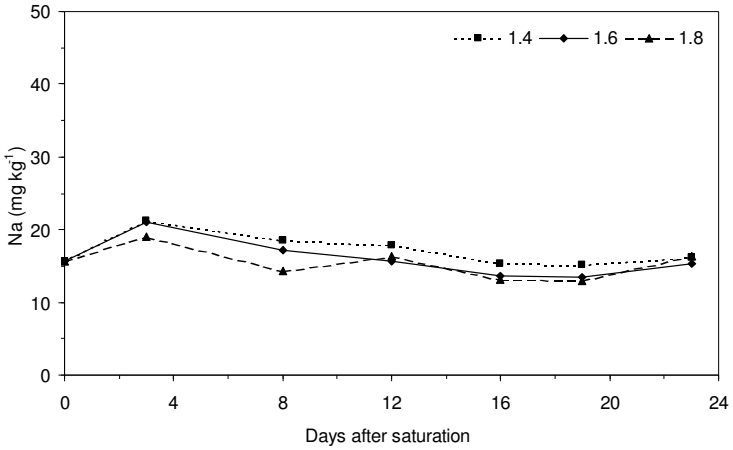

Figure 7.21 The Na^+ concentration for all bulk densities over a period of 23 days.

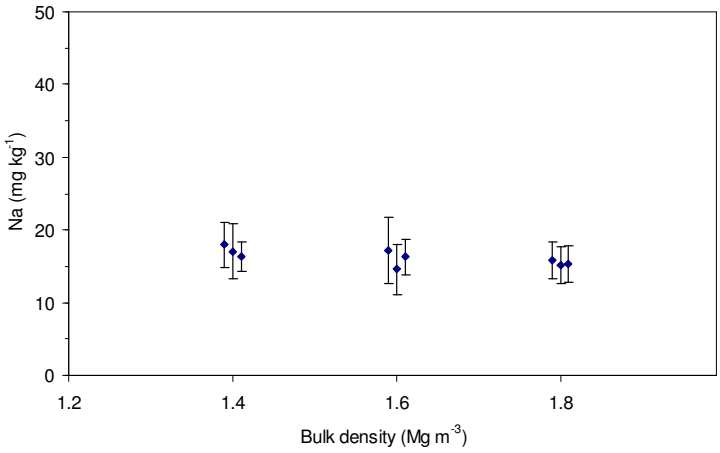

Figure 7.22 Average Na^+ concentration and standard deviation of three sets of replications consisting of 7 measurements each over a period of 23 days.

1.4 Mg m^{-3}

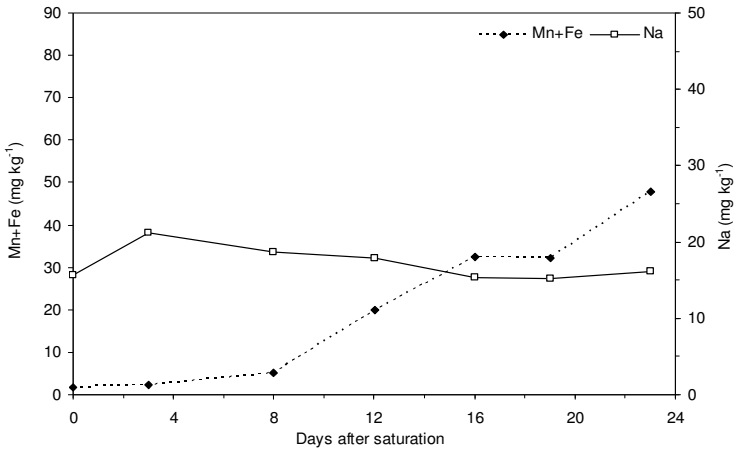

1.6 Mg m^{-3}

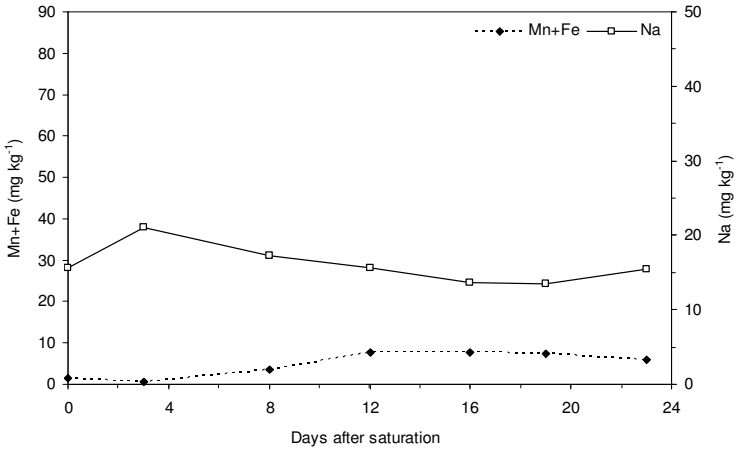

1.8 Mg m^{-3}

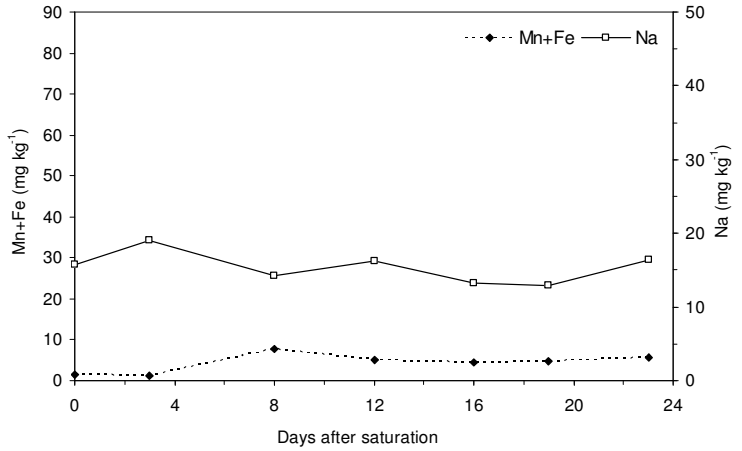

Figure 7.23 Na^+ concentration and Mn+Fe values for the bulk densities 1.4, 1.6, 1.8 Mg m^{-3}, saturated at $S_{0.8}$.

7.3.9 Comparison between phase 1 and phase 2 of experiment

To determine the effects of the warmer water used to saturate the cores, the two temperature treatments were compared. A direct comparison was made by using data from $S_{0.8}$ with a bulk density of 1.6 Mg m^{-3} in Chapter 6 and comparing it to the core saturated to $S_{0.8}$ with a bulk density of 1.6 Mg m^{-3} in Chapter 7. The data from Chapter 6 will be referred to as phase 1. These cores were saturated with room temperature water. The data from chapter 7 is referred to as phase 2, and these cores were saturated with hotter water directly from the distiller. The water in phase 2 was 6℃ hotter than the water used in phase 1 and both phases of the experiment were conducted in a laboratory at 23℃. Phase 1 of the experiment was continued for 121 days, but for the purpose of this comparison an extraction of the first 23 days of data was used.

In phase 1, the pe decreased for the first 23 days from a pe of 7.4 to a pe of 5.1. In phase 2 the pe dropped from 7.4 to 1.6 within the first three days after which it stabilized at around 6.5 (Figure 7.24).

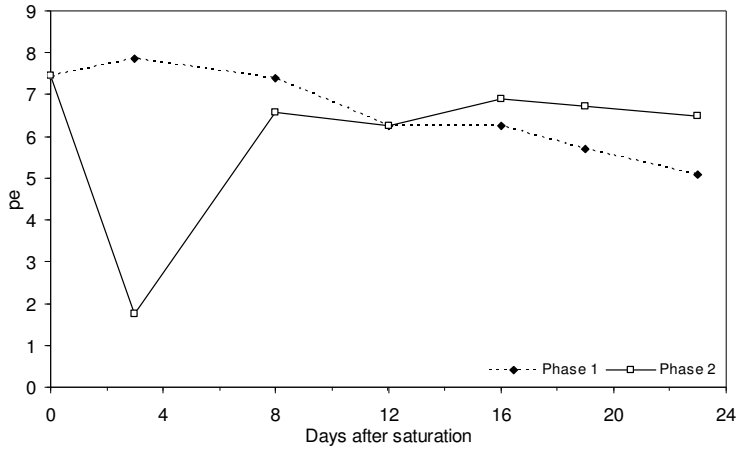

Figure 7.24 pe of phase 1 and phase 2 of the experiments respectively.

These two cores should have reacted similarly due to the fact that the experiment was carried out in the same manner. The sharp decrease in the pe of phase 2 of the experiment was not anticipated. It was also noticed that the 1.4 Mg m^{-3} bulk density core reduced to a greater extent than the 1.8 Mg m^{-3} bulk density core. This was also not anticipated as it was thought that the 1.8 Mg m^{-3} core would reduce faster due to it having less macropores than the 1.4 Mg m^{-3} at the same degree of water saturation.

The water temperature used to saturate must have played a role in this process and will be discussed in the next section. The higher water temperature (7℃) caused greater microbe activity which increased the microbe metabolism, decreasing the O_2 content in the soil and thereby caused a higher reduction rate (Glinski & Stepniewski, 1985). This could have contributed to the rapid decrease in pe in Figure 7.24.

7.4 Summary

Soil bulk density has a great effect on the amount of water a soil can hold. A soil with a higher bulk density will have less macropores and will hold less water than the same soil at a lower bulk density. The result of this is that the lower the bulk density, the more macropores, therefore the less the tendency for a soil to reduce.

A set of cores consisting of three bulk densities, 1.4, 1.6, and 1.8 Mg m^{-3} were saturated with water to $S_{0.8}$, each with three replications. A set of cores was analysed every 3.5 days, and the experiment was terminated after 23 days.

The analysis of variance (Table 7.2) showed that pH, Eh, Fe^{2+} and Mn^{2+} concentrations were all significantly affected by duration of water saturation, as well as bulk density. The Ca^{2+} and Na^{+} concentration were both significantly affected by duration of water saturation while K^{+} and Na^{+} were significantly affected by a variation in bulk density.

No trend was found between pH and bulk density or duration of water saturation. The pe increased linearly with an increase in bulk density and stabilized over time in all the bulk densities. The average pe increased from 3 in the 1.4 Mg m^{-3} bulk density core to 7 in the 1.8 Mg m^{-3} bulk density core.

Both the Mn^{2+} and Fe^{2+} concentrations were the highest in the 1.4 Mg m^{-3} bulk density core. It was anticipated that the 1.8 Mg m^{-3} bulk density core would reduce the fastest and therefore contain the highest Mn^{2+} and Fe^{2+} concentrations. The average Mn^{2+} and Fe^{2+} concentrations in the 1.4 Mg m^{-3} bulk density core decreased from 0.93 and 19.3 mg kg^{-1} to 3.62 and 0.73 in the 1.8 Mg m^{-3} bulk density core respectively. The Mn^{2+} concentration correlated better with the pH than the pe + pH. This correlation was not found for the Fe^{2+} concentrations. The Fe^{2+} correlated better to the pe + pH, with an increase in pe, leading to a decrease in Fe^{2+} concentration.

The Ca^{2+} concentration increased over time in all the treatments but was not significantly affected by a variation in bulk density. The average Ca^{2+} concentration increased from 81.0 mg kg^{-1} to 96.8, 79.9 and 83.1 mg kg^{-1} in the 1.4, 1.6 and 1.8 Mg m^{-3} bulk densities respectively. The Mg^{2+} concentration was not significantly influenced by either bulk density or duration of water saturation.

The K^+ concentration's were affected by the variation in bulk density although not affected by duration of water saturation. The K^+ concentration was the highest in the 1.4 Mg m^{-3} and lowest in the 1.6 Mg m^{-3} bulk density cores. The Na^+ concentration was significant affected by both bulk density and duration of water saturation. The Na^+ concentration decreased with a decreasing duration of water saturation in all the bulk densities. The average Na^+ concentration was the highest in the 1.4 Mg m^{-3} and lowest in the 1.8 Mg m^{-3} bulk density core.

It was hypothesised that the higher the bulk density, the higher the propensity would be to reduce. Therefore in this study, the 1.8 Mg m^{-3} bulk density core should have reduced first due to the lower amount of macropores, thereby having a lower amount of soil O_2 for the soil microbes to function aerobically. This hypothesis was not supported by the results.

If this experiment was to be repeated it is suggested that a lower degree of water saturation be used as macropores are already largely discontinuous at a degree of water saturation as high as $S_{0.8}$.

It was thought that the higher water temperature used might have caused the 1.4 Mg m^{-3} bulk density core to reduce faster than the rest due to a greater microbe activity which increased the microbe metabolism. Increased microbe metabolism would decrease the O_2 content in the soil and thereby cause a higher reduction rate. To determine the effects of the warmer water, the two temperature treatments were compared. A direct comparison was made by using data from $S_{0.8}$ with a bulk density of 1.6 Mg m^{-3} in Chapter 6 and comparing it to the core saturated to $S_{0.8}$ with a bulk density of 1.6 Mg m^{-3} in Chapter 7. The cores were set up in the same manner except for a difference in water temperature used to saturate them. It was found that the water temperature caused the cores to react differently. There was a higher Fe^{2+} concentration and the Eh decreased more rapidly in the core saturated with a higher water temperature. It was therefore decided to set up a second experiment to test what effect the water temperature had on the pH, Eh, Fe^{2+}, Mn^{2+}, Ca^{2+}, Mg^{2+}, K^+ and Na^+. These results are discussed in the next chapter.

CHAPTER 8

EFFECT OF WATER TEMPERATURE ON IRON, MANGANESE AND SELECTED BASIC CATIONS

8.1 Introduction

In phase 1, described in Chapter 6, of the experiment, the cores were saturated with distilled room-temperature water, whereas in phase 2, described in Chapter 7, the cores were saturated with distilled water taken directly from the distiller. The temperature of the water in phase 2 was 7°C higher than the water temperature used in phase 1. It was thought that the effect of the higher water temperature used in phase 2 of the experiment would wear off within an hour of saturating the cores, as the cores were stored at room temperature.

A comparison was done between phase 1 and phase 2, to determine what effect the warmer water temperature had on the pe, pH, Fe^{2+}, Mn^{2+} Ca^{2+}, Mg^{2+}, K^{+} and Na^{+}. Phase 1 of the experiment was stopped after 121 days of saturation, but for this comparison, only the first 23 days of data will be used.

8.1.1 Effect of temperature on pe, pH, Fe^{2+}, Mn^{2+} Ca^{2+}, Mg^{2+}, K^{+} and Na^{+}

The analysis of variance for the 1.6 Mg m^{-3} bulk density core saturated to $S_{0.8}$ with room temperature distilled water, phase 1, and the 1.6 Mg m^{-3} bulk density core saturated to $S_{0.8}$ with hot distilled water, phase 2 is presented in Table 8.1.

Table 8.1 Summary of the analyses of variance indicating the significant effects of duration of water saturation and water temperature on pH, Eh, Fe^{2+}, Mn^{2+}, Ca^{2+}, Mg^{2+}, K^{+} and Na^{+} at a 95% confidence level

Treatments[a]	pH	Eh	Fe^{2+}	Mn^{2+}	Cations			
					Ca^{2+}	Mg^{2+}	K^{+}	Na^{+}
A	*		*				*	
B				*	*	*	*	*
AB		*	*		*		*	

[a] A: Duration of saturation, B: Temperature, AB: Duration of saturation and Temperature

A significant (Table 8.1) decrease in pH took place with an increased duration of water saturation (Figure 8.1) for both the treatments. The pH of phase 1 decreased on a linear

scale (R^2 = 0.84). The pH in phase 2 did not have such a good correlation to duration of water saturation. The pH of phase 1 decreased to a greater extent over time than the pH in phase 2, although this difference between the treatments was not significant (Table 8.1).

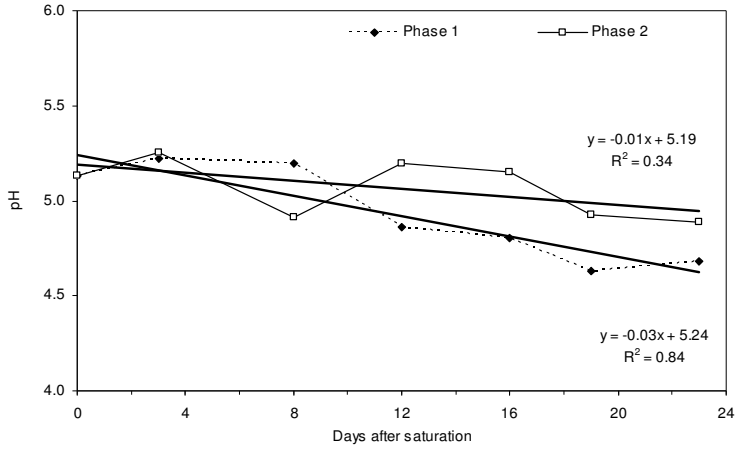

Figure 8.1 pH of phase 1 and phase 2 of the experiments respectively.

There was a good correlation (R^2 = 0.90) between pe and duration of water saturation in phase 1. The pe in phase 1 decreased linearly over the 23 day saturation period, whereas the pe in phase 2 decreased dramatically within the first 3.5 days after which it increased and stabilized with very little fluctuation. The cause of the pe stabilizing after 8 days could be due to the fact that the effects of the higher water temperature wore off as all the easily oxidisable organic matter had been depleted due to the high metabolism of the microbes during the first few days of saturation.

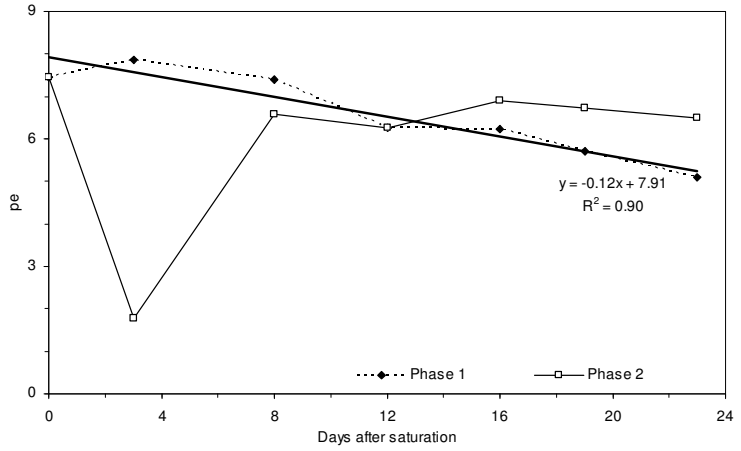

Figure 8.2 The pe of phase 1 and phase 2 of the experiments respectively.

The Fe^{2+} concentration increased during the 23 days of saturation in both the water temperatures, and therefore duration of water saturation affected the Fe^{2+} concentration significantly (Table 8.1). The water temperature treatments did not have a significant effect on the Fe^{2+} concentration in the cores (Table 8.1) and at the end of the 23 days of saturation the collective average Fe^{2+} concentration was very similar in both the treatments. An increase in Fe^{2+} concentration in phase 2 only took place after 8 days of saturation. Therefore the initial decrease in pe in phase 2 did not have an immediate effect on the Fe^{2+} concentration (Figure 8.3).

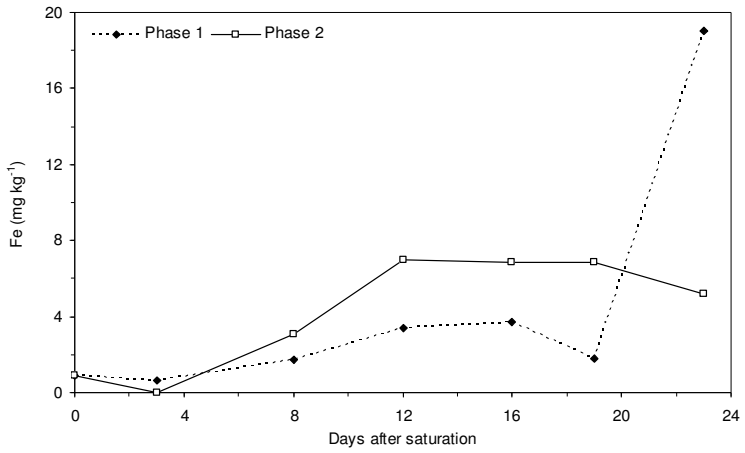

Figure 8.3 Fe^{2+} concentration for 1.6 Mg m^{-3} bulk density cores saturated to $S_{0.8}$ for phase 1, saturated with room temperature water and phase 2, saturated with hot water.

The Mn^{2+} concentration increased in the room temperature water treatment and decreased in the hot water treatment. Therefore there was a significant difference between the treatments (Table 8.1). Duration of saturation did not have a significant effect (Table 8.1) on the Mn^{2+} concentration and after two weeks of saturation the Mn^{2+} concentration stabilized in both treatments. It was anticipated that with a lower pe, more Mn^{4+} would reduce and a higher Mn^{2+} concentration would be present in the soil solution. This was not the case. With a higher temperature, less Mn^{2+} was present in the soil solution.

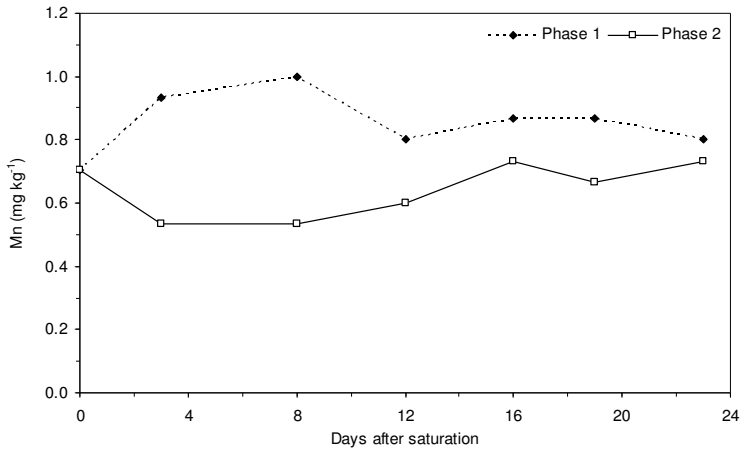

Figure 8.4 Mn^{2+} concentration for 1.6 Mg m^{-3} bulk density cores saturated to $S_{0.8}$ for phase 1, which was saturated with room temperature water and phase 2, which was saturated with hot water.

The analysis of variance showed that there was a significant difference between the two temperature treatments and the Ca^{2+} concentration. The Ca^{2+} concentration was the lowest in the hot water treatment (Figure 8.5) as with the Mn^{2+} concentration. The Ca^{2+} concentration was not significantly affected by duration of water saturation, although the treatment times could have been too short to show a significant difference. The Ca^{2+} concentration in phase 1, where the treatment lasted for 121 days, did show a significant difference, the Ca^{2+} concentration increasing with duration of water saturation.

The Mg^{2+} concentration for both the phases remained relatively stable and did not increase significantly over the duration of water saturation, except for a slight increase in Mg^{2+} on the 18^{th} day of saturation. In phase 1 the Mg^{2+} concentration was significantly influenced by time over a 121 day period. The Mg^{2+} concentration was significantly higher for room temperature treatment than the hot water treatment (Figure 8.5).

There was an initial sharp increase in K^+ over the first 12 days after saturation in the room temperature water treatment after which it stabilized (Figure 8.5). In the hot water treatment, K^+ did not increase as dramatically, but remained relatively stable throughout the 23 days of saturation. In the analysis of variance, K^+ was significantly influenced by duration of water saturation as well as temperature.

The Na^+ concentration was significantly higher in the room temperature treatment than in the hot water treatment, although the Na^+ concentration did not increase significantly with

duration of water saturation. The Na^+ concentration did show a significant difference in relation to duration of water saturation with the room temperature treatment over a 121 day period, therefore the period of 23 days might have been too short to show an increase of Na^+ over time.

The reason for the initial decrease in pe in the phase 2 experiment might be due to the effect of temperature on the microbes within the soil. This was probably due to the higher temperature of the distilled water used to saturate the cores, as well as the lower O_2 content of the water taken directly from the distiller.

It was decided to set up an experiment to test the hypothesis that the water temperature of the cores affected the varying bulk densities differently. The results are discussed in the next section.

Ca^{2+}

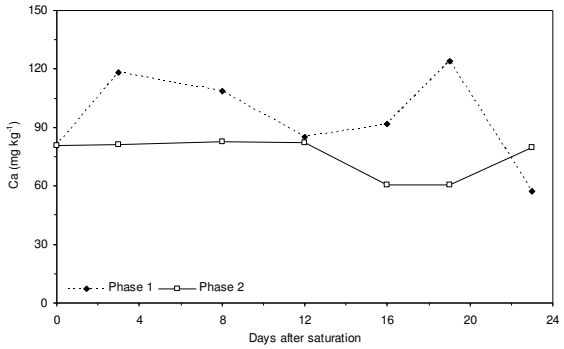

Mg^{2+}

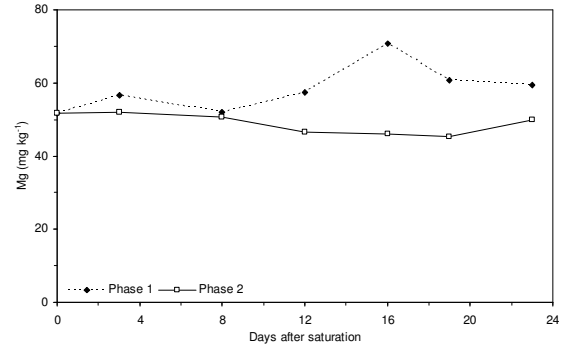

K^{+}

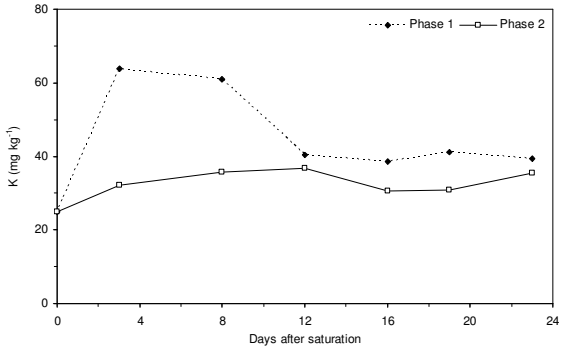

Na^{+}

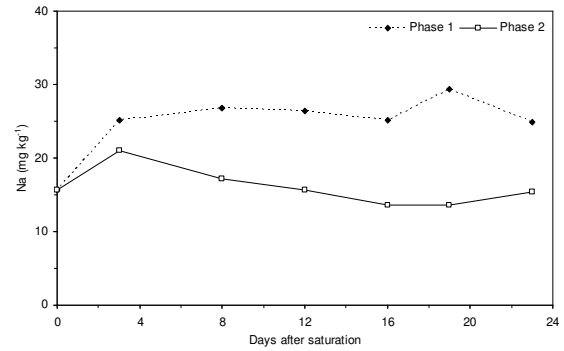

Figure 8.5 Ca^{2+}, Mg^{2+}, K^{+} and Na^{+} concentrations for 1.6 Mg m^{-3} cores saturated to $S_{0.8}$ for phase 1 which was saturated with room temperature water and phase 2 which was saturated with hot water.

8.1.1.1 Hot and room temperature water test

In Chapter 7, the 1.4 Mg m^{-3} bulk density core reduced faster than 1.8 Mg m^{-3} bulk density core. This could have been as a result of more hot water being added to the 1.4 Mg m^{-3} core than in the 1.6 and 1.8 Mg m^{-3}. In the 1.4 Mg m^{-3} bulk density core, 320 cm^3 of the hot water was added when saturating the core and no water was added before to aid in the packing process. In the 1.8 Mg m^{-3} bulk density core, 168 cm^3 room temperature water was first added to the core to bring it to a porosity of 0.5 to aid in the packing process, after which 50 cm^3 hot water was added to bring it up to the correct degree of water saturation. Therefore an greater amount (270 cm^3) of hot water was added to the 1.4 Mg m^{-3} core. The 1.4 Mg m^{-3} bulk density core needed more water in volume to saturate the core to $S_{0.8}$ as it had a greater amount of pores(Figure 7.1). It was hypothesised that the larger volume of hot water added to the 1.4 Mg m^{-3} bulk density core was the reason for the intense reaction in this core.

It was decided to set up a test experiment to test the hypothesis. Cores were set up in exactly the same manner as in the previous experiment. One set of cores was saturated with room temperature distilled water as had been used in phase 1 of the experiment, and the other set was saturated with hotter water directly from the distiller as in phase 2. The first measurement took place 3 days after saturation and the experiment was stopped after 10 days.

In the soil packed to 1.4 Mg m^{-3}, a rapid decrease in pe took place in both the hot and room temperature cores although the hotter water caused the soil to become more reduced than the room temperature water (Figure 8.6). In the core packed to a bulk density of 1.6 Mg m^{-3} the room temperature core gradually decreased whereas a more rapid decrease in pe took place in the core saturated with hotter water. In 1.8 Mg m^{-3} the room temperature core (23°C) maintained a relatively stable pe whereas the core saturated with hotter water (30°C) fluctuated with a pe value of two units. In both the water temperatures the pe remained the lowest in the 1.4 Mg m^{-3} and the highest in the 1.8 Mg m^{-3} (Figure 8.6).

pe
(Room temperature)

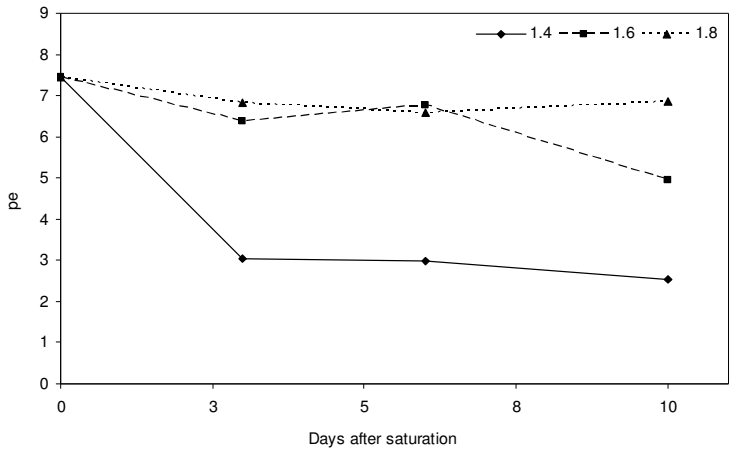

pe
(Hot)

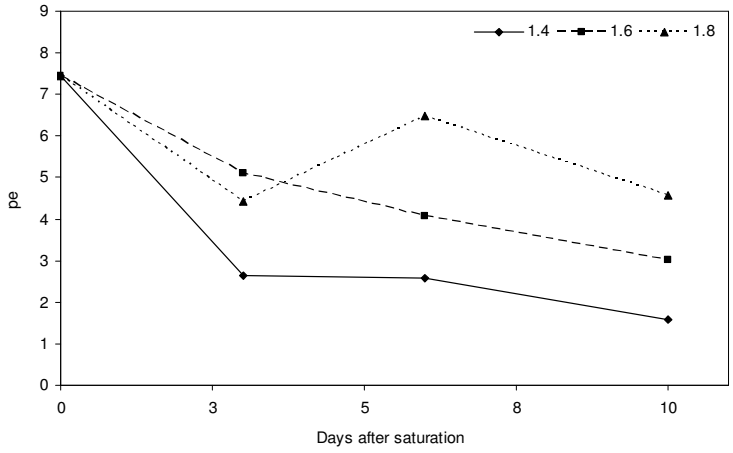

Figure 8.6 pe for the hot and the room temperature treatments for all the bulk densities.

The cores saturated with room temperature water had a relatively stable Fe^{2+} concentration, with the 1.8 Mg m^{-3} bulk density core having the lowest Fe^{2+} concentration. The Fe^{2+} concentration was considerably higher in the core packed to a bulk density of 1.4 Mg m^{-3} and saturated with hot water than any of the other treatments (Figure 8.7). At the end of 10 days, the Fe^{2+} in the 1.4 Mg m^{-1} bulk density core had an average concentration of 74.4 mg kg^{-1} in the hot water treatment compared to 16.7 mg kg^{-1} in the room temperature treatment. The 1.8 Mg m^{-3} bulk density core had the lowest Fe^{2+} concentration at the end of the 10 days of saturation in both the room temperature and hot water treatments.

Fe^{2+}
(Room temperature)

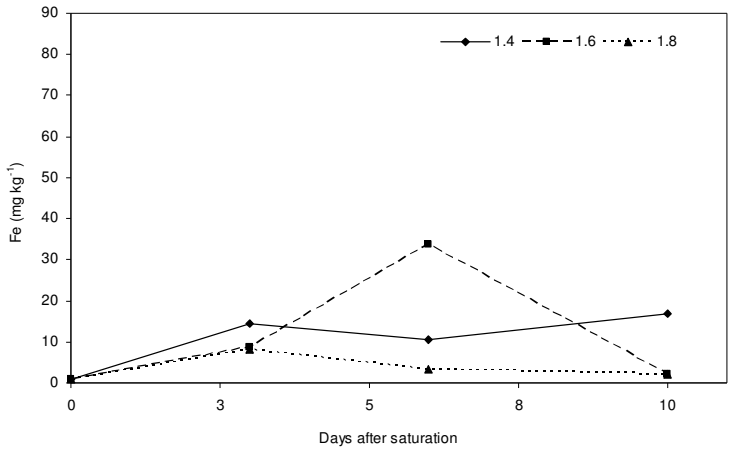

Fe^{2+}
(Hot)

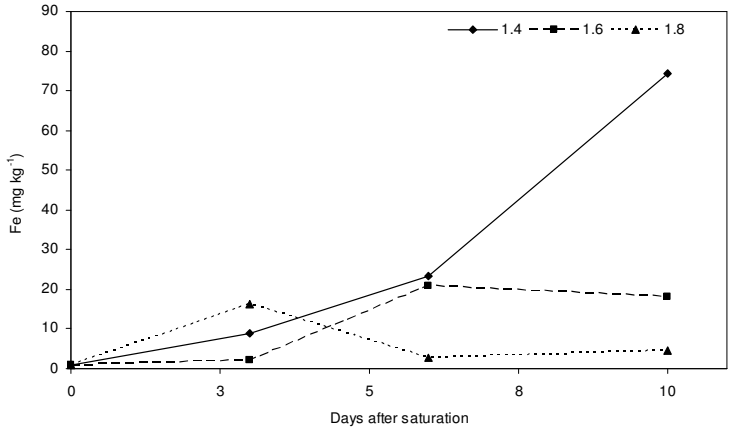

Figure 8.7 Fe^{2+} concentration for the hot and the room temperature treatments for all the bulk densities.

The 1.6 Mg m^{-3} and 1.8 Mg m^{-3} bulk density cores had a very similar Mn^{2+} concentration throughout the 10 days of saturation, whereas the Mn^{2+} concentration in the 1.4 Mg m^{-3} bulk density core varied sporadically. In the hot water treatment the Mn^{2+} concentration was the highest in the 1.4 Mg m^{-3} bulk density core, although the Mn^{2+} concentration did not vary as much as in the room temperature treatment. In both treatments, the Mn^{2+} concentration was the highest in the 1.4 Mg m^{-3} bulk density core, and the lowest in the 1.8 Mg m^{-3} bulk density core (Figure 8.8).

Mn^{2+}
(Room temperature)

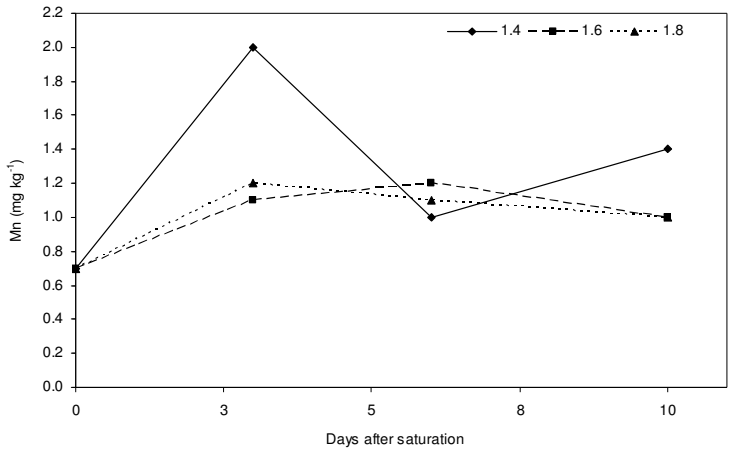

Mn^{2+}
(Hot)

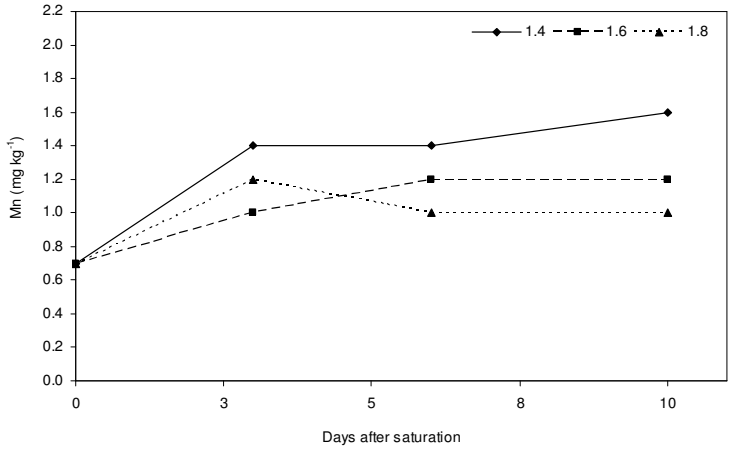

Figure 8.8 Mg^{2+} concentration for the hot and the room temperature treatments for all the bulk densities.

The Ca^{2+} concentration for the 1.6 Mg m^{-3} and 1.8 Mg m^{-3} bulk densities in both treatments were very similar. The Ca^{2+} concentration was the highest in the 1.4 Mg m^{-3} bulk density core in the room temperature water treatment and the lowest in the hot water treatment. The 1.4 Mg m^{-3} bulk density had the highest average cation concentration in all the treatments except for the Mg^{2+} and K^{+} in the room temperature treatment and the Ca^{2+} concentration in the hot water treatment.

Therefore an initial higher water temperature lead to a higher average concentration of Fe^{2+} released in the soil. In this experiment the water temperature had no effect on the average Mn^{2+} concentration, although the bulk density did play a role in the Mn^{2+} concentration. The lower bulk density produced a higher Mn^{2+} concentration than the higher bulk density.

A higher initial water temperature did not affect Ca^{2+} and Mg^{2+} in the same way as the Fe^{2+} concentration. The room temperature treatments delivered a higher average concentration in these two basic cations. These findings were confirmed by the previous experiments. Therefore one can say that the hotter water, which lead to a higher amount of reduction, in turn lead to a decrease in Ca^{2+} concentration. This was confirmed in Figure 8.5 and Figure 8.9.

The K^{+} concentrations seemed to fluctuate more under the room temperature water treatments, and were more stable in the hot water treatment, as confirmed in Figure 8.5 and Figure 8.9. The average Na^{+} concentration was higher in the hot water treatment. This was also confirmed by the previous experiments, where it was shown that Na^{+} was significantly affected by temperature (Table 8.1).

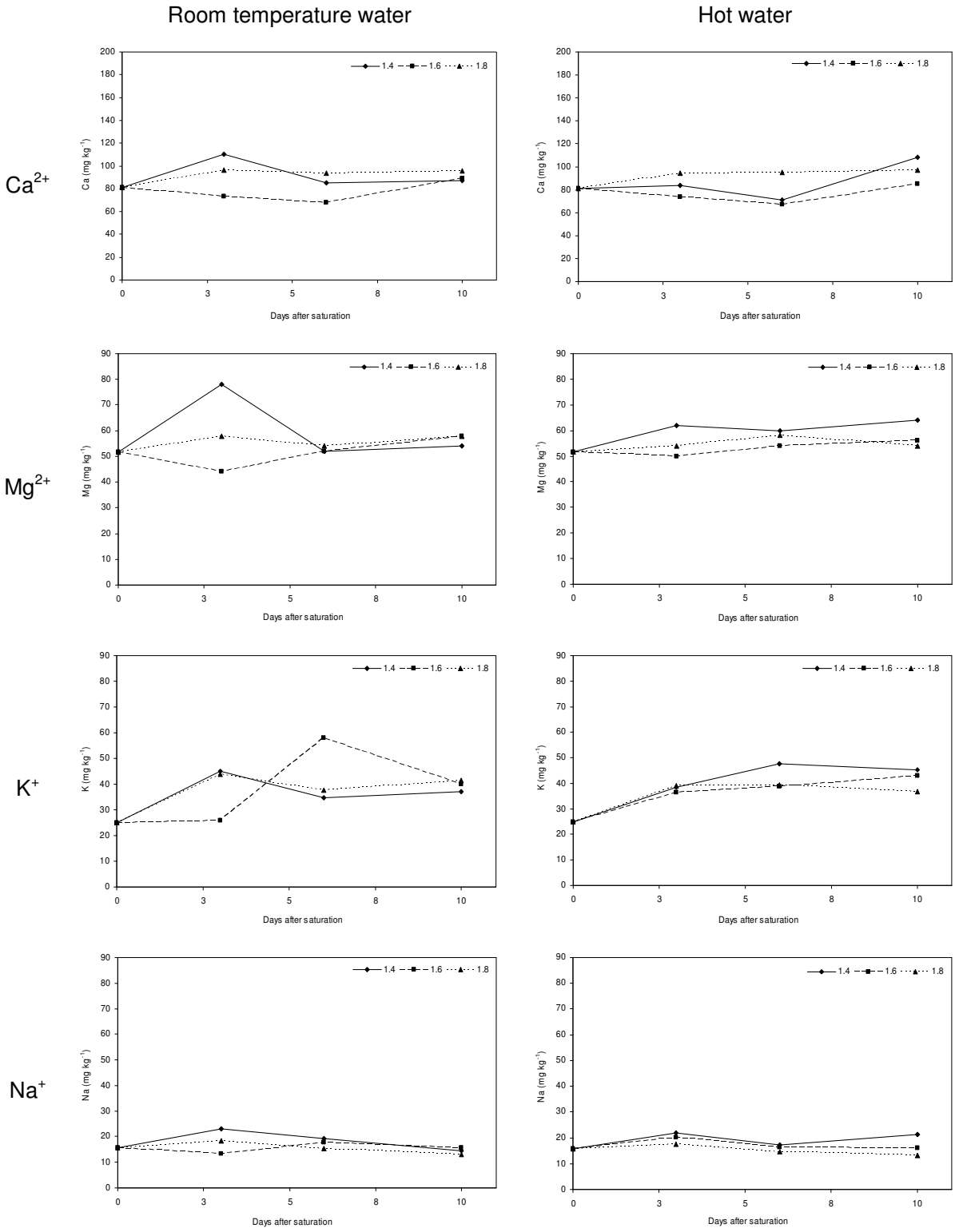

Figure 8.9 Ca^{2+}, Mg^{2+}, K^{+} and Na^{+} concentrations for 1.6 Mg m^{-3} cores saturated to $S_{0.8}$ for phase 1 which was saturated with room temperature water and phase 2 which was saturated with hot water.

8.2 Summary

It was anticipated that a soil with a higher bulk density would have a higher propensity to reduce. This is due to less macropores at a higher bulk density and therefore less soil air available for microbes at low air filled porosities (< 0.2 m^3m^{-3}). A decrease in soil respiratory activity therefore occurs (Glinski & Stepniewski, 1985).

This was not the case in this set of experiments. The lowest bulk density, at 1.4 Mg m^{-3}, reduced much faster and to a greater extent than the highest bulk density which was 1.8 Mg m^{-3}. It was thought that an experimental error could have caused the anomalous results. The error could have taken place due to a greater volume of the higher water temperature (±7°C). More of the hotter water, therefore more heat, was added to the 1.4 Mg m^{-3} core and therefore it reduced faster. This could have been the case for the rapid reduction in the 1.4 Mg m^{-3} bulk density core that was initially saturated to a higher temperature. However it was found that even in the room temperature water treatment the Fe^{3+} and Mn^{4+} reduced faster in the 1.4 Mg m^{-3} bulk density core than in the 1.8 Mg m^{-3} bulk density core.

These results still do not agree with the hypothesis that a soil with a lower bulk density will reduce faster than a soil with a higher bulk density. In both cases of water temperature, the lower bulk density reduced faster than the higher bulk density. No conclusive reason could be given for this phenomenon and further research is needed in this area.

CHAPTER 9

SUMMARY AND RECOMMENDATIONS

This dissertation describes the relationship between duration and degree of water saturation, with varying degrees of bulk density. It aims to determine the effect of duration and degree of water saturation on the reduction of Fe and Mn and the impact thereof on cations in the soil. The study was based on the hypothesis that for a soil horizon with sufficient micoorganisms, organic carbon, and iron and with a specific bulk density, there is a critical degree of water saturation at which the onset of reduction will occur and a certain time period in which the reducing conditions will occur.

There were three key aims to the study: to establish the relationship between the degree of water saturation (s) and the onset of reduction; and to establish the relationship between the degree of water saturation (s) and the duration of reduction; to establish the effect of bulk density and pore size distribution on the above-mentioned processes.

To address the first aim, a column experiment was set up and soil water was extracted under vacuum via micro tensiometer cups. This proved to be insufficient to meet the aims of the experiment and it was then decided to use single cores. The first and second aims were then addressed through a detailed soil core study. Soil cores using the same soil and bulk density were saturated to four different degrees of water saturation ($S_{0.6,\ 0.7,\ 0.8,\ 0.9}$). The experiment was terminated after 121 days. Redox potential was measured *in situ* every 3.5 days for the first three months after which weekly measurements were made for a further month. To address the third aim, a second experiment was set up with three bulk densities and a constant degree of water saturation ($S_{0.8}$). Redox potential was measured *in situ* every 3.5 days and the experiment was terminated after 23 days of water saturation.

A soil profile in the Weatherley catchment was selected due to the considerable amount of data available on the area. The profile chosen was a 1.6 m deep Avalon 2100 which is profile 234 in the Weatherley catchment, Eastern Cape, South Africa. It consisted of an orthic A, on a yellow brown apedal B1 and B2 horizon, with a soft plinthic B, on an unspecified material with signs of wetness. The yellow brown apedal B1 and B2 horizon was used for all experiments.

The aim of the column experiment was to determine the extent to which water could be extracted from all segments in a soil column wetted through capillary rise. It was thought that the degree of water saturation would decrease from the bottom of the column upwards. Once the water was extracted it would be analysed to determine if and when reduction took place through the measurement of Eh, pH, Mn^{2+}, Fe^{2+}, Ca^{2+}, Mg^{2+}, K^{+} and Na^{+}.

The artificial soil column was constructed by packing the soil in a PVC pipe, 1 m high, and 0.104 m inner diameter. The complete column consisted of ten 0.1 m sections sealed with silicon sealant and held together with duct tape, making the column 1 m high. The column was packed to a bulk density of 1.6 Mg m^{-3} and the bottom of the column was sealed with a PVC base and silicon sealant. A water table was established at 0.3 m and kept constant by means of a Marriott bottle. Capillary rise was very slow through the column. Water could only be sufficiently extracted using an -85 kPa vacuum pump from the first three segments and from the fourth one with difficulty, even though the fourth segment was below the water table level. The experiment was terminated after 42 days after which there were still no signs of wetness at the top of the column. After 7 months (252 days), the column was deconstructed into the 0.1 m sections. All the segments were moist except the top segment. No colour changes or morphological features were observed.

A second soil column was built in an attempt to accelerate the wetting process by creating a -85 kPa vacuum at the top of the column. It was also thought that the tensiometer cups had not made sufficient contact with the soil to ensure a sufficient flow of soil water from the soil matrix into the tensiometer cups. Silica flour, which has a very fine texture, was thought to enhance the movement of water from the soil matrix into the tensiometer cup. Even though the column had been sufficiently wetted through the suction applied to the top of the column, extraction of soil water still proved to be too difficult. The extraction process through tensiometer cups was still too slow even though the silica flour around the tensiometer cups aided slightly. It was also thought that a continual feeding of distilled water into the column, as the water was extracted would be undesirable due to the continual introduction of oxygenated water. The saturation of a soil column through capillary rise was therefore deemed inpractical for the analysis of redox conditions at different degrees of water saturation, because very little soil solution could be extracted just below the water table and no water could be extracted above it. Another problem with column analysis was that there was no way to determine at which degree of water saturation the segments were.

It was decided to change the experimental setup to single cores, each with its unique degree of water saturation. It was also determined that creating a decreasing degree of

wetness in a column needed more research as it had been unsuccessful on two occasions. The core method was tested and it was concluded that individual core analysis of redox conditions delivered more satisfactory results than column analysis. It was ensured through this method that the cores were kept at a constant known degree of water saturation and that no O_2 rich water entered the core, therefore the redox conditions could be monitored accurately.

Individual cores were packed to a bulk density of 1.6 Mg m^{-3}. Four water saturation treatments were used, namely $S_{0.6, 0.7, 0.8}$ and $S_{0.9}$. Triplicates were made of each set. The cores were kept at their respective s values for 121 days, after which the experiment was terminated.

The pH showed a significant difference in relation to duration of water saturation although not in degree of water saturation. Even though there was no significant difference between the different water saturations, the standard deviation between them varied more with increasing degree of water saturation, from a standard deviation of 0.08 in $S_{0.6}$ to a standard deviation of 0.16 in $S_{0.9}$. The average pH decreased from 5.1 units in $S_{0.6}$ to 4.9 units in $S_{0.9}$. This was due to the fact that H^+ ions were used in reducing reactions, thereby affecting the pH.

The Eh varied markedly during the study from a maximum of 463 mV in the $S_{0.6}$ core to a minimum of 124 mV in the $S_{0.9}$ core, and was significantly affected by the duration as well as the degree of water saturation. The Eh was interpreted as pe to aid in better correlation with pH. The pe is directly related to the Eh, therefore it was also significantly affected by these two factors. There was a good correlation ($R^2 = 0.95$) between pe and degree of water saturation, with a decrease in pe from a pe of 8 units in $S_{0.6}$ to a pe of 4 units in $S_{0.9}$. The standard deviation of Eh also increased as the s value increased from 17 in $S_{0.6}$ to 72 in $S_{0.9}$. This was a result of the greater redox activity in the higher water saturations, thereby leading to increased micro site activity.

The Mn^{2+} concentration was significantly affected by degree of water saturation as well as duration of water saturation. There was a good correlation ($R^2 = 0.91$) between the Mn^{2+} concentration and an increase in degree of water saturation. The standard deviation also increased with an increase in degree of water saturation from an average standard deviation of 0.09 in $S_{0.6}$ to 0.18 in $S_{0.9}$. This was as a result of the increased redox activity as the degree of water saturation increased. There was an inverse relationship between Mn^{2+} concentration and pH. As the pH became more acidic, the Mn^{2+} concentration increased.

This is because Mn^{2+} is more soluble in acidic environments. It could therefore be concluded that Mn^{2+} concentration is dominated by pH in lower pH environments. Therefore it is not advised to use Mn^{2+} as a redox indicator in acidic pH environments.

The Fe^{2+} concentration was significantly affected by duration of water saturation as well as degree of water saturation. The Fe^{2+} concentration showed a good relationship with pe. The lower the pe in the cores, the higher the Fe^{2+} concentration in the soil. The average Fe^{2+} concentration increased dramatically from the lower degree of water saturation to the higher degree of water saturation, with an average Fe^{2+} concentration of 2.36 mg kg^{-1} in $S_{0.6}$ to an average Fe^{2+} concentration of 25.7 mg kg^{-1} in $S_{0.9}$ over a 121 day period. This reinforces the hypothesis that reduction takes place more intensely the higher the degrees of water saturation at a certain bulk density. The Fe^{2+} concentration fluctuation also increased with time as observed by the standard deviations that increased with an increase in degree of water saturation. The Fe^{2+} concentration correlated well with the combined pe+pH concentration. An increase in pe+pH lead to a decrease in Fe^{2+} concentration and *vice versa*. The lower Fe^{2+} concentrations at higher pe values occurred as a result of the higher reduction potential in the soil and less Fe^{3+} being reduced. The reason for the correlation between pH and Fe^{2+} concentration is because as the pH decreases, a shift occurs in the ferric/ferrous couple as the reduction potential increases. At a pH of 2 and 3, the standard reduction potential for Fe^{3+} is ±770 mV, as the pH increases the reduction potential lowers to values close to ± 200 mV.

The Ca^{2+} concentration in the soil was affected by factors such as $Mn^{2+} + Fe^{2+}$ concentration, pe and to a large extent pH. There was an inverse relationship between $Mn^{2+} + Fe^{2+}$ concentration and the Ca^{2+} concentration in the soil, and a direct relationship between Ca^{2+} concentration and pH. The Mg^{2+} concentration was significantly influenced by degree as well as duration of water saturation. The $S_{0.7}$ and $S_{0.8}$ treatments had a higher average Mn^{2+} concentration than the $S_{0.6}$ and $S_{0.9}$ treatments. The $Mn^{2+} + Fe^{2+}$ concentration did not affect the Mg^{2+} concentration to a large extent, although it was found that the Mg^{2+} concentration reacted inversely to the pH of the soil. The K^{+} concentration was significantly affected by duration of water saturation and not by degree of water saturation. The K^{+} concentration behaved very similarly in all the cores. The K^{+} concentration decreased over the first 28 days of saturation after which it stabilised over the next 70 and then increased in concentration. The Na^{+} concentration did not differ between the different water saturations. The Na^{+} concentration decreased with time, irrespective of the water saturation. This decrease was as a result of the Na^{+} being adsorbed on the clay complex as the other cations became displaced and left the exchange complex.

In conclusion it can be said that the cations did not behave in a similar fashion to each other in relation to the degree and duration of saturation. Ca^{2+} and K^{+} concentrations were significantly affected by duration of saturation although the degree of saturation did not have a significant effect. The Mg^{2+} and Na^{+} concentrations were significantly affected by both degree and duration of saturation. The average Ca^{2+} concentration did not change over the 121 days of saturation. Increases and decreases in the concentration took place although the average remained the same. The Mg^{2+} concentration increased on average over the 121 day period, whereas the Na^{+} concentration decreased on average. The K^{+} concentration increased during the first 24 days of saturation after which it decreased and then remained stable after which it increased again after 85 days of saturation.

In a separate experiment where cores were packed to a bulk density of 1.6 Mg m^{-3} and saturated to $S_{0.9}$, redox accumulations and depletions occurred within 12 months water saturation. This confirmed that this soil with 0.22% organic carbon at a bulk density of 1.6 Mg m^{-3} will produce morphological features within a year of water saturation at $S_{0.9}$.

In the light of these findings, it was determined that for this soil, Fe^{2+} and to a certain extent Mn^{2+} will start reducing at a pe of 6 and a degree of water saturation of $S_{0.78}$. These findings have shed new light on the first approximation that $S_{0.7}$ was sufficient for reduction. It is proposed that the new value of $S_{0.78}$ be used in future calculations.

A separate experiment was set up to determine the effect of bulk density on the degree and duration of water saturation. The cores were packed in the same manner as the previous experiment. A set of cores consisting of three bulk densities, 1.4, 1.6, and 1.8 Mg m^{-3} were saturated with water to $S_{0.8}$, each with three replications. A set of cores was analysed every 3.5 days, and the experiment was terminated after 23 days.

The analysis of variance showed that pH, Eh, Fe^{2+} and Mn^{2+} concentrations were all significantly affected by duration of water saturation, as well as bulk density. The Ca^{2+} and Na^{+} concentrations were both significantly affected by duration of water saturation; K^{+} and Na^{+} were significantly affected only by a variation in bulk density. No trend was found between pH and bulk density or duration of water saturation. The pe increased linearly with an increase in bulk density ($R^2 = 0.90$) and stabilized over time in all the bulk densities. Both the Mn^{2+} and Fe^{2+} concentrations were highest in the 1.4 Mg m^{-3} bulk density core. It was anticipated that the 1.8 Mg m^{-3} bulk density core would reduce the fastest and therefore contain the highest Mn^{2+} and Fe^{2+} concentrations. A better relationship existed between the

Mn^{2+} concentration and pH than pe + pH. This correlation was not found for the Fe^{2+} concentrations. A better relationship existed between the Fe^{2+} concentration and the combined pe+pH then the Mn^{2+} concentration and pe+pH. This was because the Mn^{2+} is soluble at low pH values and the pH in the bulk density experiment were all low (> 5.5 units). An increase in pe+pH lead to a decrease in Fe^{2+} concentration and *vice versa*. The lower Fe^{2+} concentrations at higher pe values occurred as a result of the higher reduction potential in the soil and less Fe^{3+} is reduced. The reason for the correlation between pH and Fe^{2+} concentration is because as the pH decreases, a shift occurs in the ferric/ferrous couple as the reduction potential increases. At a pH of 2 and 3, the standard reduction potential for Fe^{3+} is ±770 mV, as the pH increases the reduction potential lowers to values close to ± 200 mV.

It was hypothesised that the higher the bulk density, the higher the propensity to reduce, because there would be less macropores. Therefore in this study, the 1.8 Mg m^{-3} bulk density core should have reduced first due to the lower amount of macropores, because there would have been a lower amount of soil O_2 for the soil microbes to function aerobically. This hypothesis was not supported by the results obtained.

A higher water temperature was used in the bulk density experiment than in the degree of water saturation experiment. It was thought that the higher water temperature used might have caused the different results. To determine the effects of the warmer water, two temperature treatments were compared. A direct comparison was made by using data from $S_{0.8}$ with a bulk density of 1.6 Mg m^{-3} in the degree of water saturation experiment and comparing it to the core saturated to $S_{0.8}$ with a bulk density of 1.6 Mg m^{-3} in the bulk density experiment. The cores were set up in the same manner except for a difference in water temperature used to saturate them. It was found that the water temperature caused the cores to react differently. It was decided to set up a second experiment to test what effect the water temperature had on the pH, Eh, Fe^{2+}, Mn^{2+}, Ca^{2+}, Mg^{2+}, K^{+} and Na^{+}.

Cores packed to 1.4, 1.6, and 1.8 Mg m^{-3} were saturated with room temperature water (23°C) to $S_{0.8}$ in the first experiment and with the warmer water (30°C) in the second experiment. It was found that the lowest bulk density, at 1.4 Mg m^{-3}, reduced much faster in both water temperature treatments than the highest bulk density which was 1.8 Mg m^{-3}. The hypothesis that a higher bulk density will reduce faster than a lower bulk density due to less macropores did not prove to be true in this case.

Based on the results of this study it was decided against the use of $S_{0.8}$ in bulk density experiments and to rather use a lower degree of water saturation when such experiments are carried out and thereby one could determine the effect of bulk density to a more accurate degree. It was also decided that the use of room temperature water is better than the use of warmer water to ensure that the results would not be affected by the temperature of the water.

The first aim of this study was satisfied in saying that significant reduction did not take place in the $S_{0.6}$ and $S_{0.7}$ treatments and only started in the $S_{0.8}$ treatment. Therefore 70% of water saturation was not sufficient to initiate reduction in this closed soil system. A new value of $S_{0.78}$ was identified as the critical degree of saturation for the initiation of reduction. The pe and Fe^{2+} concentration of the $S_{0.8}$ and $S_{0.9}$ cores did not stabilise during the 121 days of analysis. In the second column experiment, segment 1 saturated to $S_{0.81}$ had a pe of 2.81 and an average Fe^{2+} concentration of 66.67 mg kg^{-1} after 330 days. Therefore Fe^{2+} reduction will continue to take place as long as there is sufficient organic matter and the pe stays low in favour of reducing conditions. The third aim was to establish the effect of bulk density on reduction. The results obtained were the opposite of what was anticipated, as the cores with a lower bulk density reduced sooner and to a greater extent than the higher bulk density cores. These results were not conclusive and it was decided that further research was needed into the effect of bulk density on reduction in a closed system.

Since this study was only concerned with the yellow brown apedal B soil horizon, the results might not hold true for the rest of the horizons in the profile, or with other yellow brown apedal B horizons with more or less organic matter contents.

Further research is needed to develop an improved methodology for soil column analyses of redox reactions. Extraction of water through tensiometer cups inserted into the column proved difficult for regular redox determinations. A more conclusive answer also needs to be found to determine the interrelationship between degree of water saturation, bulk density and the onset of reduction. A study is further proposed to determine the effect of soil temperature and varying levels of organic carbon contents on redox reactions and how these parameters affect the degree of water saturation at which reduction is initiated. It also needs to be determined if the $S_{0.78}$ value holds true for different soil horizons, soils with varying organic carbon contents, bulk densities and at varying temperatures.

REFERENCES

ASHWORTH, D.J. & SHAW, G., 2004. Soil migration and plant uptake of technetium from a fluctuating water table. *J. Environ. Radioactivity*. 81, 155-171.

AUST, W.M. & LEA, R., 1992. Comparative effects of aerial and ground logging on soil properties in a tupelo-cypress wetland. *For. Ecol. Manage.* 50, 57-73.

AUSTIN, W.E. & HUDDLESTON, J.H., 1999. Viability of permanently installed platinum redox electrodes. *Soil Sci. Soc. Am. J.* 63, 1757-1762.

BARTLETT, R.J., 1986. Soil redox behavior. In D. L. Sparks (ed.). Soil physical Chemistry. CRC Press, Boca Raton, Florida.

BEEH., 2003. Weatherley database V1.0. School of Bioresources Engineering and Environmental Hydrology, University of Natal, Pietermarizburg.

BLAKE, G.R. & HARTGE, K.H., 1986. Bulk density. In. Klute (ed.). Methods of soil analysis. Part 1. Physical and mineralogical methods. 2nd ed. ASA, Madison, Wis.

BOHN, H., McNEAL, B.L. & O'CONNOR, G.A., 1985. Oxidation and Reduction, Soil Chemistry, John Wiley & Sons, USA.

BOHN, H.L., 1969. The EMF of platinum electrodes in dilute solutions and its relation to soil pH. *Soil Sci. Soc. Am. Proc.* 33, 639-640.

BRINKMAN, R., 1970. Ferrolysis, a hydromorphic soil forming process. *Geoderma.* 3, 199-206.

BRINKMAN, R., 1977. Surface-water gley soils in Bangladesh; Genesis. *Geoderma*. 7, 111-144.

BROOKINS, D.G., 1988. Eh-pH-diagrams for geochemistry. Springer-Verlag, New York.

BUOL, S.W., HOLE, F.D. & McCRACKEN, R.J., 1989. Soil genesis and classification. 3rd edition. Iowa State University Press, Ames.

CALLEBAUT, F., GABRIELS, D., MINJAUW, W. & DE BOODT, M., 1982. Redox potential, oxygen diffusion rate, and soil gas composition in relation to water table level in two soils. Soil Sci. 134, 149–156.

CASEY, K.C. & EWEL, K.C., 1998. Soil redox potential in small pondcypress swamps after harvesting. *For. Ecol. Manage.* 112, 281-287.

CHEN, J., GU, B., ROYER, R.A. & BURGOS, W.D., 2003. The role of natural organic matter in chemical and microbial reduction of ferric iron. *Sci. Total Environ.* 307, 167-178.

CHIEF DIRECTOR OF SURVEYS AND MAPPING, 1993. South Africa 1:50 000 sheet 3128AB Maclear. Chief Director of Surveys and Mapping, Mowbray.

CHILDS, C.W., 1981. Field test for ferrous iron and ferric-organic complexes (on exchange sites or in water-soluble forms) in soils. *Aust. J. Soil Res.* 19, 175-180.

CLARK, W.M., 1923. Studies on Oxidation-Reduction. I. Introduction: *Public Health Reports*, 38, 443-455

CLARK, W.M., 1960. Oxidation-Reduction potentials of organic systems. Williams & Wilkins, Baltimore.

CRAFT, C.B., 2001. Biology of wetland soils. In J. L. Richardson and M. J. Vepraskas. (ed.). Wetland soils: genesis, hydrology, landscapes, and classification. Lewis Publishers, Washington, D. C.

CROWN, P.H. & HOFFMAN, D.W., 1970. Relationship between water table levels and type of mottles in four Ontario gleysols. *Can. J. Soil Sci.* 50, 453-455.

CROZIER, C.R., DEVAI, I. & DeLAUNE, R.D., 1995. Methane and reduced sulphur gas production by fresh and dried wetland soils. *Soil Sci. Soc. Am. J.* 59, 277-284.

CUOTO, W., SANZONOWICZ, C. & De O BARCELLOS, A., 1985. Factors affecting oxidation-reduction processes in a Oxisol with a seasonal water table. *Soil Sci. Soc. Am. J.* 49, 1245-1248.

CZYZ, E.A., 2004. Effects of traffic on soil aeration, bulk density and growth of spring barley. *Soil Tillage Res.* 79, 153-166.

DANIELS, R.B., GAMBLE, E.E. & BUOL, S.W., 1973. Oxygen content in the ground water of some North Carolina Aquults and Udalts. In R. R. Bruce *et al*. (ed.). Field soil water regime. SSSA Special Publication 5. SSSA, Madison, Wis.

DOBOS, R.R., CIOLKOSZ, E.J. & WALTMAN, W.J., 1990. The effect of organic carbon, temperature, time, and redox conditions on soil colour. *Pennsylvania Agric. Exp. Stn.* 150, 506-512.

DOWDY, H. & STELLY, M., 1981. Chemistry in the soil environment, ASA Spec. Publ. No. 40, American Society of Agronomy, Madison, Wis.

ESPREY, L.J., 1997. Hillslope experiments in the North Eastern Cape to measure and model subsurface flow processes. M.Sc. Dissertation. University of Natal, Pietermarizburg.

EVANS, C.V. & FRANZMEIER, D.P., 1986. Saturation, aeration, and colour patterns in a toposequence of soils in north-central Indiana*. Soil Sci. Soc. Am. J.* 50, 975-980.

FAO., 1998. World Reference Base For Soil Resources. World Soil Resources Reports 84. FAO, Rome.

FAO., 2006. World Reference Base For Soil Resources. World Soil Resources Reports 103. FAO, Rome.

FAULKNER, S.P. & PATRICK, W.H., 1992. Redox processes and diagnostic wetland indicators. in bottomland hardwood forests. *Soil Sci. Soc. Am. J.* 56:856-865.

FAULKNER, S.P., PATRICK, W.H. & GAMBRELL, R.P., 1989. Field techniques for measuring wetland soil parameters. *Soil Sci. Soc. Am. J.* 53, 883–890.

FIEDLER, S. & SOMMER M., 2000. Methane emissions, groundwater table and redox potentials along a gradient of redoximorphic soils in a temperate-humid climate. *Global Biogeochem. Cycle.* 14, 1081-1093.

FIEDLER, S. & SOMMER M., 2004. Water and redox conditions in wetland soils-their influence on pedogenic oxides and morphology. *Soil Sci. Soc. Am. J.* 68, 326-335.

FIEDLER, S., 2000. *In situ* long-term measurements of redox potentials in hydromorphic soils. In J. Schüring *et al.* (ed.). Redox-fundamentals, processes and measuring techniques. Springer-Verlag, New York.

FIEDLER, S., JUNGKUNST, H.P.F., JAHN, R., KLEBER, M., SOMMER, M. & STAHR, K., 2002. Linking soil classification and soil dynamics – pedological and ecological perspectives. *J. Plant Nutr. Soil Sci*. 165, 517-529.

FIEDLER, S., VEPRASKAS, M.J. & RICHARDSON, J.L., 2007. Soil redox potential: importance, field measurements, and observations. *Adv. Agron*. 94, 1-54.

FITZPATRICK, E.A., 1980. Soils: Their formation, classification and distribution. Longman, London.

FOTH, H.D., 1978. Fundamentals of Soil Science. 6th ed. Wiley, New York.

FRANSON, M.A.H., GREENBERG, A.E., TRUSSELL, R.R. & CLESCERI, L.S., 1995. Standard methods for the examination of water and wastewater. American Public Health Association, Washington DC.

FRANZMEIER, D.P., YAHNER, J.E., STEINHARDT, G.C. & SINCLAIR, H.R. Jr., 1983. Color patterns and water table levels in some Indiana soils. *Soil Sci. Soc. Am. J.* 47, 1196–1202.

GALSTER, H., 2000. Technique of measurement, electrode processes and electrode treatment. In J. Schuring *et al*. (ed.). Redox: Fundamentals, processes and applications. Springer Press, Berlin Germany.

GAST, R.C., 1977. Surface and colloid chemistry. In Dixon J.B., Weed, S.B., Kittrick, J.A., Milford, M.H., and White, J.L. (Eds). Minerals in Soil Environments. *SSSA*. Madison, Wis.

GLINSKI, J. & STEPNIEWSKI, W., 1985. Soil aeration and its role for plants. CRC Press, Boca Raton, Florida.

GLINSKI, J., STAHR, K., STEPNIEWSKA, Z. & BRZEZINSKA, M., 1996. Changes of redox and pH conditions in a flooded soil amended with glucose and manganese oxide or iron oxide under laboratory conditions. *Z. Pflanzenerahr. Boden*. 159, 297–304.

HAVLIN, J.L., BEATON, J.D., TISDALE, S.L. & NELSON, W.L., 1999. Soil Fertility and Fertilizers, an introduction to Nutrient Management. 6th ed. Simon & Schuster, New Jersey.

HERBAUTS, J., EL BAYAD, J. & GRUBER, W., 1996. Influence of logging traffic on the hydromorphic degradation of acid forest soils developed on loessic loam in middle Belgium. *For. Ecol. Manage.* 87, 193-207.

HESSE, P.R., 1971. A textbook of Soil Chemical Analysis, John Murray, London.

HILLEL, D., 1980. Application of soil physics, Academic Press, New York.

HILLEL, D., 1998. Environmental Soil Physics, Academic Press, New York.

HINTZE, J.L., 1997. Number cruncher statistical systems 2000, Kaysville, Utah.

HSEU, Z.Y. & CHEN, Z.S., 1996. Saturation, reduction, and redox morphology of seasonally flooded alfisols in Taiwan. *Soil Sci. Soc. Am. J.* 60, 941-949.

IUSS WORKING GROUP WRB.,. 2006. *World reference base for soil base for soil resources* 2006. World Soil Resources Reports No. 103. FAO, Rome.

JACOBS, M.P., WEST, L.T & SHAW, J.N., 2002. Redoximorphic features as indicators of seasonal saturation, Lowndes County, Georgia. *Soil Sci. Soc. Am. J.* 66, 315-323.

JAHN, R., BLUME, H.-P., ASIO, V.B., 2003. Student guide for soil description, soil classification and site evaluation, Halle/Saale.

KLUTE, A., 1986. Water retention: Laboratory methods. In A. Klute (ed.). Methods of soil analysis. Part 1. 2nd ed. Agron. Monogr. 9. ASA and SSSA, Madison, Wis.

KUTILEK, M. & NIELSEN, D.R., 1994. Interdisciplinarity of hydropedology. *Geoderma*. 138, 252-260.

LARSON, K.D., GRAETZ, D.A. & SCHAFFER, B., 1991. Flood-induced chemical transformations in calcareous agricultural soils in south Florida. *Soil Sci.* 152, 33-40.

LE ROUX, P.A.L., DU PREEZ, C.C. & BÜHMANN, C., 2005. Indications of ferrolysis and structure degradation in an Estcourt soil and possible relationships with plinthite formation. *S. Afr. J. Plant & Soil.* 22, 199-206.

LIN, H.S., BOUMA, J., WILDING, L.P., RICHARDSON, J.L., KUTILEK, M. & NIELSEN, D. R. 2005. Advances in hydropedology. *Adv. Agron.* 85, 1-89.

LOVLEY, D.R., 2001. Environmental microbe-metal interactions. ASM Press, Washington, DC.

MANSFELDT, T., 2003. *In situ* long-term redox potential measurements in a dyked marsh soil. *J. Plant Nutr. Soil Sci*. 166, 210-219.

MAUSBACH, M.J. & RICHARDSON, J.L., 1994. Biochemistry processes in hydric soil formation. *In* W. H. Patrick, Jr. (ed). *Current Topics in Wetland Biogeochemistry.* 1, 68-127.

MCBRIDE, M.B., 1994. Environmental chemistry of soils, Oxford University Press, New York.

McDANIEL, P.A. & BUOL, S.W., 1991. Manganese distributions in acid soils of the North Carolina piedmont. *Soil Sci. Soc. Am. J.* 55, 125-158.

McKEAGUE, J.A., 1965. A laboratory study on gleying. *Can. J. Soil. Sci.* 45, 199-206.

McKEAGUE, J.A., BRYDON, J.E. & MILES, N.M., 1971. Differentiation of forms of extractable iron and aluminium in soils. *Soil Sci. Soc. Am. J.* 35, 33-38.

MEHRA, O.P. & JACKSON, M.L., 1960. Iron oxide removal from soils and clays by a dithionite-citrate system buffered with sodium bicarbonate. *Clay Miner.* 7, 317-327.

MOKMA, D.L. & SPRECHER, S.W., 1994. Water table depths and colour patterns in Spodosols of two hydrosequences in Northern Michigan, USA. *Catena.* 22, 275-286.

MOORE, P.A., READDY, K.R. & GRAETZ, D.A., 1992. Nutrient transformations in sediments as influenced by oxygen supply. *J. Environ. Qual.* 21, 387-393.

MUELLAR, S.C., STOLZY, L.H. & FICK, G.W., 1985. Constructing and screening platinum microelectrodes for measuring soil redox potential. *Soil Sci*. 139, 558-560.

MUNSELL COLOR COMPANY, 1980. Munsell book of colour. Munsell colour, Baltimore.

NATIONAL RESEARCH COUNCIL (NRC), 2001. Basic Research Opportunities in Earth Science. National Academy Press, Washington, DC.

PARKIN, T.B., 1987. Soil microsites as a source of denitrification variability. *Soil Sci. Soc. Am. J.* 51, 1194-1199.

PATRICK, W.H. & JUGUJINDA, A., 1992. Sequential reduction and oxidation of inorganic nitrogen, manganese, and iron in a flooded soil. *Soil Sci. Soc. Am. J.* 56, 1071-1073.

PATRICK, W.H., GAMBRELL, R.P & FAULKNER, S.P., 1996. Redox measurement in soils. In D.L. Sparks (ed.). Methods of soil analysis. Part 3. 2nd ed. ASA and SSSA, Madison, Wis.

PAUL, E.A. & CLARK, F.E., 2001. Soil microbiology and biochemistry, Academic Press, New York.

PHILLIPS, L.R. & GREENWAY, M., 1998. Changes in water-soluble and exchangeable ions, cation exchange capacity, and $Phosphorus_{max}$ in soils under alternating waterlogged and drying conditions. *Commun. Soil. Sci. Plant Anal.* 29, 51-65.

PONNAMPERUMA, F.N., 1972. The Chemistry of Submerged Soils. *Adv. Agron.* 24, 26-96

RABENHORST, M.C. & LINDBO, D.L., 1998. Micromorphology of sandy epipedons along an upland-wetland transect. In M.C. Rabenhorst *et al*. (ed.). Quantifying soil hydromorphology. SSSA Spec. Publ. 54. SSSA, Madison, Wis.

RABENHORST, M.C., & PARIKH, S., 2000. Propensity of soils to develop redoximorphic colour changes. *Soil Sci. Soc. Am. J.* 64, 1904-1910.

REUTER, R.J. & BELL, J.C., 2001. Soils and Hydrology of a wet-sandy catena in East-central Minnesota. *Soil Sci. Soc. Am. J.* 65, 1559-1569.

RICHARDSON, J.L. & HOLE, F.D., 1979. Mottling and iron distribution in a Glossoboralf Haplaquoll hydrosequence on a glacial moraine in northwestern Wisconsin. *Soil Sci. Soc. Am. J.* 43, 552-558.

RICHARDSON, J.L., ARNDT, J.L. & MONTGOMERY, J.A., 2001. Hydrology of Wetland and Related Soils. In J. L. Richardson, M. J. Vepraskas. (ed.). Wetland soils: genesis, hydrology, landscapes, and classification. Lewis Publishers, Washington.

ROBERTS, V.G., HENSLEY, M., SMITH-BAILLIE, A.L. & PATTERSON, D.G., 1996. Detailed soil survey of the Weatherley catchment. ISCW Report No. GW/A/96/33. ARC-ISCW, Pretoria.

SCHOENEBERGER, P.J. & WYSOCKI, D.A., 2005. Hydrology of soils and deep regolith: A nexus between soil geography, ecosystems and land management. *Geoderma*, 126, 117-128.

SCHULTEN, H., 1993. Analytical pyrolysis of humic substances and soils: geochemical agricultural and ecological consequences. *J. Anal. Appl. Pyrolysis.* 25, 97-122.

SCHÜRING, J.S., SCHULZ, H.D., FISCHER, W.R., BÖTTCHER, J. & DUIJNISVELD, W.H.M., 2000. Redox, fundamentals, processes and applications. Springer-Verlag Berlin, Heidelberg.

SCHWERTMANN, U., & FANNING, D.S., 1976. Iron-manganese concretions in hydrosequences of soils in loess in Bavaria. *Soil Sci. Soc. Am. J.* 40, 731–738.

SCHWERTMANN, U., 1971. Transformation of hematite to goethite in soils, *Nature*, 232, 624-625.

SCHWERTMANN, U., 1985. The effect of pedogenic environments on iron oxide minerals. *Adv. Soil Sci.* 1, 171-200.

SCHWERTMANN, U., 1991. Solubility and dissolution of iron oxides. *Plant Soil.* 130, 1-25.

SIGG, L., 2000. Redox potential measurements in natural waters: Significance, Concepts and Problems. In Schüring *et al.* (ed.). Redox, fundamentals, processes and applications. Springer-Verlag Berlin, Heidelberg.

SIMONSON, G.H. & BOERSMA, L., 1972. Soil morphology and water table relations: II. Correlation between annual water table fluctuations and profile features. *Soil Sci. Soc. Am. J.* 67, 1952-1958.

SOIL CLASSIFICATION WORKING GROUP, 1991. Soil classification - A taxonomic system for South Africa. Mem. Agric. Nat. Resour. S. Afr. No 15. Dept. Agric. Dev., Pretoria.

SOIL SURVEY STAFF, 1975. Soil Taxonomy. USDA Handbook, 436, Washington, D.C.

SOIL SURVEY STAFF, 1999. Soil taxonomy - A basic system of soil classification for making and interpreting soil surveys, 2nd ed., USDA, Washington, DC.

SPOSITO, G., 1989. The chemistry of soils. Oxford Univ. Press, New York.

SSSA., 1997. Glossary of Soil Science Terms. SSSA, Madison, Wis.

STOLT, M.H., GENTHNER, M.H., DANIELS, W.L., GROOVER, V.A.L. & NAGLE, S., 1998. Quantifying Iron, Manganese, and Carbon Fluxes within Palustrine Wetlands. Quantifying soil hydromorphology. SSSA Special Publication, 54. SSSA, USA.

TAN, H.K., 1993. Principles of soil chemistry. 2nd ed. Marcel Deker, inc, New York.

TAREKEGNE, A., 2001. Studies on genotypic variability and inheritance of water logging tolerance in wheat. Ph.D. Thesis, University of the Free State, Bloemfontein.

TAYLOR, S.A. & ASHCROFT, G.L., 1972. Physical Edaphology, the physics of irrigated and non-irrigated soils. Freeman, San Fransisco.

THE NON-AFFILIATED SOIL ANALYSIS WORK COMMITTEE, 1990. Handbook of standard soil testing methods for advisory purposes. SSSSA, Pretoria.

TICEHURST, J.L., CRESSWELL, H.P, McKENZIE, N.J., & GLOVER M.R., 2007. Interpreting soil and topographic properties to conceptualise hillslope hydrology. *Geoderma.* 137, 279-292.

TURNER, F.T. & PATRICK, W.H. Jr., 1968. Chemical changes in waterlogged soils as a result of oxygen depletion. In Trans. Int. Congr. Soil Sci. 9th 1968. Adelaide, Australia. ISSS.

VAN DER WATT, H.V.H. & VAN ROOYEN T.H., 1995. A glossary of soil science. 2nd ed. Soil Science Society of Southern Africa. Pretoria.

VAN HUYSSTEEN, C.W., 2004. The relationship between the water regime and morphology of soils in the Weatherley catchment, northerly Eastern Cape. Ph.D Thesis. University of the Free State, Bloemfontein.

VAN HUYSSTEEN, C.W., HENSLEY, M., LE ROUX, P.A.L., ZERE, T.B., & DU PREEZ, C.C., 2005. The relationship between soil water regime and soil profile morphology in the Weatherley catchment, and afforestation area in the North Eastern Cape. Final report on WRC project no K5/1317. WRC, Pretoria.

VENEMAN, P.L.M., VEPRASKAS, M.J. & BOUMA, J., 1976. The physical significance of soil mottling in a Wisconsin toposequence. *Geoderma.* 15, 103–118.

VEPRASKAS, M. J. AND SPRECHER, S.W., 1997. Overview of aquic conditions and hydric soils. In: M.J. Vepraskas and S.W. Sprecher, Editors, Aquic Conditions and Hydric Soils: The Problem Soils SSSA Spec. Publ. vol. 50, SSSA, Madison, Wis.

VEPRASKAS, M.J. & BOUMA, J., 1976. Model experiments on mottle formation simulating field conditions. *Geoderma*, 15, 217-230.

VEPRASKAS, M.J., & FAULKNER, S.P., 2001. Redox Chemistry of Hydric Soils. In J. L. Richardson, M. J. Vepraskas. (ed.). Wetland soils: genesis, hydrology, landscapes, and classification. Lewis Publishers, Washington, D. C.

VEPRASKAS, M.J., 2001. Morphological Features of Seasonally Reduced Soils. In J. L. Richardson, M. J. Vepraskas. (ed.). Wetland soils: genesis, hydrology, landscapes, and classification. Lewis Publishers, Washington, D. C.

WEAVER, J.M.C., 1992. Ground water sampling. A comprehensive guide for sampling methods. WRC Project No 339. TT 54/92. WRC, Pretoria.

WHITFIELD, M., 1969. Eh as an operational parameter in estuarine sediments, *Limnol. Oceanogr*. 14, 547–558.

WOLT, J.D., 1994. Soil solution chemistry: Applications to environmental science and agriculture. John Wiley & Sons, New York.

ZACHARA, J.M., FREDRICKSON, J.K., SMITH, S.C., & GASSMAN, P.L., 2000. Solubilization of Fe(III) oxide-bound trace metals by dissimilaratory Fe(III) reducing bacterium*. Geochim. Cosmochim. Acta.* 65, 75-93.

APPENDIX A

Profile data

Table A1 Profile description for profile 234 (Avalon 2100) (Van Huyssteen *et al.*, 2005)

Profile No: 234
Map/photo: 3128AB
Latitude & Longitude: 31° 06' 02.8" / 28° 20' 18.2"
Surface stoniness: None
Altitude: 1 333 m
Terrain unit: Midslope
Slope: 11 %
Slope shape: Concave
Aspect: West
Microrelief: None
Parent material solum: Origin single, local colluvium
Underlying material: Feldspathic sandstone
Geological Group: Elliot

Soil form: Avalon
Soil family: 2100
Surface rockiness: None
Occurrence of flooding: None
Wind erosion: None
Water erosion: None
Vegetation / Land use: Grassveld, closed
Water table: None
Described by: M. Smit & A.Q. Weldeyohannes
Date described: 19/06/2001
Weathering of underlying material: Strong physical, moderate chemical
Alteration of underlying material: Ferruginised

Horizon	Depth(mm)	Description	Diagnostic horizons / material
A	0 - 500	**Moisture status:** moist; **dry colour:** 10YR4/2 (95 %), 10YR4/3 (5 %); **moist colour:** 10YR3/2 (95 %), 10YR4/3 (5 %); 9.8 % clay; coarse sandy loam; no 10YR4/3 dry, 10YR3/2 moist, humus mottles; apedal massive; hard, friable, non-sticky, non-plastic; few normal fine and very fine pores; few normal medium and coarse pores; no slickensides; no cracks; no cutans; no coarse fragments; water absorption 1 second(s); many normal roots; gradual smooth transition;	orthic A horizon
B1	500 - 880	**Moisture status:** moist; **dry colour:** 10YR5/4 (90 %), 10YR4/2 (10 %); **moist colour:** 10YR4/4 (90 %), 10YR3/2 (10 %); 14.3 % clay; coarse sandy loam; common medium distinct 10YR4/2 dry, 10YR3/2 moist, humus mottles; apedal massive; hard, friable, non-sticky, non-plastic; few normal fine and very fine pores; few normal medium and coarse pores; no slickensides; no cracks; no cutans; no coarse fragments; water absorption 1 second(s); many normal roots; gradual smooth transition;	yellow-brown apedal B horizon
B2	880 - 1070	**Moisture status:** moist; **dry colour:** 10YR6/4 (85 %), 10YR6/6 (10 %), 10YR5/2 (5 %); **moist colour:** 10YR5/4 (85 %), 10YR4/6 (10 %), 10YR3/2 (5 %); 17.1 % clay; sandy loam; common medium distinct 10YR6/6 dry, 10YR4/6 moist, humus mottles; apedal massive; hard, friable, non-sticky, non-plastic; many normal fine and very fine pores; few normal medium and coarse pores; no slickensides; no cracks; no cutans; no coarse fragments; water absorption 1 second(s); common normal roots; gradual smooth transition;	yellow-brown apedal B horizon
B3	1070 - 1300	**Moisture status:** moist; **dry colour:** 10YR7/3 (90 %), 10YR8/1 (10 %); **moist colour:** 10YR5/6 (90 %), 10YR5/6 (10 %); 18.7 % clay; loam; common fine distinct 10YR8/1 dry, 10YR5/6 moist, iron oxide mottles; common fine distinct 10YR8/1 dry, 10YR5/6 moist, iron oxide mottles; apedal massive; very hard, friable, very sticky, plastic; many normal fine and very fine pores; few normal medium and coarse pores; no slickensides; no cracks; no cutans; no coarse fragments; water absorption 1 second(s); few bleached roots; clear smooth transition;	soft plinthic B horizon
C1	1300 - 1500	**Moisture status:** moist; **dry colour:** 10YR8/1 (70 %), 2.5YR4/8 (30 %); **moist colour:** 10YR6/2 (70 %), 10YR4/8 (30 %); 15.1 % clay; loam; common fine distinct 2.5YR4/8 dry, 10YR4/8 moist, iron oxide mottles; many fine prominent 2.5YR4/8 dry, 10YR4/8 moist, iron oxide mottles; moderate coarse prismatic; very hard, very firm, very sticky, very plastic; few bleached fine and very fine pores; few bleached medium and coarse pores; many slickensides; no cracks; common clay & cutans; very few 2-6 mm round Fe & Mn concretions; water absorption 4 second(s); very few bleached roots; abrupt smooth transition;	unspecified material with signs of wetness
C2	1500 - 1600	**Moisture status:** moist; **dry colour:** 10YR7/1 (60 %), 10YR5/8 (40 %); **moist colour:** 10YR5/4 (60 %), 10YR4/6 (40 %); 15.1 % clay; loam; many coarse distinct 10YR5/8 dry, 10YR4/6 moist, iron oxide mottles; moderate coarse prismatic; very hard, very firm, very sticky, very plastic; few bleached fine and very fine pores; few bleached medium and coarse pores; many slickensides; no cracks; common clay & cutans; no coarse fragments; water absorption 1 second(s); no roots; transition not reached;	unspecified material with signs of wetness

Table A2 Soil analyses for profile 234 (Avalon 2100)

Horizon	Depth	Diagnostic horizon	Soluble cations			CEC soil	Exchangeable cations					
			Ca	Mg	Na		Ca	K	Mg	Na	Fe	Mn
	mm		$cmol_c\ kg^{-1}$								$mg\ kg^{-1}$	
A	0-500	ot	0.55	0.52	0.15	7.3	1.60	0.16	0.78	0.05	13.5	20.8
B1	500-900	ye	0.38	0.49	0.18	7.1	0.46	0.09	0.49	0.06	0.4	1.0
B2	900-1100	ye	0.92	0.50	0.17	4.2	0.49	0.07	0.58	0.05	0.2	1.4
B3	1100-1300	sp	0.88	1.03	0.18	10.6	2.11	0.27	2.46	0.11	0.5	1.2
C	1300-1500	on	0.81	0.89	0.70	14.5	2.85	0.35	2.70	0.13	0.4	1.4
B1+B2	500-1100	ye	0.61	0.47	0.16	5.4	0.47	0.07	0.52	0.05	0.4	1.1

Horizon	Depth	Diagnostic horizon	pH	Org C	N	C:N	Fe	Mn
			H_2O				CBD	
	mm		%	%	$mg\ kg^{-1}$	ratio	$mg\ kg^{-1}$	
A	0-500	ot	5.14	1.10	551.0	19.5	6253.0	6.5
B1	500-900	ye	5.33	0.25	151.0	17.8	5412.0	13.5
B2	900-110	ye	5.55	0.15	74.0	21.1	4487.0	6.0
B3	1100-1300	sp	5.81	0.29	351.0	7.4	5219.0	6.5
C	1300-1500	on	5.69	0.26	267.0	8.8	6318.0	7.0
B1+B2	500-1100	ye	5.47	0.22	137.6	17.0	4856.0	8.8

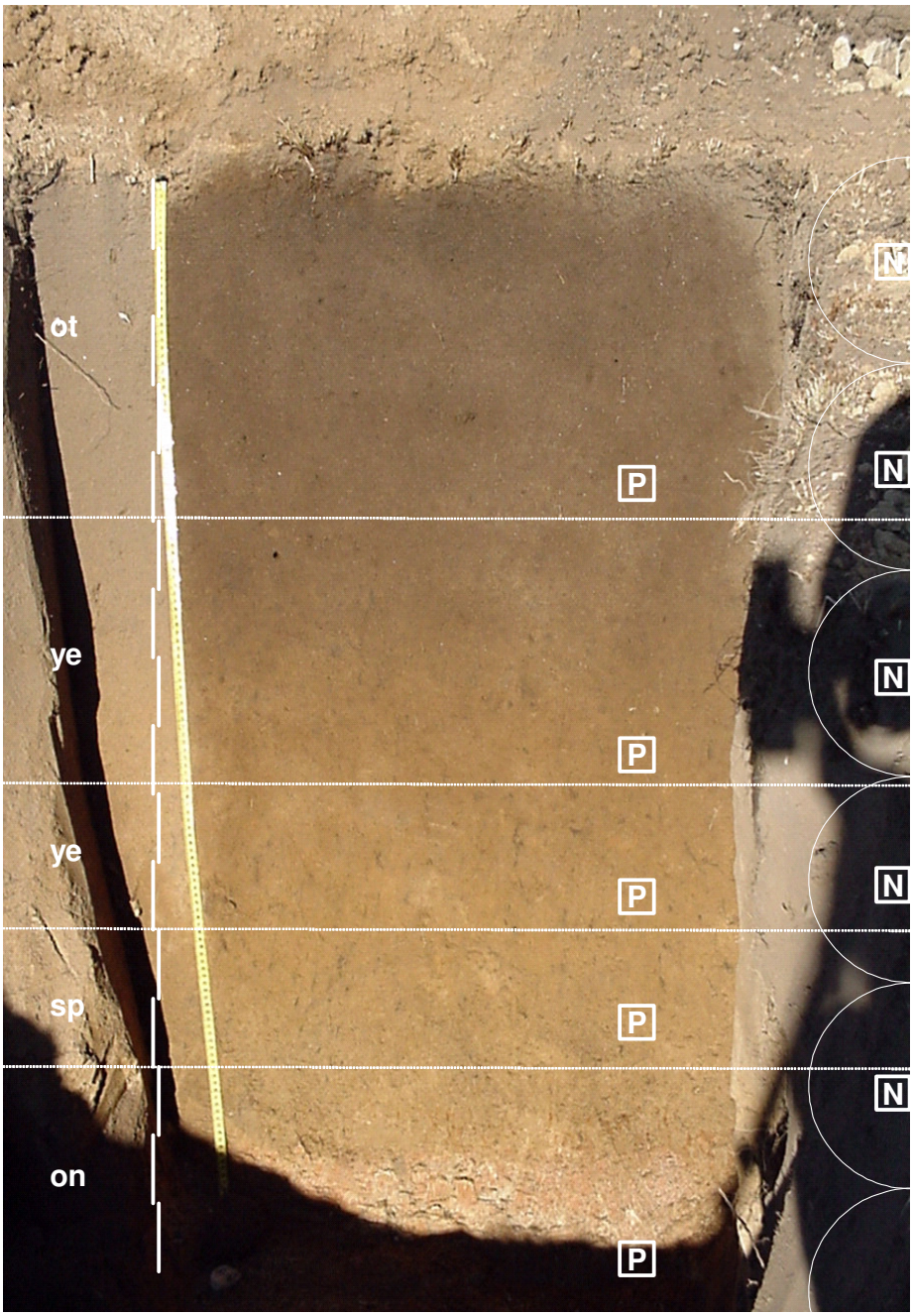

Figure A1 Profile 234 (Avalon 2100), indicating diagnostic horizons as well as measurement depths for neutron water meter [N] and piezometers [P] measurements.

APPENDIX B

Data for column experiment 1

Table B1 Data for segment 1 (0 - 100 mm) over a 42 day period

Days after saturation	Segment 1											
	pH	Eh	rH	pe	pe + pH	Fe	Mn	Fe+Mn	Ca	K	Mg	Na
		(mV)				(mg kg^{-1})						
0	5.13	439.3	25.15	7.45	12.58	0.01	0.10	0.11	0.61	0.12	0.51	0.16
2	5.62	154.4	16.47	2.62	8.24	0.01	0.10	0.11	0.38	0.17	0.30	0.22
3	5.59	171.0	16.98	2.90	8.49	0.07	0.11	0.18	0.45	0.19	0.21	0.20
4	5.71	159.0	16.81	2.69	8.40	0.18	0.08	0.26	0.75	0.54	0.48	0.37
8	5.89	167.0	17.44	2.83	8.72	1.58	0.10	1.68	0.59	0.25	0.37	0.27
9	6.02	154.0	17.26	2.61	8.63	1.92	0.06	1.98	0.54	0.19	0.25	0.24
10	6.10	124.0	16.40	2.10	8.20	2.89	0.06	2.95	0.52	0.17	0.18	0.21
13	6.12	111.2	16.01	1.89	8.01	2.14	0.06	2.20	0.55	0.31	0.19	0.30
20	5.09	204.0	17.10	3.46	8.55	4.73	0.05	4.78	0.39	0.25	0.13	0.42
25	6.13	53.8	14.08	0.91	7.04	6.70	0.06	6.76	0.55	0.21	0.14	0.37
28	6.01	34.8	13.20	0.59	6.60	7.99	0.05	8.04	0.39	0.20	0.14	0.48
31	5.59	58.8	13.17	1.00	6.59	4.86	0.01	4.87	0.14	0.01	0.00	0.02
34	5.60	60.3	13.24	1.02	6.62	8.35	0.06	8.41	0.29	0.11	0.10	0.32
35	5.45	71.8	13.33	1.22	6.67	11.84	0.11	11.95	0.44	0.21	0.19	0.62
38	5.53	109.5	14.77	1.86	7.39	3.47	0.05	3.52	0.35	0.34	0.11	0.56
42	5.42	96.9	14.12	1.64	7.06	0.12	0.02	0.14	0.33	0.16	0.08	0.43

Table B2 Data for segment 2 (100 - 200 mm) over a 42 day period

Days after saturation	Segment 2											
	pH	Eh	rH	pe	pe + pH	Fe	Mn	Fe+Mn	Ca	K	Mg	Na
		(mV)				(mg kg^{-1})						
0	5.13	439.3	25.15	7.45	12.58	0.01	0.10	0.11	0.16	0.12	0.51	0.16
2	6.07	150.4	17.24	2.55	8.62	0.01	0.14	0.15	0.39	0.31	0.34	0.39
3	6.08	148.2	17.18	2.51	8.59	0.03	0.13	0.16	0.35	0.28	0.39	0.35
4	6.09	151.0	17.30	2.56	8.65	0.41	0.12	0.53	0.47	0.49	0.64	0.47
8	6.11	148.0	17.24	2.51	8.62	0.25	0.07	0.32	0.60	0.40	0.39	0.60
9	6.18	101.0	15.78	1.71	7.89	3.59	0.10	3.69	0.32	0.33	0.33	0.32
10	6.21	110.0	16.15	1.86	8.07	5.33	0.08	5.41	0.34	0.27	0.25	0.34
13	6.25	89.3	15.53	1.51	7.76	2.52	0.06	2.58	0.41	0.55	0.22	0.41
20	6.34	38.0	13.97	0.64	6.98	7.36	0.07	7.43	0.34	0.33	0.18	0.34
25	6.38	-13.4	12.31	-0.23	6.15	12.19	0.07	12.26	0.26	0.53	0.19	0.26
28	5.81	99.8	15.00	1.69	7.50	13.26	0.07	13.33	0.30	0.34	0.21	0.30
31	5.86	104.0	15.25	1.76	7.62	8.13	0.06	8.19	0.27	0.26	0.24	0.27
34	5.71	118.2	15.43	2.00	7.71	4.28	0.05	4.32	0.24	0.26	0.19	0.24
35	5.64	303.6	21.57	5.15	10.79	0.42	0.03	0.45	0.21	0.26	0.13	0.21
38	6.13	118.7	16.28	2.01	8.14	0.14	0.01	0.15	0.21	0.28	0.10	0.21
42	6.05	101.2	15.53	1.71	7.76	0.10	0.01	0.11	0.30	0.22	0.06	0.30

Table B3 Data for segment 3 (200 - 300 mm) over a 42 day period

Days after saturation	Segment 3											
	pH	Eh	rH	pe	pe + pH	Fe	Mn	Fe+Mn	Ca	K	Mg	Na
		(mV)				(mg kg^{-1})						
0	5.13	439.3	25.15	7.45	12.58	0.01	0.10	0.11	0.16	0.12	0.51	0.16
2	6.59	185.1	19.45	3.14	9.73	0.15	0.04	0.19	0.66	0.54	0.51	0.66
3	6.62	191.0	19.71	3.24	9.86	0.10	0.06	0.16	0.64	0.55	0.53	0.64
4	6.76	166.5	19.16	2.82	9.58	0.25	0.07	0.32	0.60	0.40	0.39	0.60
8	6.77	156.5	18.85	2.65	9.42	0.19	0.04	0.23	0.54	0.39	0.33	0.54
9	6.81	125.1	17.86	2.12	8.93	0.11	0.08	0.19	0.55	0.35	0.29	0.55
10	6.87	112.0	17.54	1.90	8.77	0.15	0.04	0.19	0.41	0.28	0.22	0.41
13	6.54	109.1	16.78	1.85	8.39	0.19	0.05	0.24	0.57	0.68	0.19	0.57
20	6.88	104.3	17.30	1.77	8.65	0.68	0.07	0.75	0.50	0.45	0.20	0.50
25	6.21	102.2	15.88	1.73	7.94	0.95	0.05	1.00	0.36	0.38	0.19	0.36
28	6.32	64.6	14.83	1.09	7.41	1.94	0.04	1.98	0.37	0.38	0.17	0.37
31	6.01	88.0	15.00	1.49	7.50	0.64	0.03	0.67	0.31	0.28	0.10	0.31
34	6.89	91.2	16.87	1.55	8.44	0.55	0.02	0.57	0.31	0.31	0.09	0.31
35	5.84	162.9	17.20	2.76	8.60	0.45	0.01	0.46	0.31	0.34	0.08	0.31
38	5.25	221.4	18.01	3.75	9.00	0.17	0.01	0.18	0.25	0.30	0.06	0.25
42	5.21	201.5	17.25	3.42	8.63	0.10	0.01	0.11	0.38	0.23	0.06	0.38

APPENDIX C

Data for column experiment 2

Table C1 Chemical analysis of column wet by suction, 330 days after analysis stopped

Segment	Eh (mV)	pH	pe	pe+pH	Fe	Mn	Ca	Mg	K	Na	Mn+Fe	Fe	Mn	Ca	Mg	K	Na
					(mg kg^{-1})							(Cmolckg^{-1})					
9	379.1	5.48	6.43	11.9	27.13	0.73	78.27	58.0	36.80	17.53	27.87	0.10	0.00	0.39	0.29	0.18	0.09
8	396.8	5.70	6.72	12.4	3.73	0.47	80.33	84.0	37.53	19.47	4.20	0.01	0.00	0.40	0.42	0.19	0.10
7	476.5	4.60	8.08	12.7	0.53	0.60	85.13	58.7	28.87	16.73	1.13	0.00	0.00	0.42	0.29	0.14	0.08
6	432.8	5.52	7.33	12.9	0.93	0.60	84.33	57.3	28.00	15.73	1.53	0.00	0.00	0.42	0.29	0.14	0.08
5	476.0	4.68	8.07	12.7	7.40	0.67	84.60	55.3	31.93	16.67	8.07	0.03	0.00	0.42	0.28	0.16	0.08
4	455.3	4.55	7.72	12.3	1.47	0.73	86.80	58.7	30.80	17.47	2.20	0.01	0.00	0.43	0.29	0.15	0.09
3	480.0	4.67	8.14	12.8	0.93	0.80	80.87	54.0	28.33	15.33	1.73	0.00	0.00	0.40	0.27	0.14	0.08
2	471.3	4.66	7.99	12.6	31.00	0.93	84.33	54.7	29.60	15.27	31.93	0.11	0.00	0.42	0.27	0.15	0.08
1	165.8	5.37	2.81	8.2	66.67	0.93	52.00	61.3	23.20	11.33	67.60	0.24	0.00	0.26	0.31	0.12	0.06

APPENDIX D

Data for degree of water saturation experiment

Table D1 Analysis of single cores saturated to $S_{0.6}$ over a period of 121 days, data represented is the average of replications

Days after saturation	Eh (mV)	pH	pe	pe+pH	Fe	Mn	Ca	Mg	K	Na	0.6 Mn+Fe	Eh	pH	Fe	Mn	Ca	Mg	K	Na	Fe	Mn	Ca	Mg	K	Na
					(mg kg^{-1})							(Std. deviation)								($cmol_c kg^{-1}$)					
0	439	5.1	7.4	12.6	0.7	0.9	81.0	51.7	25.0	15.7	1.6	17	0	0	0	11	11	5	3	0.003	0.003	0.40	0.43	0.06	0.07
3	441	5.1	7.5	12.6	0.6	0.0	104.8	48.0	58.8	26.8	0.6	21	0	0	0	0	0	0	0	0.000	0.002	0.52	0.40	0.15	0.12
8	435	5.2	7.4	12.6	0.6	0.5	107.9	50.7	57.7	27.5	1.1	8	0	0	0	1	3	2	1	0.002	0.002	0.54	0.42	0.15	0.12
12	448	4.9	7.6	12.5	0.6	0.5	93.1	64.0	40.6	39.3	1.1	9	0	0	0	0	2	1	0	0.002	0.002	0.46	0.53	0.10	0.17
16	449	4.7	7.6	12.3	0.7	4.3	77.0	113.3	33.7	24.3	4.9	12	0	5	0	1	3	1	0	0.015	0.002	0.38	0.93	0.09	0.11
19	460	4.7	7.8	12.5	0.7	1.9	99.3	52.0	39.1	28.5	2.5	5	0	2	0	1	2	0	0	0.007	0.002	0.50	0.43	0.10	0.12
23	455	4.7	7.7	12.4	0.9	9.6	97.4	52.0	51.3	26.9	10.5	2	0	1	0	0	2	1	0	0.034	0.003	0.49	0.43	0.13	0.12
26	463	5.0	7.8	12.8	0.9	0.8	78.9	84.7	31.5	25.3	1.7	0	0	0	0	1	5	1	0	0.003	0.003	0.39	0.70	0.08	0.11
30	459	4.7	7.8	12.5	0.5	1.7	86.0	5.2	38.3	26.6	2.3	7	0	0	0	6	0	2	1	0.006	0.002	0.43	0.04	0.10	0.12
33	457	4.7	7.7	12.5	0.7	4.4	78.4	5.3	32.9	26.6	5.1	5	0	5	0	3	0	3	1	0.016	0.002	0.39	0.04	0.08	0.12
37	427	4.9	7.2	12.1	0.7	1.5	81.3	4.9	35.0	26.7	2.3	60	0	0	0	2	0	2	0	0.005	0.003	0.41	0.04	0.09	0.12
43	457	5.0	7.8	12.7	0.7	1.7	79.6	50.0	31.3	26.7	2.4	3	0	0	0	6	2	4	1	0.006	0.002	0.40	0.41	0.08	0.12
46	426	5.2	7.2	12.4	0.8	5.8	92.7	52.0	31.0	17.6	6.6	36	0	8	0	6	2	4	0	0.021	0.003	0.46	0.43	0.08	0.08
50	455	5.0	7.7	12.7	0.9	2.0	95.3	52.0	32.5	18.1	2.9	2	0	0	0	4	2	4	1	0.007	0.003	0.48	0.43	0.08	0.08
53	460	4.8	7.8	12.6	0.8	1.3	92.7	50.0	30.8	17.6	2.1	6	0	0	0	5	5	1	0	0.005	0.003	0.46	0.41	0.08	0.08
57	451	5.1	7.6	12.7	0.5	0.9	81.2	62.7	35.7	18.7	1.4	8	0	0	0	4	1	2	1	0.003	0.002	0.41	0.52	0.09	0.08
60	451	4.7	7.6	12.3	0.6	1.7	76.5	60.7	35.5	16.8	2.3	4	1	0	0	1	3	1	0	0.006	0.002	0.38	0.50	0.09	0.07
64	449	4.7	7.6	12.3	0.7	1.9	76.3	55.3	35.0	17.3	2.6	8	0	3	0	4	2	2	0	0.007	0.003	0.38	0.46	0.09	0.08
67	443	4.6	7.5	12.1	0.7	7.7	48.5	51.3	37.6	14.1	8.4	14	0	4	0	12	7	5	0	0.027	0.003	0.24	0.42	0.10	0.06
71	452	4.6	7.7	12.2	0.8	1.0	67.5	52.7	36.3	13.9	1.8	2	0	0	0	6	2	1	0	0.004	0.003	0.34	0.43	0.09	0.06
74	432	4.7	7.3	12.0	0.9	1.9	74.9	52.0	35.3	14.1	2.9	4	0	1	0	2	2	2	0	0.007	0.003	0.37	0.43	0.09	0.06
78	436	4.7	7.4	12.1	1.1	6.6	74.5	53.3	36.5	14.7	7.7	10	0	9	0	2	1	3	1	0.024	0.004	0.37	0.44	0.09	0.06
81	460	4.6	7.8	12.4	1.0	1.1	73.7	51.3	34.4	13.1	2.1	6	0	1	0	2	2	0	1	0.004	0.004	0.37	0.42	0.09	0.06
85	401	4.8	6.8	11.6	0.6	1.7	64.9	60.0	34.4	16.4	2.3	81	0	1	0	2	5	1	0	0.006	0.002	0.32	0.49	0.09	0.07
88	420	4.8	7.1	11.9	0.6	3.1	73.3	60.0	33.1	16.0	3.7	5	0	2	0	3	5	1	0	0.011	0.002	0.37	0.49	0.08	0.07
92	398	4.8	6.7	11.6	0.5	1.0	96.1	62.7	36.1	16.5	1.5	74	0	1	0	3	4	1	0	0.004	0.002	0.48	0.52	0.09	0.07
99	462	5.3	7.8	13.1	0.9	1.6	116.9	66.7	47.1	31.8	2.5	4	0	1	0	9	8	14	13	0.006	0.003	0.58	0.55	0.12	0.14
107	437	5.1	7.4	12.5	0.7	1.3	105.7	66.7	54.9	18.2	2.0	6	0	1	0	6	5	17	1	0.005	0.003	0.53	0.55	0.14	0.08
114	456	4.9	7.7	12.6	1.0	1.1	107.9	64.7	54.0	18.4	2.1	3	0	0	0	7	10	6	1	0.004	0.004	0.54	0.53	0.14	0.08
121	433	4.9	7.3	12.3	0.8	1.3	101.1	73.3	39.3	17.4	2.1	7	0	1	0	13	5	4	2	0.005	0.003	0.50	0.60	0.10	0.08

Table D2 Analysis of single cores saturated to $S_{0.7}$ over a period of 121 days, data represented is the average of 3 replications

Days after saturation	Eh (mV)	pH	pe	pe+pH	Fe	Mn	Ca	Mg	K	Na	Mn+Fe	Eh	pH	Fe	Mn	Ca	Mg	K	Na	Fe	Mn	Ca	Mg	K	Na
					(mg kg^{-1})							(Std. deviation)								($cmol_c kg^{-1}$)					
0	439.33	5.13	7.45	12.58	0.89	0.70	81.00	51.67	25.00	15.67	1.60	17	0	0	0	11	11	5	3	0.00	0.00	0.40	0.43	0.06	0.07
3	445.78	5.16	7.56	12.72	1.20	0.73	110.73	52.67	63.80	28.53	1.93	23	0	0	0	3	4	12	5	0.00	0.00	0.55	0.43	0.16	0.12
8	443.33	5.13	7.51	12.65	1.33	0.87	94.93	53.33	56.73	26.73	2.20	54	0	0	0	13	3	12	3	0.00	0.00	0.47	0.44	0.15	0.12
12	385.67	4.90	6.54	11.44	1.40	0.73	86.93	57.33	38.00	24.13	2.13	9	0	1	0	2	1	0	0	0.01	0.00	0.43	0.47	0.10	0.10
16	389.22	4.76	6.60	11.36	3.60	0.80	84.20	76.00	36.73	24.47	4.40	60	0	2	0	2	23	1	0	0.01	0.00	0.42	0.63	0.09	0.11
19	417.33	4.67	7.07	11.74	2.73	0.73	95.73	63.33	38.40	27.67	3.47	6	0	2	0	23	2	6	5	0.01	0.00	0.48	0.52	0.10	0.12
23	357.56	4.67	6.06	10.73	13.20	0.73	59.60	58.67	36.67	23.47	13.93	14	0	17	0	22	5	3	1	0.05	0.00	0.30	0.48	0.09	0.10
26	398.78	4.88	6.76	11.64	2.47	0.80	82.47	78.67	34.53	27.67	3.27	73	0	1	0	3	3	0	1	0.01	0.00	0.41	0.65	0.09	0.12
30	354.11	4.71	6.00	10.71	7.53	0.67	77.93	100.00	33.73	27.53	8.20	50	0	10	0	4	7	3	1	0.03	0.00	0.39	0.82	0.09	0.12
33	375.44	4.59	6.36	10.96	10.80	0.80	87.73	106.67	39.27	27.13	11.60	72	0	11	0	3	2	3	1	0.04	0.00	0.44	0.88	0.10	0.12
37	417.11	4.64	7.07	11.71	4.87	0.73	81.20	101.33	38.40	26.73	5.60	38	0	2	0	1	2	0	0	0.02	0.00	0.41	0.83	0.10	0.12
43	416.67	5.09	7.06	12.15	2.27	0.60	80.20	47.33	33.13	27.60	2.87	29	0	1	0	1	8	5	1	0.01	0.00	0.40	0.39	0.08	0.12
46	420.00	5.05	7.12	12.17	4.33	0.67	90.60	53.33	33.33	17.87	5.00	32	0	5	0	2	1	5	1	0.02	0.00	0.45	0.44	0.09	0.08
50	444.67	4.93	7.54	12.46	3.60	0.80	101.47	50.67	34.20	18.53	4.40	5	0	1	0	10	1	0	1	0.01	0.00	0.51	0.42	0.09	0.08
53	420.98	4.93	7.14	12.07	2.07	0.80	91.60	49.33	31.00	17.60	2.87	42	0	1	0	0	4	2	1	0.01	0.00	0.46	0.41	0.08	0.08
57	431.22	5.04	7.31	12.35	0.60	0.60	77.47	60.00	33.73	17.40	1.20	43	0	0	0	2	4	1	0	0.00	0.00	0.39	0.49	0.09	0.08
60	410.67	4.85	6.96	11.81	1.73	0.60	73.60	56.00	33.73	16.07	2.33	59	0	1	0	1	2	1	0	0.01	0.00	0.37	0.46	0.09	0.07
64	400.89	4.21	6.79	11.01	7.13	0.80	75.13	54.67	35.73	18.47	7.93	42	0	9	0	5	3	1	1	0.03	0.00	0.37	0.45	0.09	0.08
67	376.56	4.56	6.38	10.95	21.27	0.67	66.73	50.00	33.53	13.53	21.93	71	0	26	0	5	5	5	1	0.08	0.00	0.33	0.41	0.09	0.06
71	431.44	4.57	7.31	11.89	5.67	1.00	68.80	50.67	35.13	14.00	6.67	42	0	8	0	3	4	4	0	0.02	0.00	0.34	0.42	0.09	0.06
74	442.67	4.66	7.50	12.16	1.87	0.87	73.73	53.33	37.20	14.87	2.73	5	0	1	0	1	3	2	0	0.01	0.00	0.37	0.44	0.10	0.06
78	448.44	4.65	7.60	12.25	1.67	1.00	73.80	53.00	36.33	13.80	2.67	8	0	1	0	1	1	3	0	0.01	0.00	0.37	0.44	0.09	0.06
81	417.44	4.73	7.08	11.81	20.47	1.27	74.27	49.33	38.20	15.07	21.73	6	0	19	0	4	2	6	0	0.07	0.00	0.37	0.41	0.10	0.07
85	421.33	4.72	7.14	11.86	5.13	0.60	74.33	59.33	34.73	16.33	5.73	23	0	4	0	1	2	0	0	0.02	0.00	0.37	0.49	0.09	0.07
88	438.44	4.76	7.43	12.19	2.00	0.67	74.33	60.00	33.07	16.60	2.67	3	0	1	0	1	2	2	1	0.01	0.00	0.37	0.49	0.08	0.07
92	439.11	4.92	7.44	12.37	0.40	0.67	101.80	101.80	37.47	17.33	1.07	7	0	0	0	13	13	4	1	0.00	0.00	0.51	0.84	0.10	0.08
99	453.56	5.24	7.69	12.93	0.33	1.07	119.67	70.00	58.00	18.80	1.40	9	0	0	0	7	7	11	2	0.00	0.00	0.60	0.58	0.15	0.08
107	455.11	5.13	7.71	12.84	4.40	0.73	108.07	65.33	47.20	19.47	5.13	6	0	4	0	4	5	12	1	0.02	0.00	0.54	0.54	0.12	0.08
114	440.78	4.87	7.47	12.34	1.13	1.13	108.47	68.00	49.93	18.80	2.27	5	0	1	0	3	2	12	2	0.00	0.00	0.54	0.56	0.13	0.08
121	445.67	4.98	7.55	12.53	3.07	0.67	91.60	62.67	34.67	16.40	3.73	2	0	2	0	7	3	4	1	0.01	0.00	0.46	0.52	0.09	0.07

Table D3 Analysis of single cores saturated to $S_{0.8}$ over a period of 121 days, data represented is the average of 3 replications

Days after saturation	Eh (mV)	pH	pe	pe+pH	0.8 Fe (mg kg^{-1})	Mn	Ca	Mg	K	Na	Mn+Fe	Eh	pH	Fe (Std. deviation)	Mn	Ca	Mg	K	Na	Fe ($cmol_c kg^{-1}$)	Mn	Ca	Mg	K	Na
0	439	5.13	7.45	12.58	0.89	0.70	81.00	51.67	25.00	15.67	1.60	17	0	0	0	11	11	5	3	0.003	0.003	0.40	0.43	0.06	0.07
3	464	5.22	7.87	13.09	0.67	0.93	118.07	56.67	63.87	25.13	1.60	17	0	1	0	9	1	5	1	0.002	0.003	0.59	0.47	0.16	0.11
8	436	5.19	7.40	12.59	1.73	1.00	108.67	52.00	61.07	26.73	2.73	14	0	0	0	2	2	1	2	0.006	0.004	0.54	0.43	0.16	0.12
12	369	4.86	6.26	11.13	3.40	0.80	84.93	57.33	40.47	26.40	4.20	50	0	5	0	18	1	13	5	0.012	0.003	0.42	0.47	0.10	0.11
16	368	4.81	6.24	11.05	3.73	0.87	92.00	70.67	38.47	25.13	4.60	41	0	2	0	6	14	2	0	0.013	0.003	0.46	0.58	0.10	0.11
19	337	4.63	5.71	10.34	1.80	0.87	124.20	60.67	41.27	29.40	2.67	26	0	2	0	58	1	10	5	0.006	0.003	0.62	0.50	0.11	0.13
23	300	4.68	5.08	9.76	19.07	0.80	57.00	59.33	39.40	24.93	19.87	53	0	11	0	20	9	4	1	0.068	0.003	0.28	0.49	0.10	0.11
26	341	4.81	5.78	10.59	1.60	0.80	82.27	81.33	33.60	26.53	2.40	32	0	1	0	2	7	2	1	0.006	0.003	0.41	0.67	0.09	0.12
30	301	4.70	5.10	9.80	12.53	0.67	75.47	94.67	33.27	26.47	13.20	59	0	10	0	4	6	4	0	0.045	0.002	0.38	0.78	0.09	0.12
33	295	4.82	5.01	9.82	3.87	0.80	78.73	97.33	34.87	27.40	4.67	59	0	2	0	6	6	2	1	0.014	0.003	0.39	0.80	0.09	0.12
37	216	4.46	3.66	8.12	19.60	0.93	78.73	96.00	35.00	27.53	20.53	26	0	23	0	6	7	3	1	0.070	0.003	0.39	0.79	0.09	0.12
43	253	4.93	4.29	9.22	26.47	0.93	78.27	47.33	33.20	26.87	27.40	14	1	24	0	2	6	5	1	0.095	0.003	0.39	0.39	0.08	0.12
46	331	5.29	5.61	10.89	22.93	0.87	90.13	52.67	31.53	17.87	23.80	42	0	25	0	3	2	2	0	0.082	0.003	0.45	0.43	0.08	0.08
50	278	4.61	4.72	9.32	23.73	0.93	90.07	49.33	33.73	19.07	24.67	93	0	17	0	3	4	1	0	0.085	0.003	0.45	0.41	0.09	0.08
53	327	4.82	5.54	10.36	5.27	1.00	95.07	51.33	31.80	18.60	6.27	91	0	2	0	1	3	0	0	0.019	0.004	0.47	0.42	0.08	0.08
57	318	4.75	5.40	10.14	2.67	0.60	78.13	59.33	34.93	18.40	3.27	64	1	1	0	3	3	2	1	0.010	0.002	0.39	0.49	0.09	0.08
60	388	4.72	6.57	11.29	43.33	0.87	73.33	55.33	36.27	18.00	44.20	46	0	40	0	3	6	3	1	0.155	0.003	0.37	0.46	0.09	0.08
64	325	4.73	5.51	10.24	13.80	0.87	74.73	58.67	37.00	19.07	14.67	54	0	21	0	3	3	3	1	0.049	0.003	0.37	0.48	0.09	0.08
67	269	4.49	4.56	9.05	13.00	0.67	65.60	50.67	32.20	14.53	13.67	119	0	13	0	3	2	3	1	0.047	0.002	0.33	0.42	0.08	0.06
71	311	4.63	5.27	9.89	4.20	0.87	69.20	50.67	35.53	14.27	5.07	55	0	2	0	1	1	1	1	0.015	0.003	0.35	0.42	0.09	0.06
74	318	4.63	5.39	10.02	16.00	0.93	72.67	52.67	35.13	13.93	16.93	14	0	14	0	1	5	2	0	0.057	0.003	0.36	0.43	0.09	0.06
78	357	4.58	6.04	10.62	4.87	1.20	76.00	53.33	34.33	14.07	6.07	30	0	3	0	3	4	2	0	0.017	0.004	0.38	0.44	0.09	0.06
81	300	4.51	5.08	9.60	2.00	1.07	72.00	52.67	33.67	14.93	3.07	17	0	2	0	3	6	3	1	0.007	0.004	0.36	0.43	0.09	0.06
85	311	4.71	5.27	9.99	7.20	0.67	68.67	56.67	34.07	16.20	7.87	44	0	4	0	5	5	1	1	0.026	0.002	0.34	0.47	0.09	0.07
88	323	4.90	5.47	10.37	7.93	0.73	73.13	59.33	33.67	16.87	8.67	15	0	8	0	4	6	0	0	0.028	0.003	0.36	0.49	0.09	0.07
92	436	4.72	7.39	12.11	6.27	0.80	93.27	93.27	34.00	16.93	7.07	194	0	6	0	2	2	3	1	0.022	0.003	0.47	0.77	0.09	0.07
99	414	5.25	7.02	12.27	1.60	0.73	110.93	62.67	38.80	21.47	2.33	57	0	0	0	3	3	1	3	0.006	0.003	0.55	0.52	0.10	0.09
107	388	5.04	6.57	11.61	0.47	0.80	123.47	65.33	41.93	21.07	1.27	88	0	0	0	8	8	12	2	0.002	0.003	0.62	0.54	0.11	0.09
114	308	4.69	5.22	9.91	1.20	0.87	110.93	68.67	44.00	18.20	2.07	65	0	1	0	5	4	10	2	0.004	0.003	0.55	0.57	0.11	0.08
121	378	4.94	6.41	11.35	8.20	1.00	99.47	64.67	40.00	17.53	9.20	57	0	6	0	25	11	12	2	0.029	0.004	0.50	0.53	0.10	0.08

Table D4 Analysis of single cores saturated to $S_{0.9}$ over a period of 121 days, data represented is the average of 3 replications

Days after saturation	Eh (mV)	pH	pe	pe+pH	Fe	Mn	Ca	Mg	K	Na	0.9 Mn+Fe	Eh	pH	Fe	Mn	Ca	Mg	K	Na	Fe	Mn	Ca	Mg	K	Na
					(mg kg^{-1})									(Std. deviation)						($cmol_c kg^{-1}$)					
0	439	5.13	7.45	12.58	0.89	0.70	81.00	51.67	25.00	15.67	1.60	17	0	0	0	11	11	5	3	0.003	0.003	0.404	0.425	0.064	0.068
3	400	5.10	6.79	11.88	1.33	1.07	117.13	58.67	61.27	26.07	2.40	7	0	1	0	5	1	5	1	0.005	0.004	0.584	0.483	0.157	0.113
8	395	4.72	6.69	11.41	1.20	1.00	116.80	57.60	55.20	26.20	2.20	6	1	0	0	7	2	10	4	0.004	0.004	0.583	0.474	0.141	0.114
12	265	5.09	4.49	9.58	2.47	0.67	85.87	59.33	38.07	27.33	3.13	80	0	3	0	12	8	2	7	0.009	0.002	0.428	0.488	0.097	0.119
16	174	4.83	2.95	7.77	19.40	0.93	82.87	60.00	38.93	28.33	20.33	10	0	14	0	9	5	7	10	0.069	0.003	0.414	0.494	0.100	0.123
19	180	4.86	3.05	7.91	15.07	0.93	186.27	61.33	52.33	30.67	16.00	34	0	3	0	90	1	15	4	0.054	0.003	0.929	0.505	0.134	0.133
23	172	4.73	2.92	7.65	5.27	0.87	81.00	59.33	35.00	23.40	6.13	7	0	1	0	7	3	4	1	0.019	0.003	0.404	0.488	0.090	0.102
26	222	4.59	3.76	8.35	2.53	0.80	72.27	74.00	26.60	23.87	3.33	39	0	1	0	10	6	6	2	0.009	0.003	0.361	0.609	0.068	0.104
30	221	4.88	3.74	8.61	15.13	1.07	86.00	54.67	35.27	27.13	16.20	31	0	2	0	4	1	2	0	0.054	0.004	0.429	0.450	0.090	0.118
33	229	4.89	3.88	8.77	30.60	0.80	53.47	47.33	32.60	27.13	31.40	42	0	17	0	6	1	2	0	0.110	0.003	0.267	0.390	0.083	0.118
37	203	5.03	3.44	8.47	27.67	1.00	81.93	50.00	36.07	27.87	28.67	24	0	13	0	7	3	3	1	0.099	0.004	0.409	0.412	0.092	0.121
43	280	4.83	4.75	9.58	23.53	0.80	68.93	53.33	32.87	28.20	24.33	22	0	13	0	15	3	1	1	0.084	0.003	0.344	0.439	0.084	0.123
46	218	4.90	3.69	8.59	6.93	0.80	83.93	53.33	32.67	21.47	7.73	87	0	6	0	12	5	4	5	0.025	0.003	0.419	0.439	0.084	0.093
50	282	4.88	4.78	9.65	15.73	0.87	82.53	50.67	28.33	18.53	16.60	56	0	10	0	6	1	2	1	0.056	0.003	0.412	0.417	0.072	0.081
53	223	4.92	3.78	8.70	26.53	1.13	92.73	52.00	34.13	19.33	27.67	6	0	9	0	5	0	3	1	0.095	0.004	0.463	0.428	0.087	0.084
57	294	4.87	4.98	9.84	43.33	1.00	66.67	60.00	34.80	17.07	44.33	70	0	68	0	13	4	7	1	0.155	0.004	0.333	0.494	0.089	0.074
60	179	4.71	3.03	7.75	38.20	0.87	70.73	59.33	36.60	18.40	39.07	36	0	19	0	5	1	2	0	0.137	0.003	0.353	0.488	0.094	0.080
64	254	4.66	4.30	8.96	43.67	1.00	72.67	61.33	37.73	18.87	44.67	24	0	3	0	5	5	4	1	0.156	0.004	0.363	0.505	0.097	0.082
67	244	4.45	4.14	8.59	55.33	1.20	62.93	55.33	36.07	14.33	56.53	16	0	66	1	13	4	5	1	0.198	0.004	0.314	0.455	0.142	0.062
71	274	4.64	4.65	9.29	12.53	1.00	60.67	50.67	35.67	14.87	13.53	61	0	6	0	8	3	0	1	0.045	0.004	0.303	0.417	0.130	0.065
74	124	4.84	2.10	6.94	64.13	1.20	71.07	52.67	39.53	14.47	65.33	4	0	50	0	4	3	1	0	0.230	0.004	0.355	0.433	0.135	0.063
78	181	4.76	3.07	7.83	38.27	1.60	74.27	52.00	37.60	14.53	39.87	81	0	19	0	4	0	0	1	0.137	0.006	0.371	0.428	0.133	0.063
81	155	4.62	2.62	7.24	64.07	1.53	81.13	51.33	39.20	15.27	65.60	36	0	74	0	8	3	9	1	0.229	0.006	0.405	0.422	0.131	0.066
85	249	4.64	4.22	8.86	39.20	1.07	71.80	58.00	33.13	16.67	40.27	101	0	59	1	2	2	3	1	0.140	0.004	0.358	0.477	0.148	0.072
88	245	4.64	4.15	8.79	57.80	1.07	68.80	66.67	38.20	16.87	58.87	27	0	60	0	7	4	3	1	0.207	0.004	0.343	0.549	0.171	0.073
92	270	4.86	4.57	9.43	17.13	1.47	87.93	65.33	39.33	18.20	18.60	26	0	7	1	20	6	4	0	0.061	0.005	0.439	0.538	0.167	0.079
99	323	5.23	5.48	10.71	2.80	0.87	109.60	68.67	68.67	20.53	3.67	64	0	4	0	6	7	7	4	0.010	0.003	0.547	0.565	0.176	0.089
107	305	5.06	5.18	10.24	6.20	1.13	124.40	58.67	51.27	21.47	7.33	83	0	9	0	7	11	12	3	0.022	0.004	0.621	0.483	0.150	0.093
114	255	5.19	4.32	9.52	13.40	0.93	108.47	68.00	38.33	18.73	14.33	47	0	22	0	7	7	6	1	0.048	0.003	0.541	0.560	0.174	0.081
121	250	5.02	4.23	9.25	81.60	1.53	83.40	68.00	42.47	17.73	83.13	62	0	49	0	39	3	3	0	0.292	0.006	0.416	0.560	0.174	0.077

APPENDIX E

Data for bulk density experiment

Table E1 Analysis of single cores packed to a bulk density of 1.4 Mg m^{-3} saturated to $S_{0.8}$ over a period of 23 days, data represented is the average of 3 replications

1.4 Mg m^{-3}																								
Days after saturation	Eh (mV)	pH	pe	pe+pH	Fe	Mn	Ca	Mg	K	Na	Mn+Fe	Eh	pH	Fe	Mn	Ca	Mg	K	Na	Fe	Mn	Ca	Mg	K	Na
					(mg kg^{-1})							(Std. deviation)								($cmol_c kg^{-1}$)					
0	439	5.1	7.4	12.6	0.9	0.7	81.0	51.7	25.0	15.7	1.6	17	0	0	0	11	11	5	3	0.003	0.003	0.40	0.43	0.06	0.07
3	-93	5.6	-1.6	4.1	1.5	0.9	87.4	53.3	40.3	21.1	2.3	92	0	1	0	3	1	1	1	0.005	0.003	0.44	0.44	0.10	0.09
8	178	5.1	3.0	8.1	4.4	0.7	64.6	50.0	33.5	18.6	5.1	11	0	2	0	10	5	3	5	0.016	0.002	0.32	0.41	0.09	0.08
12	169	5.1	2.9	8.0	18.9	0.9	59.7	54.0	40.9	17.9	19.8	25	0	18	0	26	9	11	3	0.068	0.003	0.30	0.44	0.10	0.08
16	191	5.3	3.2	8.6	31.2	1.3	75.4	50.8	37.9	15.3	32.5	40	0	19	1	11	7	4	0	0.112	0.005	0.38	0.42	0.10	0.07
19	135	5.1	2.3	7.4	31.2	1.0	75.2	50.7	37.2	15.1	32.2	20	0	19	0	11	6	3	0	0.112	0.004	0.38	0.42	0.10	0.07
23	169	5.1	2.9	7.9	46.7	1.1	96.8	50.0	39.0	16.1	47.7	19	0	38	0	23	5	3	2	0.167	0.004	0.48	0.41	0.10	0.07

Table E2 Analysis of single cores packed to a bulk density of 1.6 Mg m^{-3} saturated to $S_{0.8}$ over a period of 23 days, data represented is the average of 3 replications

1.6 Mg m^{-3}																									
Days after saturation	Eh (mV)	pH	pe	pe+pH	Fe	Mn	Ca	Mg	K	Na	Mn+Fe	Eh	pH	Fe	Mn	Ca	Mg	K	Na	Fe	Mn	Ca	Mg	K	Na
					(mg kg^{-1})							(Std. deviation)								($cmol_c kg^{-1}$)					
0	439	5.1	7.4	12.6	0.9	0.7	81.0	51.7	25.0	15.7	1.6	17	0	0	0	11	11	5	3	0.003	0.003	0.40	0.43	0.06	0.07
3	104	5.5	1.8	7.2	0.0	0.5	81.2	52.0	32.1	21.1	0.5	213	0	0	0	1	2	1	1	0.000	0.002	0.41	0.43	0.08	0.09
8	388	4.9	6.6	11.5	3.1	0.5	82.5	50.7	35.9	17.2	3.6	36	0	2	0	1	3	4	7	0.011	0.002	0.41	0.42	0.09	0.07
12	370	5.2	6.3	11.5	7.0	0.6	82.1	46.7	36.7	15.6	7.6	43	0	8	0	4	2	5	1	0.025	0.002	0.41	0.38	0.09	0.07
16	407	5.2	6.9	12.0	6.9	0.7	60.6	46.0	30.7	13.6	7.6	19	0	3	0	6	10	6	1	0.025	0.003	0.30	0.38	0.08	0.06
19	397	4.9	6.7	11.7	6.9	0.7	60.5	45.3	30.9	13.5	7.5	33	0	3	0	6	10	7	1	0.025	0.002	0.30	0.37	0.08	0.06
23	383	4.9	6.5	11.4	5.2	0.7	79.9	50.0	35.4	15.4	5.9	65	0	6	0	11	11	4	2	0.019	0.003	0.40	0.41	0.09	0.07

Table E3 Analysis of single cores packed to a bulk density of 1.8 Mg m^{-3} saturated to $S_{0.8}$ over a period of 23 days, data represented is the average of 3 replications

1.8 Mg m^{-3}																								
Days after saturation	Eh (mV)	pH	pe	pe+pH	Fe	Mn	Ca	Mg	K	Na	Mn+Fe	Eh	pH	Fe	Mn	Ca	Mg	K	Na	Fe	Mn	Ca	Mg	K	Na
					(mg kg^{-1})							(Std. deviation)								($cmol_c kg^{-1}$)					
0	439	5.1	7.4	12.6	0.9	0.7	81.0	51.7	25.0	15.7	1.6	17	0	0	0	11	11	5	3	0.003	0.003	0.40	0.43	0.06	0.07
3	321	5.6	5.4	11.0	0.7	0.5	83.0	52.7	33.6	19.1	1.2	115	0	1	0	3	2	1	0	0.002	0.002	0.41	0.43	0.09	0.08
8	383	5.0	6.5	11.5	6.9	0.7	91.5	56.0	43.2	14.3	7.6	55	0	10	0	16	9	9	1	0.025	0.003	0.46	0.46	0.11	0.06
12	427	5.2	7.2	12.5	4.4	0.7	81.5	49.3	37.1	16.3	5.1	13	0	1	0	1	1	3	2	0.016	0.003	0.41	0.41	0.09	0.07
16	437	5.0	7.4	12.4	3.7	0.8	65.8	50.2	34.8	13.2	4.5	12	0	1	0	9	2	1	1	0.013	0.003	0.33	0.41	0.09	0.06
19	419	5.0	7.1	12.1	3.9	0.7	65.8	50.0	35.1	12.9	4.7	8	0	2	0	9	2	0	1	0.014	0.003	0.33	0.41	0.09	0.06
23	425	5.0	7.2	12.2	4.9	0.9	83.1	55.3	37.0	16.4	5.7	5	0	1	0	2	2	2	1	0.017	0.003	0.41	0.46	0.09	0.07